The influence of three different intercalation methods on the properties of exfoliated graphite

Xandra van Heerden

Submitted in partial fulfilment of the requirements for the degree
Master's degree (Chemical Engineering) in the Faculty of Engineering,
Built Environment and Information Technology,
University of Pretoria, Pretoria, South Africa

2015

UNIVERSITEIT VAN PRETORIA
UNIVERSITY OF PRETORIA
YUNIBESITHI YA PRETORIA

CVD 800

The influence of three different intercalation methods on the properties of exfoliated graphite

By: Xandra van Heerden
Supervisor: Dr. Heinrich Badenhorst
Department: Chemical Engineering
Degree: M.Eng (Chemical Engineering)

Synopsis

It is unclear whether all intercalation techniques truly lead to the insertion of atoms between the graphite layers, or also lead to other effects which contribute to expansion. The objective of this project is to better understand the effects caused by different intercalation methods. Three intercalation methods were explored to determine the method which incurs the least damage to the surface and microstructure of the graphite intercalated compounds, yet achieves the best intercalation and therefore expansion.

All the main findings are summarised below:

- The gas phase sample had virtually no mass loss at the point where expansion took place. Therefore the intercalation was very efficient, producing large expansion without significant mass loss.
- The mass loss that only occurs at the sublimation of iron chloride (320 ºC) indicates the excessive "un-intercalated" or residual iron chloride.
- After oxidation, before purification, the gas phase sample has 25 % residual mass; this also proves the presence of impurities and residual iron chloride in the exfoliated sample.

- For the Hummers and electrochemical samples, expansion and mass loss occur over a wide temperature range, this indicates that graphite oxide was formed rather than the theoretically expected "insertion of atoms between the sheets".
- The mass losses before 200 ˚C of the samples of the Hummers and electrochemical methods are more evidence that graphite oxide and graphite surface complexes with oxygen were produced.
- The Hummers and electrochemical intercalation methods show similar expansion and mass loss curves, therefore it can be concluded that the reaction mechanism for both these methods is alike.
- The gas phase method yields the best expansion of 250 % using the TMA, whereas both the other methods deliver approximately 220 %.
- Using microwave expansion the electrochemical intercalation method yields the best bulk volume expansion of 1500 %, with the gas phase sample delivering a volume expansion of 1450 %.

The Hummers samples are extremely damaged. This is clear from the several and deep oxidation pits visible throughout the basal plane of these samples. The basal plane and the edges are even eroded before purification and oxidation. This intercalation technique employs oxidisers in the preparation method which additionally oxidises the samples. This explains why the Hummers method renders the most damage.

The residual material on the gas phase sample acts as catalysts making the sample very reactive and consequently damaging the surface during oxidation. The partially oxidised purified gas phase sample visibly shows the pits and roughened edges.

There are two “types” of intercalation. The first intercalation “type” is the actual insertion of atoms or molecules between the graphite layers, whereas the other “type” of intercalation is the production of graphite oxide. The compound comprises carbon, oxygen and hydrogen, obtained by treating graphite with strong oxidisers. The functional groups usually found in graphite oxide are carbonyl (C=O), hydroxyl (-OH),

phenol amongst others and also some impurities of sulphur when sulphuric acid is used. Both these intercalation types lead to expansion.

It is recommended that a more efficient method for removal of residual material in the gas phase samples be explored. It is also recommended that more research be done to determine the reaction mechanisms during the three different intercalation methods. The graphite surface complexes of the intercalated compounds and the evolved gases during expansion should be analysed.

Keywords: Graphite, Hummers intercalation, Gas phase intercalation, Electrochemical intercalation, Expanded graphite, Exfoliated Graphite

Acknowledgements

'It is the Lord who gives me wisdom;
from Him come knowledge and understanding.'
(Proverbs 2:6)

My Lord and Saviour, **Jesus Christ**; for my talents and His guidance and grace.

My dearest husband, **Jacques van Heerden**; who has been a constant source of support and encouragement and for his committed love and personal sacrifices so that I could pursue my dreams.
"You don't marry the person you can live with… you marry the person you can't live without!" – Unknown author

My parents, **Philip and Petro Nice**, for their unconditional love, support and encouragement.
"At the end of the day, the most overwhelming key to a child's success is the positive involvement of parents" – Jane D. Hull

My supervisor, **Dr. Heinrich Badenhorst**, for his guidance and encouragement. It was an honour to work with him.
"A single conversation with a wise man is better than ten years of study."
– Chinese Proverb

All of the staff at the University of Pretoria, and the Institute of Applied Materials for their time and the use of their equipment.

'I can do all things through Christ who strengthens me.'
(Philippians 4:13)

Table of contents

List of figures

List of tables

1. Introduction

Graphite has a layered structure, which allows the introduction of various molecules or atoms between these layers, producing a material known as graphite intercalated compounds (GICs). This process is known as intercalation. There are various methods of intercalation, such as different liquid phase intercalation methods, gas phase intercalation methods, hydrothermal and electrochemical intercalation methods. It is also possible to intercalate more than one substance, producing a ternary graphite intercalation compound (TGIC). GICs have many applications because of its unique properties. GICs can be used as additives, electrodes, conductors, etc. GICs can be expanded to produce a low density, large surface area, worm-like structure known as expanded graphite (EG). Expansion can be achieved by using different methods such as microwave irradiation and rapid heating, also known as thermal shock.

It is unclear whether all intercalation techniques truly lead to the insertion of atoms, or also lead to other effects which contribute to expansion. The objective of this project is to better understand the effects caused by different intercalation methods. GICs will be used as additives to increase electrical and thermal conductivity of various material, thus the microstructure, surface structure and atomic structure is therefore of high importance. Another objective will be to understand the trade-off between achieving good intercalation and effective separation of the graphite layers, versus the damage caused to the final microstructure and surface, therefore the influence of the different intercalation techniques and conditions on the surface and microstructure of the final expanded and exfoliated graphite must be investigated.

Three methods were investigated and compared; liquid phase, gas phase and electrochemical intercalation. In order to determine the extent of damage of each sample, the samples were analysed using Thermogravimetric analysis (TGA) for oxidation and mass loss data, RAMAN spectroscopy, but also visually investigated using the High Resolution Field Emission Gun Scanning Electron Microscope (HR FEG-SEM). The extent of intercalation was determined using manual expansion employing microwave irradiation, as well as Thermomechanical analysis (TMA).

2. Theoretical Background

2.1. Graphite

2.1.1. Structure

The word “graphite” is derived from the Greek word “graphein”, which means to write. There are generally two types of graphite namely synthetic graphite and natural graphite where natural graphite can be classified into three different types namely flakes, high crystalline and amorphous. These three types of natural graphite can further be classified into more subdivisions, depending on the particle size, impurities and graphite content (Kalyoncu, 1998). Natural graphite has a unique structure, comprising ‘graphene’ layers stacked on one another. The carbon atoms in graphite have sp^2 hybridised orbitals directed 120º apart on a layer plane rendering a trigonal structure. Graphene has a hexagonal unit cell. The formation of σ-bonding between the carbon atoms on the layer plane is due to the overlapping of the sp^2 hybridised orbitals. The delocalised orbitals result in loosely bound π-electrons which form weak van der Waals forces between the layers in the *c*-direction. Graphite has an intraplanar C–C bond length of 1,42 Å and an interplanar spacing (*c*-axis spacing) of 3,35 Å as shown in Figure 2-1 (Chung, 2002).

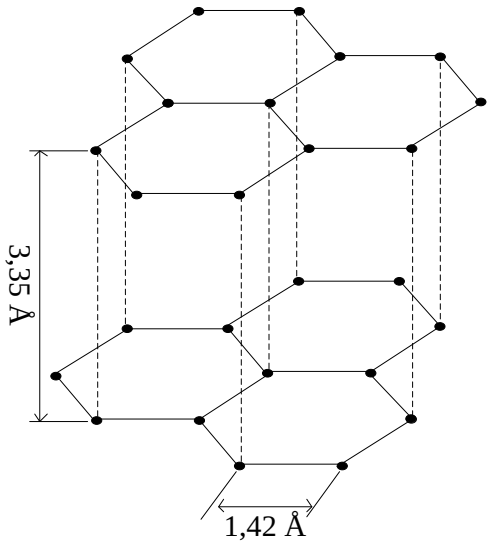

Figure 2-1: The crystal structure of graphite illustrating the hexagonal structure.

The basal planes are stacked on one another by π – π interaction, which is weak van der Walls interlayer bonding. The irregular surface which is parallel to the *c*-axis, and perpendicular to the *a*-axis or 'basal plane', is known as the 'edge plane'. These 'edge planes' may comprise many functional groups containing oxygen. Natural graphite contains various inorganic impurities quantified as ash content (McCreery, 2008; Noel & Santhanam, 1998).

2.1.2. Properties

Graphite has a distinct grey to black colour, is opaque and has a metallic gloss. It is flexible, but not elastic and soft with a Mohs hardness of 1 to 2. The specific gravity of graphite is between 2,20 and 2,30 depending on the purity (Kalyoncu, 1998). Graphite is anisotropic. The electrical and thermal conductivity is good in the direction of the layers, due to the in-plane metallic bonds, but it is poor perpendicular to the layers, due to the weak van der Waals forces between the layers (Chung, 2002). Graphite has unique chemical and physical properties. Graphite has excellent lubrication. Because of its anisotropy, graphite has the ability to allow chemical molecules to be intercalated between the graphite layers (Chung, 2002; Graphit Kropfmuhl AG (*sa*) "What is graphite", http://www.graphite.de/englisch/pdf/blaehgraphitprospekt_e.pdf [2013, July 10]).

2.2. Graphite intercalation compounds

2.2.1. Intercalation

Due to the layered structure of graphite, many different substances (molecules or atoms) can be introduced between the graphene layers. This process is called intercalation, where the various substances are known as intercalants. The product of this process is called graphite intercalated compounds (GICs), also known as expandable graphite. A diagram of a GIC is illustrated in Figure 2-2.

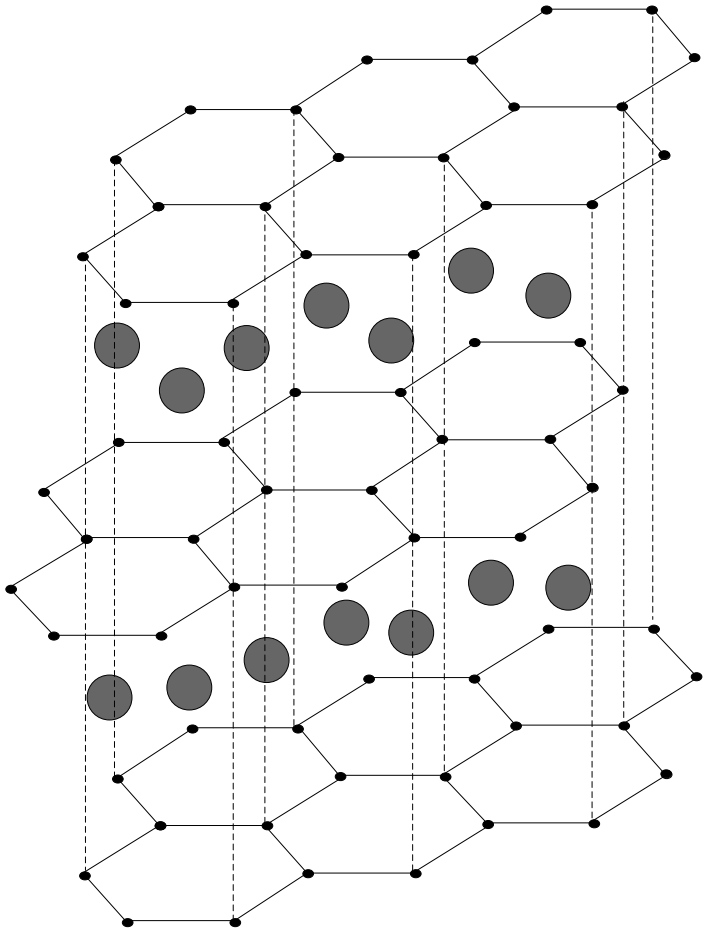

Figure 2-2: A graphite intercalated compound (GIC) shown graphically.

There are various different methods of intercalation. The methods employed to synthesise these GICs include vapour absorption, immersion in solution, aqueous solution, and molten salt as well as electrochemical methods (Zhu, Chen & Wang, 2003; Asano *et al*, 1996). An acceptor-type GIC is produced when electronegative species accept an electron and form an ionic bond with the π-electron network (denoted by C_x) as illustrated in Equation 2-1;

$$C_x + A \rightleftharpoons C_x^+ \cdot A^- \quad (2\text{-}1)$$

But in contrast, a donor-type GIC is produced when an electron is donated to the network, this happens with metal atoms as shown in Equation 2-2.

$$C_x + M \rightleftharpoons C_x^- \cdot M^+ \quad (2\text{-}2)$$

(Noel & Santhanam, 1998).

2.2.2. Applications

GICs have novel features and diverse properties like their structural, electronic and optical properties which would suggest a number of applications. A few of the promising applications are its use as electrode material, conductors, superconductors, catalysts, hydrogen storage, batteries, displays and polarisers (Dresselhaus, MS & Dresselhaus, G, 2002; Zhao *et al*, 2011).

Another application of GICs is their use as a flame retardant. As the heat of the flame is exposed to the expandable graphite, the intercalants vaporise and the graphite expands and creates an intumescent layer on the surface of the material. This retards the spread of fire and minimise the formation of toxic gases and fumes. The advantages of expandable graphite as flame retardants are that it has an excellent flame retardant effect with low material use, is free from halogens and heavy metal, it is non-polluting and also reduces fume formation and is low in cost. It is suitable for a wide range of applications such as insulation and soft foams, carpets, textiles, coatings and plastic foils, rubber products as well as in pipe closing systems (Graphit Kropfmuhl AG (*sa*) “What is graphite”, http://www.graphite.de/englisch/pdf/blaehgraphitprospekt_e.pdf [2013, July 10]).

GICs are also used as graphite foils, where it is compacted and rolled out in a calendering process to produce foils. Gaskets and compounds with excellent chemical and thermal resistance can be produced from these foils. Another application is the employment of GICs as a covering material in the metallurgical industry for hot molten metal; here graphite is used for thermal insulation and protection against oxidation. Expandable graphite can also act as an absorption medium to absorb liquids (Graphit Kropfmuhl AG (*sa*) “What is graphite”, http://www.graphite.de/englisch/pdf/blaehgraphitprospekt_e.pdf [2013, July 10]).

2.2.3. Properties

The most distinguishing property of GICs is the staging index *n*. This involves the intercalant layers being arranged periodically in the matrix of graphene layers. The resultant GIC is titled in terms of the staging index *n*, which denotes the number of graphite layers that lie between adjacent intercalant layers. Therefore, with a stage-1 GIC, one graphene layer is sandwiched by two intercalant layers and in the case of a stage-2 GIC, an intercalant layer is sandwiched by two graphite layers, and so on, as illustrated in Figure 2-3 (Zhao *et al*, 2011; Abe *et al*, 1995).

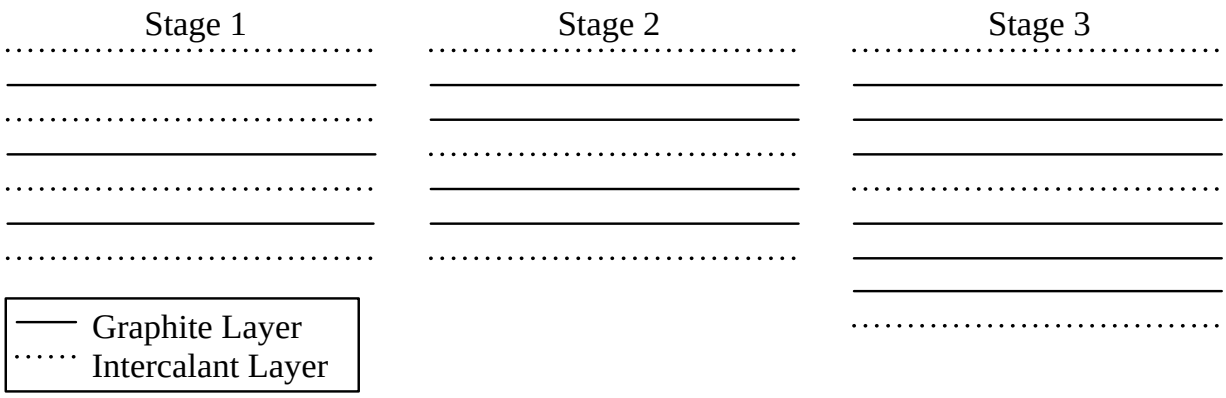

Figure 2-3: A schematic illustration of different stages (Noel & Santhanam, 1998).

Dresselhaus, MS & Dresselhaus, G (2002) states that when using RAMAN experiments, it is indicated that donor intercalants cause the in-plane graphite layers to expand as the electrons are added, whereas acceptor intercalants remove electrons. It is also implied that the carbon-carbon bonds in the bonding layer plane have stage-dependent stiffening and softening, for acceptors and donors respectively, due to the electron transfer.

The most important structural characteristic of GICs is the strong intraplanar binding and weak interplanar binding. This ensures the graphite and intercalant layers stay separated, which ensures that the graphite layer maintains all the basic properties of pristine graphite, and the intercalant layer behaves like the parent intercalant material. The spacing between consecutive graphite layers in GICs is the same as in pristine graphite, C_0 = 3,35 Å. The distance between graphite layers wherein the intercalant layer is sandwiched, d_s also known as the intercalant sandwich thickness is

used to determine another important characteristic of GICs, which is the *c*-axis identity period, also known as the repeat distance (I_c) using Equation 2-3:

$$I_c = d_s + (n - 1)C_0 \qquad (2\text{-}3)$$

It is observed by Dresselhaus, MS & Dresselhaus, G (2002) that the intercalant sandwich thickness d_s increases from stage 1 to stage 2 for most donor compounds but decreases for acceptor compounds, but is independent for stages greater than 2 for both acceptor and donor compounds (Dresselhaus, MS & Dresselhaus, G, 2002; Sorokina *et al*, 2001).

The most widely studied property of GICs is their electrical conductivity due to the fact that it has high in-plane (basal plane) conductivity, but relatively low *c*-axis conductivity. A large increase in the in-plane conductivity is observed with an increasing concentration of both donor and acceptor intercalants. The *c*-axis conductivity increases with a donor, but decreases with an acceptor compound (Dresselhaus, MS & Dresselhaus, G, 2002).

2.2.4. Ternary graphite intercalated compounds

It is possible to intercalate more than one intercalant into graphite layers; this is known as ternary graphite intercalated compounds (TGICs) (Hamwi *et al*, 1993). TGICs can contain more than one type of donor, acceptor, or even a mixture of donor-acceptor systems (Noel & Santhanam, 1998). These TGICs can either be co-intercalated or bi-intercalated graphite compounds. Co-intercalation compounds occur where the two intercalants lie within the same galleries. Such compounds can be prepared by the reaction (in liquid or gas phase) of one intercalant alone with an unsaturated binary GIC of stage ≥ 2, and then a ternary compound of lower stage is obtained. Bi-intercalation systems occur when the intercalants occupy separate consecutive galleries. This type of compound can only be produced by subsequently intercalating into a stage ≥ 2 binary GIC with another intercalant. Two metal chlorides or two alkali metals are most commonly used (Hamwi *et al*, 1993).

The difference between bi-intercalation and co-intercalation compounds is illustrated in a schematic diagram in Figure 2-4.

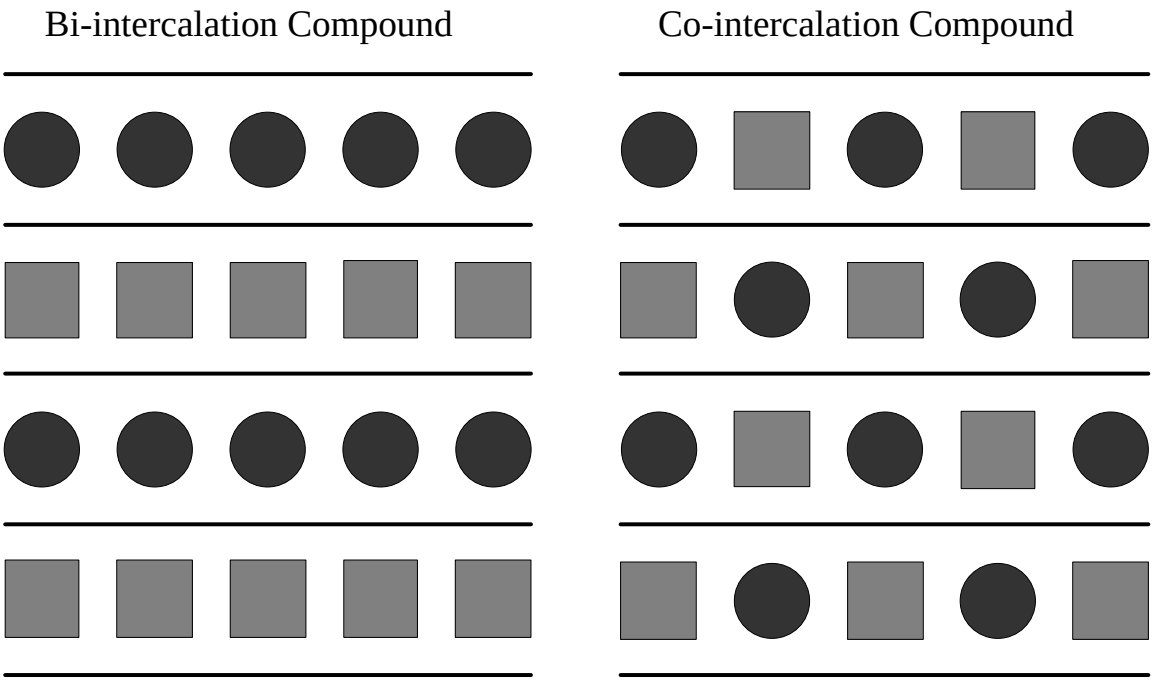

Figure 2-4: An illustration of bi-intercalation and co-intercalation compounds.

2.2.5. Intercalants

In principle any molecule or atom can be used as an intercalant. These intercalants are generally classified according to whether they form donor or acceptor compounds. The most common and most widely studied donor compounds are the alkali metal compounds, i.e. compounds containing K, Rb, Cs and Li, although alkaline earth metals, lanthanides and metal alloys are other known donor compounds. Alkali metals with hydrogen or any other polar molecules (ammonia, tetrahydrofuran (THF)), or aromatic molecules (benzene) have also been used successfully for the preparation of ternary donor compounds (Dresselhaus, MS & Dresselhaus, G, 2002).

For the preparation of acceptor compounds different intercalants may be used. These intercalants may be Lewis acid intercalants like halogen Br_2 or halogen mixtures, metal chlorides, bromides, fluorides and oxyhalides, or strong Brönsted acids like sulphuric acid (H_2SO_4) and nitric acid (HNO_3) or acid oxides such as N_2O_2 and SO_3 (Dresselhaus, MS & Dresselhaus, G, 2002).

The most common GIC, according to Chung (1987), is graphite bisulphate, which is obtained by the reaction of graphite with a mixture of sulphuric and nitric acid. The ratio of concentrated sulphuric acid to nitric acid (65 %) is either 3:1 or 4:1, which

yields expansion of up to 300. Using potassium and tetrahydrofuran (THF) as intercalants produces the ternary GIC, $C_{24}K(THF)_2$, with the ability to yield an expansion of 300 as well (Chung, 1987).

GICs which contain transition metal chlorides have attracted much attention because of its good electrical conductivity and magnetic properties, as well as its very high coefficient of thermal expansion. Expanded graphite (EG) made from these GICs has promising adsorbent ability. $FeCl_3$, $AlCl_3$, $CuCl_2$ and $NiCl_2$ are known to be used as intercalants, among others (Shornikova *et al*, 2006).

Intercalation of organic molecules (THF and benzene) into the unoccupied galleries of binary GICs (Fe-GIC, Co-GIC, or Cu-GIC), which will result in a TGIC, is not found. But TGICs with Brönsted acids have been obtained. Several bi-intercalation compounds with inorganic fluorides (VF_6, TiF_6, SbF_5, AsF_5 or WF_6) have been reported. These fluoride-GICs are very unstable in air, as opposed to chloride-GICs, this is due to the fluoride volatility which yields high diffusion of the fluoride species between graphite layers (Hamwi *et al*, 1992).

There are many GICs which are unstable in air. Donor compounds are unstable in air since it is easily oxidised, while acceptor compounds are unstable by reason of ease of desorption. Because of this instability, most of these GICs require encapsulation to ensure chemical stability (Dresselhaus, MS & Dresselhaus, G, 2002).

Graphite nitrate (GN) is a very unstable GIC, as GN is reduced by water and spontaneously decomposes. The decomposition of GN can occur without the presence of water to produce gaseous products such as CO, CO_2, NO and NO_2 which is formed when NO_3^- turns into an unstable radical. Co-intercalation of carboxylic acids is a promising approach in the stabilisation of GN (Savoskin *et al*, 2006).

2.3. Expansion

2.3.1. Expanded graphite

Expanded graphite is GICs that have expanded and has a low density and large surface area. In general expanded graphite is prepared by the rapid heating of GICs. It is the product of the thermal decomposition of GICs (Afanasov *et al*, 2010; Inagaki *et al*, 2004).

Expansion of graphite involves a phase transition where the intercalant in the graphite vaporises, forming gas pockets that may or may not burst. If the gas pockets do not burst, and the heating is not excessive, the expansion can be reversible upon subsequent cooling. With excessive heating and if the gas pockets burst, it results in a large unidirectional irreversible expansion of up to hundreds of times along the *c*-axis of initial graphite flakes. The resultant material is puffed-up with a low density and high temperature resistance (Wei *et al*, 2011; Chung, 1987; Chung, 2002). EG is a promising material which is being used in the production of flexible sheets, gaskets, seals, thermal insulators and fire-retardant composites, and it also exhibits excellent adsorption for spilled oil in water (Wei *et al*, 2011; Inagaki *et al*, 2004).

2.3.2. Methods

There are different methods of expansion. True expansion occurs at elevated temperatures, therefore internal or external heating is required for true expansion to occur. The most conventional external heating source is a flame in a furnace. The flame provides rapid heating with flame temperatures as high as 1200 ºC, but as low as 700 ºC. Expansion is negligible when particles are too small (the minimum particle size is 75 µm) or when the *c*-axis stack (l_c) is between 20 nm – 75 nm. As the particle size of graphite and the volatility of the intercalant are increased, the expansion volume is increased. Internal heating is achieved by passing an electrical current through the intercalated graphite. Recently heating methods involving infrared, microwave and laser have been employed. Microwave irradiation is very promising as it can be executed in a short period of time and at room temperature, consuming less energy (Chung, 1987; Kang *et al*, 2002).

2.3.3. Properties

Expanded graphite attained from acceptor-type and donor-type GICs have different morphologies. Expansion of acceptor-type GICs present large balloons with worm-like particles through the original graphite flakes, as opposed to the expansion of donor-type GICs which leads to small balloons with very small graphite layers. Usually expanded graphite was characterised mostly by expansion volume or bulk density. More detailed and quantitative characterisation of the pore structure of expanded graphite is required. Currently, no relation between pore structure and preparation conditions was found. An electrochemical method is able to both quantitatively characterise and control the intercalation process (Kang *et al*, 2002).

Expanded graphite is mechanically weak. The transport properties, such as the electrical resistivity and the thermal conductivity are enhanced when expanding. The *a*-axis electrical resistivity is increased by expansion, but expansion decreases the electrical resistivity along the *c*-axis, due to the bending of the graphite layers, therefore *c*-axis conduction path. Expansion decreases the *c*-axis thermal conductivity due to the decrease in density. The *a*-axis thermal conductivity is also decreased with expansion because of the bending of the graphite layers and the increased photon-photon scattering. Since the thermal conductivity along both the *a*-axis and the *c*-axis is decreased by expansion, expanded graphite is a beneficial thermal insulator material (Chung, 1987).

2.4. Sonication

Sonication is the act of applying sound energy to disturb particles in a sample. This process is also known as ultra-sonication due to ultrasonic frequencies (>20 kHz) usually utilised. This is done by using various instruments, including a sonication horn or a sonication bath. Sonication is used to exfoliate, or break down the expanded graphite to yield graphene sheets, or few-layered graphite sheets. This is to expose the extra surface within the flakes in order to examine the surface. These samples are known as exfoliated graphite.

2.5. Characterisation

GICs are very sophisticated material. GICs are three-dimensional and are solid-state material. They have different stages of intercalation and expansion paths, as well as different sizes of intercalation areas. The host material, which is the graphite, can comprise various defects, and the guest species, which is the intercalant, may be ionic, solvated ionic or complex ionic species. This makes the characterising of GICs daunting (Noel & Santhanam, 1998).

A number of techniques are exploited for the characterisation of GICs, which includes visual inspection, weight uptake and weight loss, chemical analyses, *c*-axis expansion, diffraction measurements and electron microscopy. Visual inspection provides information on the sample colour, and the colour gives qualitative information on the staging index (for a stage 1 alkali metal compounds a yellow, gold or red colour is observed, for a stage 2 compound, a steel blue, and for a stage 3 compound a dark blue colour is witnessed and a graphite-metallic colour for higher stages, among other examples). By observing the *c*-axis expansion under a travelling microscope, one can assume qualitative information on staging. Direct chemical analyses provide the chemical formula for the GIC. If the chemical formula is known, and the stoichiometry is assumed, the weight uptake can give information on the sample stage. All of the above gives qualitative information because of the inhomogeneities, vacancies, microcracks, defects among others (Dresselhaus, MS & Dresselhaus, G, 2002).

Diffraction studies such as X-ray diffraction (XRD) are employed to determine the staging index and give information on the stage fidelity, repeat distance (I_c), and to provide information on in-plane order and to characterise the host lattice and the GICs produced from these host lattices (Dresselhaus, MS & Dresselhaus, G, 2002; Noel & Santhanam, 1998; Zhao *et al*, 2011).

There is a wide variety of spectroscopic techniques for compositional analysis. X-ray fluorescence spectroscopy (XRF) is a very suitable technique for the analysis of bulk samples such as GICs.

Thermomechanical analysis (TMA) is employed to determine the thermal expansion of GICs, whereas Thermogravimetric analysis (TGA) is used to determine the mass loss of a GIC as a function of increasing temperature, where the mass loss suggests evaporation or even decomposition of the sample. The sample displays thermal stability at the temperature region where no mass loss is observed (Shornikova *et al*, 2006). TGA also quantifies the oxidation rate which can be used to determine the extent of damage on the sample, as the faster the oxidation occurs, the more damaged the sample is.

Irreversible surface transformations such as intercalated stages, surface expansion among others can be scrutinised by applying microscopic techniques. By using a scanning electron microscope (SEM) it is possible to analyse the micro- and surface structure of GICs and can also provide evidence of microcracks formation due to intercalation to analyse the extent of damage to the surface of the graphite. RAMAN Spectroscopy is also used to monitor intercalation and adsorption of intercalant. The RAMAN spectrum consists of a set of distinct peaks. It allows monitoring of intercalation, defects, disorder, chemical modifications, edges, strain and relative orientation of graphene layers. Each peak is characterised by position, width, height and area. The position of the G-peak, pos(G), is widely used to identify the GIC staging (Zhao *et al*, 2011).

2.6. Methods of Intercalation

2.6.1. Liquid phase intercalation

The Staudenmaier method is the most common method of intercalation. This method uses oxidisers such as fuming nitric acid (HNO_3) and potassium chlorate ($KClO_3$) to oxidise the graphite, and uses a strong acid like sulphuric acid (H_2SO_4) to intercalate. There are many modifications of this method, such as the Brodie method where the ratio of the oxidiser and intercalant is varied. There are two other modified Staudenmaier methods, named the Hofman's method where sodium nitrate ($NaNO_3$) is used as oxidiser instead of nitric acid (HNO_3), and in the Hummers method the potassium chlorate ($KClO_3$) is replaced with potassium permanganate ($KMnO_4$) (Nakajima & Matsuo, 1994).

Nakajima & Matsuo (1994) used the Staudenmaier method. Natural graphite with a flake size of between 250 µm and 830 µm was oxidised using fuming nitric acid (HNO_3), 97 % sulphuric acid (H_2SO_4) and potassium chlorate ($KClO_3$). A 300 mL flask comprising 50 mL H_2SO_4 and 25 mL HNO_3 was cooled to 5 ºC in an ice bath. 2 g of $KClO_3$ per gram of graphite was added to the solution under stirring, after 1 g of graphite was added to the solution. $KClO_3$ was added 8 times, every hour per day for 3 days. This solution was poured into 1 L of water, and immediately filtered with an aspirator and then washed with methanol until a pH value of 5 or more was reached.

2.6.2. Gas phase intercalation

Shornikova *et al* (2006) synthesised binary graphite intercalation compounds (GICs) with $FeCl_3$ by the gas-core method (Herold's method) which allowed them to obtain single phase samples of GICs. A temperature gradient of 300 ºC – 360 ºC was applied for duration of 4 h – 24 h for the $FeCl_3$ in a two-section tube. Stage 1 GIC was obtained with a graphite temperature (T_G) of 310 ºC and a $FeCl_3$ temperature (T_I) of 300 ºC for a reaction time (τ) of 18 h – 25 h and a mass gain, indicating the degree of intercalation (Δm), of between 207 % and 227 % was obtained. With a T_G of 360 ºC and T_I of 300 ºC, a stage 2 GIC was obtained with a τ of 3 h – 25 h and a Δm of between 42 % and 113 % were found. It is clear that the amount of intercalated chlo-

rides (Δm) is directly proportional to the reaction time (increases with an increase in reaction time (τ)). For stages 1 and 2 respectively, $C_{6.0–6.6}FeCl_3$ and $C_{12–32.1}FeCl_3$ were the compositions found, and the average thickness of the intercalated layer (d_i) for the synthesised GIC were 9,40 Å, whereas the measured repeat distances (I_c) were 9,40 Å and 12,76 Å, respectively. The decomposition of binary $FeCl_3$-graphite GIC starts at 310 ºC – 330 ºC as the vaporisation temperature of $FeCl_3$ is at 320 ºC (Shornikova *et al*, 2006).

Hamwi *et al* (1992) used an appropriate stoichiometric mixture of anhydrous iron (III) chloride ($FeCl_3$) and natural graphite for a composition of $C_{16,8}FeCl_3$ (determined by weight-uptake) to prepare the binary $FeCl_3$-GIC in a sealed tube under 1 atm chlorine pressure. A reaction of 1 to 2 weeks with $FeCl_3$ at a temperature of 300 ºC was necessary to prepare this GIC. In order to remove the excess of unreacted $FeCl_3$, the resulting product was washed with pure alcohol and then dried at 110 ºC for several hours. It was established by XRD that the product was a stage 2 $FeCl_3$–GICs, and the values of I_c is 1275 pm and d_i (I_c – 335) is 940 pm (Hamwi *et al*, 1992).

Mitsutani *et al* (1993) prepared stage 4 to stage 6 $FeCl_3$ – GICs by an ordinary two-bulb method from natural graphite flakes and anhydrous $FeCl_3$. The two reagents were loaded into a Pyrex glass reaction tube and sealed under vacuum and placed in a well-controlled two-zone furnace for a reaction time of approximately 20 h. The temperature of $FeCl_3$ (T_I) was held constant through all experiments while the graphite temperature (T_G) was varied. A correlation between the stage number (n = 1 – 6) of the $FeCl_3$ – GICs and the graphite temperature (T_G) was established. The temperature of $FeCl_3$ (T_I) was set at 300 ºC.

The sandwich thickness (d_s) (C/$FeCl_3$/C) of the stage 4 GIC was calculated to be 0,943 nm (c-axis repeat distance I_c = 1.9492 nm), literature reported values of between 0,938 – 0,941 nm (Abe *et al*, 1995; Metz & Hohlwein, 1975). Stage 5 and stage 6 have a c-axis repeat distance (I_c) of 2,280 nm and 2,846 nm respectively and the C/$FeCl_3$/C sandwich thickness of 0,943 nm and 0,941 nm, respectively, which is also in agreement with literature values of 0,938 nm – 0,941 nm (Abe *et al*, 1995; Metz & Hohlwein, 1975).

Abe *et al* (1995) employed the two-bulb method to produce stage 2 and stage 3 $FeCl_3$ – GICs from natural graphite and anhydrous $FeCl_3$. The temperature of the $FeCl_3$ was held constant for both reactions at 300 ºC whereas the temperature of the graphite was set at 405 ºC and 450 ºC for the preparation of stage 2 and stage 3 respectively. The reaction time for the preparation was 24 h. XRD data were collected with CuKα radiation monochromatised by highly oriented pyrolytic graphite (HOPG) and a scintillation counter, with typical working conditions of 35 kV, 20 mA, scanning speed of ⅛ º/min and a time constant of 5 s. The *c*-axis repeat distances I_c of the GICs were 1,277 nm and 1,613 nm for stage 2 and stage 3 respectively. The C/$FeCl_3$/C sandwich thickness, d_s was identified as 0,942 nm, which is in good agreement with literature. The characterisation for the perfection of the stage structure for the stage 2 and stage 3 $FeCl_3$ – GICs was done by comparing the full width at half maximum (FWHM, ΔΘ) of the [001] peaks of the GIC with that of the natural graphite flakes (Abe *et al*, 1995).

Intercalation of $FeCl_3$ was done in the gas phase by Kalucki & Morowski (1987). A mixture of natural graphite and pure anhydrous $FeCl_3$ was dried at 50 ºC under a pressure of about 6 Pa for 2 h. The dried mixture was sealed in a glass tube under a pressure of approximately 6 Pa and heated to a temperature of 300 ºC for a reaction time of 20 h. Different amounts of $FeCl_3$, ranging from 3 % to 70 % by weight, was used in the starting material during the intercalation reactions and the volume of the mixture wasn't allowed to exceed 40 % of the reactor volume. In order to remove the unreacted $FeCl_3$, the material was soaked in an aqueous solution of hydrochloric acid in a ratio of 1:1 for 2 h, filtered, washed with distilled water and then dried at 110 ºC overnight. The products were analysed by XRD and examined at room temperature by [001] reflection with MoKα radiation. The weight % content of $FeCl_3$ in the starting material is directly proportional to the weight % content of $FeCl_3$ in the resulting GIC. The relationship is given in Equation 2-4

$$y = 2{,}5325 + 1{,}288x \qquad (2\text{-}4)$$

with the weight % of $FeCl_3$ in the starting material represented by *y* and in the product represented by *x*. The *c*-axis repeat distance, I_c, was calculated using Equation 2-3, where d_s is 937 pm, C_0 is 335 pm, and *n* is the stage index. The range of stages in the product is related to the amount of intercalant in the starting material, at

a low percentage of $FeCl_3$ a wide range of stages were obtained, a narrow range was observed at a higher percentage of $FeCl_3$. Above a concentration of 60 % of $FeCl_3$ in the GIC, a homogeneous phase of $FeCl_3$ – GIC exists (Kalucki & Morowski, 1987).

The different results are compared in Table 2-1.

Table 2-1: Comparison of gas phase intercalation using different preparation methods.

Reference	T_G (ºC)	T_I (ºC)	τ (h)	I_c (Å)	Composition	Stage, n
Shornikova *et al* (2006)	310	300	18	9,39	$C_{6.6}FeCl_3$	1
Shornikova *et al* (2006)	310	300	22	9,40	$C_{6.1}FeCl_3$	1
Shornikova *et al* (2006)	310	300	25	9,41	$C_{6.0}FeCl_3$	1
Shornikova *et al* (2006)	360	300	3	12,72	$C_{32.1}FeCl_3$	2
Shornikova *et al* (2006)	360	300	6	12,75	$C_{21.2}FeCl_3$	2
Shornikova *et al* (2006)	360	300	18	12,77	$C_{16.2}FeCl_3$	2
Shornikova *et al* (2006)	360	300	25	12,81	$C_{16.2}FeCl_3$	2
Hamwi *et al* (1992)	300	300	1 – 2 weeks	12,75	$C_{16.8}FeCl_3$	2
Mitsutani *et al* (1993)	495 – 500	300	20	19,49		4
Mitsutani *et al* (1993)	516 – 518	300	20	22,80		5
Mitsutani *et al* (1993)	523 – 524	300	20	28,46		6
Abe *et al* (1995)	405	300	24	12,77		2
Abe *et al* (1995)	450	300	24	16,13		3
Kalucki & Morowski (1987)	300	300	20	$I_c = d_s + (n\text{-}1)C_0$ With $C_0 = 3{,}35$ and $d_s = 9{,}37$		

2.6.3. Hydrothermal Intercalation

2.6.3.1. Microwave intercalation

Wei *et al* (2008) employed microwave irradiation for the preparation of expanded graphite, where simultaneous intercalation and expansion occurs. Natural graphite (average flake size of 320 µm), an oxidiser (potassium permanganate ($KMnO_4$)) and an intercalation agent which promotes oxidation (68 % nitric acid (HNO_3)) was merely mixed by a glass bar at different weight ratios in a porcelain dish at room temperatures for 3 minutes before microwave irradiation. After the mixing, the porcelain dish was directly placed into a domestic microwave oven and irradiated at 700 W for a reaction time of approximately 60 s. H_2O_2 and H_2SO_4 were also used as oxidiser and intercalant for the preparation EG by MW irradiation. The expansion volume was determined by measuring the volume of the EG prepared from 0,20 g natural graphite (NG). For comparison, after the mixture of graphite, oxidiser and intercalant were mixed for 3 minutes, it was rapidly heated to 1000 ºC (Wei *et al*, 2008).

According to Wei *et al* (2008) the maximum expanded volume of 312 ml/g obtained from MW irradiation using a mixture ratio of 1:2:1 by weight (NG : HNO_3 : $KMnO_4$). At this ratio, the bulk density was 5,4 x 10^{-3} g/cm^3 which is slightly higher than that of EG prepared by MW irradiation (5,1 x 10^{-3} g/cm^3) by Kwon *et al* (2003), but lower than that prepared commercially by rapid heating accompanied by the reaction in an oxidising agent (between 6 x 10^{-3} g/cm^3 and 10 x 10^{-3} g/cm^3) by Toyoda & Inagaki (2000).

Wei *et al* (2008) stated that for successful intercalation in a short time, the edge of graphite must be oxidised and the graphite must be opened, therefore, a strong oxidiser with high oxidation rate must be used. H_2O_2 has lower oxidation ability than $KMnO_4$, consequently when used has lower expansion. The amount of oxidiser, or oxidiser ability, used in the reaction is proportional to the amount of volume expansion of the EG. As the amount of $KMnO_4$ was increased, the expanded volume was increased. If an excess of oxidiser was charged, the strong oxidiser damaged the structure of the graphite layers, and resulted in a decrease in the expanded volume (Wei *et al*, 2008).

HNO_3 functions as an intercalant and provides acidity which promotes the oxidation ability of $KMnO_4$. More HNO_3 was intercalated when the amount of HNO_3 was increased and consequently resulted in higher expansions. Once again, redundant amounts of HNO_3 lead to excessive oxidation of graphite, and therefore decreasing expansion. MW irradiation is promoted by the comparison of volume expansion by rapid heating (160 ml/g) and that of MW irradiation (275 ml/g). The samples were further investigated by XRD with CuKα radiation. The XRD data is well explained by stage theory, where the basal spacing (I_c) is calculated by Bragg's equation and Equation 3, with $n = 3$ and $d_s = 7{,}48$ Å, I_c is calculated to be 14,18 Å (Wei *et al*, 2008).

2.6.3.2. Intercalation using a non-metal oxidiser

Zhu *et al* (2003) mixed natural graphite flakes of average size of 150 µm with concentrated H_2SO_4 (90%), H_2O_2 (30%), $CuCl_2$ and $FeCl_3$-$6H_2O$ in predetermined ratios. Zhu *et al* (2003) placed the mixture into a Teflon-lined hydrothermal autoclave with a capacity of 100 mL, and then placed in an oven. The temperature was held constant at values between 70 ºC and 180 ºC for a reaction time of between 4 h and 15 h and then cooled to room temperature. The material was washed with distilled water and filtered until a pH of 7 was reached, and then dried at 60 ºC. Characterisation was done by XRD using CuKα radiation (λ = 0,154178 nm). It was confirmed that the temperature, reaction time, ratio of starting material and the amount of oxidiser affected the end group. The optimum ratio by weight of $CuCl_2$/$FeCl_3$/H_2SO_4/graphite was 0,1 : 1,0 : 9,8 : 1,0. Without an oxidiser, no intercalation took place; therefore, the use of an oxidiser was found to be crucial. H_2O_2 as the oxidiser was essential because it reacted with H_2SO_4 to produce OH-OSO_3H and water. This encouraged the intercalation reaction. The optimum reaction time and temperature attained was 12 h and 120 ºC. The results are tabulated in Table 2-2.

The distance between adjacent carbon atoms in the *c*-direction (C_0) is 3,35 Å (335 pm) and the distances of intercalant (d_i) $FeCl_3$ and H_2SO_4 were 6,10 Å and 3,658 Å respectively and therefore, the Graphite/$FeCl_3$/Graphite and Graphite/H_2SO_4/Graphite sandwich distances (d_s) were 9,45 Å and 7,008 Å respectively (Zhu *et al*, 2003).

Table 2-2: Comparative experimental conditions from Zhu *et al* (2003).

$CuCl_2/FeCl_3/H_2SO_4$/NG Weight ratio	Oxidiser	T (ºC)	τ (h)	Stage of Products
0,1 : 1,0 : 9,8 : 1,0	None	120	12	No reaction
0,1 : 1,0 : 9,8 : 1,0	H_2O_2	70	15	Small amount of stage 4
0,1 : 1,0 : 9,8 : 1,0	H_2O_2	120	12	Small amount of stage 4
0,1 : 1,0 : 9,8 : 1,0	H_2O_2	120	4	Small amount of stage 4
0,1 : 1,0 : 9,8 : 1,0	H_2O_2	120	4	Small amount of stage 4
1,0 : 1,0 : 9,8 : 1,0	H_2O_2	120	4	Only Stage 4
0,1 : 0,0 : 9,8 : 1,0	H_2O_2	180	12	Small amount of stage 4

2.6.4. Electrochemical Intercalation

Kang *et al* (2002) utilised electrochemical intercalation. 600 g of NG with an average flake size of 300 µm was sealed off in a net polypropylene bag, and then immersed the bag in 93 wt. % H_2SO_4. A 40 x 50 cm^2 stainless steel plate, to act as an anode, was inserted in the middle of the bag. Two additional stainless steel plates with the same size were introduced on both sides of the bag, which acted as cathodes. Figure 2-5 illustrates the experimental set-up for the electrochemical synthesis of H_2SO_4 – GICs (Kang *et al*, 2002).

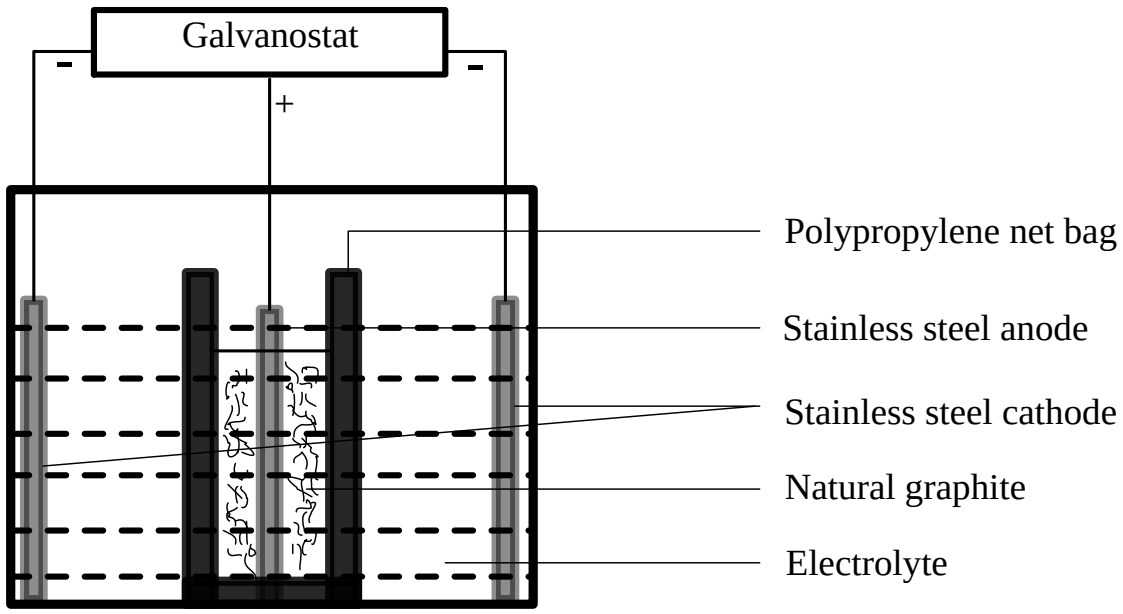

Figure 2-5: Schematic diagram of Experimental set-up for electrochemical synthesis of GIC.

The anodes and the cathode were kept parallel to ensure a uniform reaction during electrochemical intercalation. The distance between the cathode and anode was 5 cm. The electricity consumption for electrolysis was varied to control the quantity of intercalants in the resultant GIC, using a galvanostat.

The different electricity consumptions at which the GICs were prepared were 10,83 A.h/kg, 18,67 A.h/kg, 20,41 A.h/kg, 33,33 A.h/kg and 40,00 A.h/kg. The GICs were rinsed with water until the pH reached a value of between 4 and 5, and then dried at 110 ºC for 2 h. The residual compounds were rapidly heated in a muffle furnace to produce EG. Expansion of the expandable graphite prepared with different electricity consumption was achieved at a constant temperature of 1000 ºC, and expansion at temperatures of 1000 ºC, 800 ºC, 600 ºC, 400 ºC, 300 ºC and 200 ºC with expandable graphite prepared at electricity consumption of 33,33 A.h/kg. Kang *et al* (2002) concluded that expansion volume, pore volume and specific surface area at 1000 ºC were increased with increasing electricity consumption.

Shornikova, *et* al (2006) employed electrochemical graphite oxidation to obtain co-intercalation GIC of $FeCl_3$ and CH_3COOH (acetic acid). This was achieved under galvanostatic mode (I = 0,5 mA) in a three electrode cell. The graphite underwent electrochemical treatment in a mixed electrolyte of $FeCl_3$ and CH_3COOH. In order to increase the electrolyte electrical conductivity, HCl was added. Intercalation was characterised by smooth charging curves, a plateau at $E_{Ag/AgCl}$ = 1,96 V was achieved. By means of XRD it was established that a mixture of stage 3 and stage 5 GICs was first achieved after which the mixture gradually transits into stage 3 single phase ternary GIC (TGIC) with I_c = 16,18 Å (d_s = 9,48 Å) and the overweight (Δm) of stage 3 being 65 %.

There were no direct evidence with XRD that CH_3COOH was co-intercalated, because of the geometrical size difference between CH_3COOH and $FeCl_3$ molecules. Radiotracer analysis was used to confirm the presence of CH_3COOH. In this case acetic acid [1 – ^{14}C]CH_3COOH marked by isotope ^{14}C was used as a radiotracer. Accumulation of the acetic acid on the defects and the borders of the graphite samples, due to sorption, was observed without electrochemical treatment using autora-

diography, but the autoradiogram of the stage 3 TGIC with $FeCl_3$ – CH_3COOH, which were synthesised by electrochemical treatment and after galvanostatic oxidation (Q = 600 A s/g), clearly showed that the acetic acid was homogeneously distributed through the entire sample volume. Therefore, Shornikova, *et* al (2006) confirmed the co-intercalation of $FeCl_3$ and CH_3COOH, and homogeneous distribution of the weak intercalant (CH_3COOH).

Shornikova, *et* al (2006) characterised the samples using and it was concluded that a number of mass losses were observed and that it could be divided into different temperature ranges. The first mass loss deals with the decomposition and de-intercalation of the solvent molecule whereas the second mass loss is thought of as de-intercalation and partial $FeCl_3$ oxidation. The last mass loss agrees with the evolution of iron compounds which contains oxygen. The presence of $FeCl_3$ and CH_3COOH in the intercalated layer is also confirmed from the thermal analysis (Shornikova, *et* al, 2006).

2.6.5. Ternary Intercalation

Hamwi *et al* (1992) states the intercalation of a second intercalant into a stage-2 binary GIC generally occurs with a 3-step process, shown in Figure 2-6.

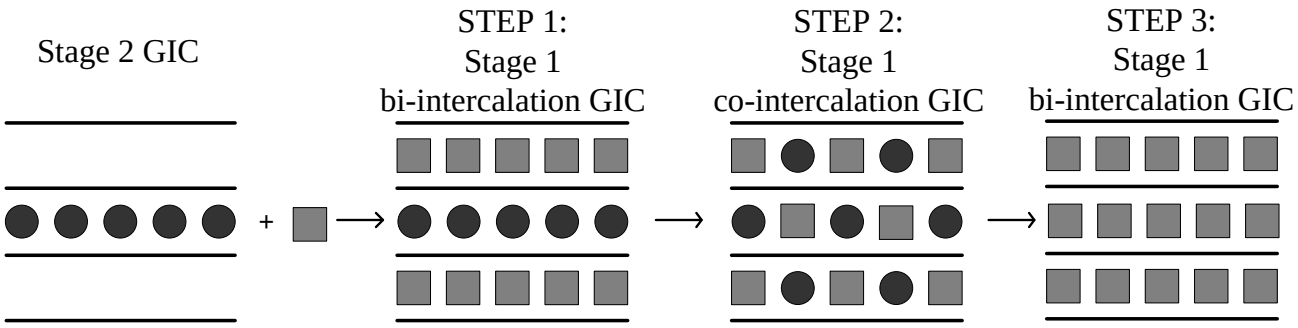

Figure 2-6: Process of intercalation of a second intercalant.

The reaction stabilises at one of the 3 steps, depending on the physical and chemical characteristics of the 2 intercalants. The expected stabilisation of a compound depends on the ability of the intercalant to diffuse between the graphite layers (Hamwi *et al*, 1992).

In the preparation of $FeCl_3$ – H_2SO_4 bi-intercalation compounds, Mitsutani *et al* (1993) poured several H_2SO_4 drops onto binary $FeCl_3$ – GICs which were mounted on the glass holder of the X-Ray diffractometer at room temperature. The excess H_2SO_4 was wiped off using glass wool filter paper, after a few minutes.

XRD data were collected with monochromatic CuKα radiation by highly oriented pyrolytic graphite (HOPG) and recorder on a computer, with typical working conditions of 32 kV, 15 mA, scanning speed of scintillation detector of 2º/min and a time constant of 0,5 s. This procedure was repeated until H_2SO_4 were fully intercalated into all the vacant interlayer spaces of the $FeCl_3$ – GICs (Mitsutani *et al*, 1993).

Mitsutani *et al* (1993) found that the *c*-axis repeat distance varied for a stage 4 GIC from 23,8 Å, which was used to establish that one of the three vacant interlayer spaces were occupied by H_2SO_4, to 33,80 Å which meant that three layers of H_2SO_4 were occupied in the GBC. With the stage 5 GIC as starting material, the two values of I_c were found to be 27,2 Å and 31,5 Å and their number of H_2SO_4 layers were determined to be one and two. When H_2SO_4 was fully intercalated (no vacant layers) I_c = 40,9 Å. For the stage 6 GIC, I_c were found to be 31,1 Å, 3,50 nm, 39,7 Å and 48,1 Å and their number of H_2SO_4 layers were found to be one, two, three and five. One vacant interlayer space could not be found in the bi-intercalation process of H_2SO_4 into stage 4 – 6 $FeCl_3$ – GICs as starting material (Mitsutani *et al,* 1993). Figure 2-7 illustrates a schematic of the bi-intercalation process of H_2SO_4 into stages 4 – 6 $FeCl_3$ – GIC.

Shornikova *et al* (2006) stated that the synthesis of TGICs with either two acids or an acid and an organic salt can be achieved by chemical and electrochemical methods. In order to obtain a TGIC, a binary GIC must be produced and be of stage ≥ 2 and then intercalated by a second intercalant, this method is used to synthesise a bi-intercalation GIC.

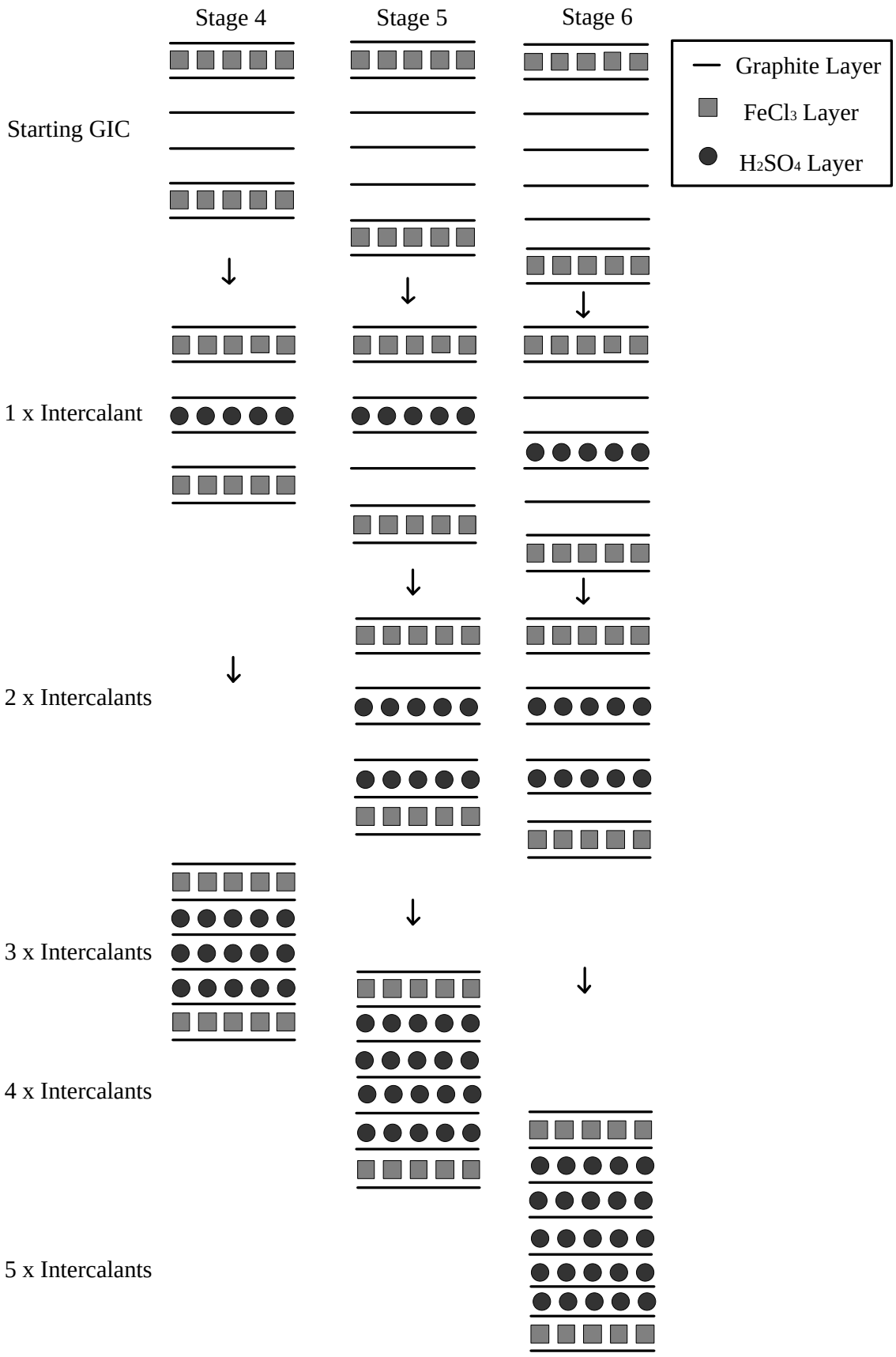

Figure 2-7: The bi-intercalation process of H_2SO_4 into stages 4 – 6 $FeCl_3$ – GIC.

A second method entails the intercalation of graphite with a mixture of two intercalants, and the third method is an incomplete change reaction between the binary GIC and a pure second intercalant. The last two methods are used to obtain co-intercalation GICs. Acids possess different acidities and therefore have different intercalation abilities. In the production of a new TGIC, interesting new properties can be expected (Shornikova *et al*, 2006).

3. Experimental

Three methods of intercalation were investigated and compared: liquid phase (Hummers method), gas phase and electrochemical. These three intercalation techniques are described in detail below.

3.1 Liquid phase intercalation – Hummers Method

The method used to prepare the liquid phase intercalation compounds was modified from the method used by Nakajima & Matsuo, 1994.

Chemicals

High purity big graphite flakes (RFL 99.5 O), with a particle size of min. 90 % > 160 µm, supplied from Graphit Kropfmühl AG and potassium permanganate, sulphuric acid (95 % – 99 %), nitric acid (65 %) and distilled water supplied by Merck Chemical (Pty) Ltd were used.

Apparatus

A mechanical stirrer and heater as well as a laboratory scale were utilised in the liquid phase intercalation. A Büchner funnel, filter flask and filter paper were used for washing and filtering of samples. A convection oven was used for drying of the samples.

Experimental design

The mass of graphite and of potassium permanganate were fixed for all of the experiments at 15 g and 3 g respectively. The independent variables were chosen to be the ratio of nitric acid to sulphuric acid, as well as the volume of each, the reaction temperature and the reaction time. These variables were chosen as independent to obtain a broad range of conditions that will affect intercalation for comparison purposes. The dependent variables were the volume expansion and the damage incurred onto the microstructure and surface of the graphite. The conditions at which the experiments were performed are summarised in Table 3-1. The conditions in Experiment 1 were chosen as basis.

Table 3-1: The conditions at which the experiments were performed.

Sample	Graphite (g)	$KMnO_4$ (g)	HNO_3 (ml)	H_2SO_4 (ml)	Temp (˚C)	Duration (min)
1	15	3	15	45	Ambient	5
2	15	3	30	90	Ambient	5
3	15	3	15	90	Ambient	5
4	15	3	15	45	50	5
5	15	3	15	45	Ambient	60

Method

The graphite and potassium permanganate was added in a beaker. First the nitric acid and then the sulphuric acid was added under continued mechanical stirring for 10 minutes at the reaction temperature. The mixture was removed from the stirrer and remained for the selected duration and then soaked in distilled water for 2 hours. The soaked mixture was washed and filter with distilled water to neutrality. The mixture was dried in a convection oven at 50 ˚C for 2 days.

3.2 Gas phase intercalation

The method used to prepare the gas phase intercalation compounds was adapted from the method used by Kalucki & Morowski, 1987.

Chemicals

High purity big graphite flakes (RFL 99.5 O), with a particle size of min. 90 % > 160 µm, supplied from Graphit Kropfmühl AG and anhydrous iron (III) chloride, hydrochloric acid (32 %) and distilled water supplied by Merck Chemical (Pty) Ltd were used.

Apparatus

A sealed aluminium cylinder was employed as a pressure vessel. High temperature resistant silicon was used as sealant. Laboratory scales, Büchner funnel, filter flask and filter paper were used. A thermopower furnace was used for the reaction, and a convection oven was used for drying of the samples.

Experimental design

The mass of graphite is fixed for all experiments at 3 g. The independent variables were chosen to be temperature, mass ratio and reaction time. This was chosen to obtain a broad range of conditions that will affect intercalation for comparative purposes. The values of the independent variables are summarised in Table 3-2.

Table 3-2: The values selected for the independent variables.

Variable	Values
Mass ratio of graphite to iron (III) chloride	2:1, 1:1, 1:2
Temperature	300˚C, 350˚C, 400˚C
Reaction time/duration	16h, 20h, 25h

The dependent variables were chosen to be the volume expansion and the damage incurred onto the microstructure and surface of the graphite.

Method

The intercalation reaction was carried out with different amounts iron (III) chloride in the starting material, with a fixed amount of 3 g of graphite. The graphite and anhydrous iron (III) chloride was mixed in an aluminium cylinder. The mixture was dried at 50 ˚C for 2 h in a convection oven. After the cylinder was perfectly sealed with high temperature silicon it was heated to the reaction temperature for the reaction time in the furnace. In order to remove the excess iron (III) chloride, the mixture was soaked in hydrochloric acid for 2 h and then filtered and washed with distilled water. Finally the sample was dried at 110 ˚C overnight.

3.3 Electrochemical intercalation

The method used to prepare the liquid phase intercalation compounds was adapted from the method used by Kang *et al*, 2002.

Chemicals

High purity big graphite flakes (RFL 99.5 O), with a particle size of min. 90 % > 160 µm, supplied from Graphit Kropfmühl AG, sulphuric acid (95 % – 99 %) and distilled water supplied by Merck Chemical (Pty) Ltd was used.

Apparatus

The electrochemical cell comprised a plastic bottle, stainless steel electrodes and a porous material bag, a galvanostat was also used and the electrolyte was sulphuric acid. The set-up of the cell is illustrated in Figure 3-1.

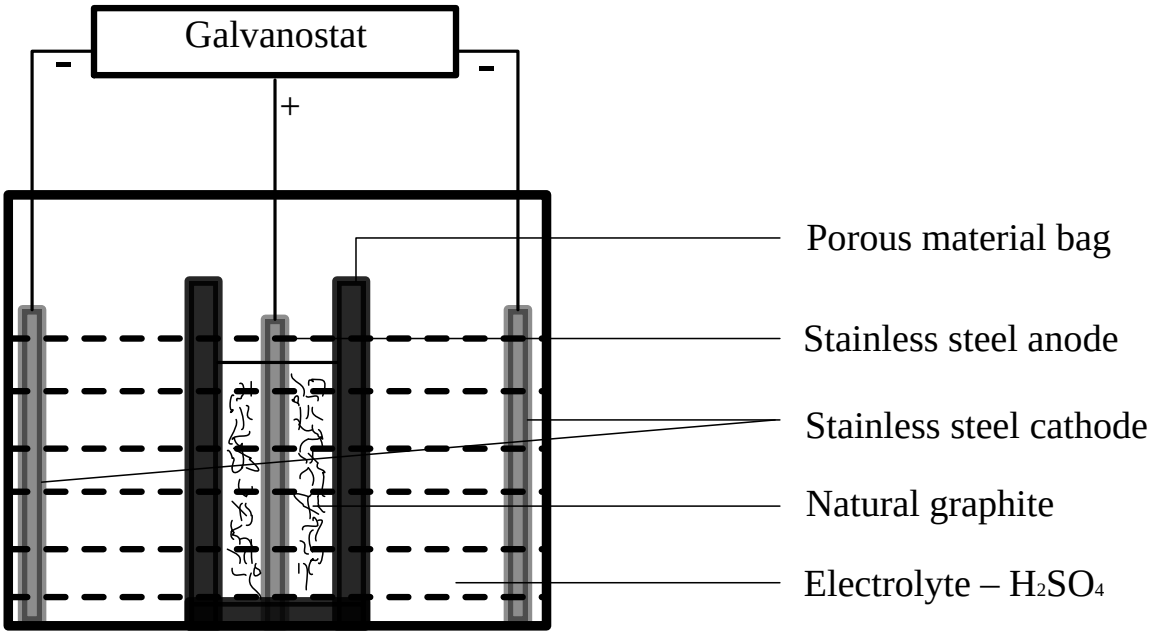

Figure 3-1: A schematic illustration of the experimental set-up for the electrochemical intercalation method.

A Büchner funnel, filter flask and filter paper were used for washing and filtering of samples. A convection oven was used for drying of the samples.

Method

For the intercalation the porous material bag was filled with graphite flakes. The stainless steel electrode was inserted in the middle of the bag to act as an anode. The other stainless steel electrodes with the same size were placed parallel on both sides of the bag. The cell was assembled and filled with the electrolyte. The electricity consumption was constant at 10 W (2,5 A and 4 V). After the reaction was left overnight, the GIC was filtered and washed to neutrality and then dried overnight at 50 ˚C. Only one sample of the electrochemical method was prepared, because the objective was to prove whether electrochemical intercalation was possible. Once this was achieved, the electrical consumption was kept constant for repeatability.

3.4 Expansion and Sonication

Microwave irradiation was employed as the main expansion method. All the samples produced from each intercalation method were expanded in the microwave for 2 minutes. The percentage volume increase of each sample was calculated manually using Equation 3-1.

$$\% V = \frac{V_{Final}}{V_{Initial}} \times 100 \qquad (3\text{-}1)$$

Once the volume expansion of each sample was calculated for all the different intercalation methods, two samples of the Hummers and gas phase methods, the best and worst samples, as well as the electrochemical intercalation sample were chosen for comparative purposes for characterisation.

These 5 samples were sonicated in order to view the surface of the samples. 300 mg of each sample was submerged in 100 ml of propan-2-ol. Under constant mechanical stirring, the samples were sonicated for 10 minutes and left overnight to settle out. The propan-2-ol is evaporated by employing a Büchi Rotavap R-114 with a Büchi Waterbath B-480 and then dried at 90 ˚C overnight.

The 5 exfoliated samples were purified in a graphitising furnace for 6 hours at a temperature of 2750 ˚C in Instrument grade Helium.

3.5 Characterisation

The intercalated samples (GICs), expanded, exfoliated and purified samples were chosen for analyses by different characterisation techniques.

3.5.1. Thermogravimetry (TGA)

Thermogravimetric analysis (TGA) was performed using a TAinstruments SDT Q600 V20.9 Build 20 DSC-TGA instrument. Alumina pans were used for the mass loss analysis and oxidation data. Platinum pans were employed to partially oxidise the samples. Temperature was scanned from 25 ˚C to 800 ˚C at a scan rate of 10 ˚C/min with N_2 gas flowing at a rate of 150 mL/min for the mass loss data. For the oxidation data, the temperature was scanned from 25 ˚C to 400 ˚C at a scan rate of 15 ˚C/min, and then to 1000 ˚C at a scan rate of 5 ˚C/min with O_2 gas flowing at a rate of 150 mL/min for the mass loss data. To partially oxidise the samples, the method for oxidation was used, until a 5 % and 30 % mass loss was visible.

3.5.2. Thermomechanical analysis (TMA)

Thermal expansion measurements were conducted on a TAinstruments TMA Q400 V22.2 Build 28 Thermo Mechanical Analyser. The GIC flakes were placed in a platinum pan just to cover the base of the pan. The flake expansion behaviour was measured with a flat-tipped standard expansion probe using an applied force of 0.2 N. The temperature was scanned from 25 ˚C to 600 ˚C at a scan rate of 10◦C/min in N_2 atmosphere.

3.5.3. X-ray diffraction (XRD)

XRD diffraction patterns were recorded using a Bruker D8 Advance powder diffractometer fitted with a Lynx eye detector. The samples were measured in KαCo-radiation and KαCu-radiation with λ_{Co} = 0,17903 nm and λ_{Cu} = 0,15418 nm. Measurements were performed in the 2θ range 10 º–100 º ◦with a 0.04◦step size and a counting time of 0.2 s. The interlayer spacing, d_{002}, was calculated using Bragg's law illustrated in Equation 3-2.

$$d = \frac{n\lambda}{2\sin\theta} \qquad (3\text{-}2)$$

3.5.4. X-ray fluorescence (XRF)

The samples were roasted at 1000 ˚C to determine the Loss On Ignition (LOI). Varying weights of the roaster samples (<0,1 g) was placed together with 6 g of $Li_2B_4O_7$ into a Pt/Au crucible and fused. The ARL Perform'X Sequential XRF was used for the analyses. Analyses were executed using the Quantas software. This software analyse all elements in the periodic table between NA and U, but only elements above the detection limits were reported. The results were also monitored and filtered to eliminate the presence of the flux, wetting and oxidising agent elements.

3.5.5. Raman spectroscopy

The Raman spectra were recorded with a T64000 series II triplespectrometer system from HORIBA Scientific, Jobin Yvon Technology using the 514.3 nm laser line of a coherent Innova®70 Ar+ laser with a resolution of 2 cm^{-1} in the range 1200 cm^{-1} – 1700 cm^{-1}. The samples were recorded in a backscattering configuration with an Olympus microscope attached to the instrument (using a LD50x objective). The laser power was set at of 6 mW and a nitrogen-cooled CCD detector was used. The accumulation time was 120 s and the spectra were baseline corrected with using LabSpec soft-ware.

3.5.6. Scanning electron microscopy (SEM)

An ultrahigh resolution field emission scanning electron microscope (HR FEGSEM Zeiss Ultra Plus 55) was used to study graphite morphologies, with an InLens detector at an acceleration voltage of 1 kV to ensure maximum resolution of surface detail. No electrically-conductive coating was applied to the graphite particles.

4. Results and Discussion

4.1 XRF

The XRF data for the intercalated and expanded samples of the different intercalation techniques (only the best of the gas phase and Hummers samples) is reported in Table 4-1.

Table 4-1: XRF results with composition indicated as wt.%.

	Electrochemical		**Gas Phase**		**Hummers**	
	Expanded	Intercalated	Expanded	Intercalated	Expanded	Intercalated
Si	0,09	0,07	0,41	0,08	0,94	0,15
Al	*<0,01*	*<0,01*	1,05	0,65	*<0,01*	0,04
Fe	0,48	0,25	7,69	8,50	0,05	0,02
Mn	*<0,01*	0,03	*<0,01*	0,10	1,07	1,96
Ca	*<0,01*	*<0,01*	*<0,01*	*<0,01*	*<0,01*	*<0,01*
Cr	0,21	0,12	0,12	*<0,01*	0,02	*<0,01*
Ni	0,21	0,12	0,22	*<0,01*	0,06	*<0,01*
S	*<0,01*	0,01	*<0,01*	*<0,01*	*<0,01*	0,11
LOI	**97,20**	**98,50**	**71,80**	**72,80**	**96,10**	**96,60**

The significance of the italic values were below the detection limits of the instrument.

From Table 4-1 it is evident that the gas phase samples, both intercalated and expanded, contain considerable amounts of iron, suggesting that these samples have “un-intercalated” or residual iron chloride. No chloride is detected due to the roasting of the samples. The oxidiser, potassium permanganate, used in the Hummers intercalation method is evident by the manganese found in both the intercalated and expanded Hummers samples. Once the intercalated Hummers sample is expanded, the manganese content is almost halved. The LOI is an indication of the carbon content in the samples, and that of the electrochemical and Hummers samples is extremely high of >97 % and >96 % respectively.

4.2 Manual expansion (Microwave irradiation)

After microwave expansion of each sample for 2 minutes, the volume expansion was calculated manually. Table 4-2 illustrates the volume increase for the Hummers method, as well as the corresponding conditions.

Table 4-2: Volume expansion obtained for the Hummers intercalation method.

Method	Sample Number	**% Volume increase**	HNO_3 (ml)	H_2SO_4 (ml)	Temp (˚C)	Duration (min)
Hummers Method	1	**775**	15	45	Ambient	5
	2	**1050**	30	90	Ambient	5
	3	**825**	15	90	Ambient	5
	4	**1025**	15	45	50	5
	5	**1075**	15	45	Ambient	60

As can be seen from Table 4-2 the baseline (sample 1) produced the lowest outcome. The best outcome was achieved by only increasing the reaction duration. This parameter certainly has a profound effect on the intercalation. Also by increasing the amount of oxidiser (HNO_3) and intercalant (H_2SO_4), but maintaining the ratio, or increasing the reaction temperature, increased the intercalation significantly. Samples 1 and 5 were chosen for further analysis.

The volume expansion after microwave expansion for the gas phase intercalation at the different conditions is summarised in Table 4-3. With a ratio of graphite to iron (III) chloride of 1:2 at 300 ˚C, the reaction vessel had so much pressure build-up that the vessel nearly cracked, therefore this ratio was not tested at higher temperatures.

It is clear from Table 4-3 that at 300 ˚C and 350 ˚C with a ratio of 2:1 there was not enough pressure build-up for a reaction to take place. Also at 400 ˚C with a ratio of 2:1 and a reaction time of 16 h, intercalation was not achieved, because of a lack of pressure.

Table 4-3: Volume expansion obtained for the gas phase intercalation method at the different conditions.

Temperature (˚C)	Time (h)			Ratio (Graphite : Iron(III)Chloride)
	16	20	25	
300	failed	failed	failed	2:1
	900	1100	850	1:1
	950	500	**1450**	1:2
350	failed	failed	failed	2:1
	850	200	1100	1:1
400	failed	200	400	2:1
	150	900	**200**	1:1

The most promising parameter for the gas phase intercalation is at a temperature of 300 ˚C, a reaction time of 25 h and a ratio of 1:2. The worst conditions for gas phase intercalation is at a temperature of 400 ˚C, a reaction time of 16 h and a ratio of 1:1. The 2 samples chosen for analysis are the samples which achieved the best and second worst intercalation (In bold in Table 4-3). The latter was chosen because a volume expansion of 150 % is too small for proper analysis.

The electrochemical intercalation method achieved a volume expansion of 1500 %. Using microwave expansion, this method is the most promising intercalation method. This sample is also chosen for further analysis for comparison purposes.

4.3 TMA

Thermomechanical Analysis (TMA) was employed to determine the onset expansion temperature, expansion rate and maximum expansion of all the chosen samples.

The mass of the samples to be analysed was kept at approximately 7 mg. Nitrogen gas was chosen for the atmosphere for analyses due to its inertness, with a mass flowrate of 50 ml/min. An initial force of 0,02 N was applied to the sample, where a

force of 0,2 N was applied on the sample throughout the analysis. The method employed was a ramp of 10 ˚C/min up to 600 ˚C. Each sample was analysed three times in order to provide a good average, summarised in Table 4-4.

Table 4-4: The average of the onset expansion temperature, expansion rate and maximum expansion of all samples.

Intercalation Method	Sample	Onset Expansion Temperature (˚C)	Expansion rate (%/˚C)	Maximum Expansion (%)
Hummers	Best	250	2,0	217
Hummers	Worst	253	1,7	158
Gas phase	Best	189	0,8	243
Gas phase	Worst	300	0,7	114
Electrochemical		258	2,1	227

The gas phase intercalation method produced the highest maximum expansion of 243 % using the TMA. The expansion method using TMA is different from that of microwave expansion, as microwave expansion employs a rapid, intense heating, whereas the TMA uses slow heating, so the result found here will be different from that of the manual expansion achieved by microwave expansion (concluded that the electrochemical intercalation method produced the highest maximum expansion). Using the TMA, the electrochemical intercalation delivered the second highest maximum expansion of 227%, but the highest expansion rate of 2,1 %/˚C, whereas the Hummers intercalation has the second highest rate of 2,0 %/˚C. The gas phase intercalation has the slowest expansion rate, but exfoliates the most. It also has the lowest onset expansion temperature of only 189˚C, which means that it starts expanding first.

One TMA expansion graph of each method is depicted in Figure 4-1. Viewing the gas phase intercalation graphs (B and D), one can note 2 distinctive expansion rates, which is different from that of the other two methods which only has one general expansion rate. In Table 4-3 only the top expansion rate was taken into account

for calculating the average, because that seems to be the main expansion rate that influenced the expansion of the gas phase intercalation method.

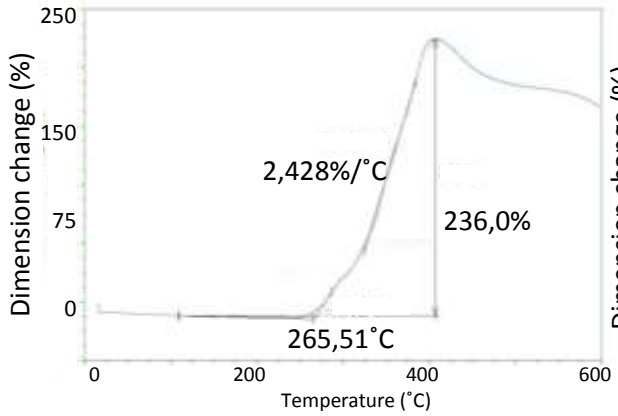

A. Electrochemical

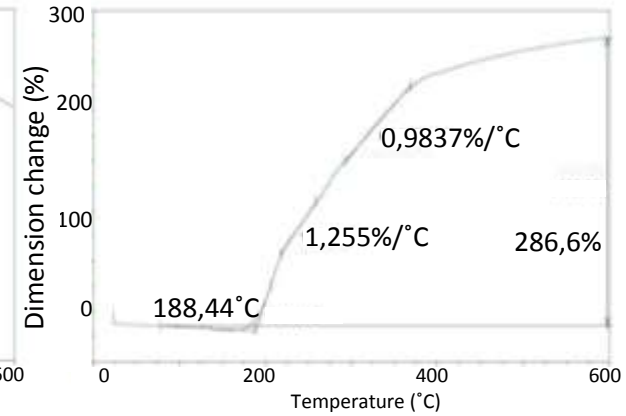

B. Gas Phase (Best)

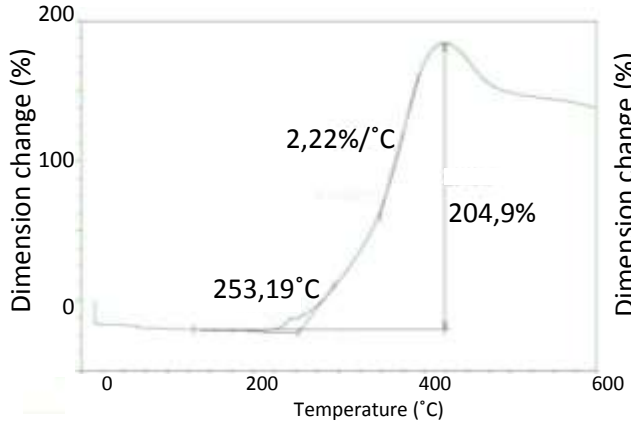

C. Hummers Intercalation (Best)

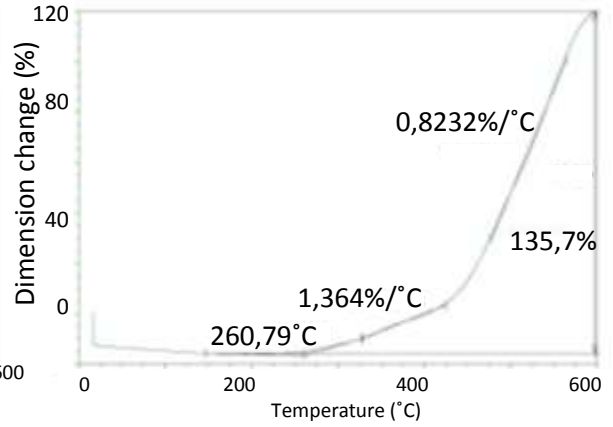

D. Gas Phase (Worst)

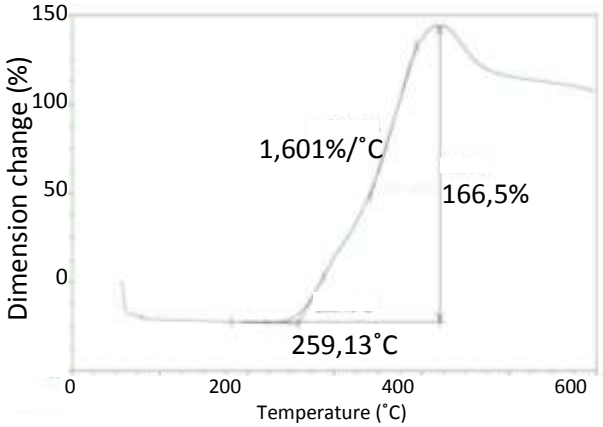

E. Hummers Intercalation (Worst)

Figure 4-1: Thermomechanical analysis graphs of all the chosen samples showing the onset expansion temperature, maximum expansion and expansion rate.

For comparative purposes, Figure 4-2 illustrates the average expansion of each method.

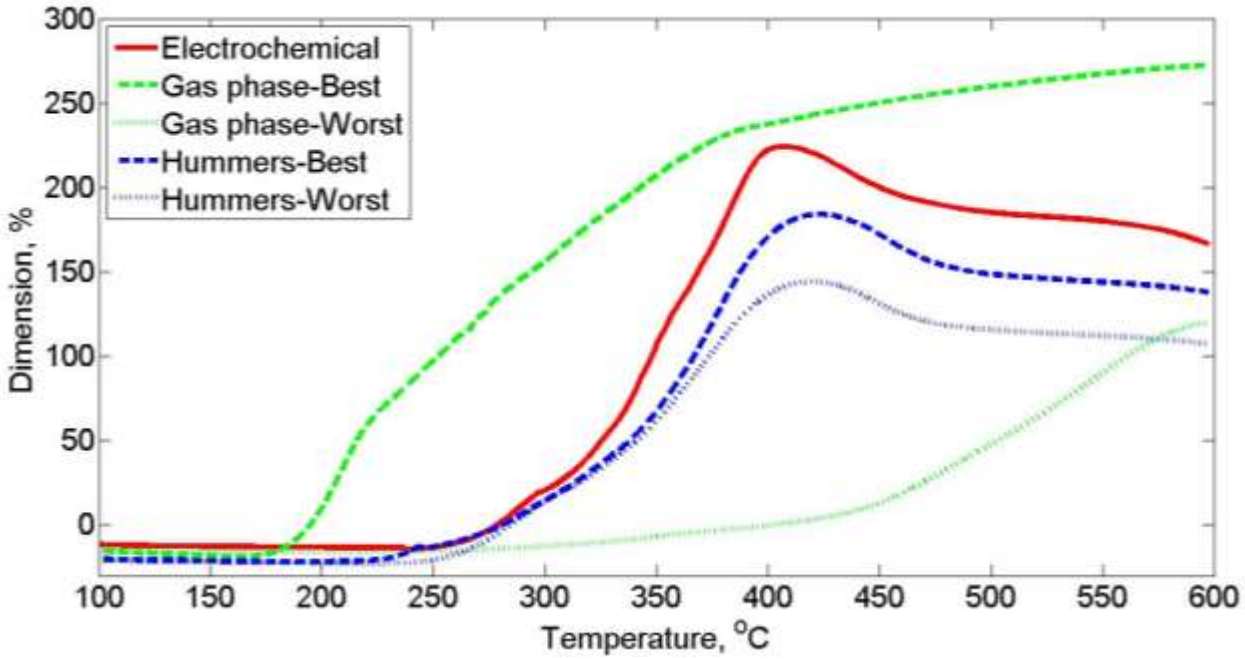

Figure 4-2: The average of the expansion for each method.

As can be seen from Figure 4-2, the gas phase delivers the best expansion. This indicates that one achieves the best intercalation using the gas phase intercalation method, at these specific conditions. The gas phase intercalation method has a very broad expected outcome, which clearly indicates that the conditions at which this method is used, is crucial. Using the Hummers method, although it is the method that delivers the lowest expansion, the various conditions will stay in the expected range shown in the Figure 4-2, making this method not as dependant to the reaction conditions. The electrochemical and Hummers methods have similar curves, which indicate that the reaction mechanism is similar, but the gas phase method employs a complete different mechanism.

4.4 TGA

The TGA was used to determine the mass loss as a function of temperature, shown in Figure 4-3. The derivative thereof was determined using MATLAB® 7.5.0 (R2007b), also illustrated in Figure 4-3.

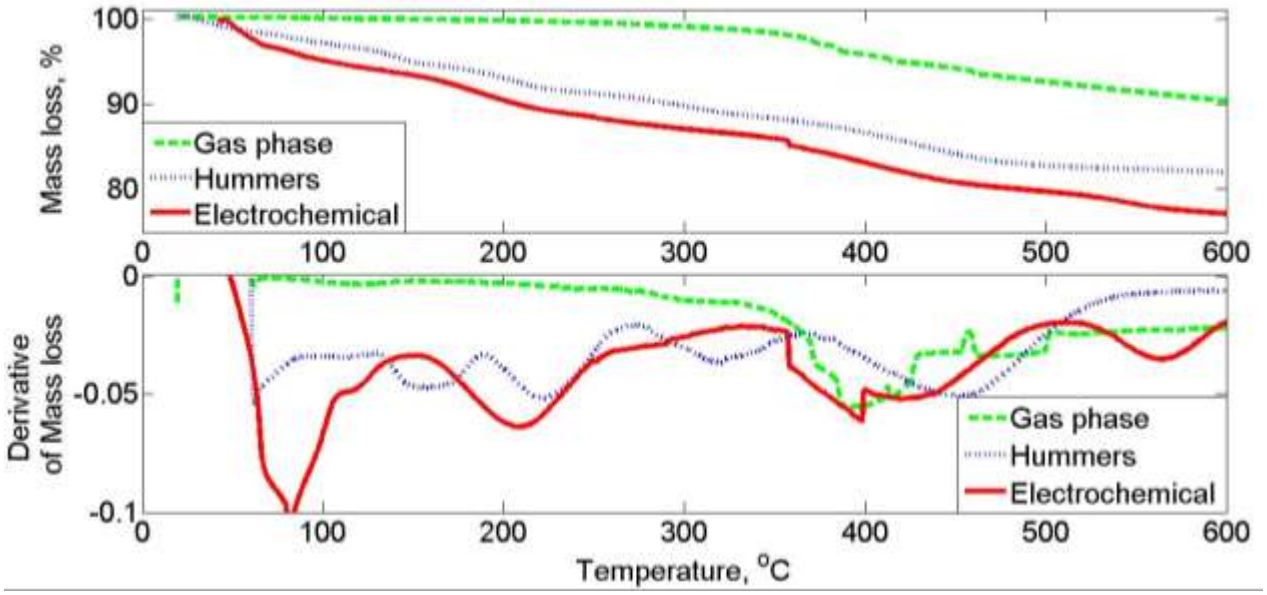

Figure 4-3: Mass loss curves and derivative thereof of the different samples in N_2 atmosphere.

The peaks in the derivative curve illustrate the major mass losses found in each sample. As can be seen from Figure 4-3, both the Hummers and electrochemical samples show mass losses below 200 ˚C, implying these mass losses are impurities and compounds bound to the surface of graphite. For the Hummers and electrochemical samples, expansion and mass loss occurs over a wide temperature range, this indicates that graphite oxide was formed rather than the theoretically expected, "insertion of atoms between the sheets". After 600 ºC the degradation of the material will take place, therefore the mass loss after this temperature is not relevant.

In Figure 4-4 the mass loss of the gas phase sample is compared to the expansion. There is a small gradual mass loss for the gas phase material up to about 3%. The gas phase sample had virtually no mass loss at the point where expansion took place. Hence the intercalation was very efficient, producing large expansion without significant mass loss. The fact that mass loss occurs only at the sublimation of iron chloride (320 ºC) indicates the amount of "un-intercalated" or residual iron chloride, also evident from Table 4-1.

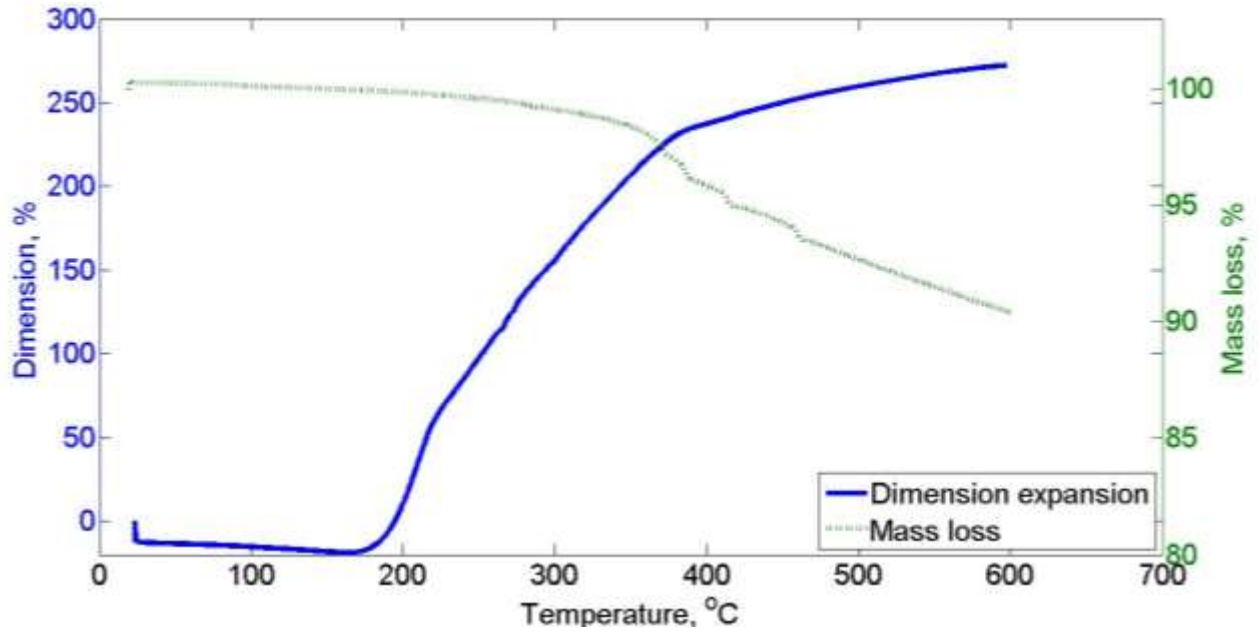

Figure 4-4: Mass loss versus dimension expansion of the gas phase sample.

The exfoliated and purified samples of the best sample of each method is oxidised. The oxidation data is illustrated in Figure 4-5.

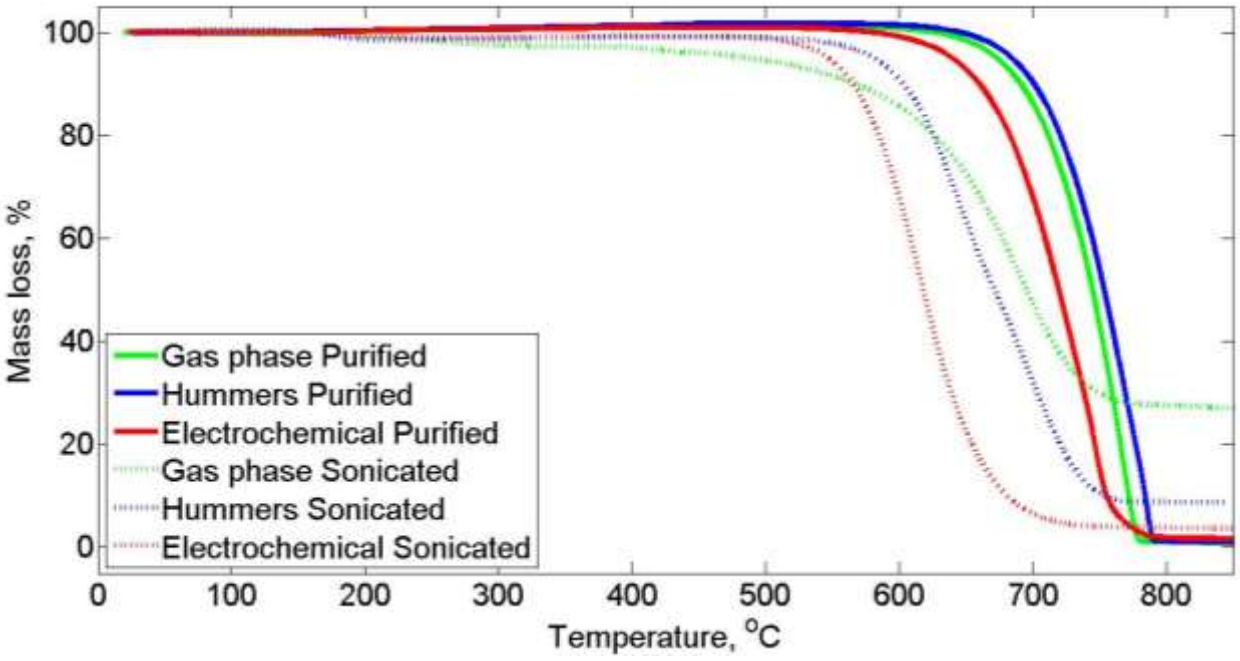

Figure 4-5: The oxidation data of the different methods.

From Figure 4-5 it is very clear that the trend for the exfoliated and purified for oxidation is similar, thus it is likely whatever caused it was already present in the exfoliat-

ed material. Most impurities within the graphite are removed during purification, and only the graphite remains. All of the carbon is reacted with oxygen to produce a mixture of carbon dioxide and carbon monoxide; therefore no residue is left. It is noticeable from the exfoliated samples that the gas phase sample starts to oxidise first, indicating that the gas phase sample has the most residual material, which acts as catalysts. The residual mass of the gas phase sample before purification is 25 %, this also proves the presence of impurities in the exfoliated samples. The electrochemical sample seems to be the most reactive as it is oxidised the most and most rapid.

4.5 RAMAN

The RAMAN spectroscopy only gives information of small regions of a sample, which makes bulk sample characterisation very difficult. These samples have many different surface structures, the edge will have a completely different spectrum than that of a flat, smooth surface and within each sample there are both smooth and uneven surfaces visible. The RAMAN spectrum was taken at 3 different locations on each intercalated and exfoliated sample. The RAMAN spectrum for the natural big flake graphite is given in Figure 4-6.

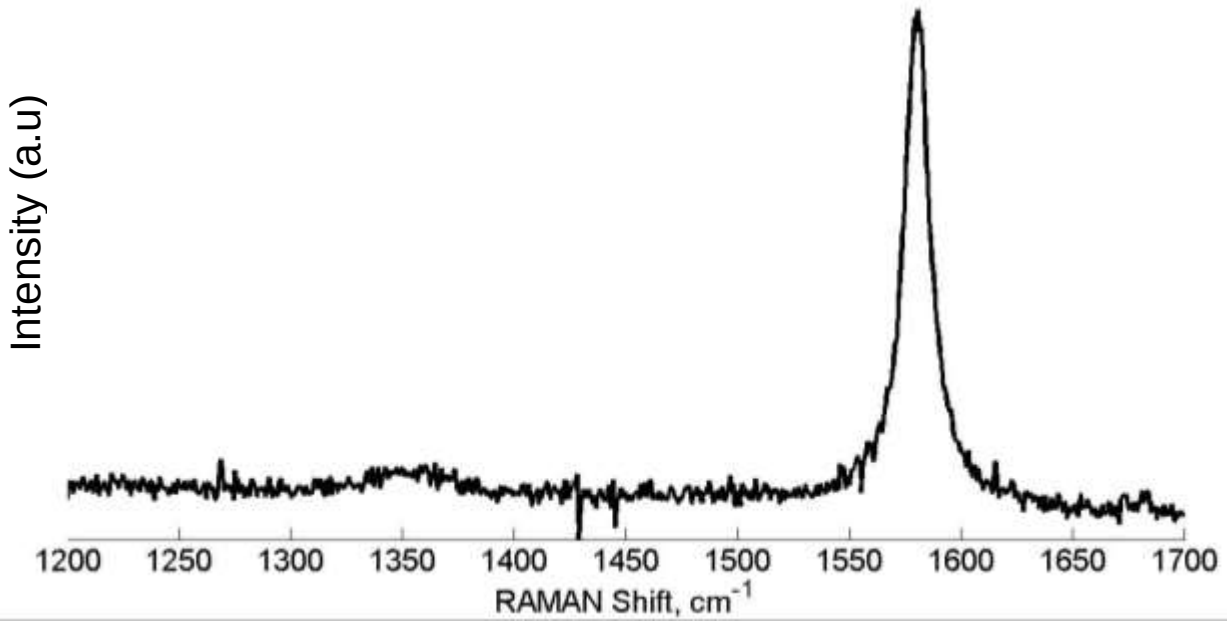

Figure 4-6: RAMAN spectrum for natural big flake graphite used.

The RAMAN spectrum of the natural graphite flakes exhibits a characteristic strong G band at 1580 cm^{-1} which is attributed to the vibration of sp^2-bonded carbon atoms in the two-dimensional hexagonal lattice. It also features a weak D band at 1349 cm^{-1} which is caused by the graphite edges and imperfections (Focke *et al*, 2014). The RAMAN spectra of the intercalated and exfoliated graphite samples are illustrated in Figure 4-7. The D-band indicates damage sustained by the intercalation process as well as possible impurities and edges.

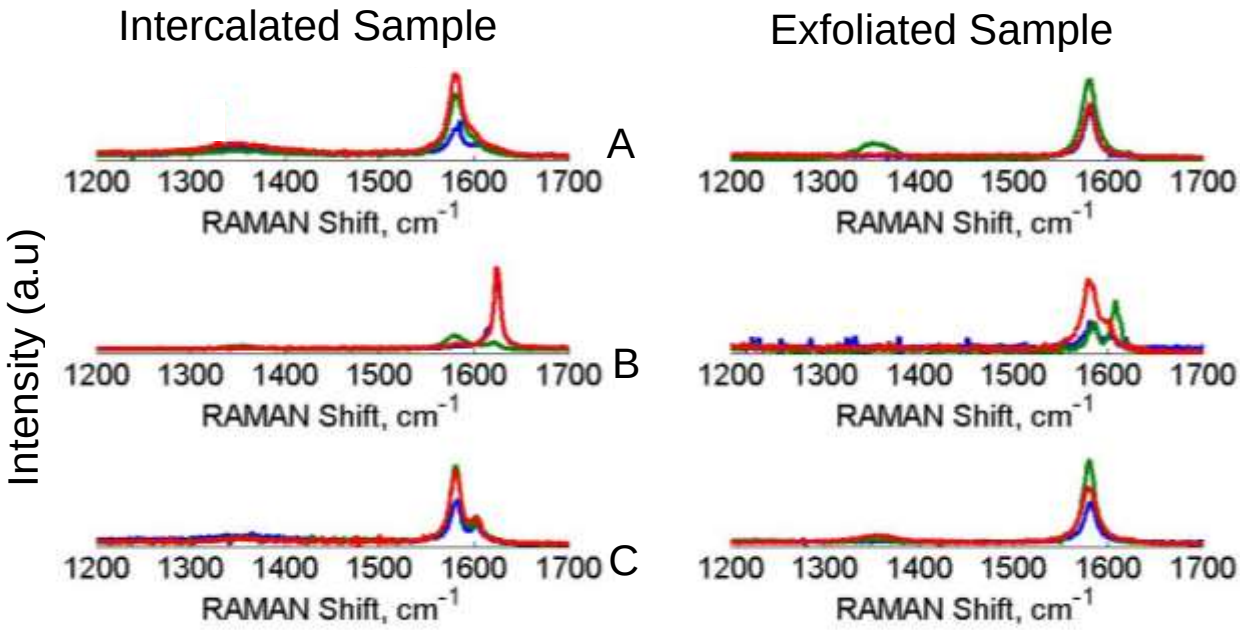

Figure 4-7: RAMAN spectra of the samples by the three intercalation methods. A – Electrochemical B – Gas phase C – Hummers.

From Figure 4-7 the G-peak (at 1580 cm^{-1}) is clearly visible in all the exfoliated samples and the intercalated electrochemical and Hummers samples. The intercalated gas phase sample merely shows a very small G-peak. All the intercalated samples exhibit a D'-peak at 1620 cm^{-1}. This peak, just as the D-peak (1349 cm^{-1}), is an indication of disorder or damage.

Table 4-5 reports the I_D/I_G peak intensity ratios for the natural graphite and the intercalated as well as exfoliated samples. Lower values for this ratio indicate increased ordering and less damage (Tuinstra & Koenig, 1970). Values of above 1 indicate extensive damage and disorder of the graphite structure.

Table 4-5: RAMAN I_D/I_G peak intensity ratios.

Sample		I_D/I_G
Graphite flake		0,03
Electrochemical:	Intercalated	0,13
	Exfoliated	0,21
Gas phase:	Intercalated	0,16
	Exfoliated	0,01
Hummers:	Intercalated	0,05
	Exfoliated	0,12

As can be seen from Table 4-5 the ratio is not very high for any of the samples. This clearly means that the surface structure of all samples was not entirely disintegrated and the graphite structure was preserved.

4.6 XRD

Figure 4-8 shows the XRD diffractograms of the graphite flakes used for all experiments and for both the intercalated and exfoliated samples.

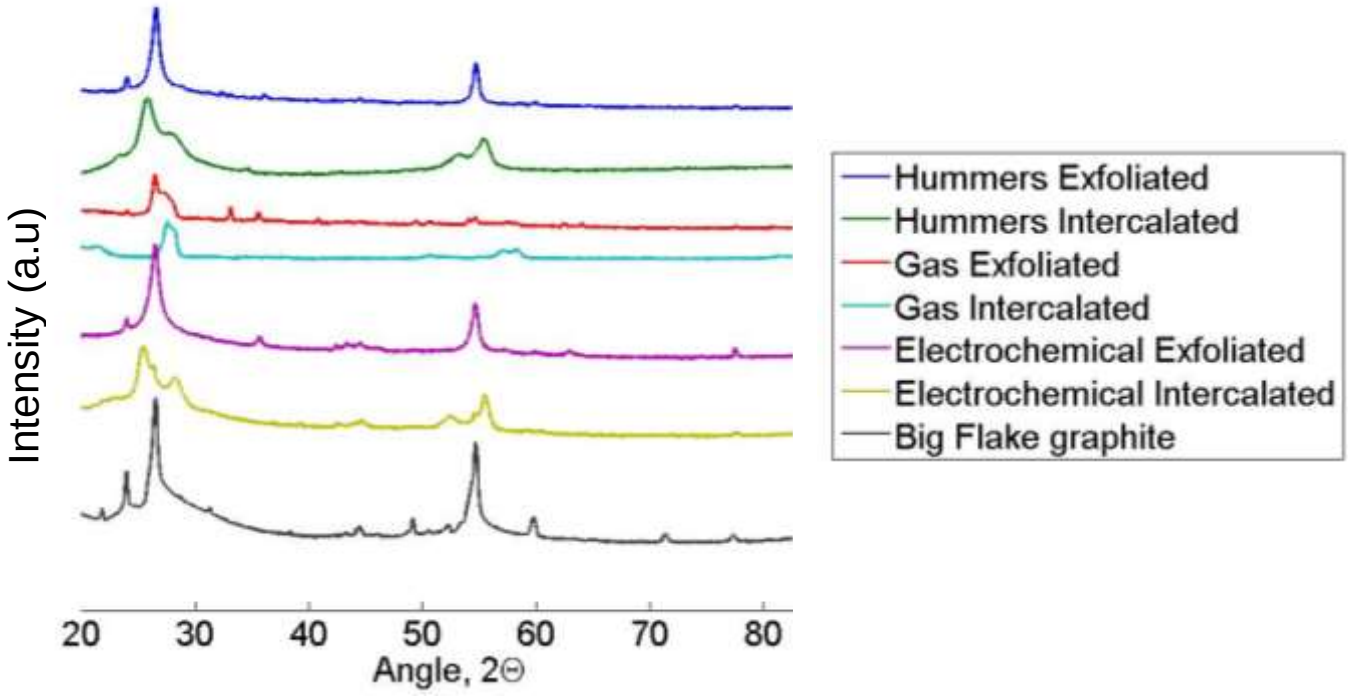

Figure 4-8: XRD patterns for the various samples (intercalated and exfoliated).

The small peaks in the diffractrogram is an indication of impurities in the material, therefore not of high importance. There are two major peaks, d_{002} and d_{004}. When analysing these diffractograms, notice that the intercalated samples clearly differ from that of the neat graphite. The electrochemical and Hummers samples have a shoulder to both the right and left of the d_{002} peak. This indicates partial modification of the material. The exfoliated samples from both the electrochemical and Hummers methods have similar graphs to that of the original graphite flakes. This indicates that after sonication, the original material is nearly completely restored with regard to the basal plane. The gas phase intercalated sample has a complete peak shift to the right, representing a modified material. The exfoliated gas sample also restores the graphite diffractrogram with a shoulder to the right, which may be due to the high amount of residual $FeCl_3$.

4.7 SEM

The structure and microstructure of the as-received graphite flakes, as well as the intercalated, expanded, exfoliated and purified samples are observed with an ultra-high resolution field emission scanning electron microscope (HR FEGSEM Zeiss Ultra Plus 55).

4.7.1 Graphite

A SEM image of the as-received material is shown in Figure 4-9. As can be seen from this figure; the sample contains large, thin and flat flakes. It is clear that the edges of these flakes are roughened and have damaged edge structures; this can also be seen in Figure 4-10. The edge of a flake is illustrated in Figure 4-10, visibly showing that the edges are curled over. Viewing the basal plane at the bottom left corner the slight damage is noticeable. The edge is examined at higher magnification in Figure 4-11. The layered structure characteristic of graphite is very clearly visible. The flakes seem to be highly crystalline, and little or no porosity noticeable.

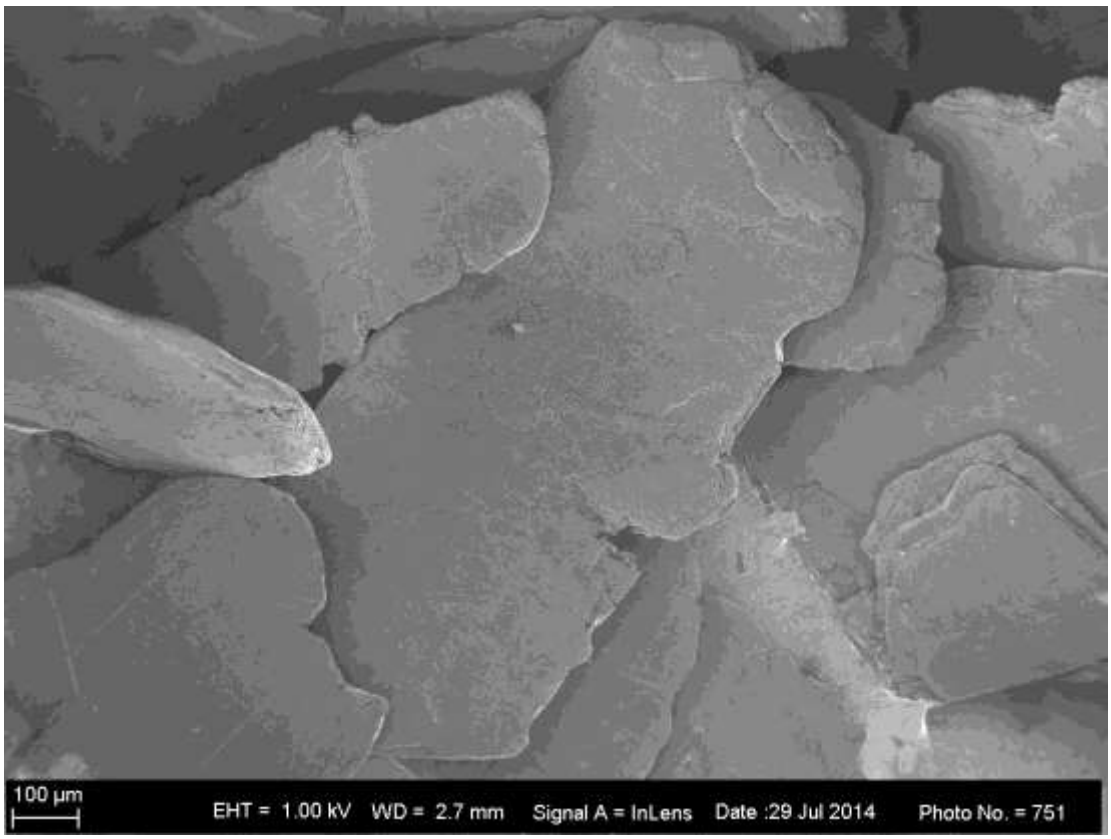

Figure 4-9: SEM image of the graphite flakes as received (180x magnification).

Figure 4-10: SEM image of the graphite flakes as received (300x magnification).

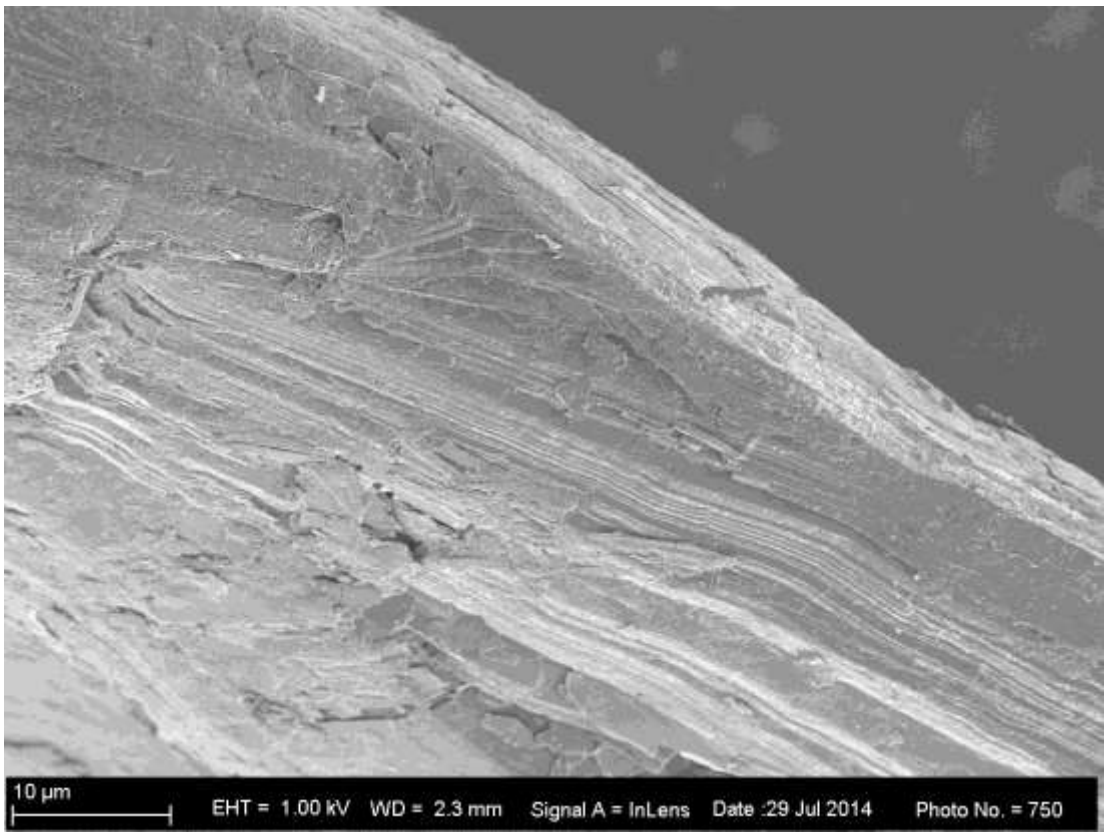

Figure 4-11: SEM image of the graphite flakes as received (4000x magnification).

4.7.2 Intercalated Samples

The basal plane of the electrochemical intercalation sample is illustrated in Figure 4-12 and Figure 4-13. From Figure 4-12 the basal plane is smooth but a residue is visible and the edges are roughened. In figure 4-13 there are cracks in the basal plane and the edges are roughened. The edge of the electrochemical intercalation sample is illustrated in Figure 4-14. From this image the layered characteristic structure of graphite is very clear. It is also very clear that the edges are slightly damaged. Figure 4-15 is another image of the edge of the electrochemical intercalated sample, illustrating the damage even clearer, and the layered structure. The edge in this image is also curled over and cracked and rugged.

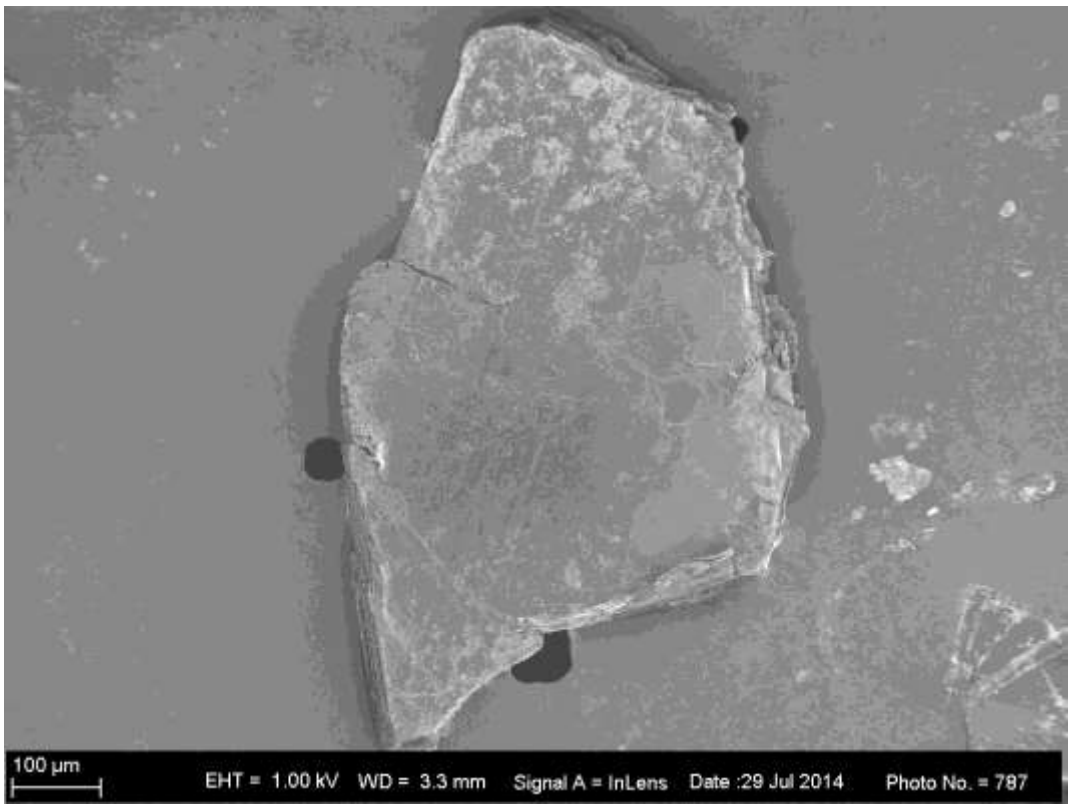

Figure 4-12: SEM image of electrochemical intercalated sample (250x magnification).

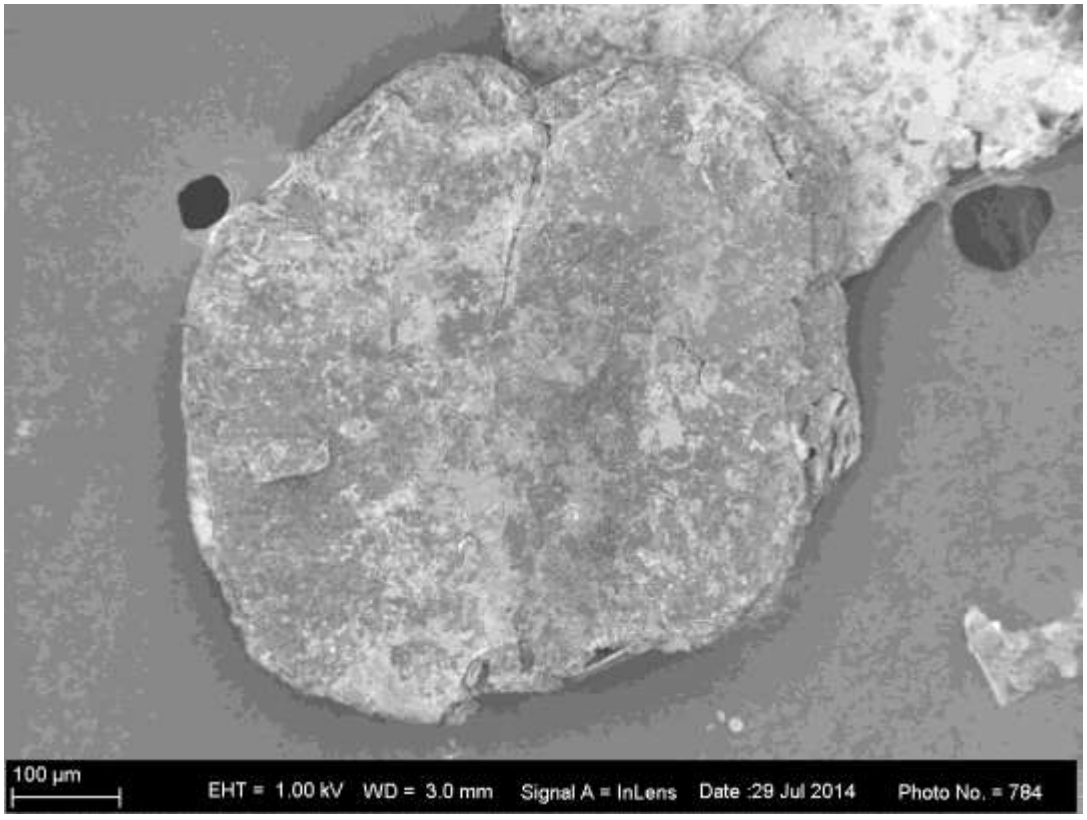

Figure 4-13: SEM image of electrochemical intercalated sample (300x magnification).

Figure 4-14: SEM image of electrochemical intercalated sample (1500x magnification).

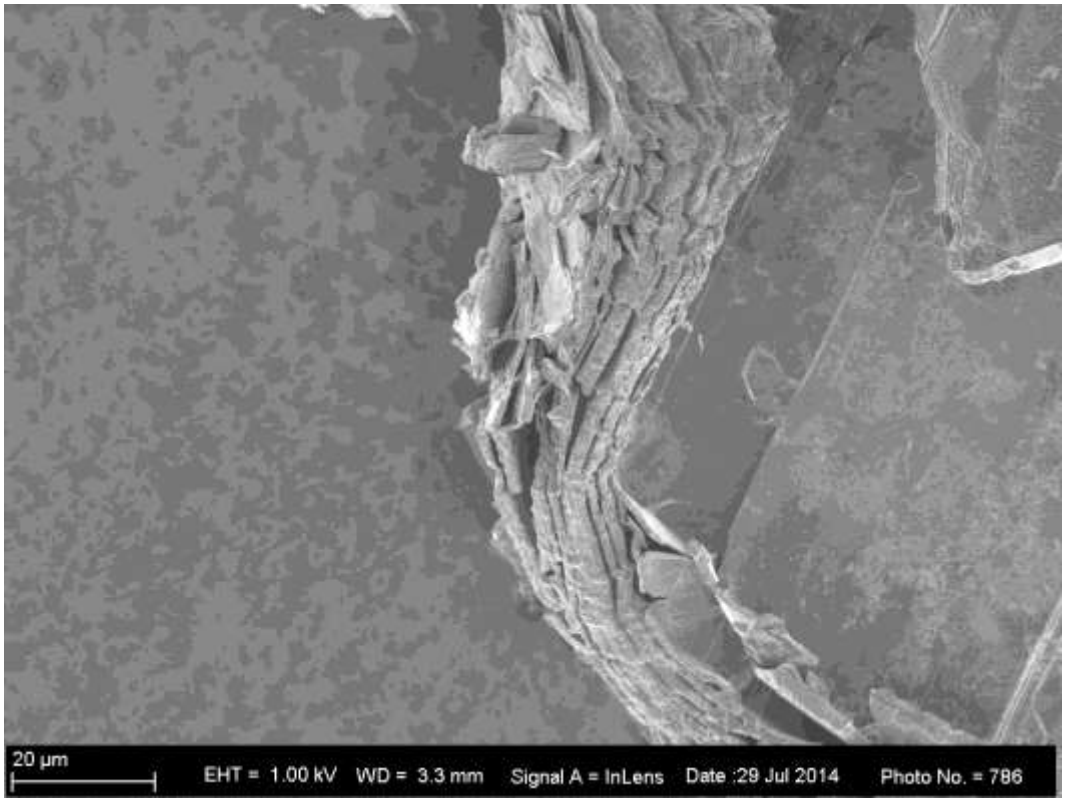

Figure 4-15: SEM image of electrochemical intercalated sample (1500x magnification).

One flake of the best gas phase intercalation sample is illustrated in Figure 4-16. The basal plane is intact, but the damage is incurred from the edge and travels to the centre. It is clear that the flake is damaged. Figure 4-17 is a magnification of the edge, to illustrate the extent of damage. The edges are curled over and very rugged. The edge of this sample is magnified in Figure 4-18. The layered structure is clear here, and the damage is extensive in this image. In Figure 4-19 the layered structure is magnified in the right of the image, but the damage on the left side of the image is an illustration of the extensive damage. The basal plane in Figure 4-20 is also severely damaged.

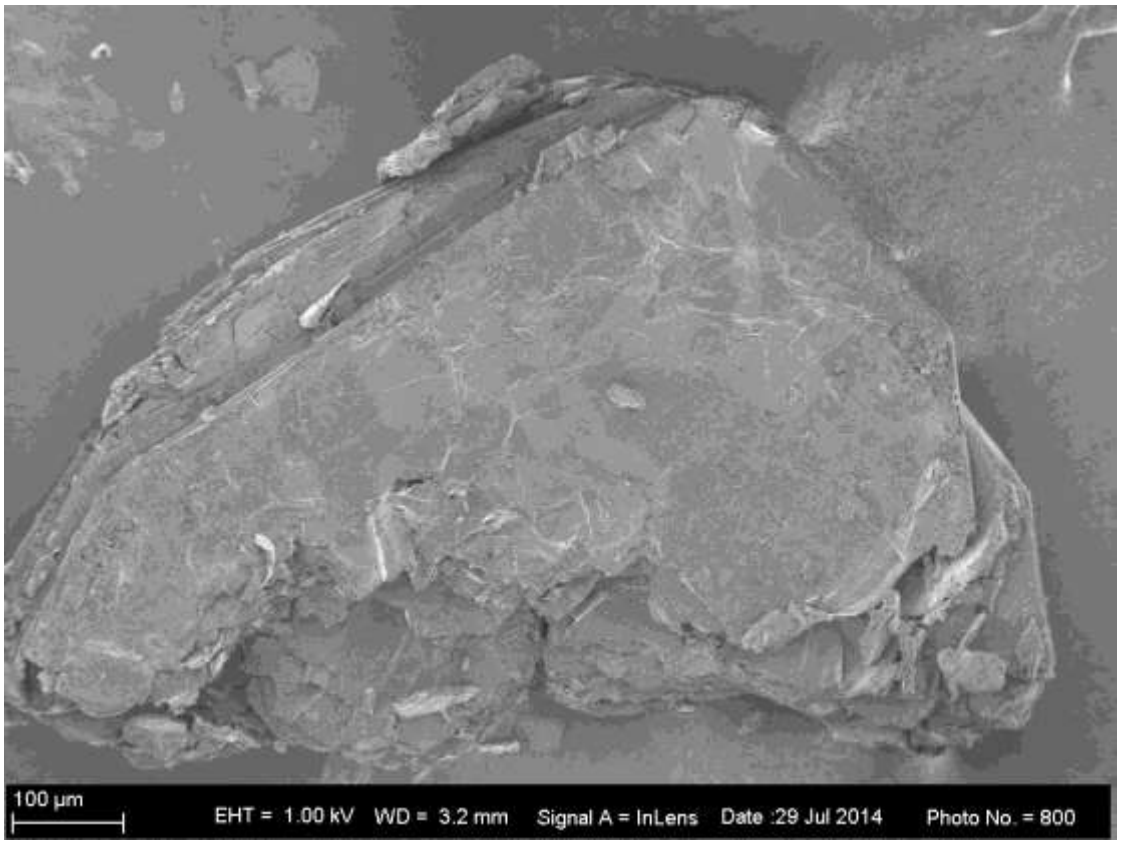

Figure 4-16: SEM of the best gas phase intercalated sample (300x magnification).

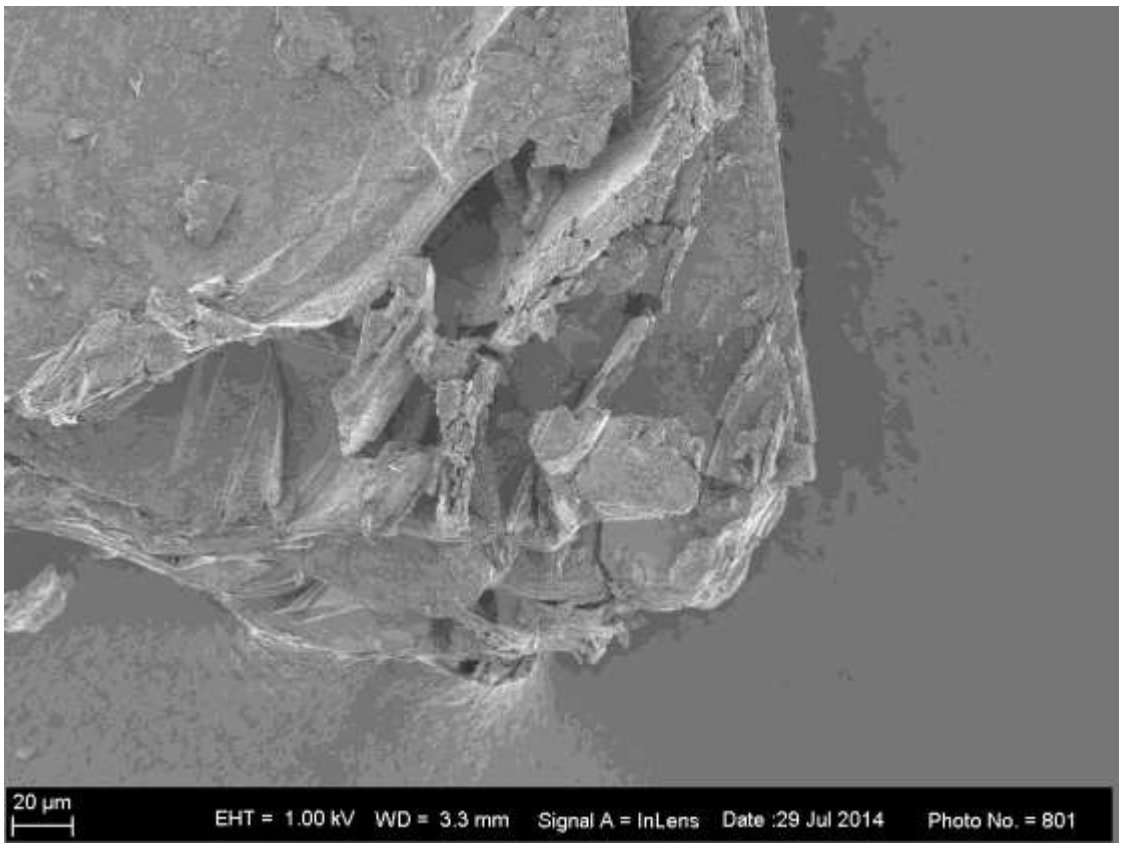

Figure 4-17: SEM of the best gas phase intercalated sample (800x magnification).

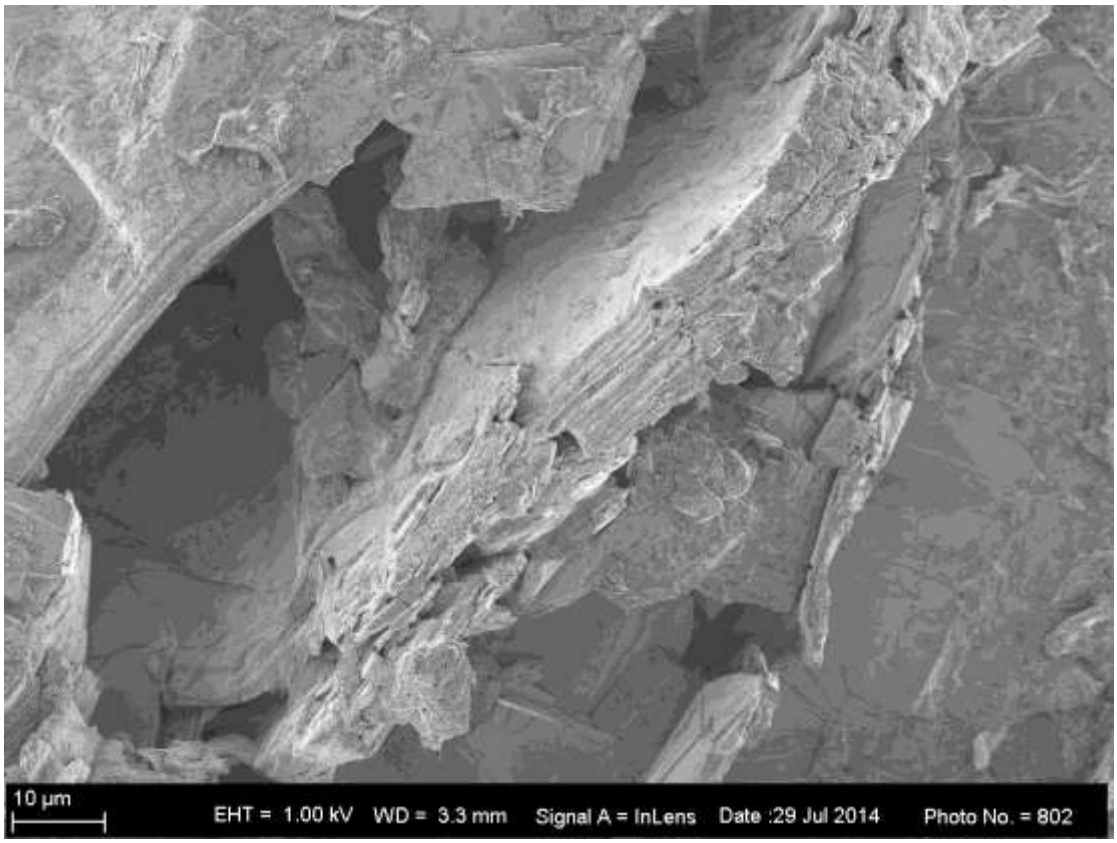

Figure 4-18: SEM of the best gas phase intercalated sample (2500x magnification).

Figure 4-19: SEM of the best gas phase intercalated sample (1000x magnification).

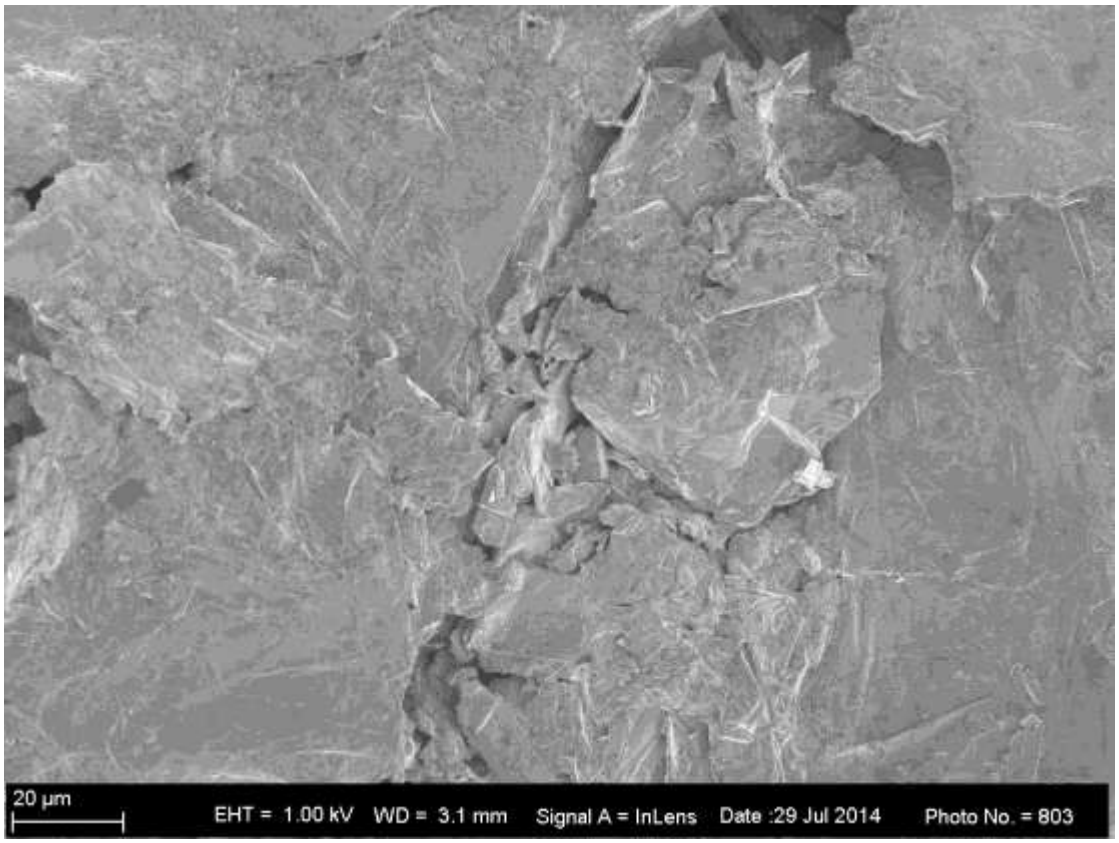

Figure 4-20: SEM of the best gas phase intercalated sample (1500x magnification).

In the next few images the worst gas phase intercalation sample is illustrated. In Figure 4-21 and Figure 4-22 the basal plane is shown. In these images, the basal plane is not as damaged, but the edge is clearly roughened in Figure 4-22. In the magnification of the edge in Figure 4-23, the damage is visible. Figure 4-24 magnifies the layered structure of the sample, here the basal plane, as well as the edges is damaged. In Figure 4-25 the edge is curled over.

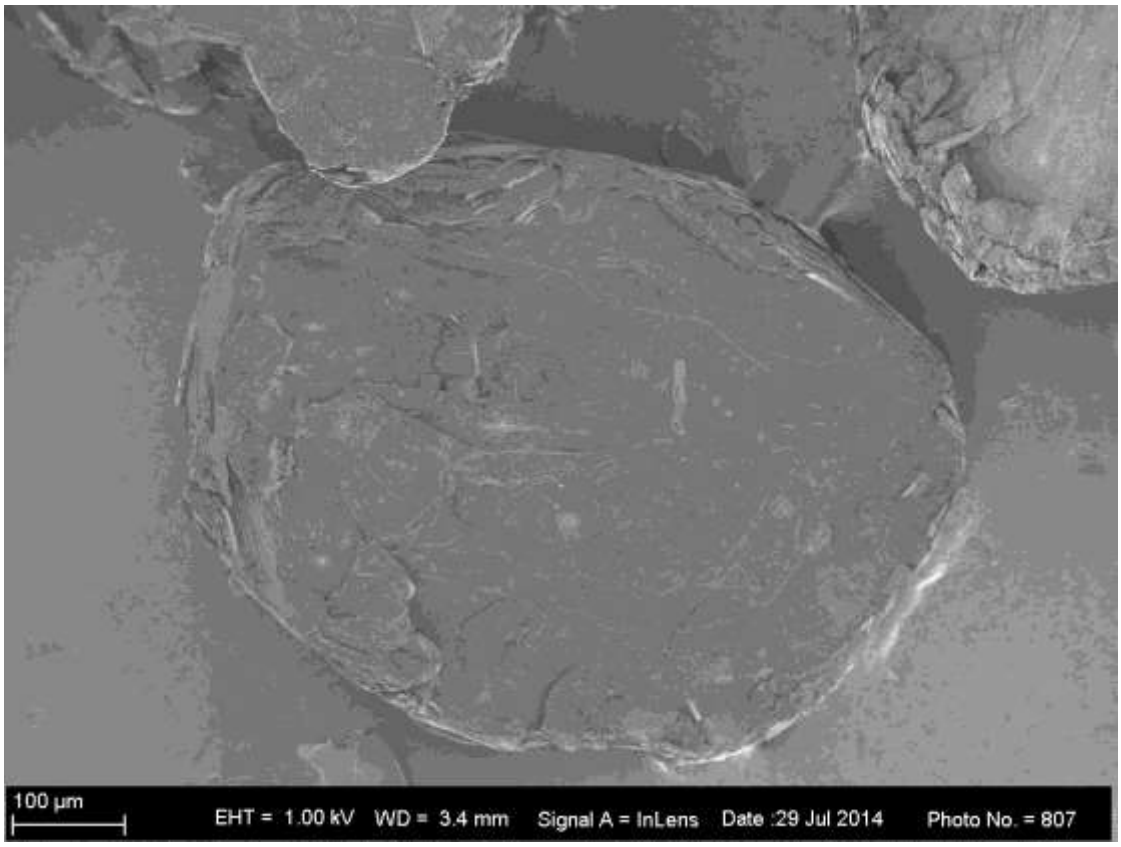

Figure 4-21: SEM of the worst gas phase intercalated sample (300x magnification).

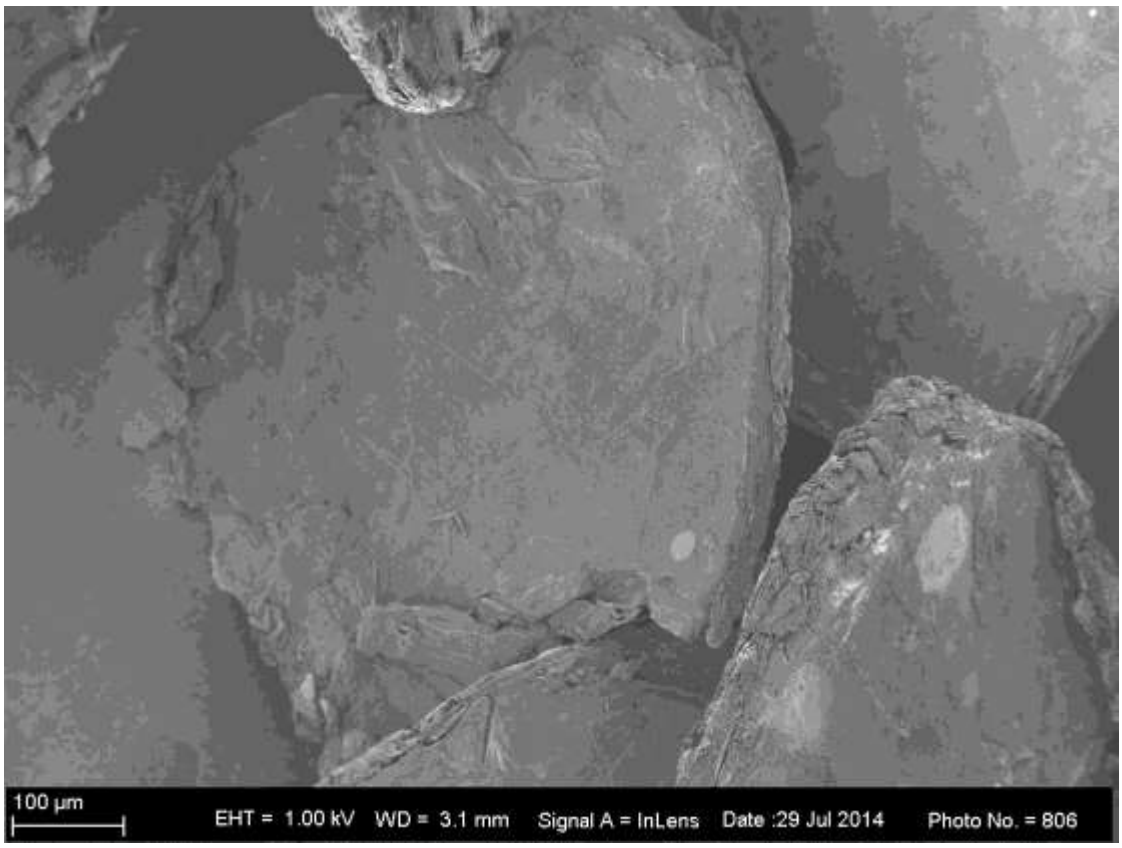

Figure 4-22: SEM of the worst gas phase intercalated sample (300x magnification).

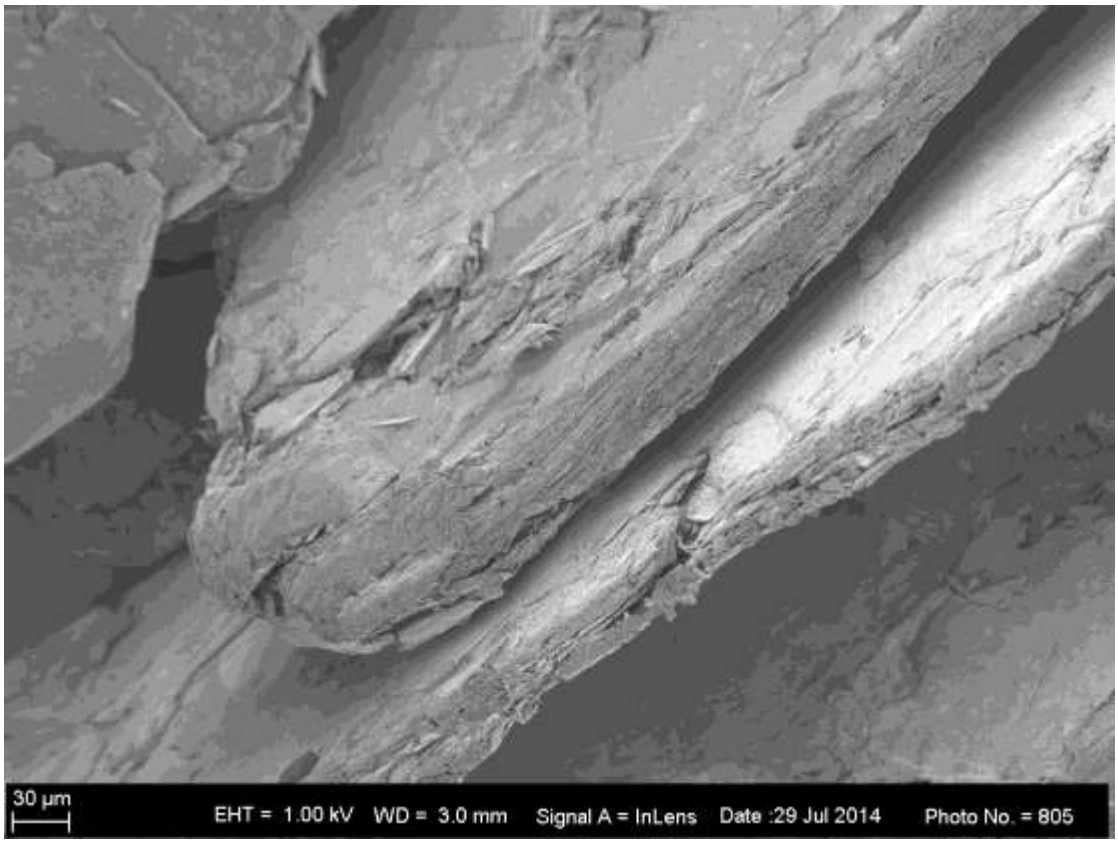

Figure 4-23: SEM of the worst gas phase intercalated sample (500x magnification).

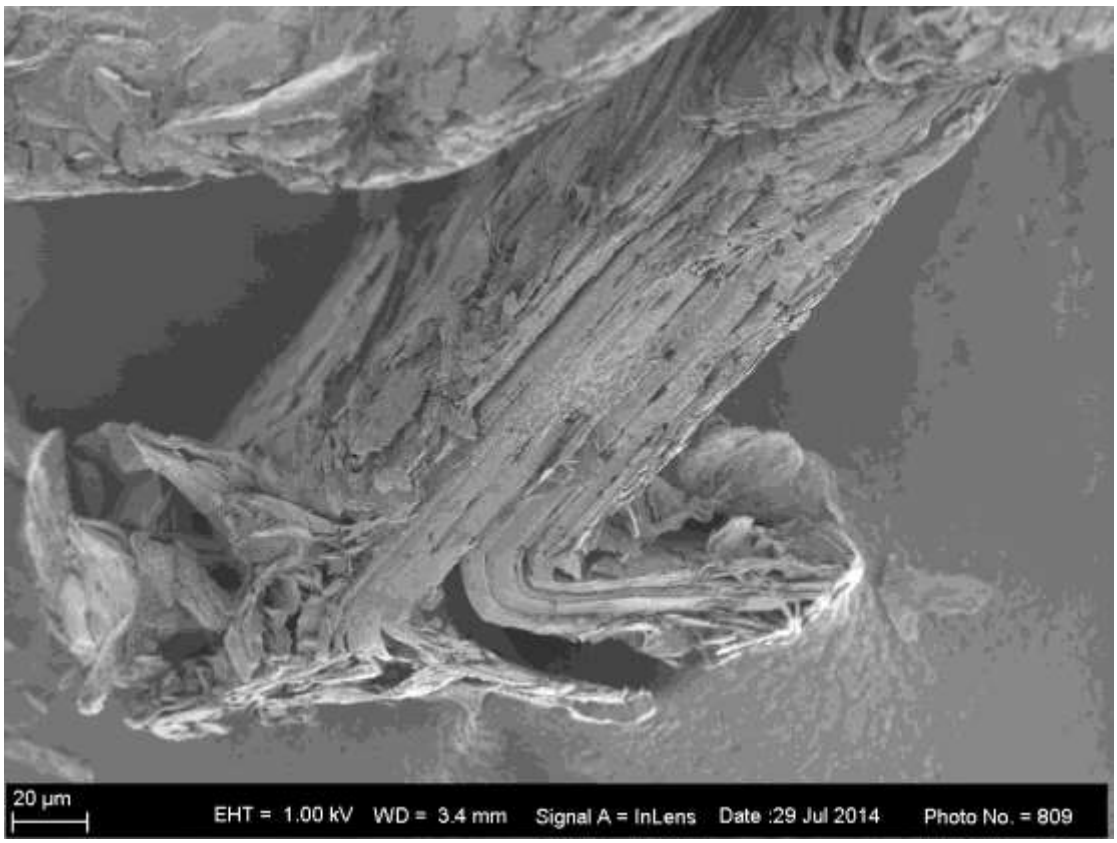

Figure 4-24: SEM of the worst gas phase intercalated sample (1000x magnification).

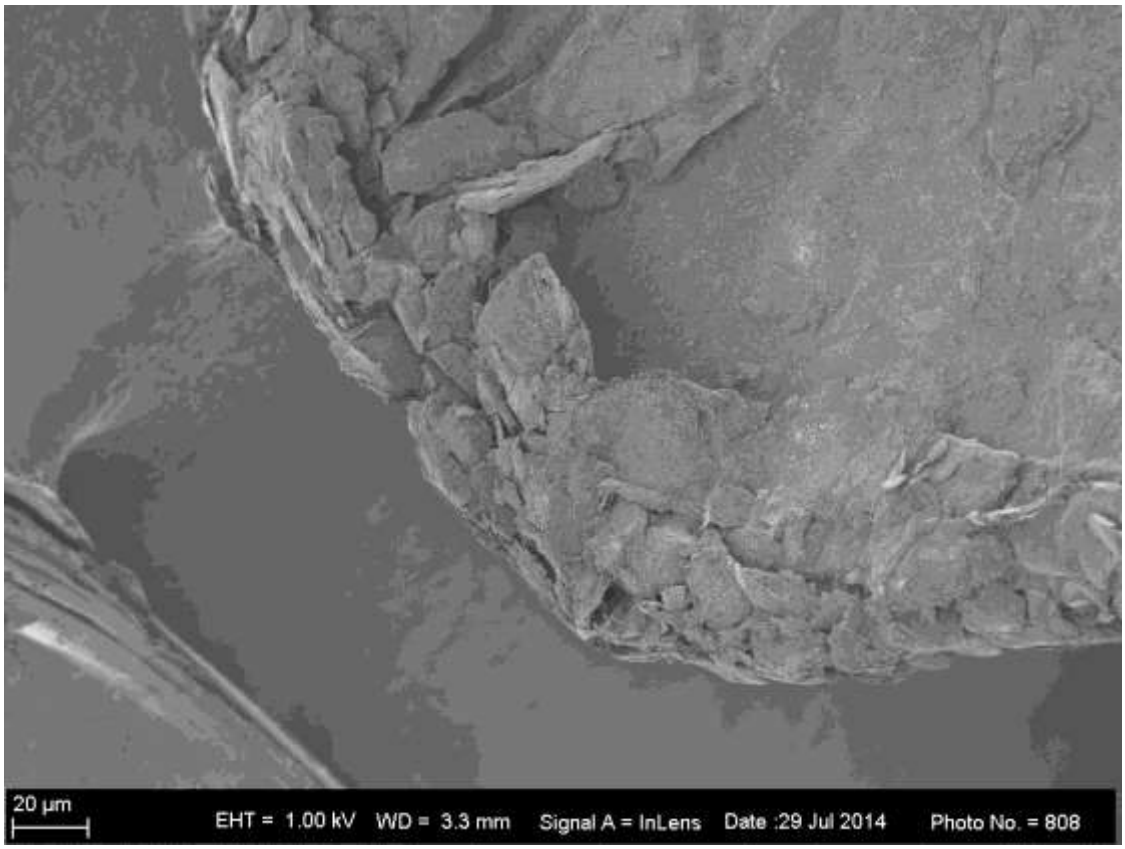

Figure 4-25: SEM of the worst gas phase intercalated sample (1000x magnification).

The best sample of the Hummers intercalation is visually examined. In Figure 4-26 the edge is curled over and in Figure 4-27 the edge is magnified. In Figure 4-27 the edge is very rugged and cracked. The basal plane is very smooth in Figure 4-28, the basal plane does not seem to be damaged. The image of this flake shows very little damage, but in the next image, Figure 4-29 the flake is extensively damaged, especially around the edges. There are cracks visible, and it is clear that the edges are curled over at the bottom right corner. In Figure 4-30 the basal plane also seems to be less damaged, however the upper right part of the sample, the basal plane is damaged, with a flaky surface.

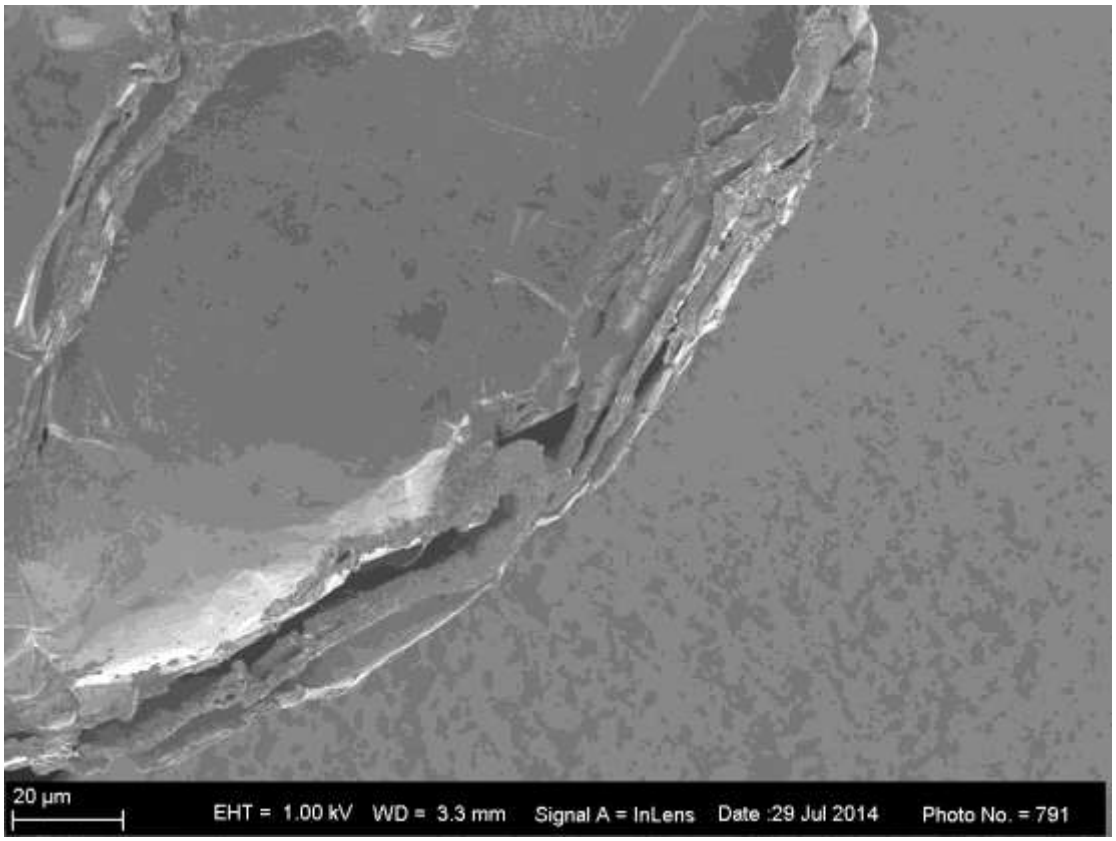

Figure 4-26: SEM of the best Hummers intercalated sample (1500x magnification).

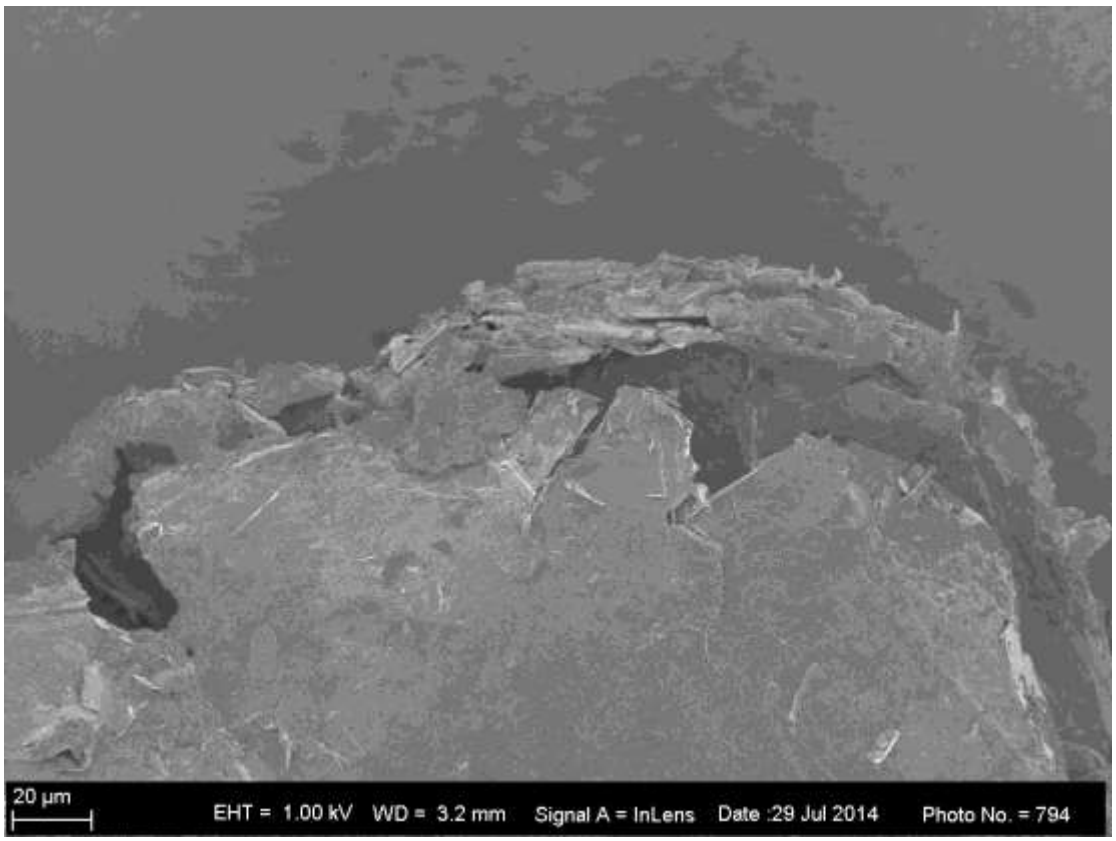

Figure 4-27: SEM of the best Hummers intercalated sample (1000x magnification).

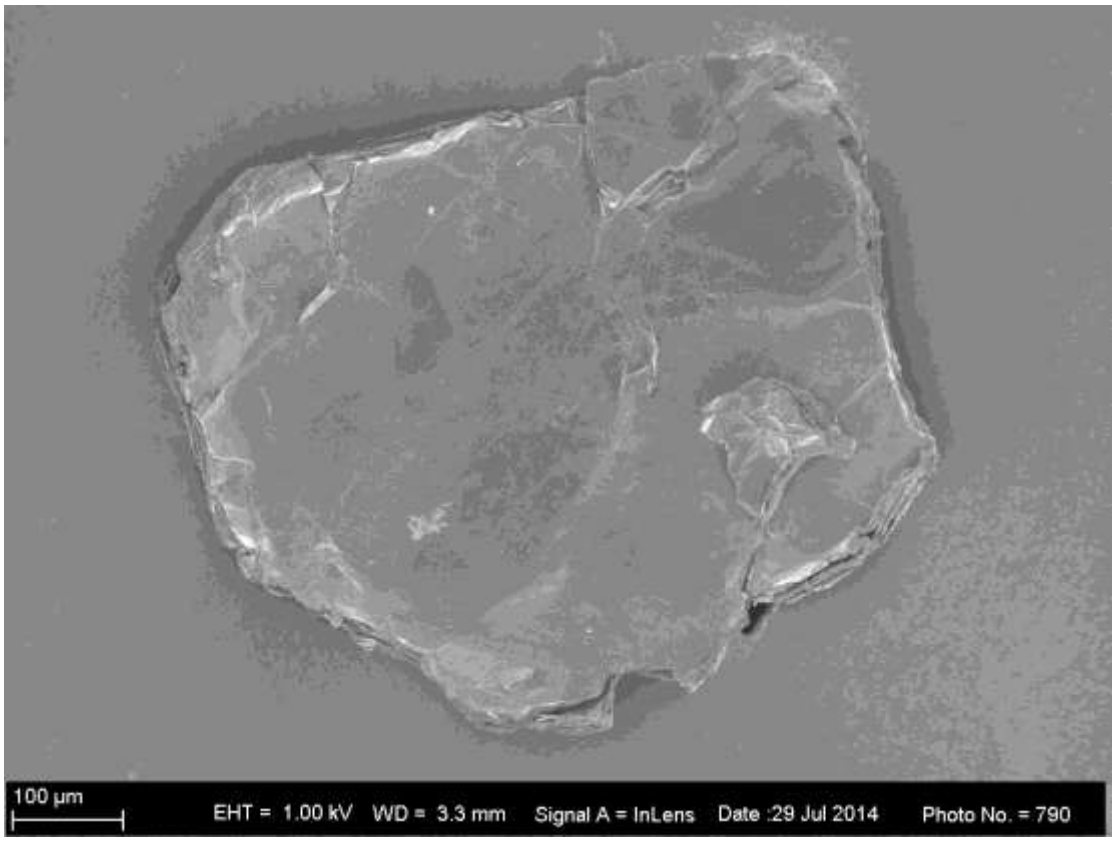

Figure 4-28: SEM of the best Hummers intercalated sample (300x magnification).

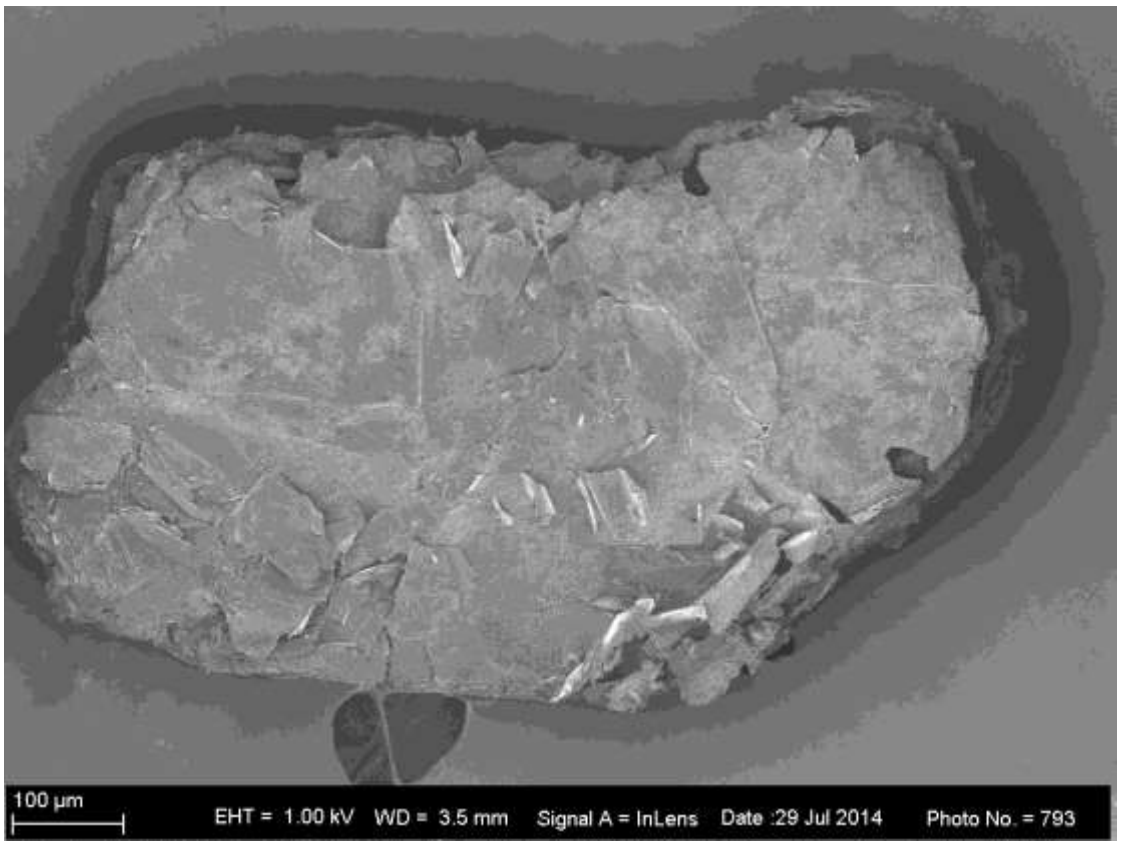

Figure 4-29: SEM of the best Hummers intercalated sample (300x magnification).

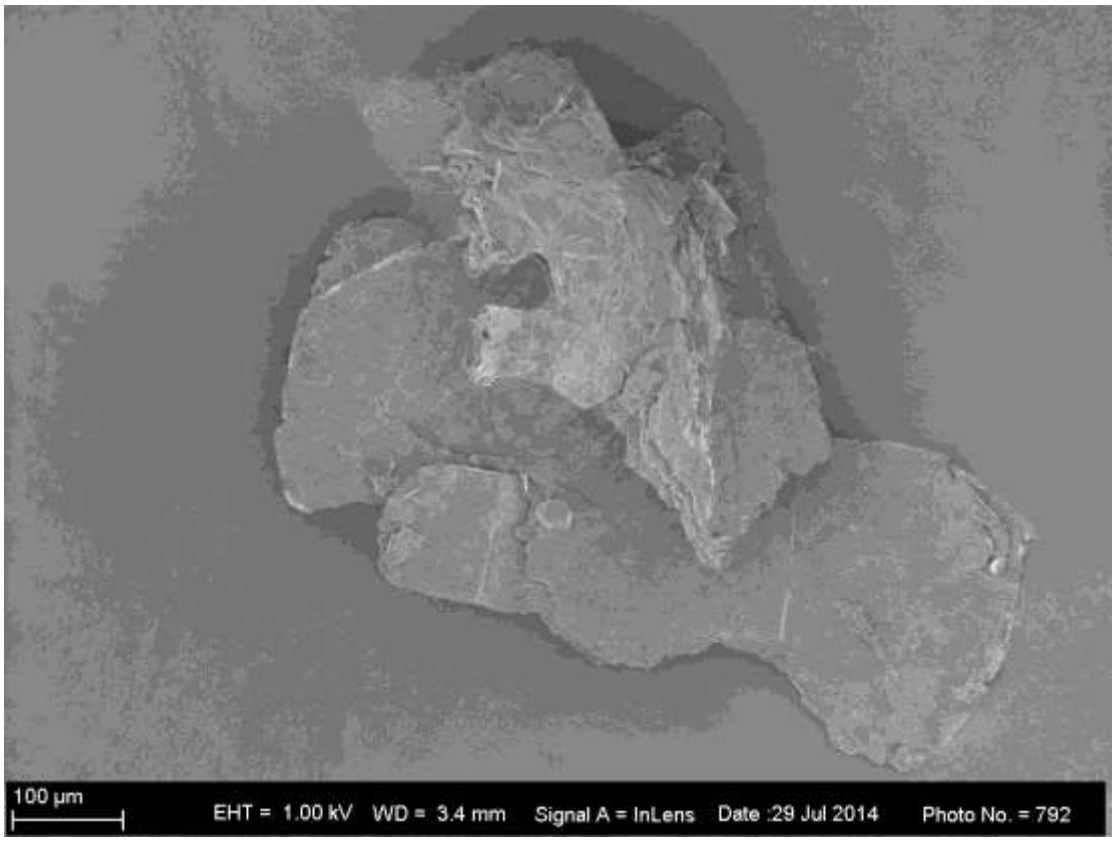

Figure 4-30: SEM of the best Hummers intercalated sample (300x magnification).

The second sample of the Hummers intercalation method is illustrated below. In Figure 4-31 the basal plane is clearly damaged, the top layer is eroded from the edge to the centre. The edge is also damaged and cracked. In the next image, Figure 4-32 the basal plane is slightly cracked but not very damaged. The edge is slightly damaged, this is shown in Figure 4-33, where the layered structure is magnified, and slight damage is visible. Figure 4-34 is an even higher magnification on the edge, which shows damage, this image indicates a smooth basal plane, but the edge is clearly rugged.

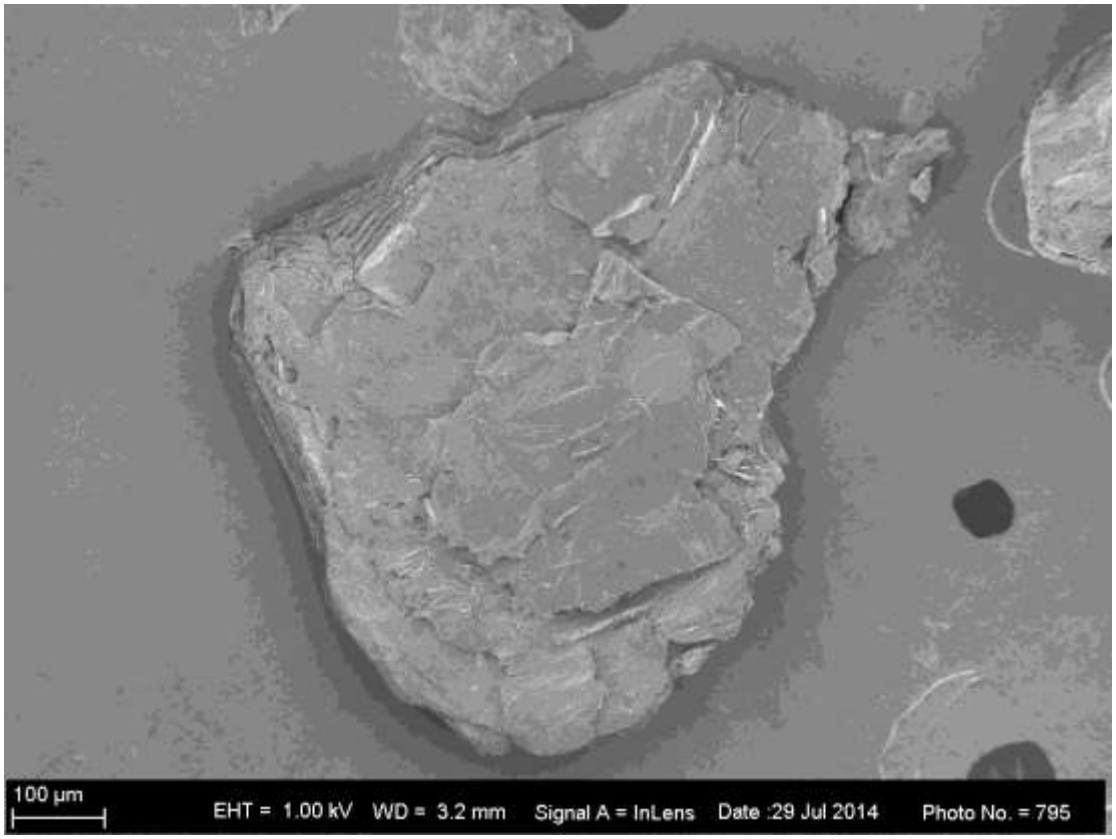

Figure 4-31: SEM of the worst Hummers intercalated sample (250x magnification).

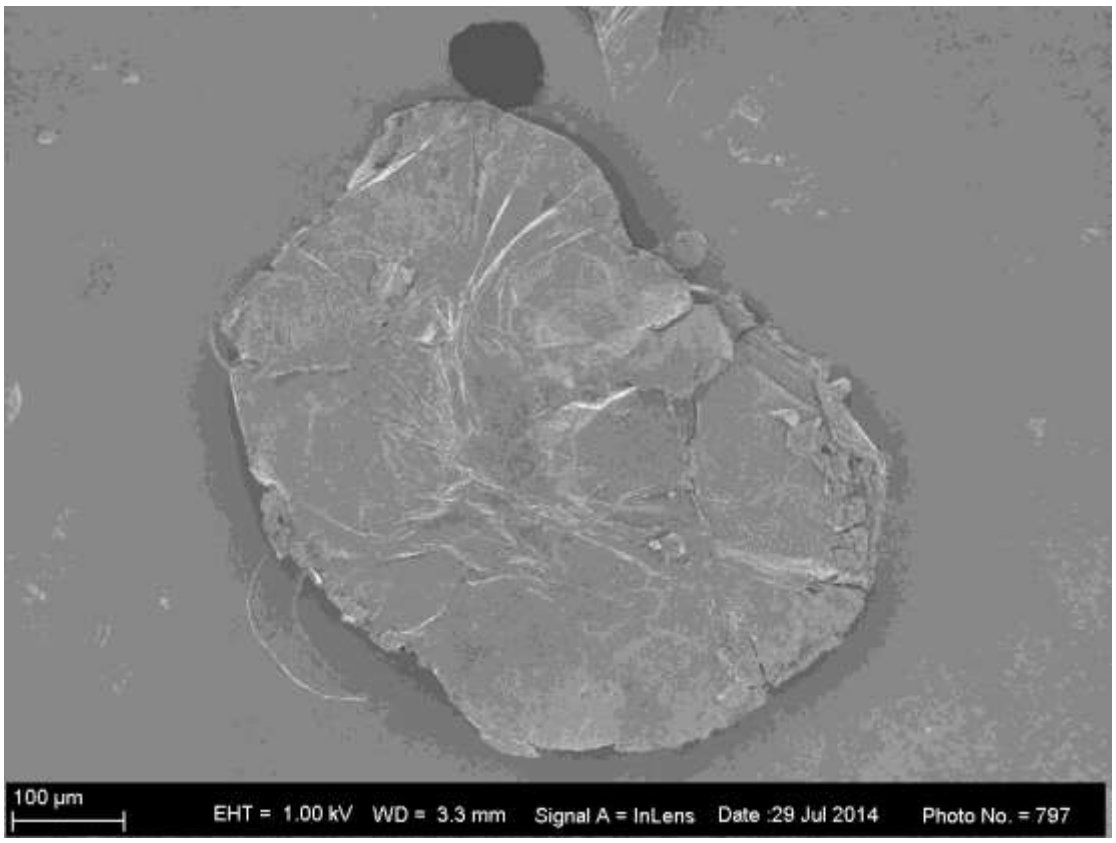

Figure 4-32: SEM of the worst Hummers intercalated sample (300x magnification).

Figure 4-33: SEM of the worst Hummers intercalated sample (1000x magnification).

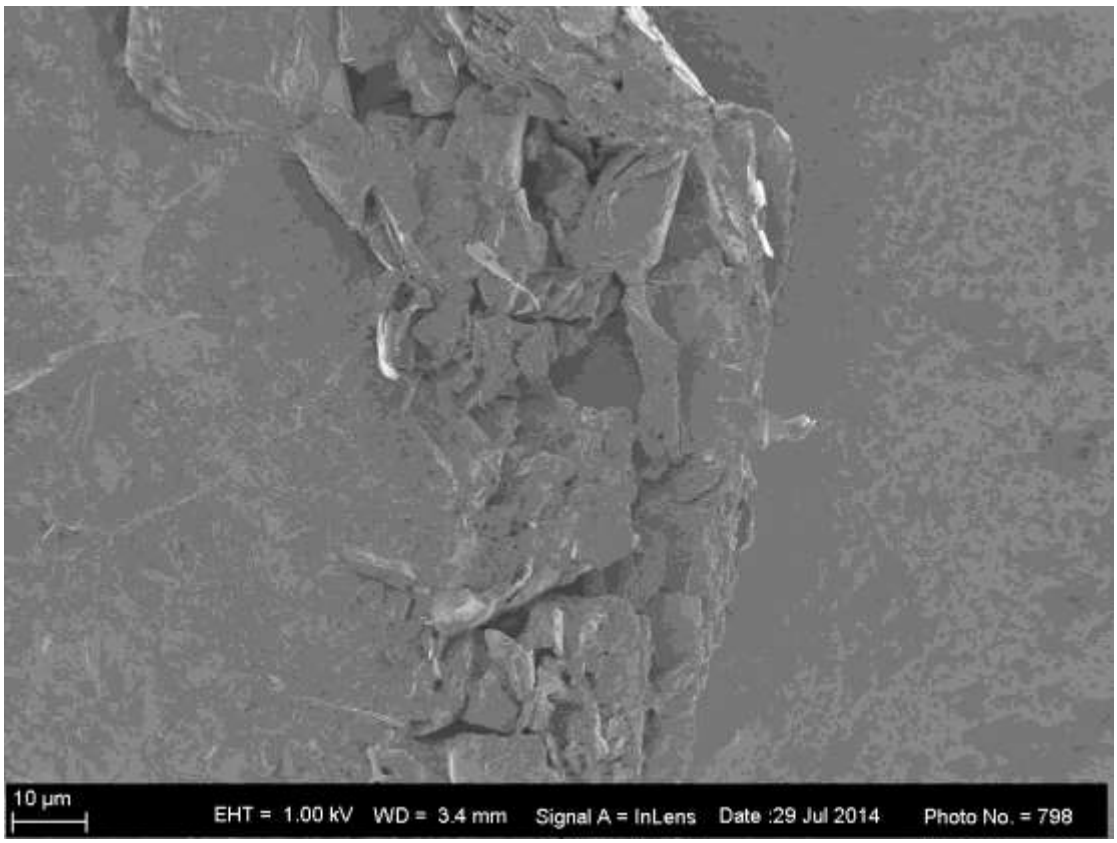

Figure 4-34: SEM of the worst Hummers intercalated sample (2000x magnification).

4.7.3 Expanded Samples

Microwave heating was employed for the expansion of all the samples. The microwave utilises rapid and intense heating, therefore damage will be sustained due to this method of heating. One expanded flake of the electrochemical sample is viewed in Figure 4-35 where the expected accordion shape is evident. This is magnified in Figure 4-36 where the presence of damage is not visible. When viewing the edges in Figure 4-37 the edge of the expanded graphite is smooth, but a residue is noticeable on the surface.

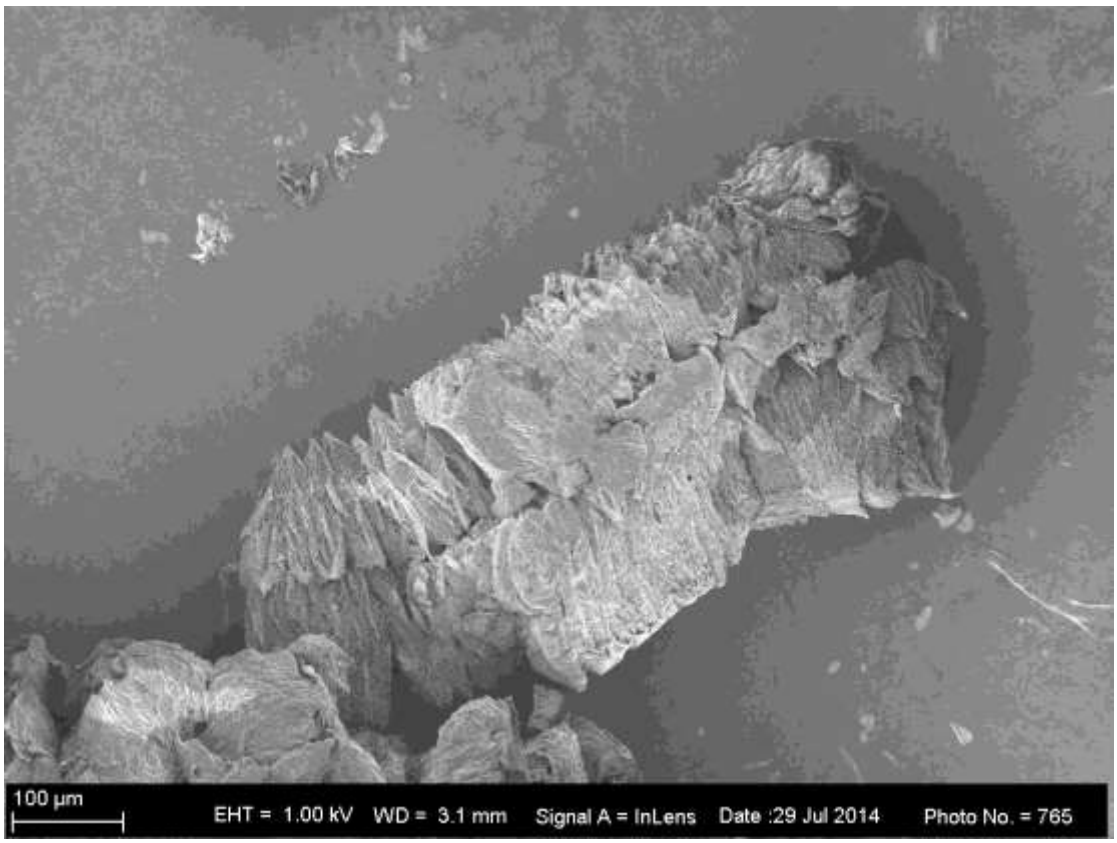

Figure 4-35: SEM of the electrochemical expanded sample (300x magnification).

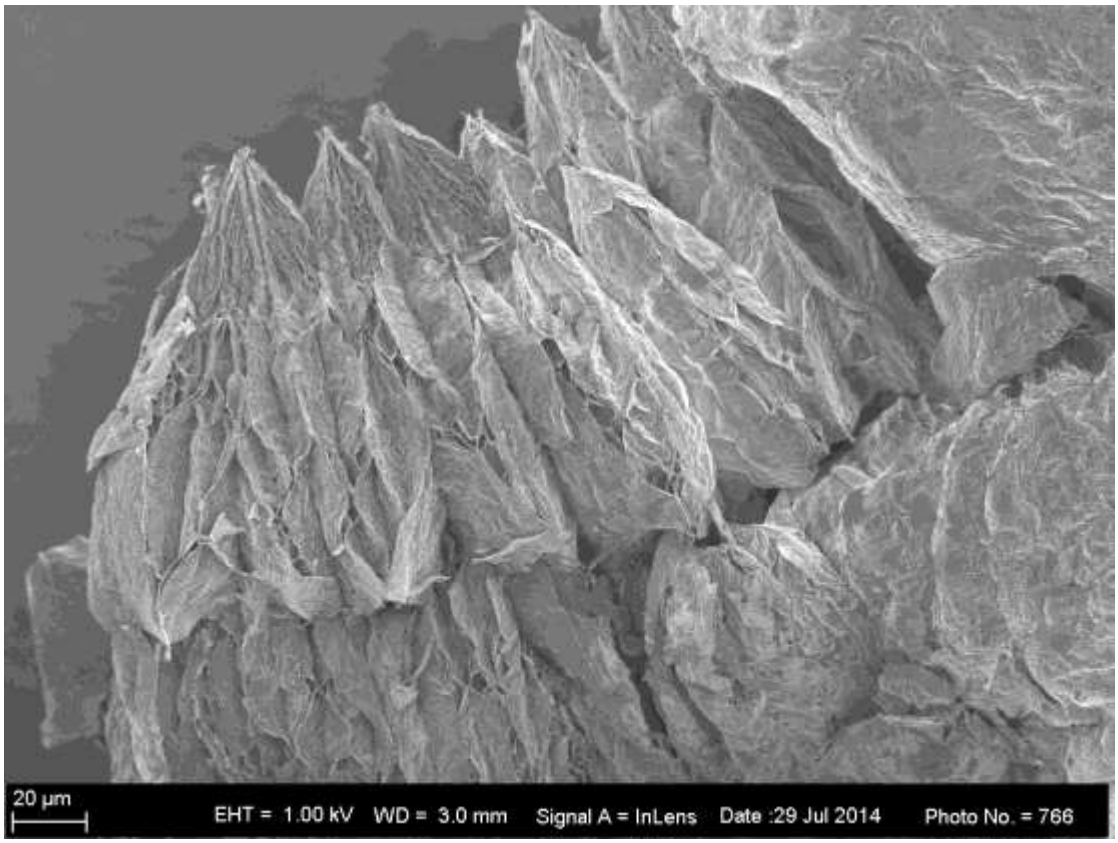

Figure 4-36: SEM of the electrochemical expanded sample (1000x magnification).

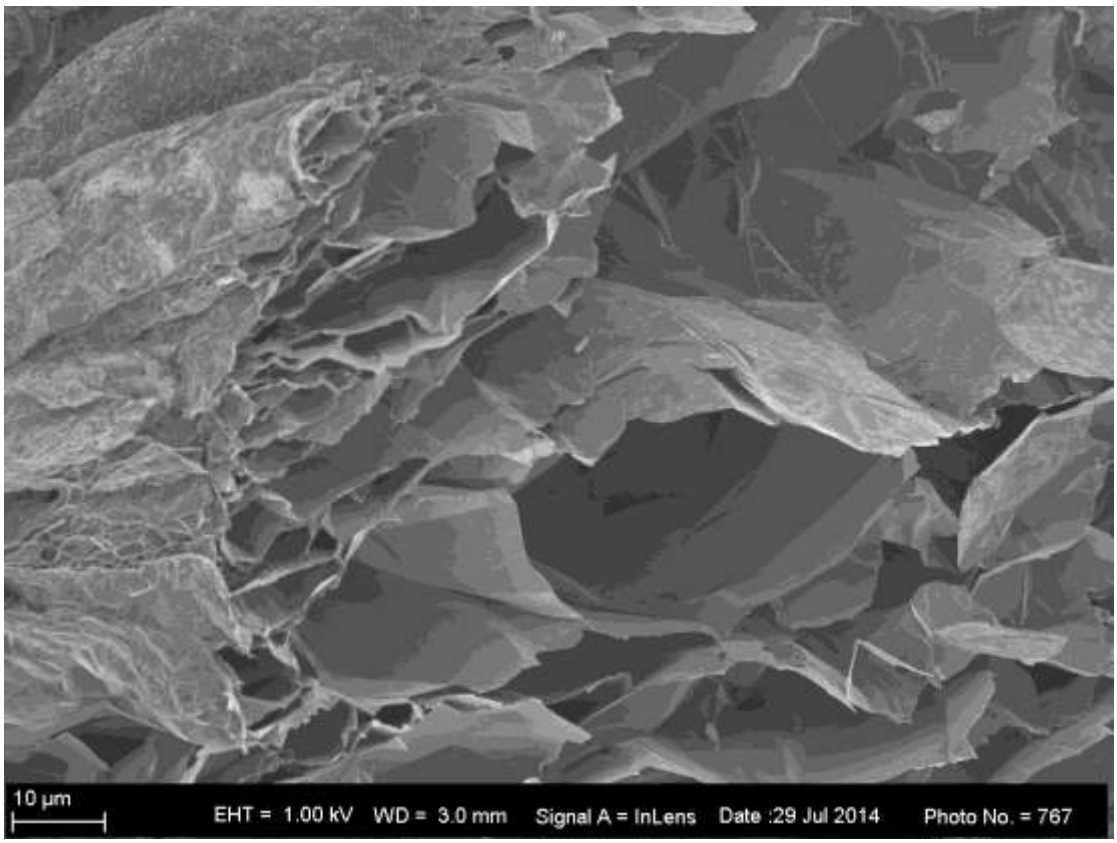

Figure 4-37: SEM of the electrochemical expanded sample (2500x magnification).

The best gas phase intercalation sample is analysed below. From Figure 4-38 the expanded sample is illustrated. The expansion looks different from that of the electrochemical expansion. The expanded edge is shown in Figure 4-39 and a magnification thereof in Figure 4-40. The residue is visible at the bottom right corner of Figure 4-40 and all over on the surface in Figure 4-39, this residue is more concentrated that that of the electrochemical sample. The surface is also clearly damaged.

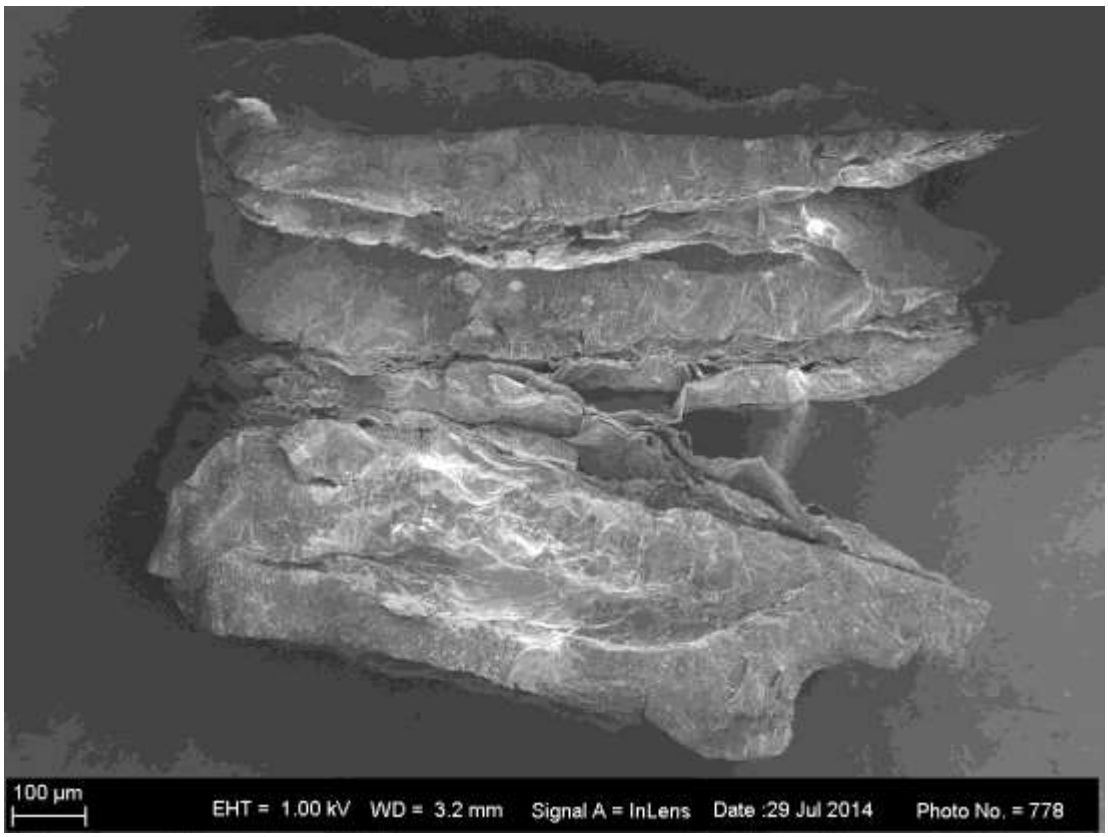

Figure 4-38: SEM of the best gas expanded sample (200x magnification).

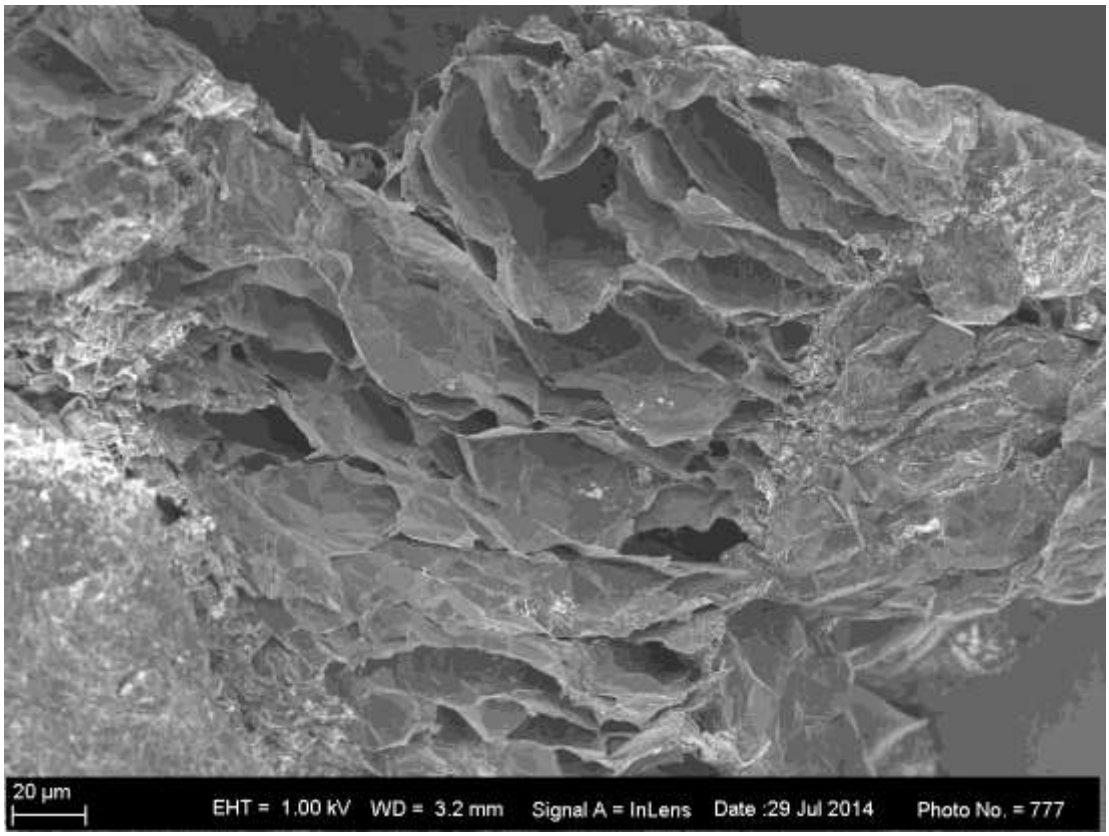

Figure 4-39: SEM of the best gas expanded sample (1000x magnification).

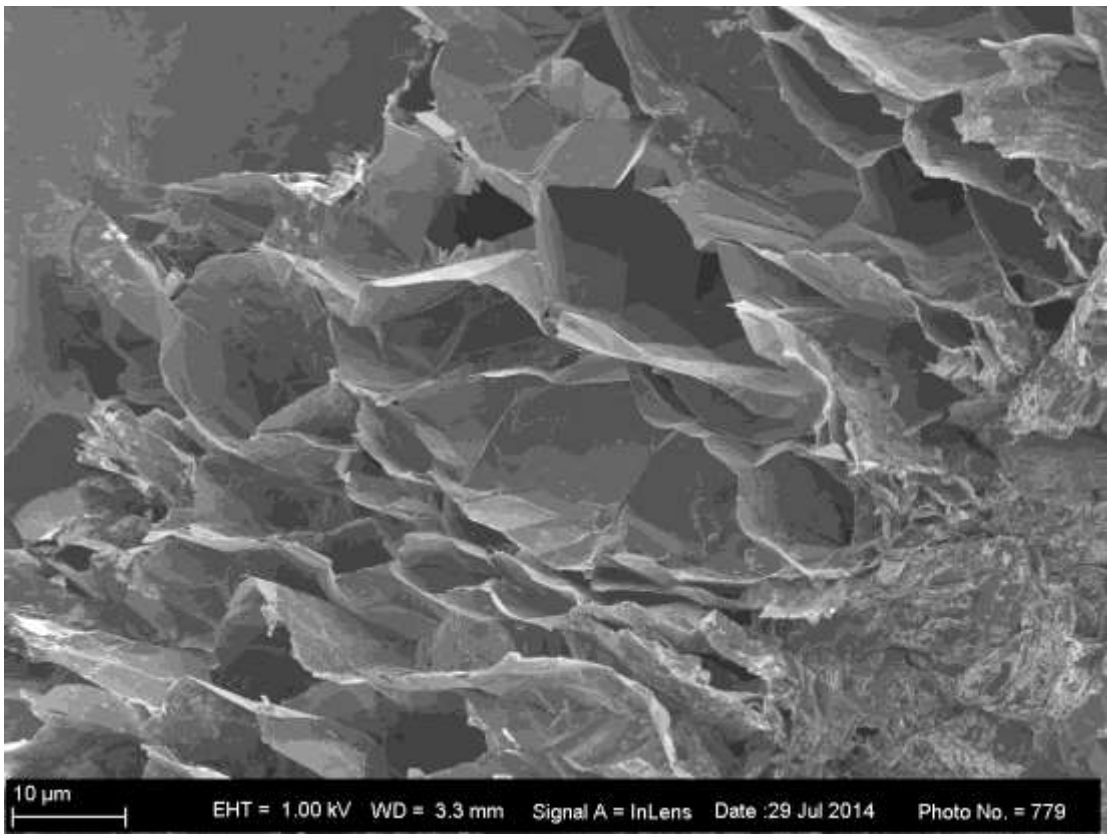

Figure 4-40: SEM of the best gas expanded sample (3000x magnification).

The worst sample of the gas phase intercalation is illustrated in Figure 4-41; this expansion is different from the other two methods. This image shows less expansion, but Figure 4-42 exhibits a very different expansion. This expansion does not show the typical accordion shape, but more similar to bubbles connected at certain places. The surface of the expanded flake on the left of the image is certainly damaged, with deposits on the surface. From Figure 4-43 the edge is magnified, and the damage on the edge is extremely evident, as the edge is rugged. There are also deposits visible. This is even more evident at a higher magnification in Figure 4-44. These deposits are the residual iron chloride on the surface of the graphite. This is evidence that the iron chloride did not bind to the graphite, but merely adheres to the surface.

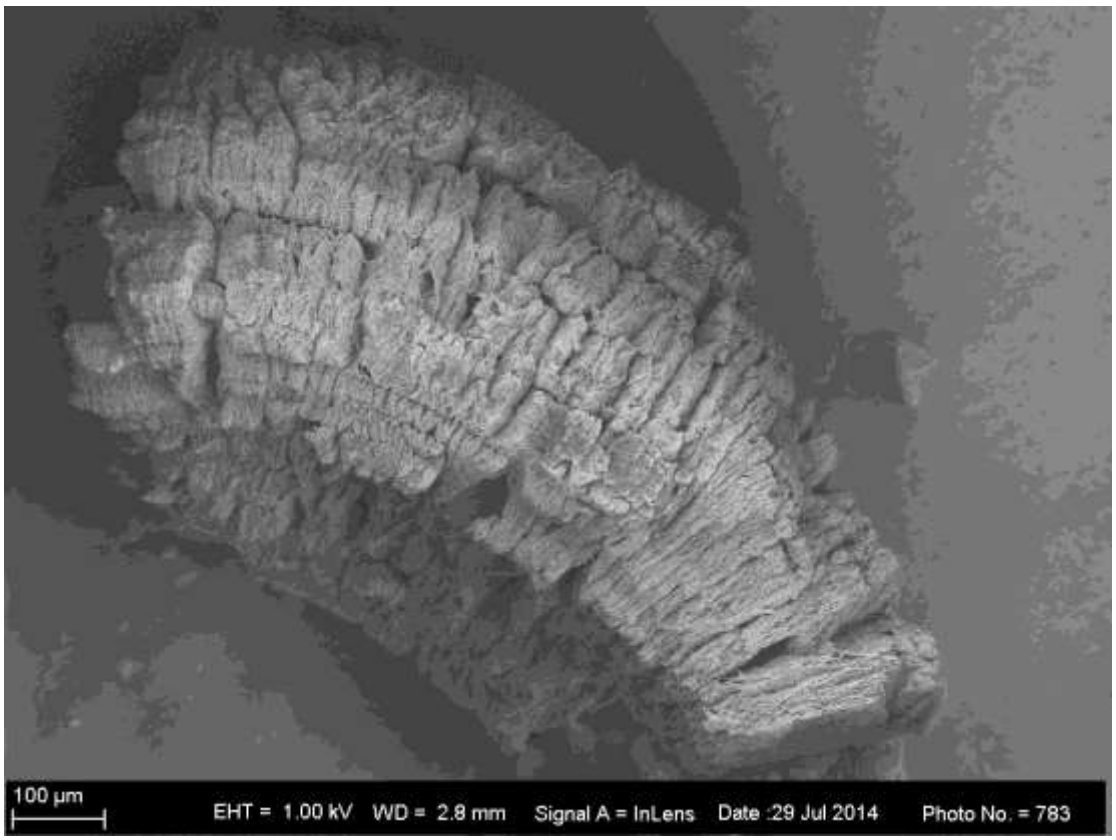

Figure 4-41: SEM of the worst gas expanded sample (250x magnification).

Figure 4-42: SEM of the worst gas expanded sample (140x magnification).

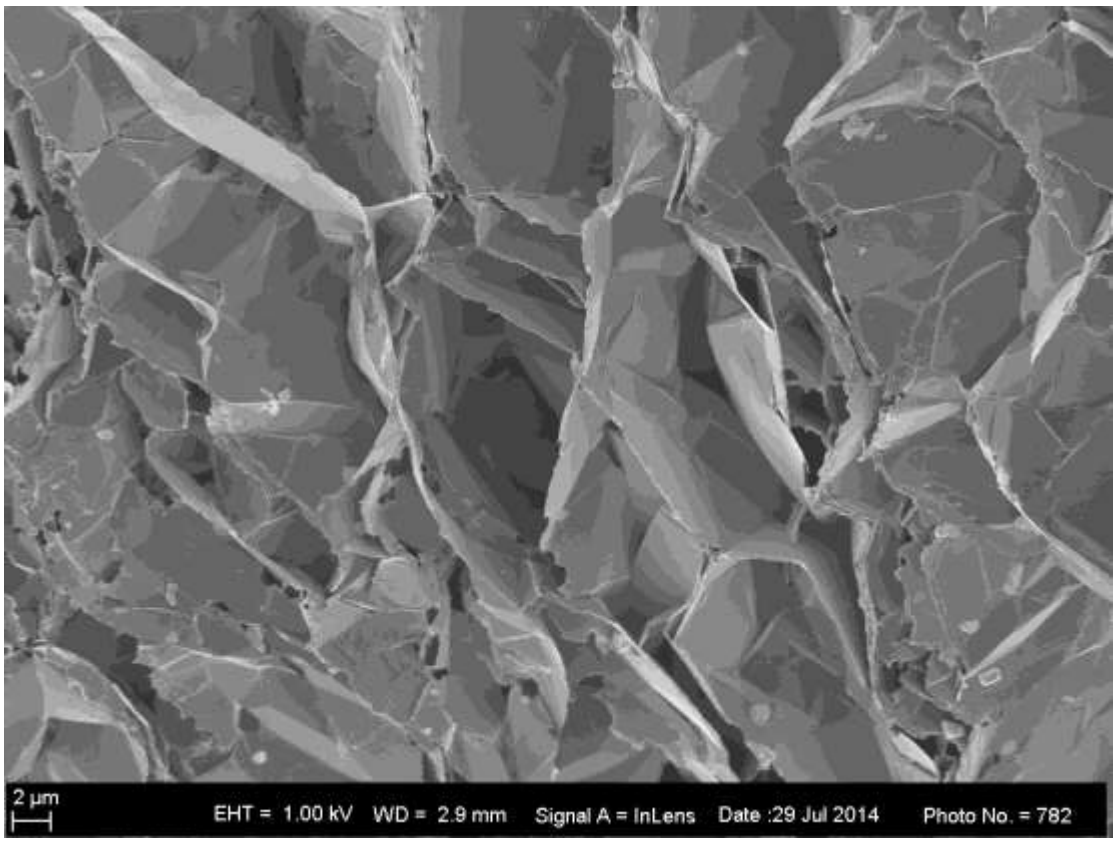

Figure 4-43: SEM of the worst gas expanded sample (5000x magnification).

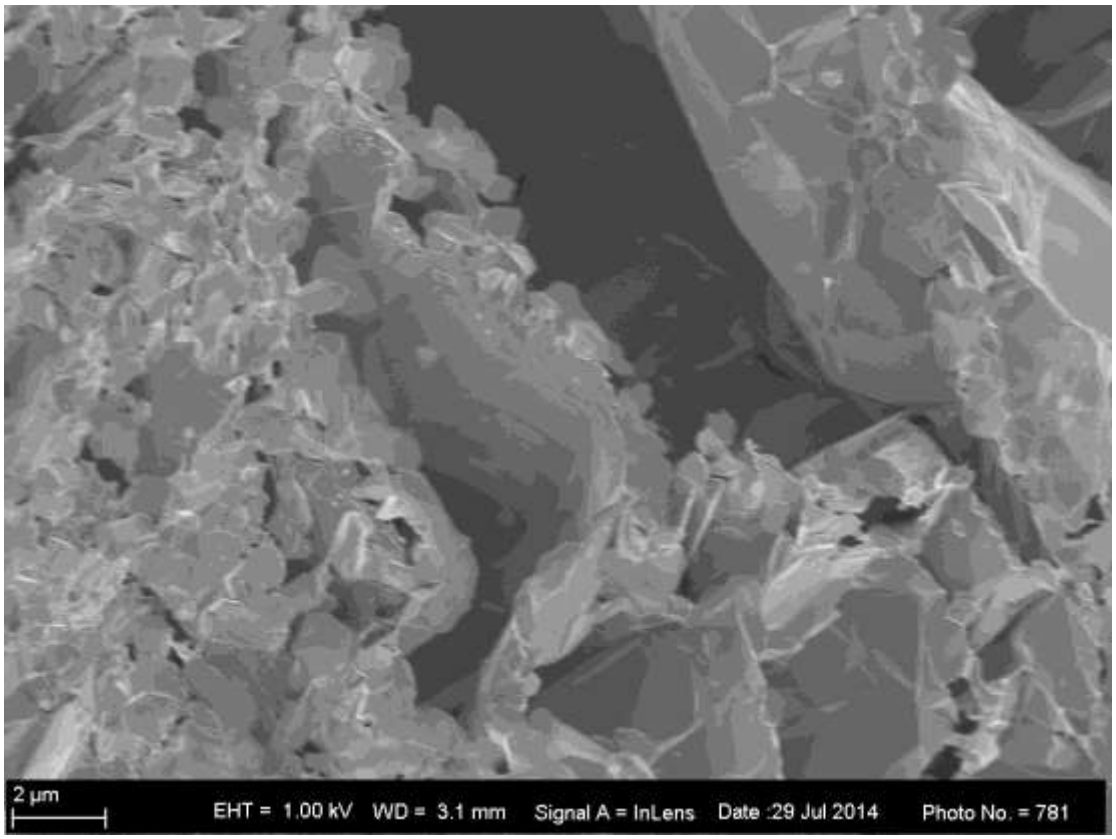

Figure 4-44: SEM of the worst gas expanded sample (13000x magnification).

The best expanded sample for the Hummers intercalation method is analysed below. Figure 4-45 illustrates the expanded flake; this image shows a rather segmented accordion structure. The surface is illustrated in Figure 4-46, the surface is severely damaged, with a lumpy surface, which has been eroded through, resulting in holes through the surface. Figure 4-47 and Figure 4-48 are magnifications of the damaged surface. The surface is extremely damaged with very uneven appearance as well as many holes. Thus far the Hummers method is the most aggressive method which damages the sample the most.

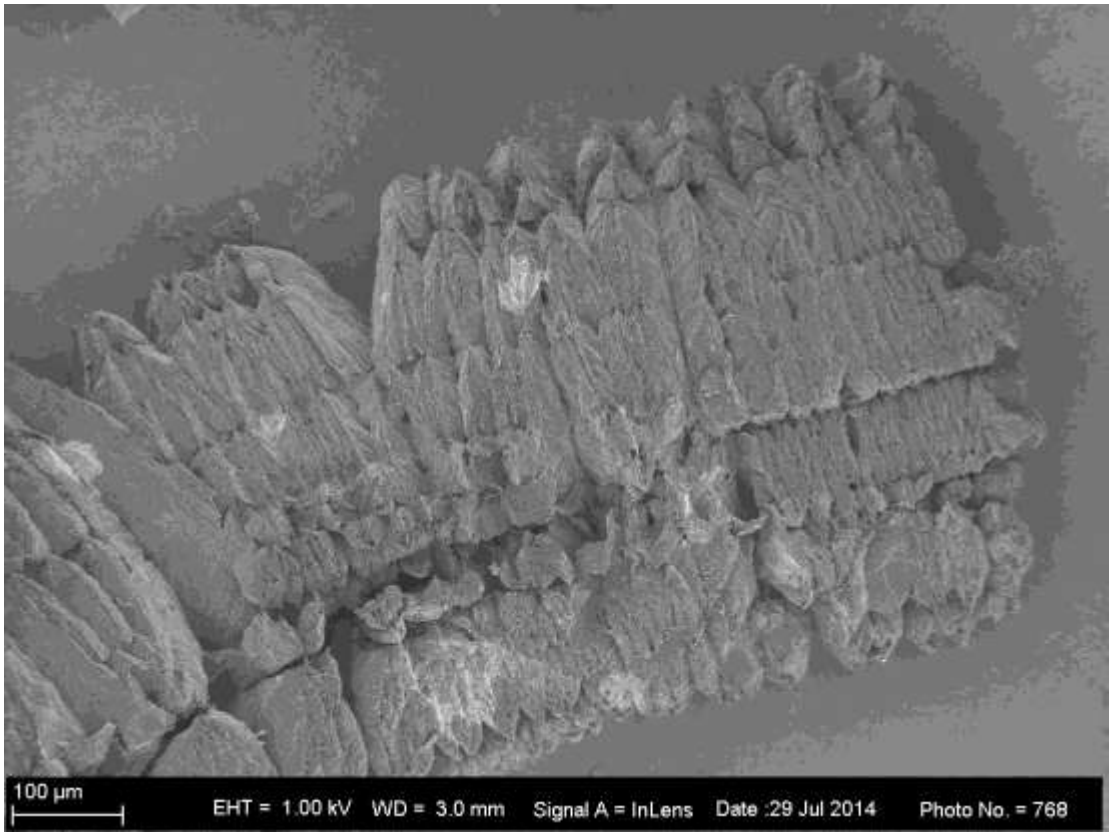

Figure 4-45: SEM of the best Hummers expanded sample (300x magnification).

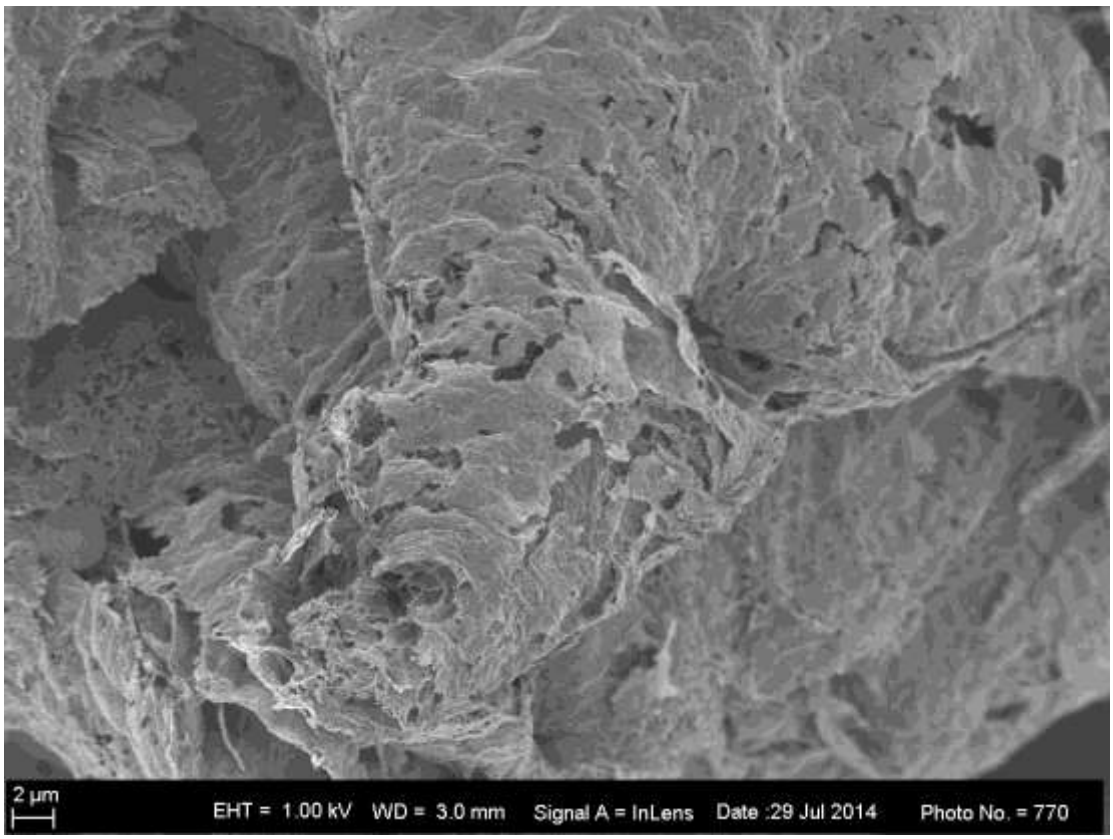

Figure 4-46: SEM of the best Hummers expanded sample (5500x magnification).

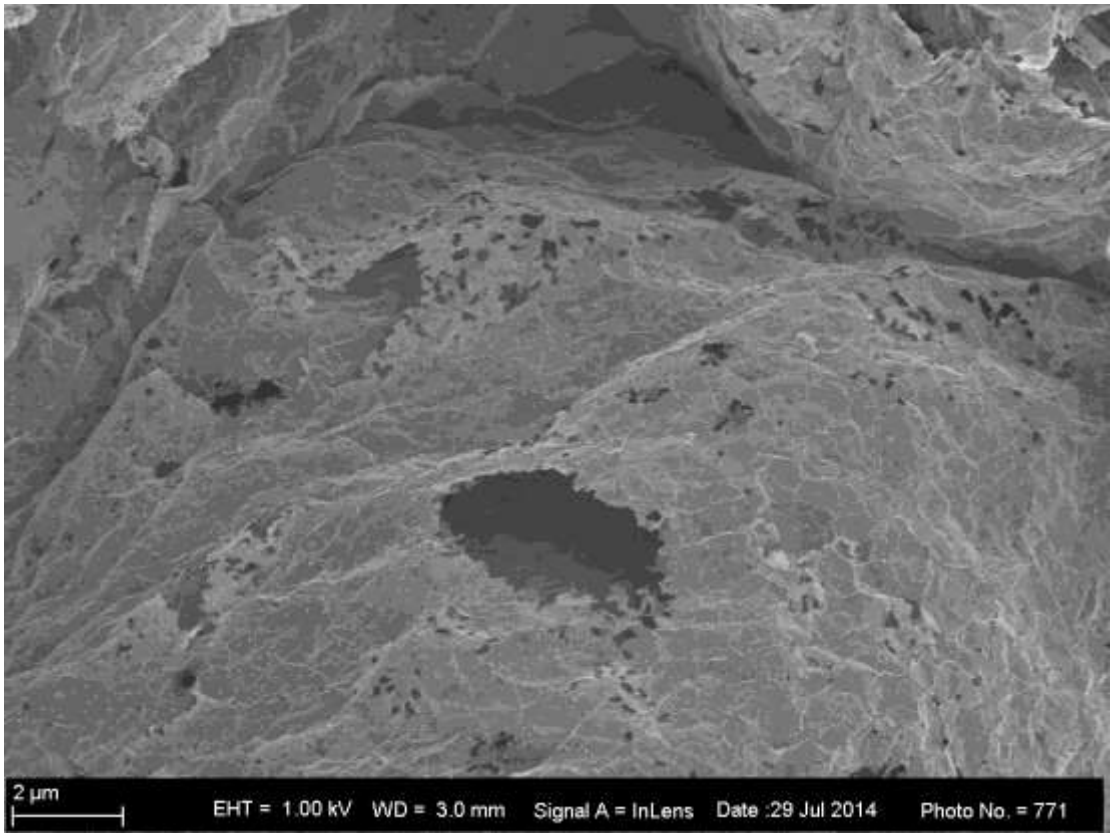

Figure 4-47: SEM of the best Hummers expanded sample (15000x magnification).

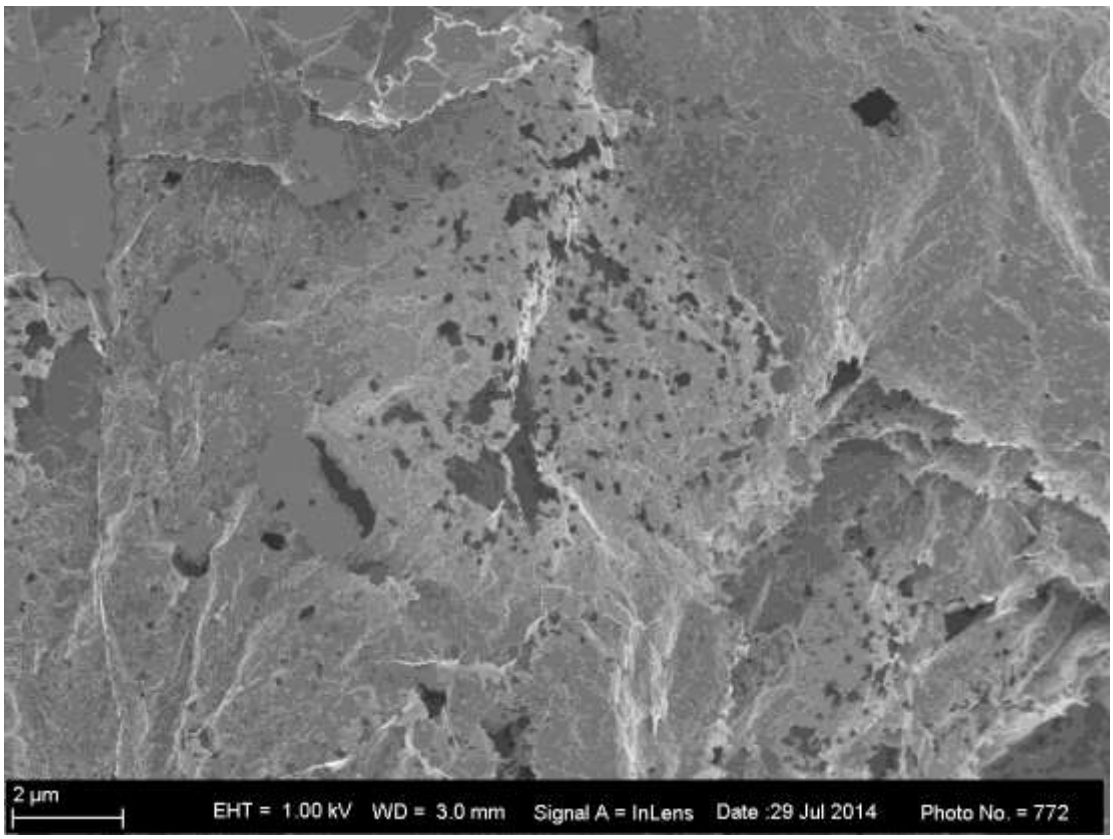

Figure 4-48: SEM of the best Hummers expanded sample (15000x magnification).

The sample of the Hummers method which expanded the least is illustrated in Figure 4-49. This expansion seems to be segmented as well. The expansion is magnified in Figure 4-50 and the surface is magnified in Figure 4-51. The surface is clearly damaged. The surface is uneven with holes visible, and the edges are rugged.

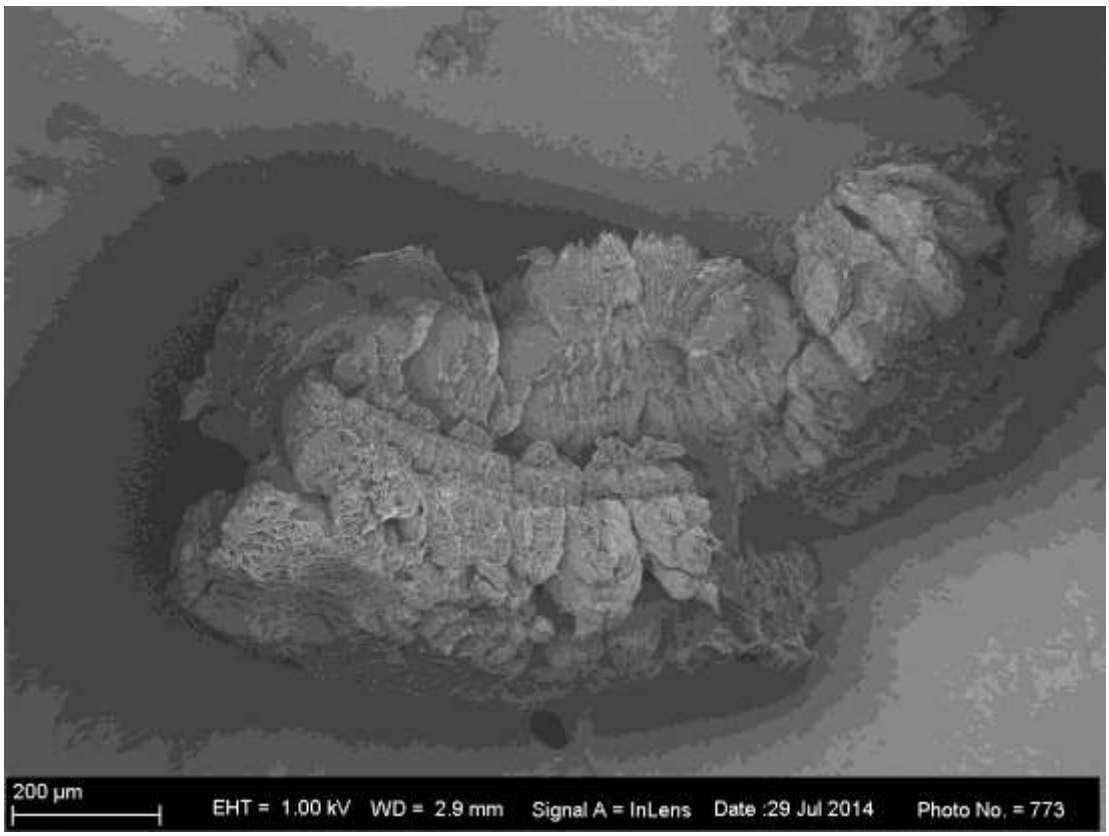

Figure 4-49: SEM of the worst Hummers expanded sample (200x magnification).

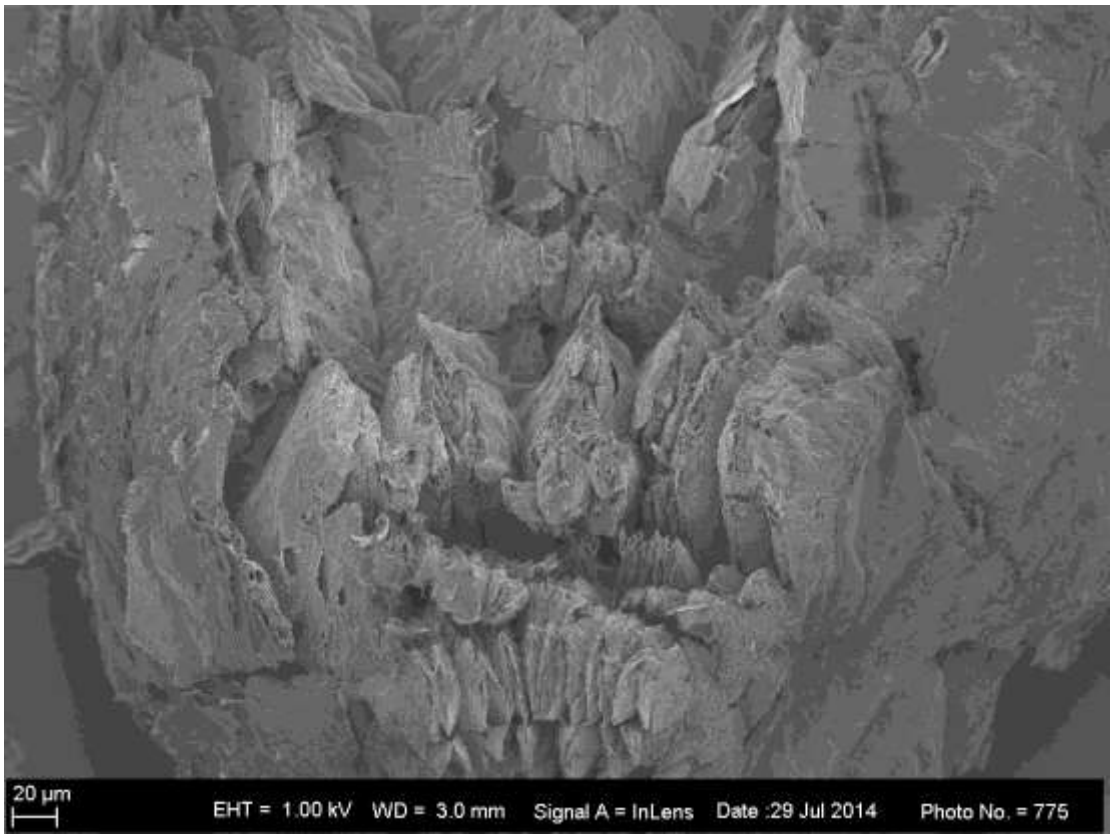

Figure 4-50: SEM of the worst Hummers expanded sample (600x magnification).

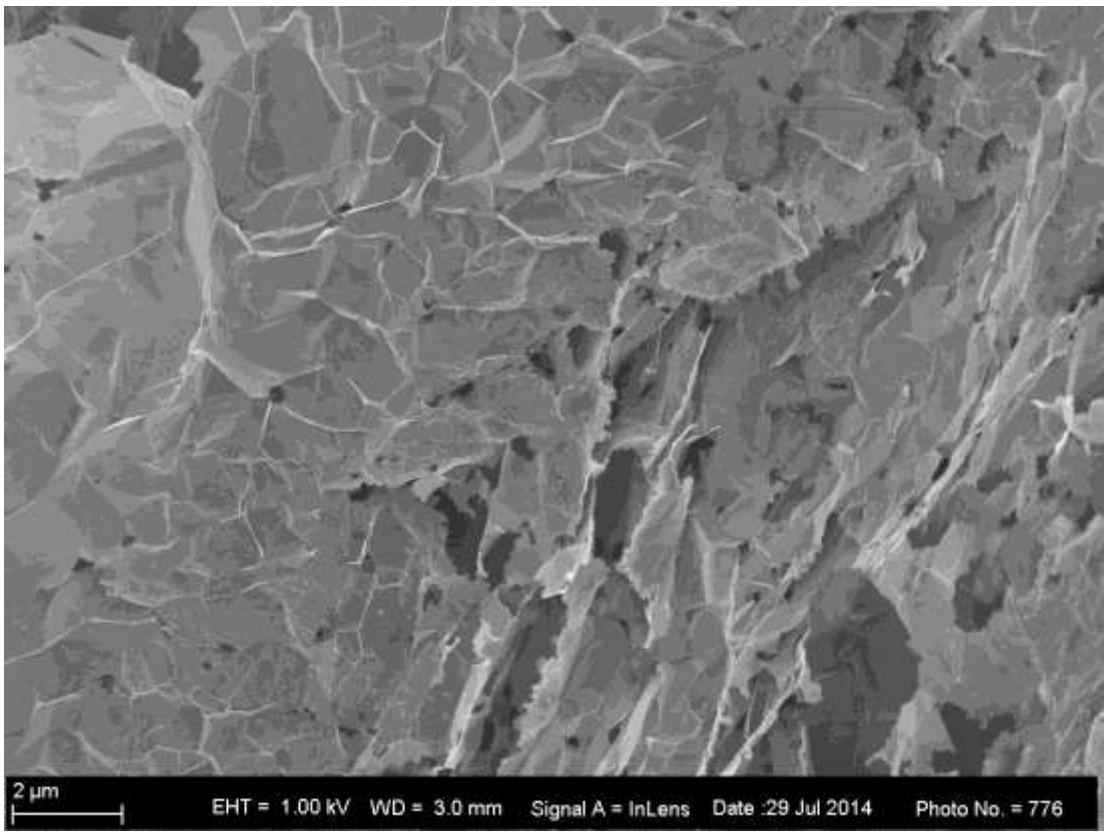

Figure 4-51: SEM of the worst Hummers expanded sample (15000x magnification).

4.7.4 Purified Samples

All the samples were sonicated in order to break the layers into few-layered graphite to view the surface and edges of the samples with more ease. The samples were then purified to remove all impurities, and so the damage can be examined. The different bulk samples are observed in the following images. Figure 4-52 illustrates the purified electrochemical sample; Figure 4-53 the best gas phase, and Figure 4-54 the worst gas phase intercalation sample. The best and worst Hummers intercalation samples are illustrated in Figure 4-55 and Figure 4-56 respectively, whereas Figure 4-57 is a magnification of the worst Hummers intercalation method. All the images are 500 times magnified, except the best Hummers, so the images are very comparable. Figure 4-53 shows slightly bigger flakes, compared to Figure 4-52. This suggests that the sonication was not as effective. Figure 4-54 illustrates a scarce amount of flakes. Comparing Figure 4-55 and Figure 4-56 is at the same magnification, and Figure 4-56 clearly has bigger flakes, with Figure 4-57 at the same magnification as the electrochemical and gas phase intercalation methods. This figure clearly shows that the flake is notably larger.

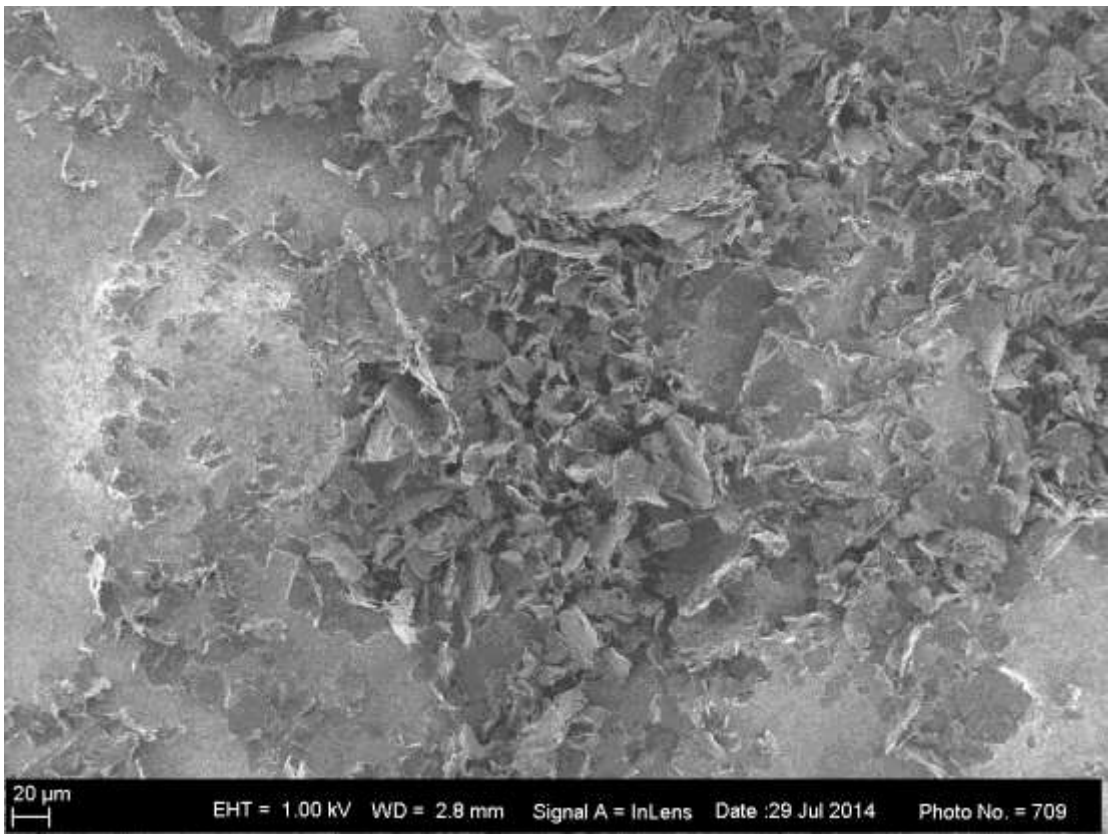

Figure 4-52: SEM of purified electrochemical sample (500x magnification).

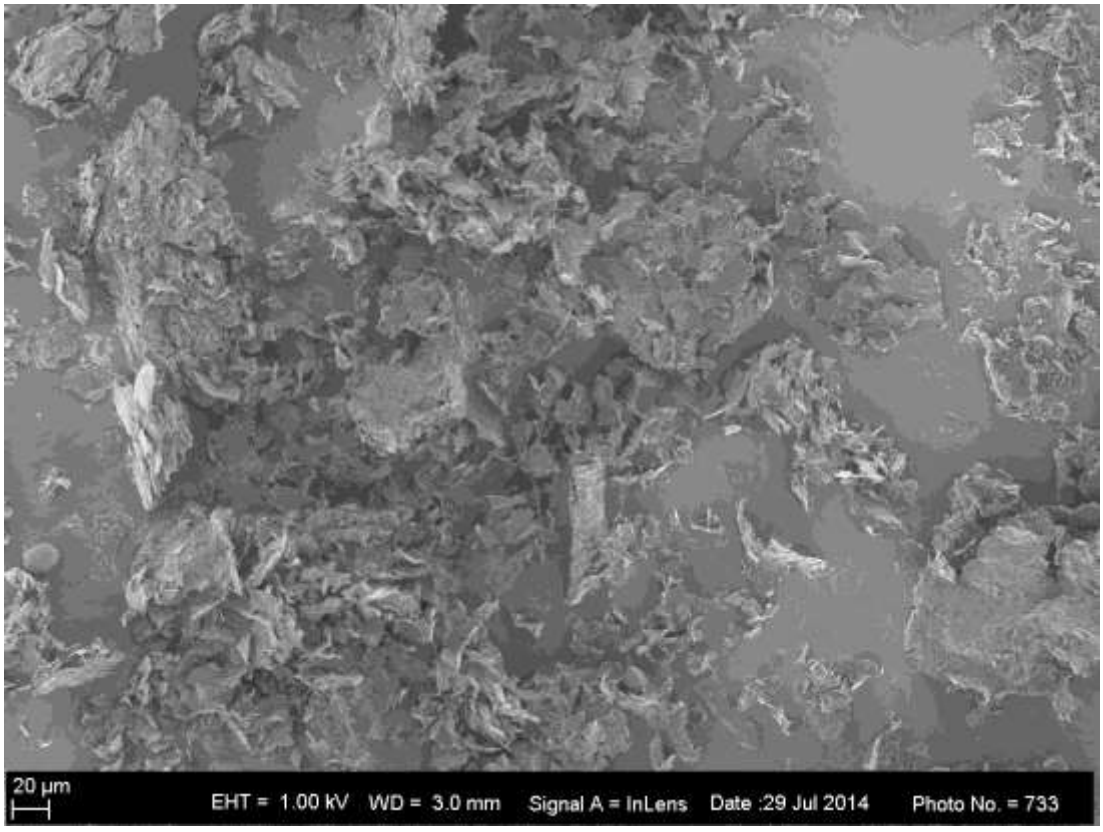

Figure 4-53: SEM of purified best gas phase sample (500x magnification).

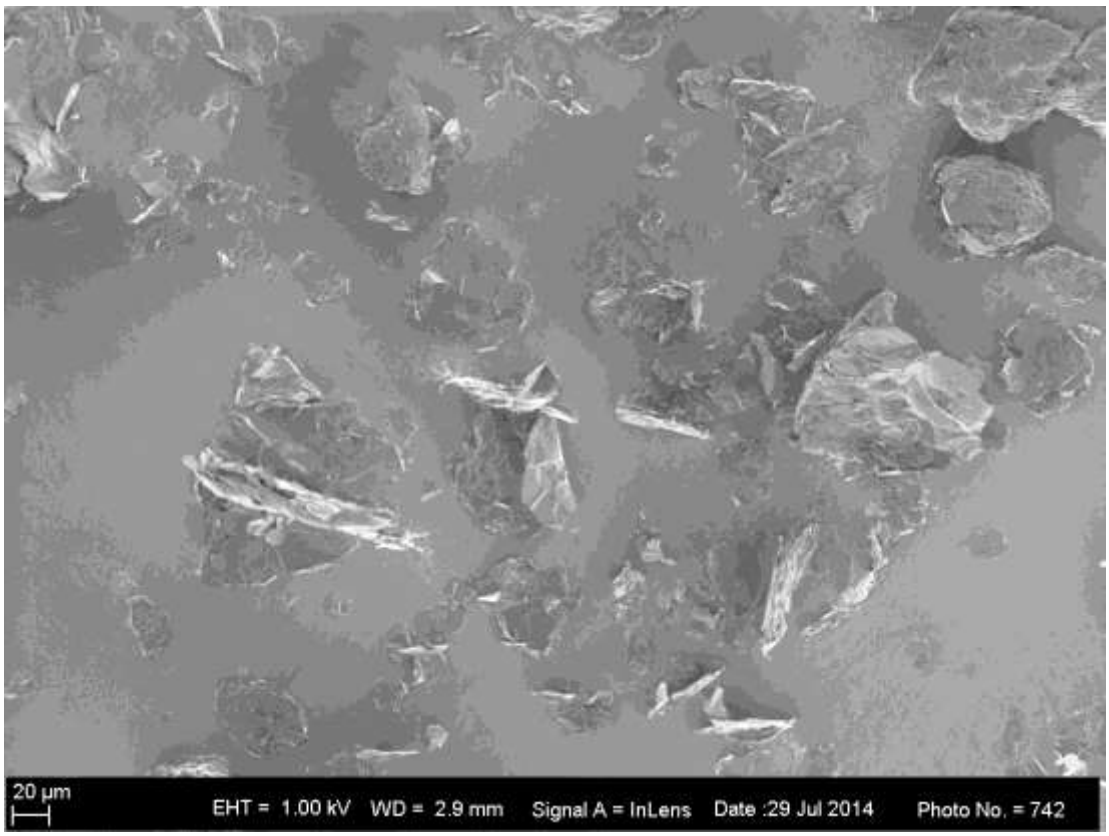

Figure 4-54: SEM of purified worst gas phase sample (500x magnification).

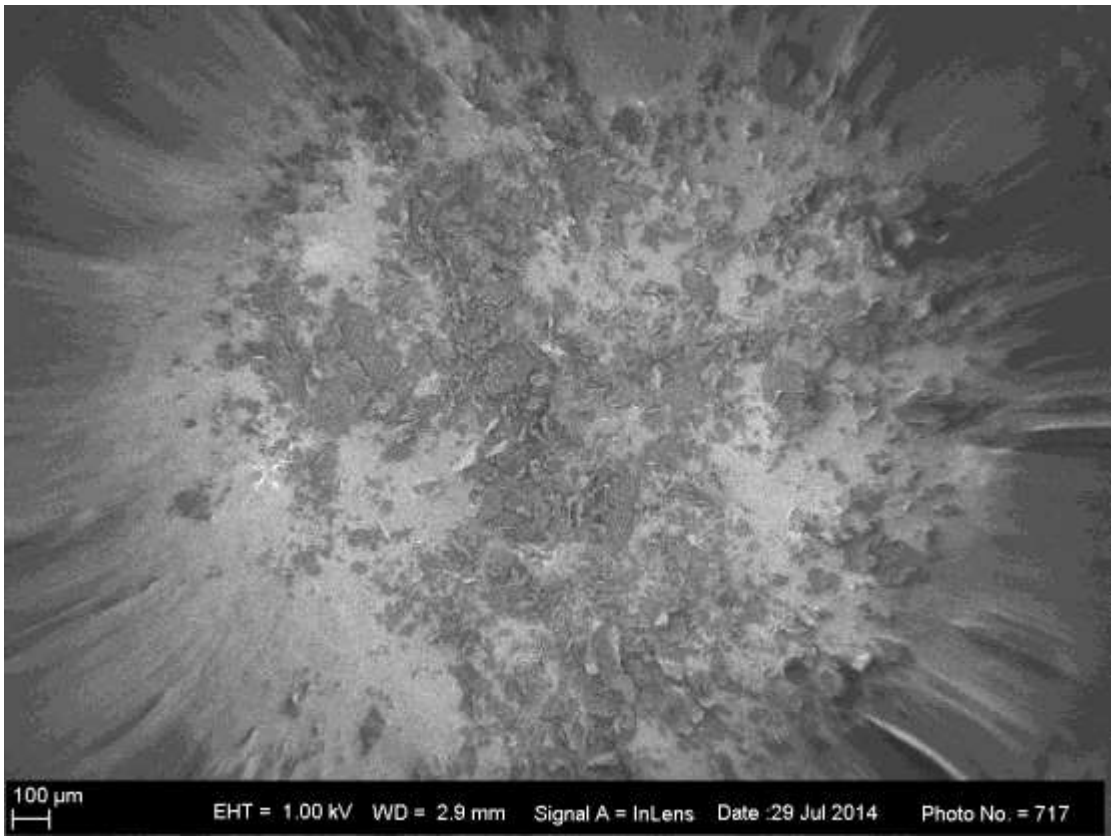

Figure 4-55: SEM of purified best Hummers sample (100x magnification).

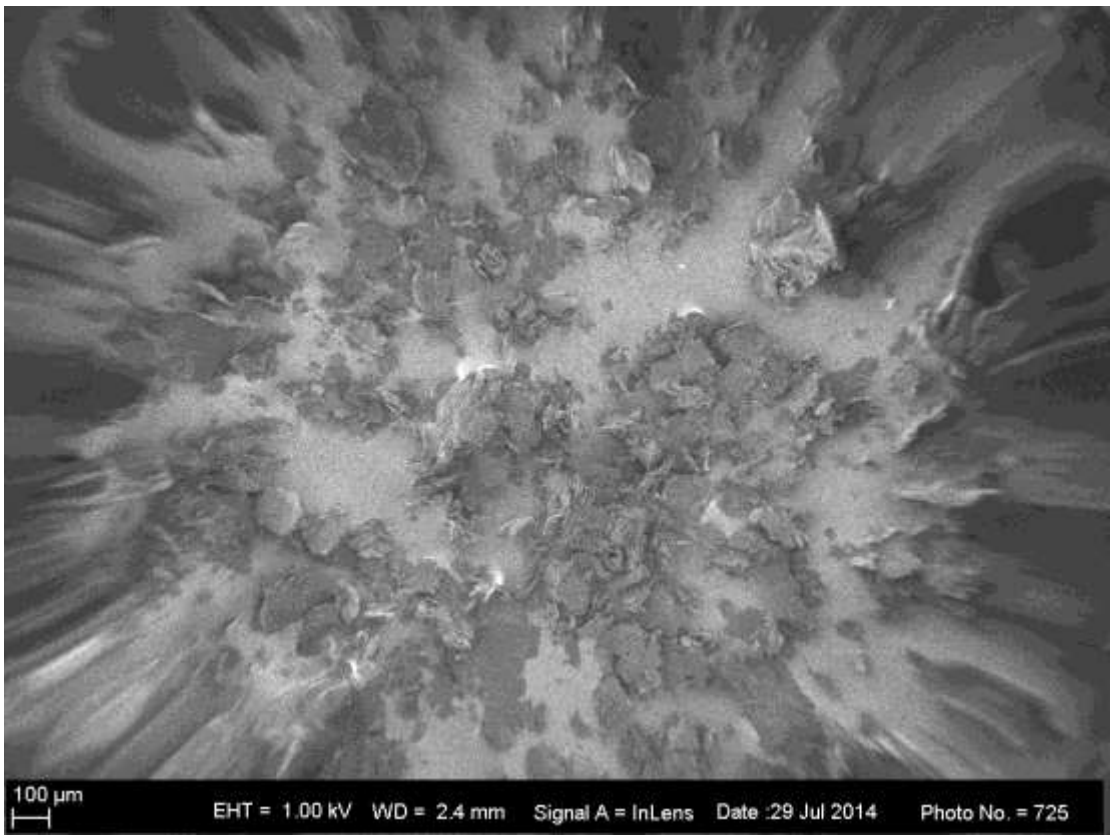

Figure 4-56: SEM of purified worst Hummers sample (100x magnification).

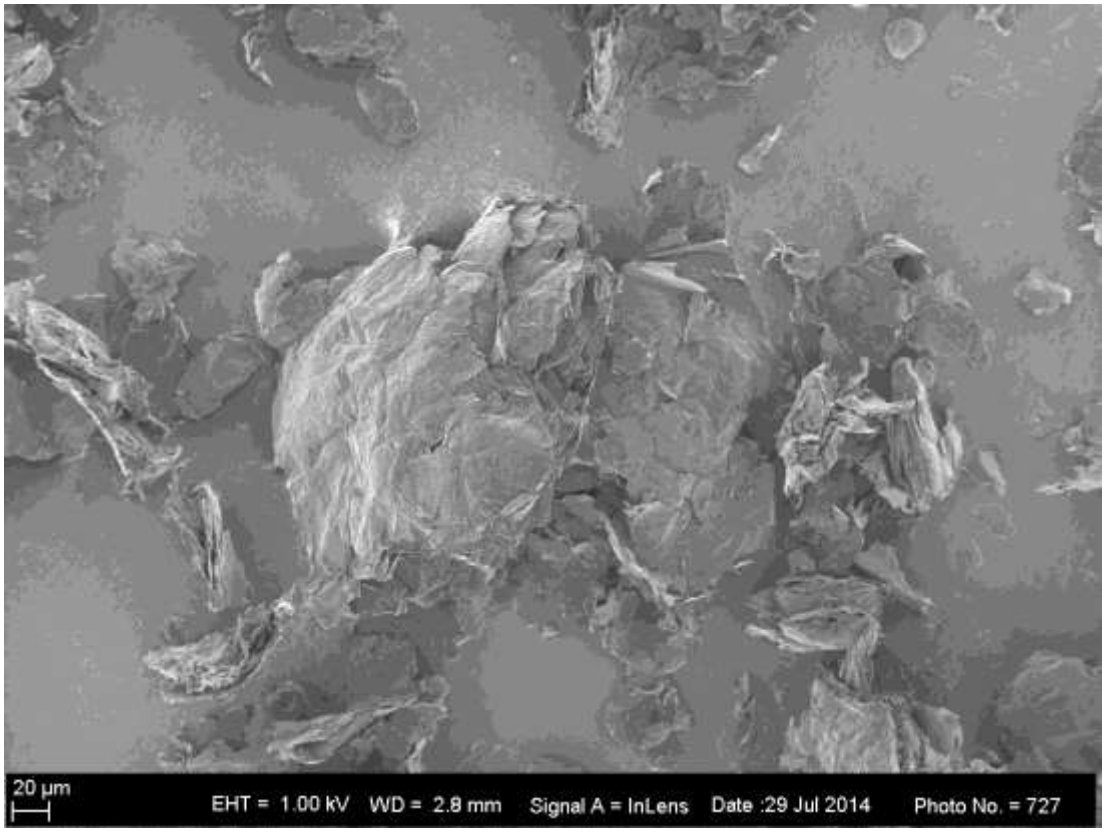

Figure 4-57: SEM of purified worst Hummers sample (500x magnification).

These figures are magnified and compared. Figure 4-58 and Figure 4-59 are images of the electrochemical intercalation method magnified 5000 times. The best gas phase sample is magnified 8000 times in Figure 4-60, whereas the worst gas phase is magnified 5000 times in both Figure 4-61 and Figure 4-62. Figure 4-63 (4000x) and Figure 4-64 (6000x) are the best Hummers intercalation sample and Figure 4-65 the worst Hummers sample magnified 5000 times.

It is very clear that the surface of the electrochemical sample is damaged, and uneven. The best gas phase sample also has uneven surface, but it is certainly less damaged than that of electrochemical sample, and the edges are rougher. The first image of the worst gas phase sample illustrates the basal plane, which is more crystalline than the electrochemical sample, whereas the next image shows the edge which is clearly more damaged. The edge of the best Hummers intercalation in the first image is the most damaged, but the basal plane, in the next image, is enormously damaged. The worst Hummers sample is not as damaged, with uneven surface. The best Hummers sample is the most damaged.

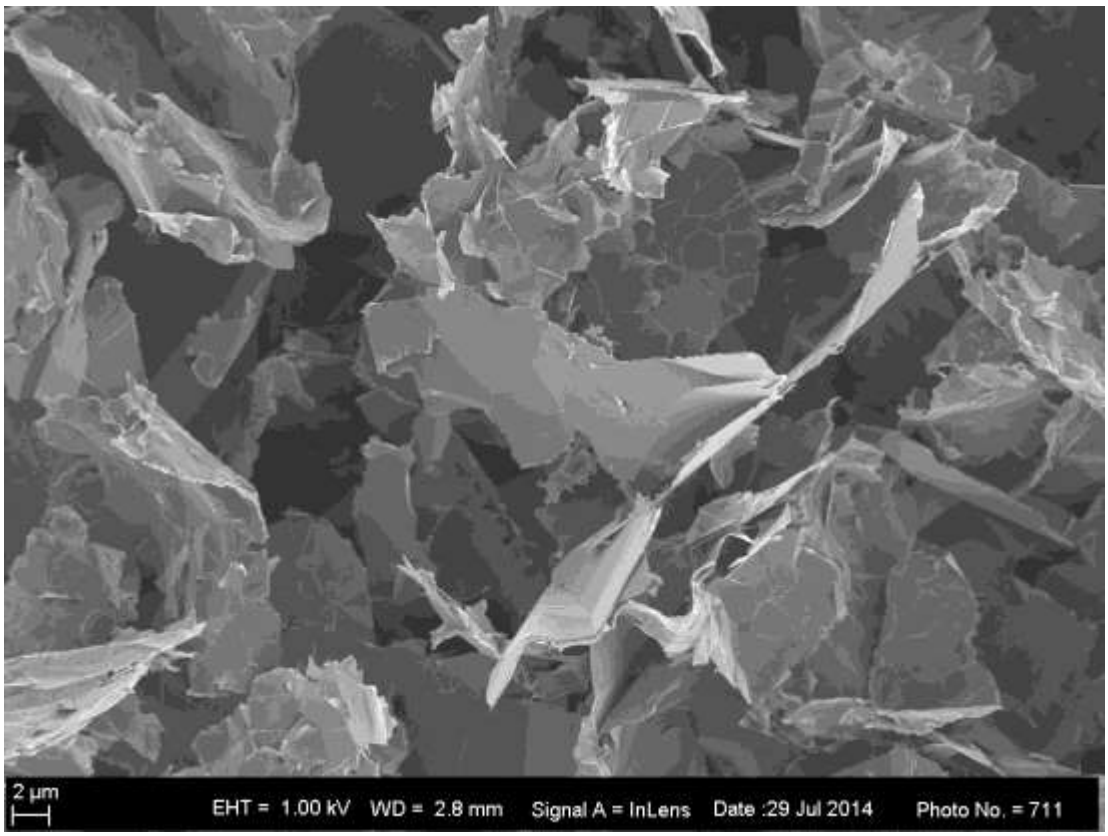

Figure 4-58: SEM of purified electrochemical sample (5000x magnification).

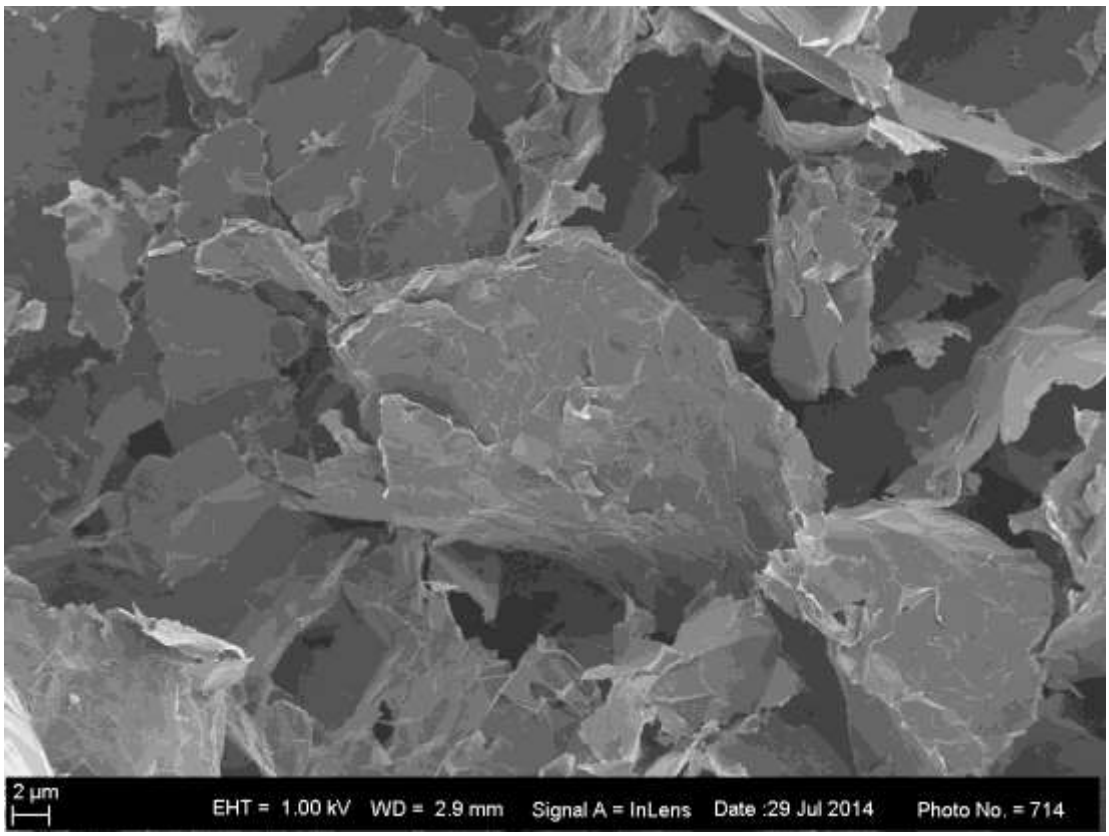

Figure 4-59: SEM of purified electrochemical sample (5000x magnification).

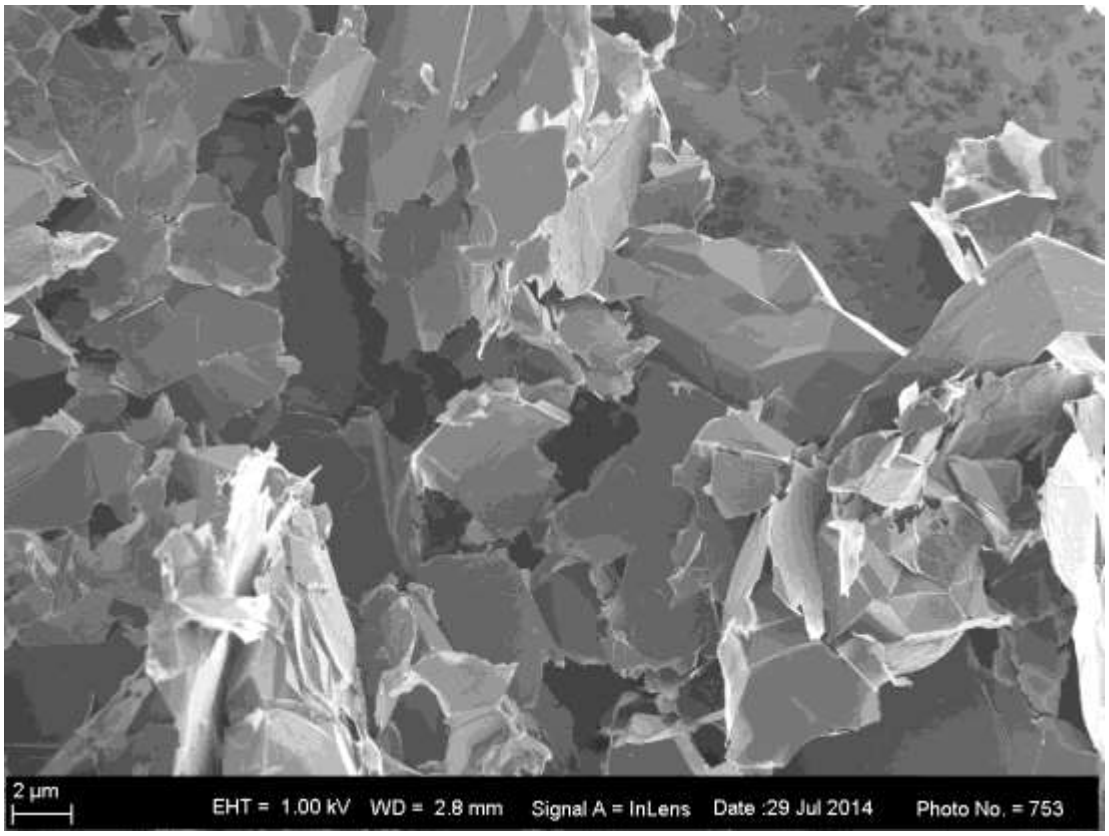

Figure 4-60: SEM of purified best gas sample (8000x magnification).

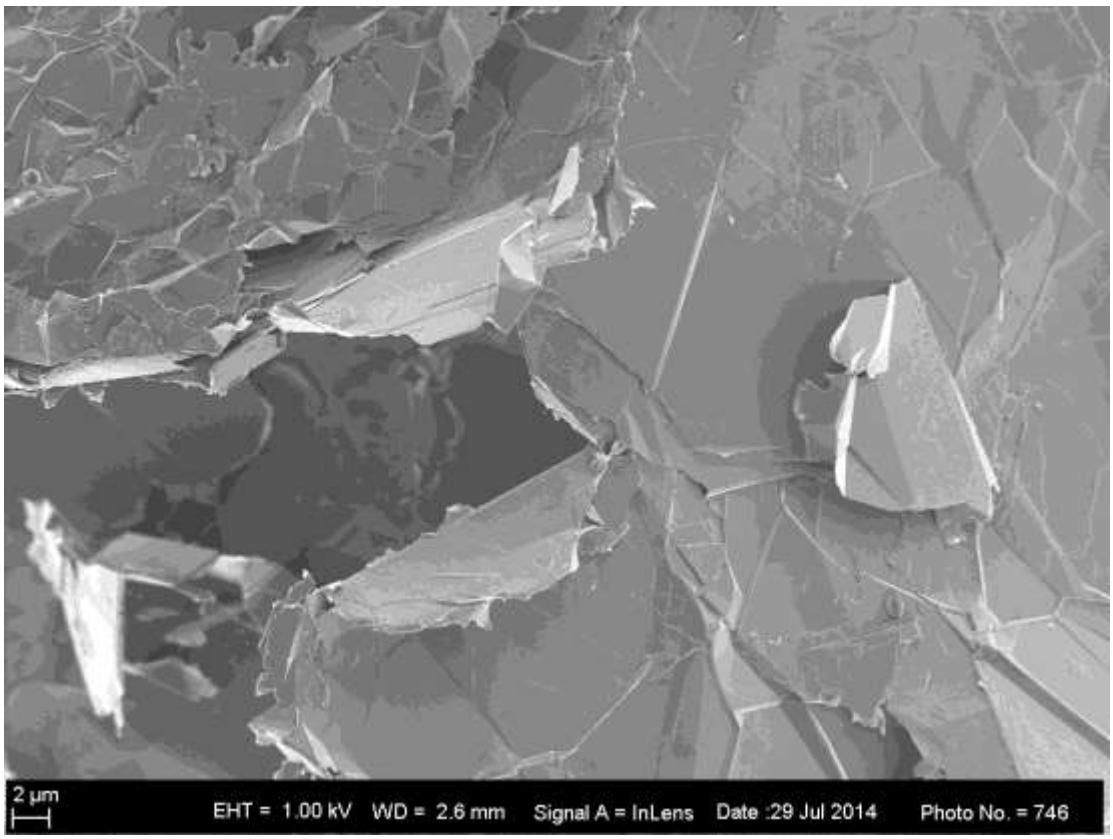

Figure 4-61: SEM of purified worst gas phase sample (5000x magnification).

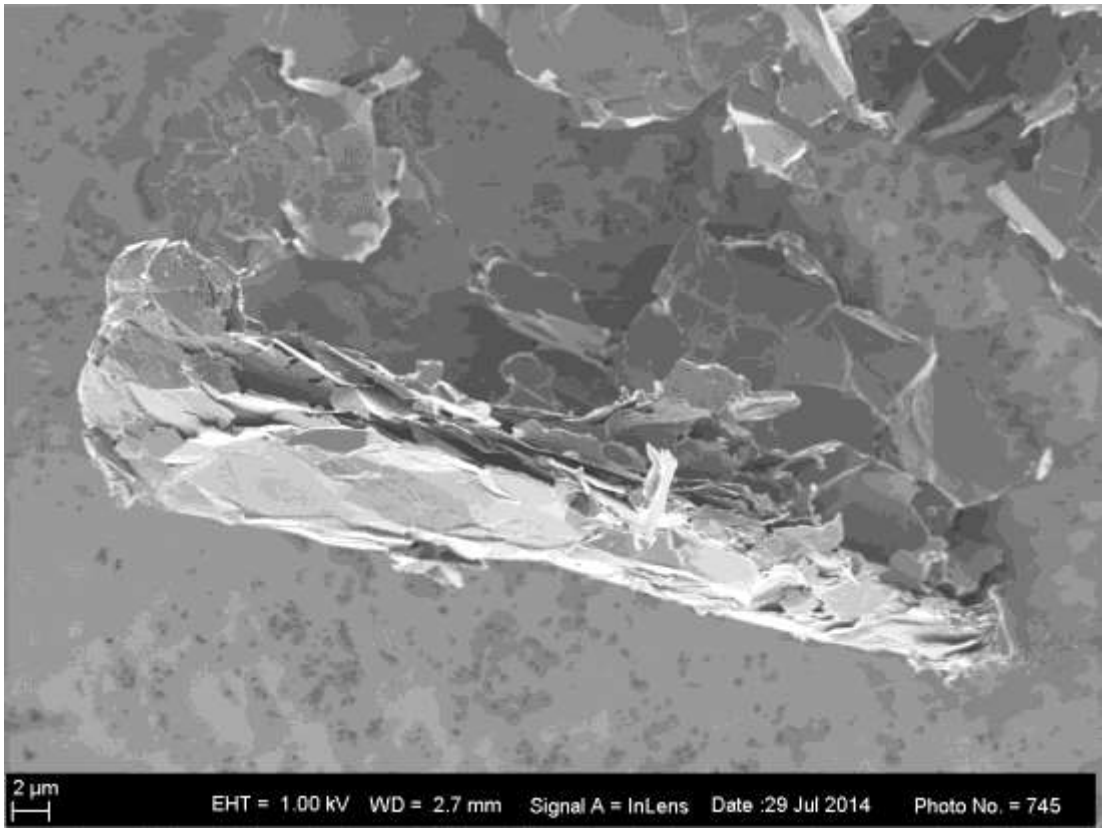

Figure 4-62: SEM of purified worst gas phase sample (5000x magnification).

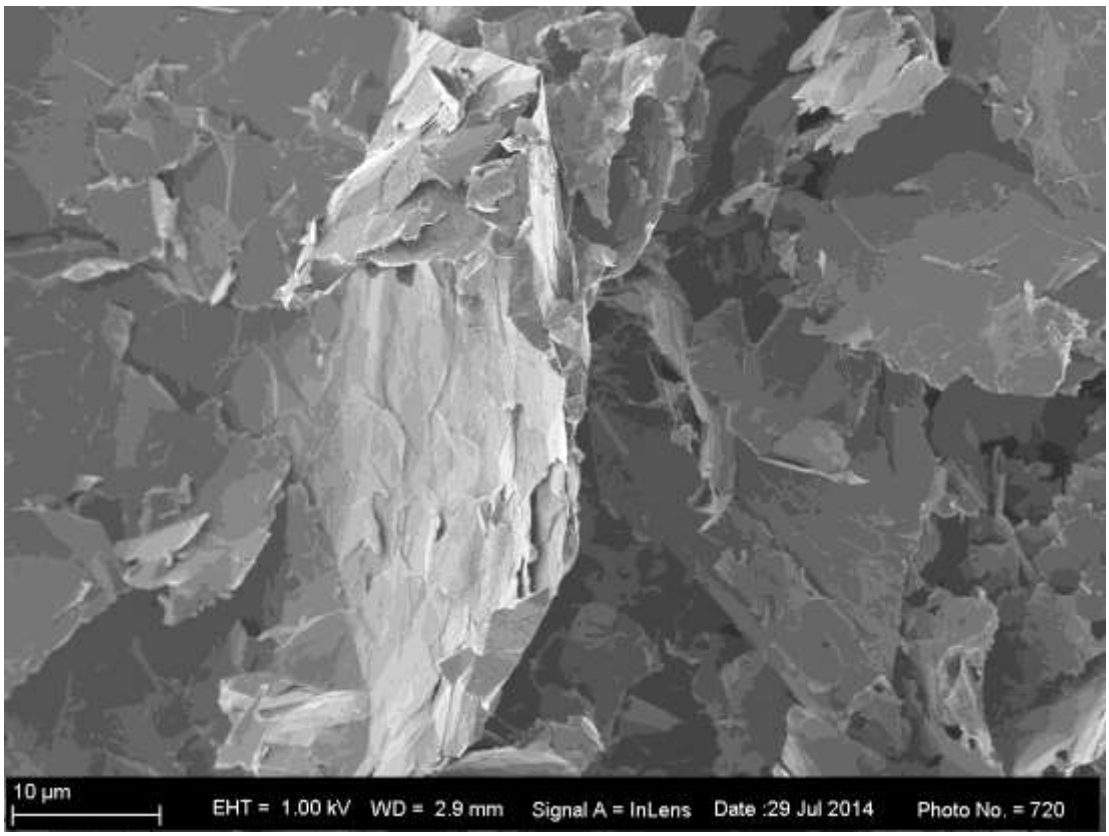

Figure 4-63: SEM of purified best Hummers sample (4000x magnification).

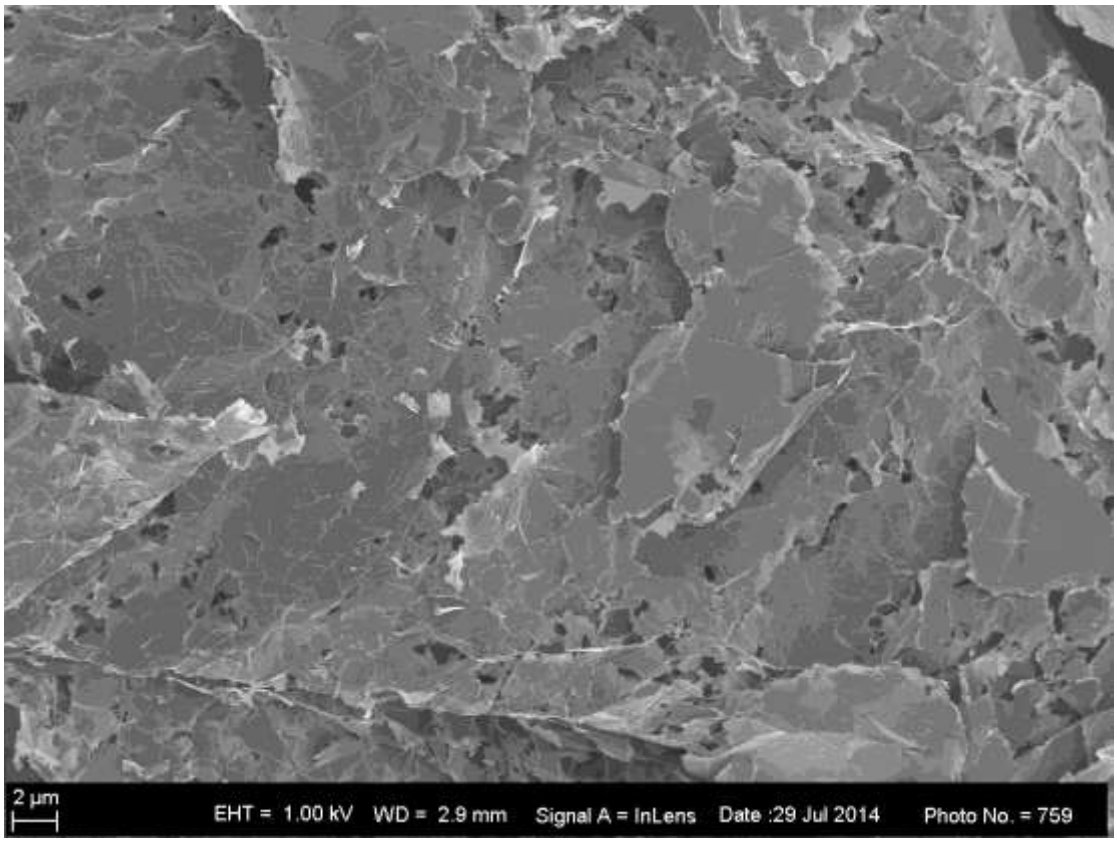

Figure 4-64: SEM of purified best Hummers sample (6000x magnification).

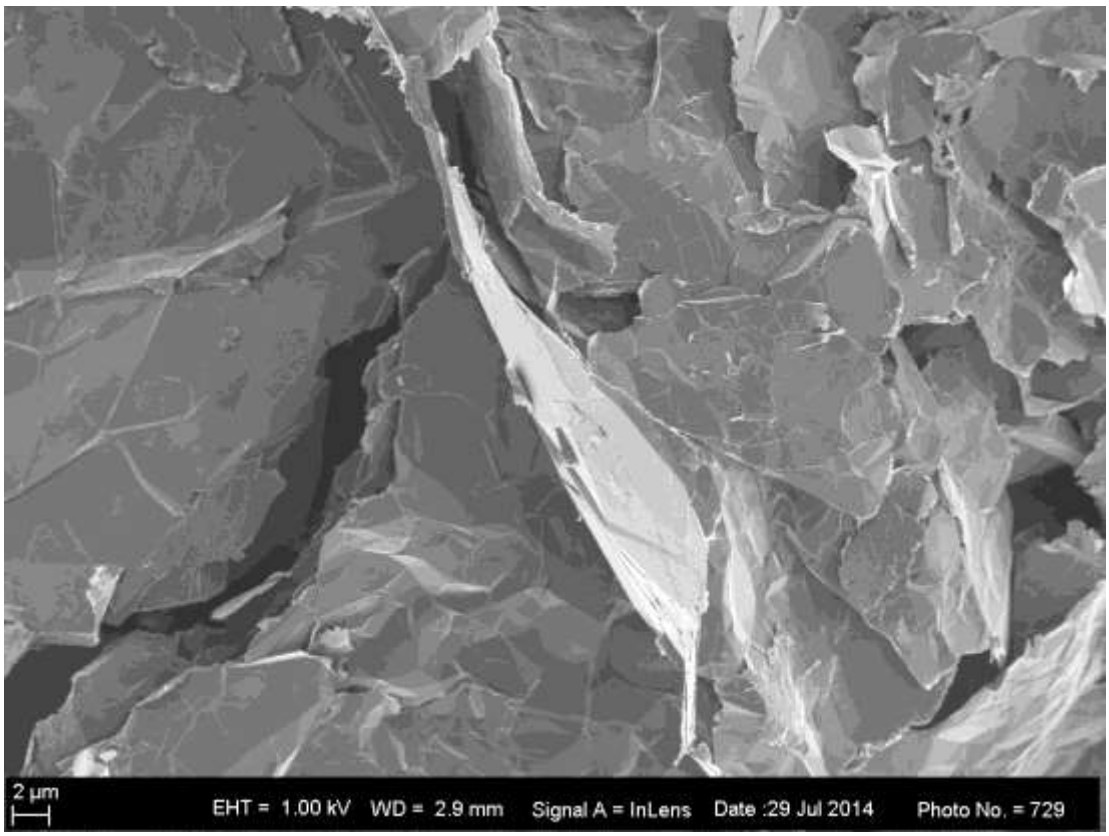

Figure 4-65: SEM of purified worst Hummers sample (5000x magnification).

The images are even more magnified to compare the basal plane and edges of the various samples. The electrochemical sample is magnified 10000 times and 20000 times in Figure 4-66 and Figure 4-67. The best gas phase sample is magnified 10000 times in Figure 4-68 and Figure 4-70, and 20000 times in Figure 4-69 and Figure 4-71. The best Hummers sample is magnified 10000 times and 15000 times in Figure 4-72 and Figure 4-73, whereas in Figure 4-74 and Figure 4-75 the worst Hummers sample is magnified 10000 times and 20000 times respectively.

The basal plane of the electrochemical sample is uneven and rough (Figure 4-6), and the few-layered structure from the sonication is evident (Figure 4-67). The gas phase sample has a more uneven surface (bottom right corner of Figure 4-68). The damage incurred onto the surface of the gas phase sample is apparent (Figure 4-70), the flakes are broken, small and the edges are rough. The basal plane at 20000 times magnification is smooth. The best Hummers sample is clearly the most damaged. The basal plane is visibly very uneven and the edge is very rough. The worst Hummers sample is also uneven and rough (Figure 4-74 and Figure 4-75).

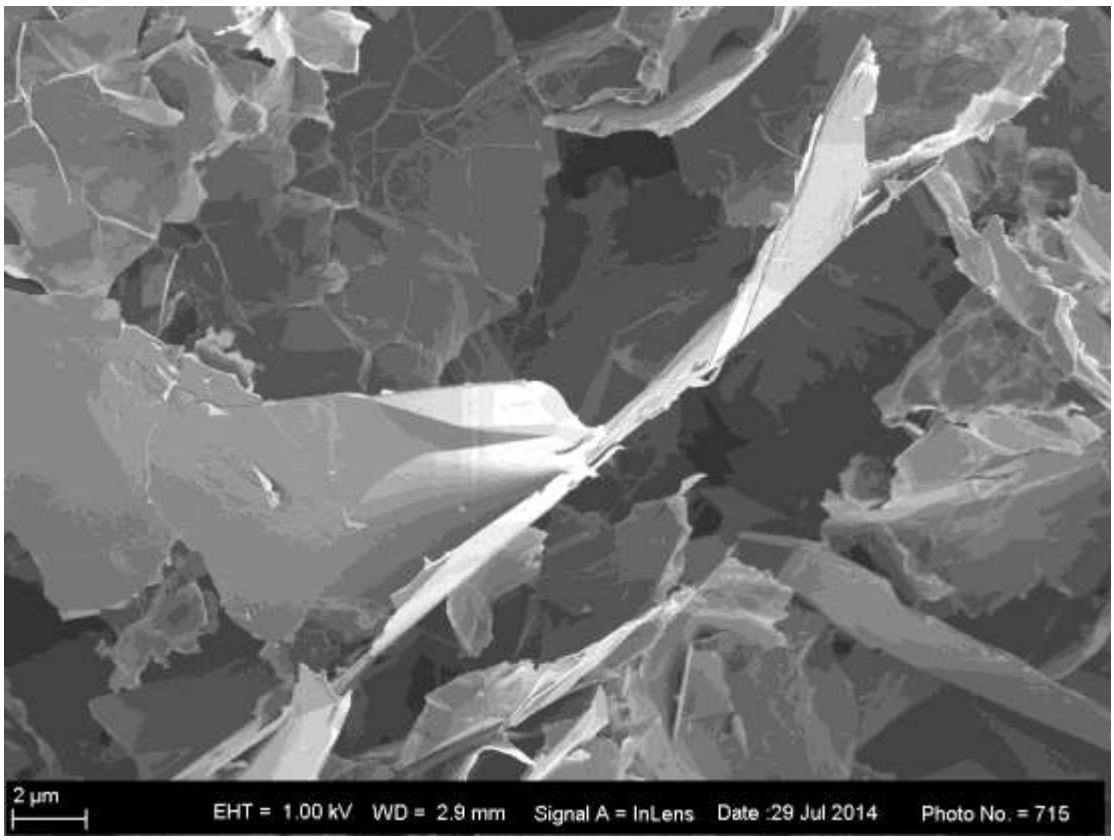

Figure 4-66: SEM of purified electrochemical sample (10000x magnification).

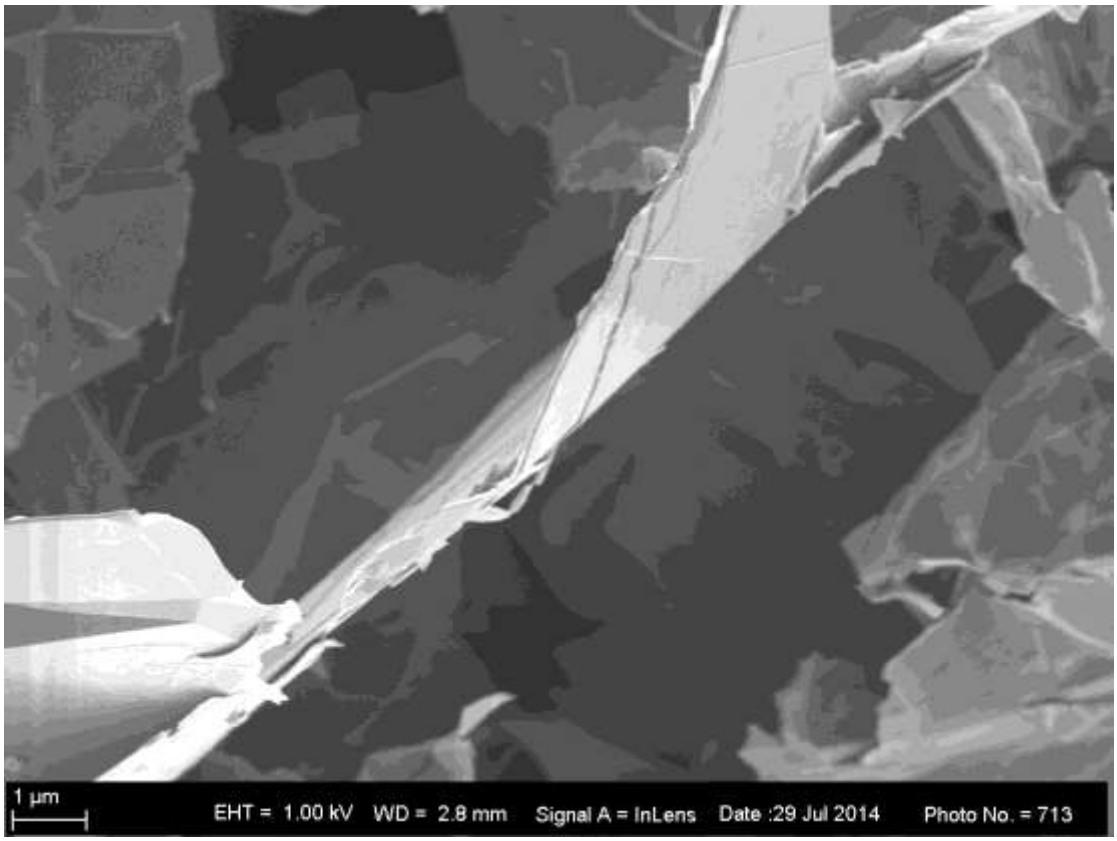

Figure 4-67: SEM of purified electrochemical sample (20000x magnification).

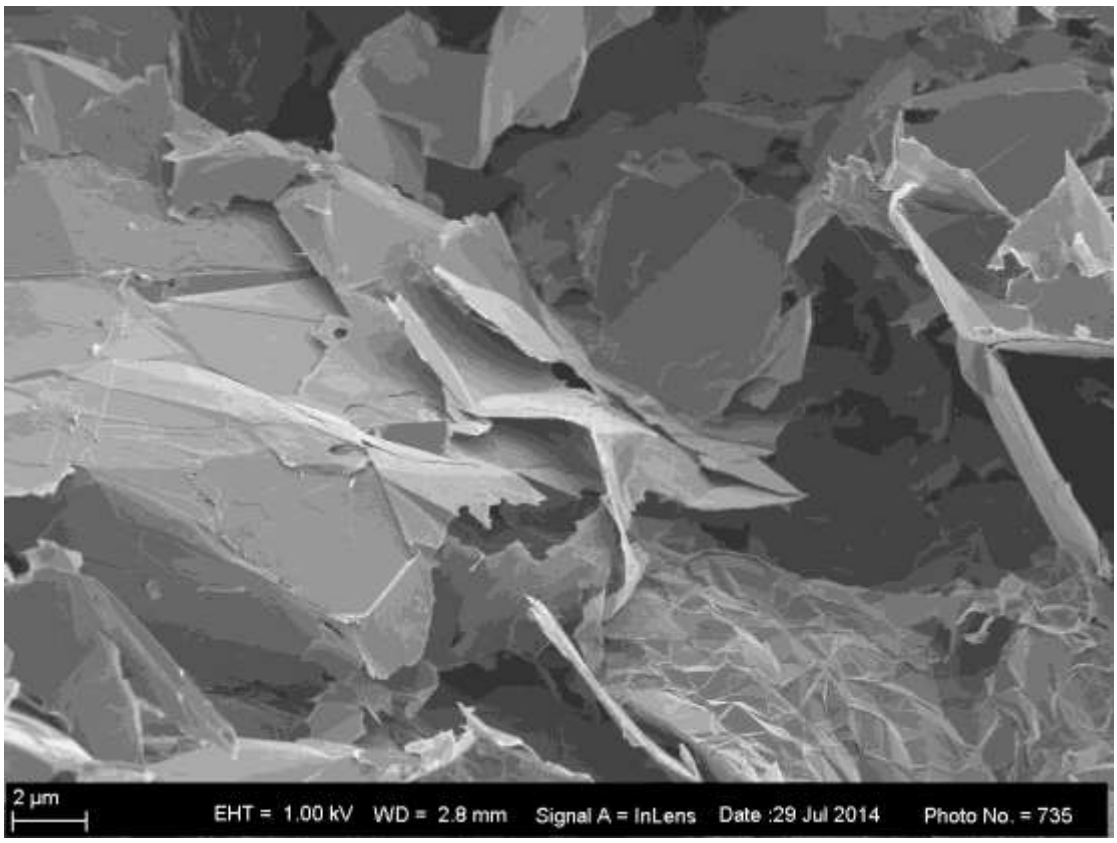

Figure 4-68: SEM of purified best gas phase sample (10000x magnification).

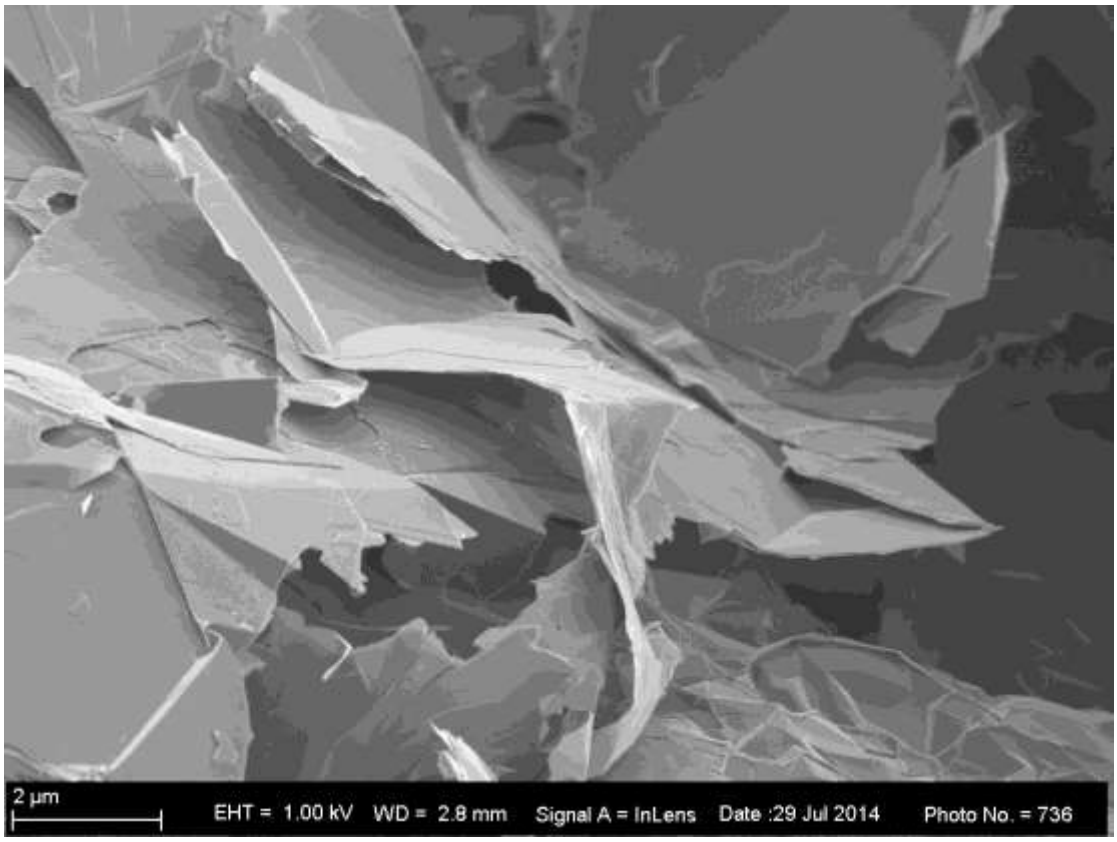

Figure 4-69: SEM of purified best gas phase sample (20000x magnification).

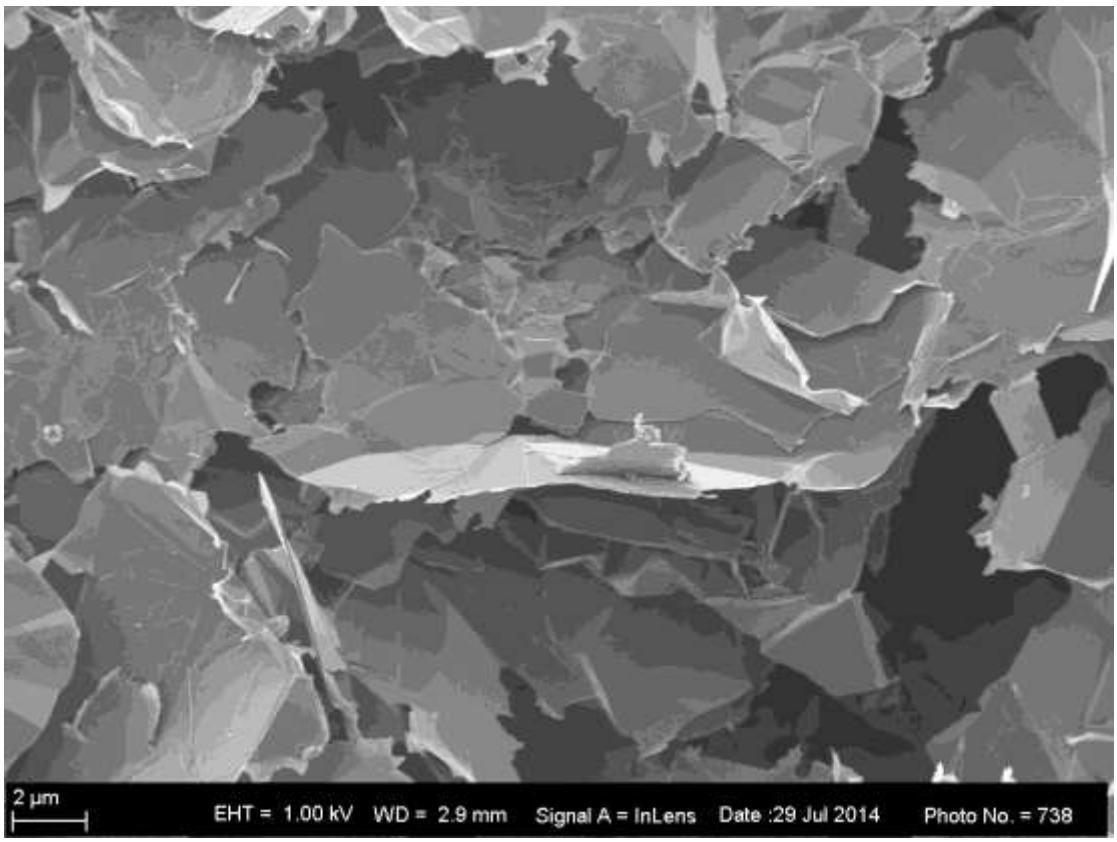

Figure 4-70: SEM of purified best gas phase sample (10000x magnification).

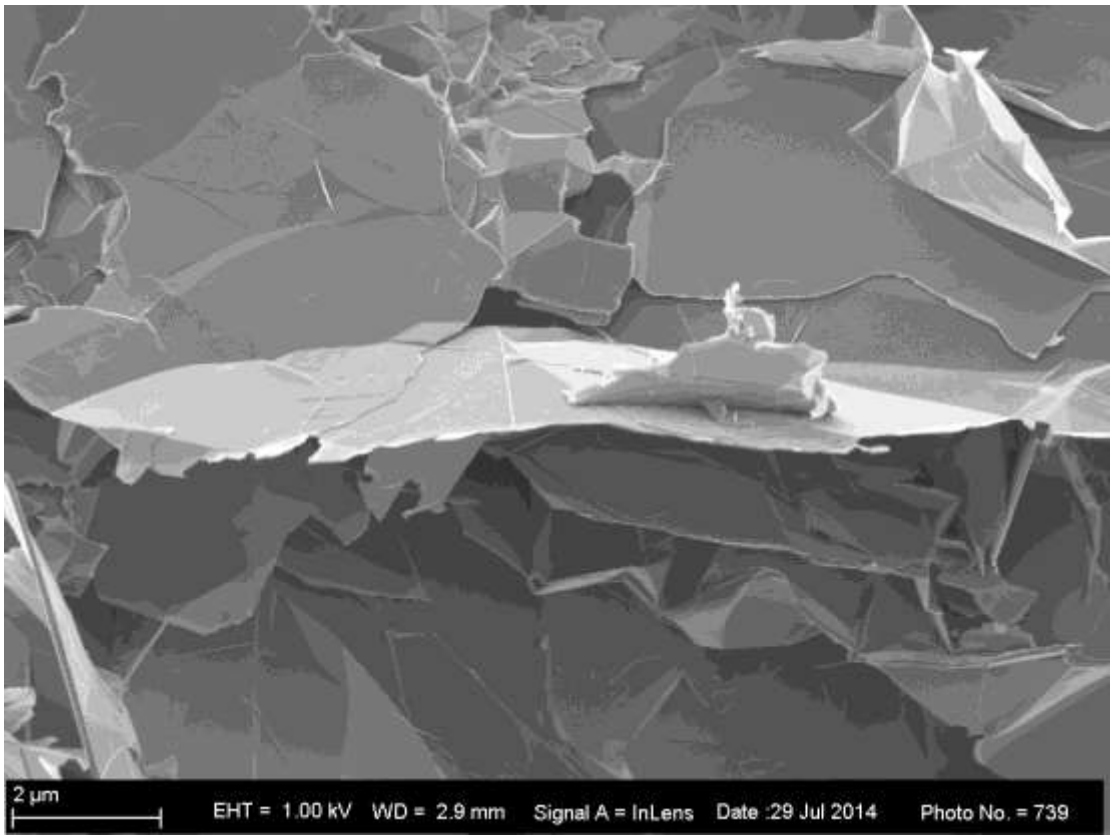

Figure 4-71: SEM of purified best gas phase sample (20000x magnification).

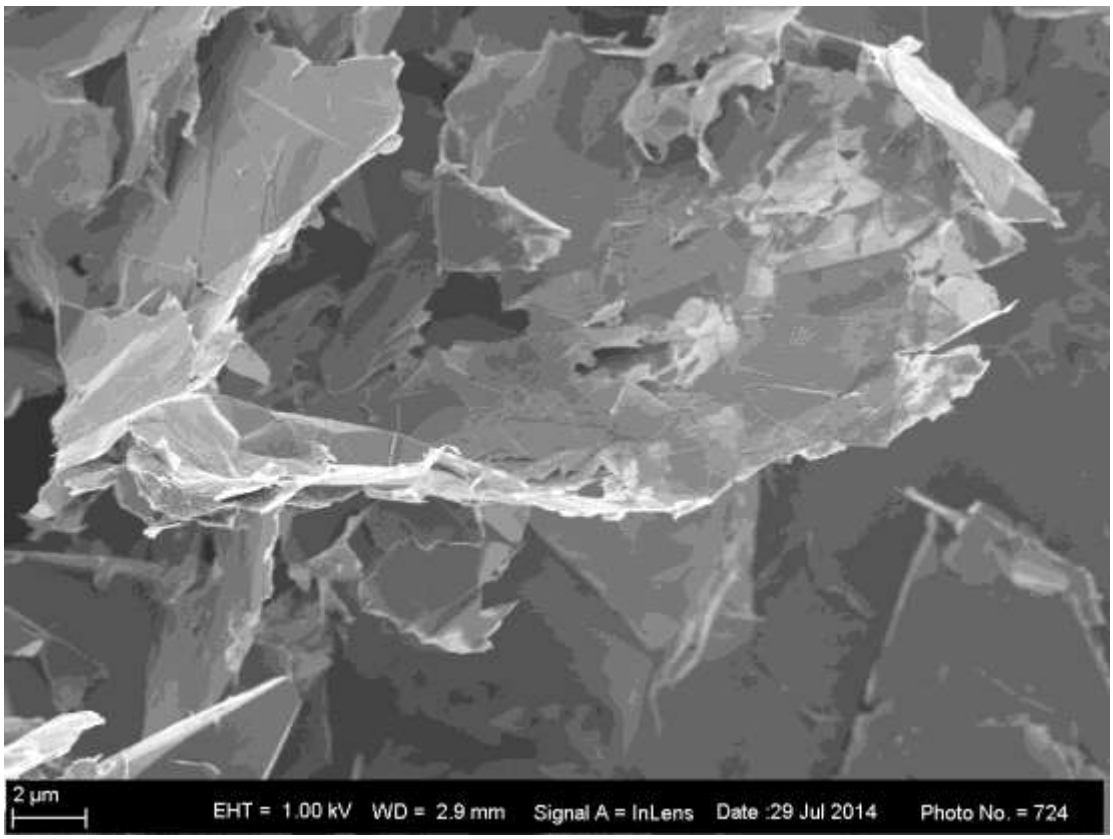

Figure 4-72: SEM of purified best Hummers sample (10000x magnification).

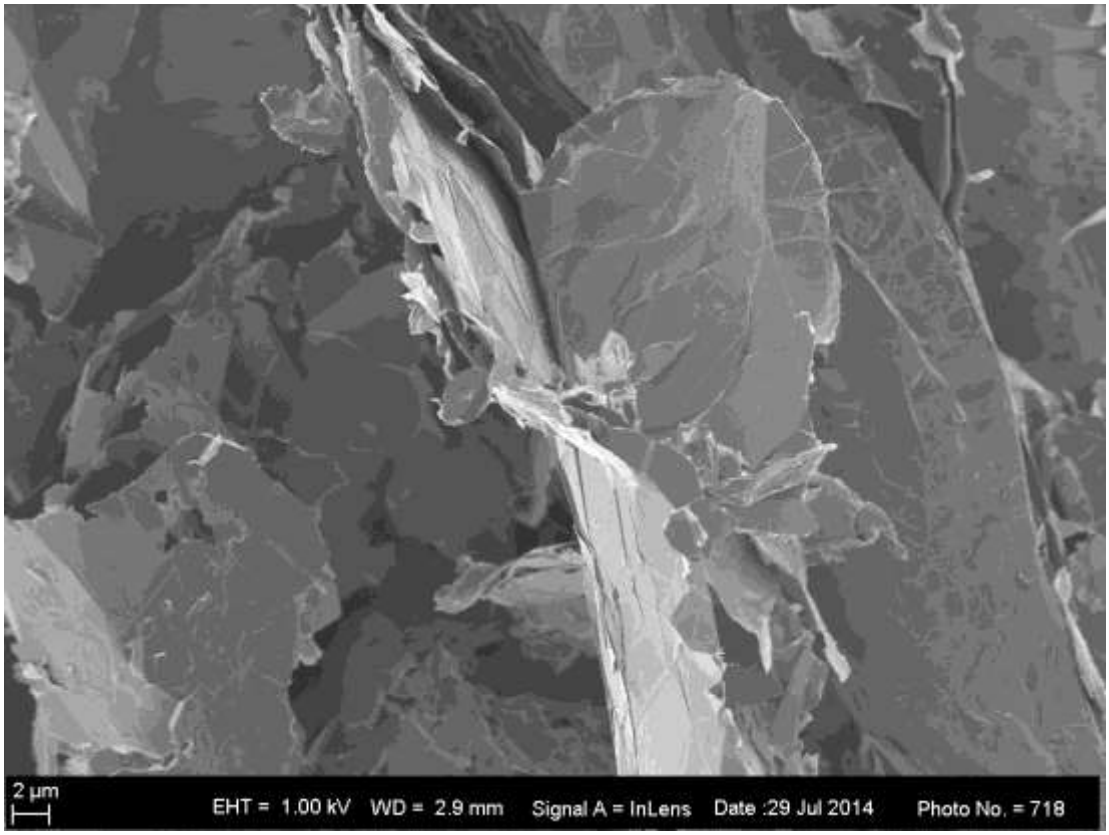

Figure 4-73: SEM of purified best Hummers sample (15000x magnification).

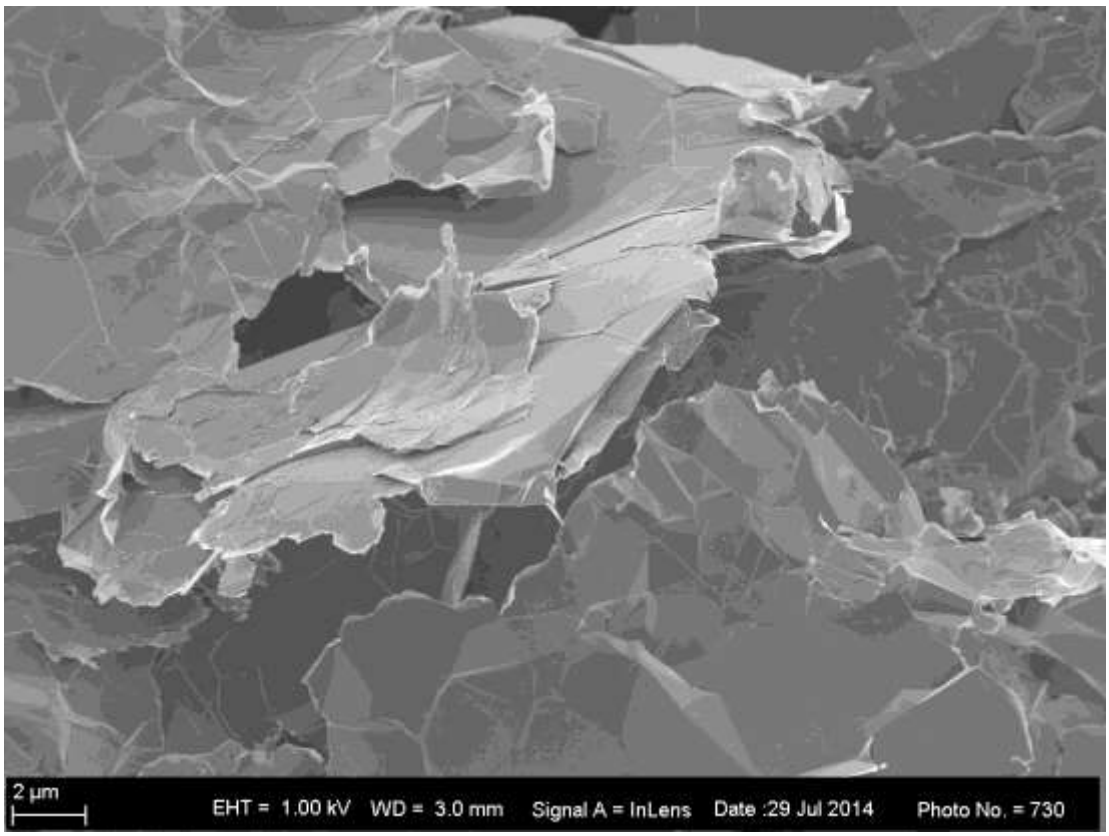

Figure 4-74: SEM of purified worst Hummers sample (10000x magnification).

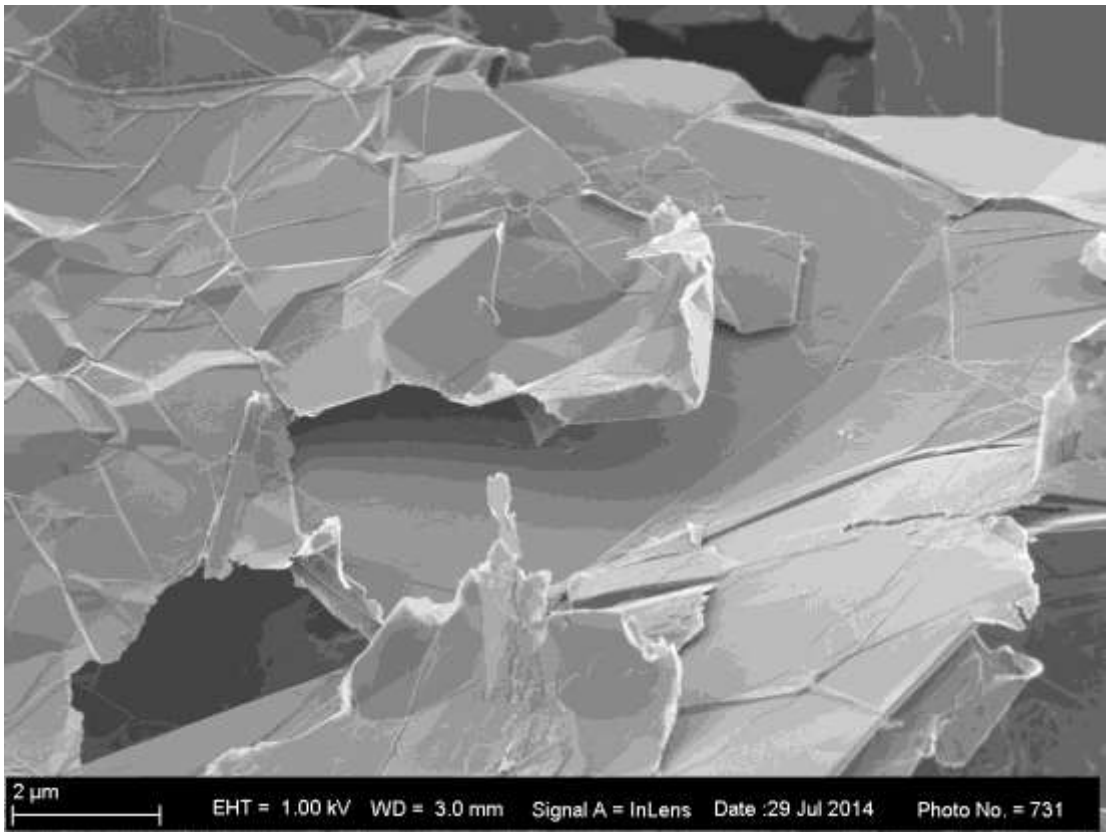

Figure 4-75: SEM of purified worst Hummers sample (20000x magnification).

The following images magnify the surface and the edge of the graphite flakes. It is very clear that these flakes are few-layered graphite. Figure 4-76 is the surface of electrochemical sample which magnifies the surface (45000x), which visibly illustrates the flaky surface. Figure 4-77 illustrates the edge (50000x), the few-layers are evident with slight damage. The best gas phase sample is magnified 60000 times in Figure 4-78 and Figure 4-79, where the edge is clearly bent as well as the surface with damage very clear in Figure 4-79. But once again, the best Hummers sample is obviously the most damaged at a magnification of 50000 times. The surface structure is completely destroyed; random irregular channelling is visible in Figure 4-80.

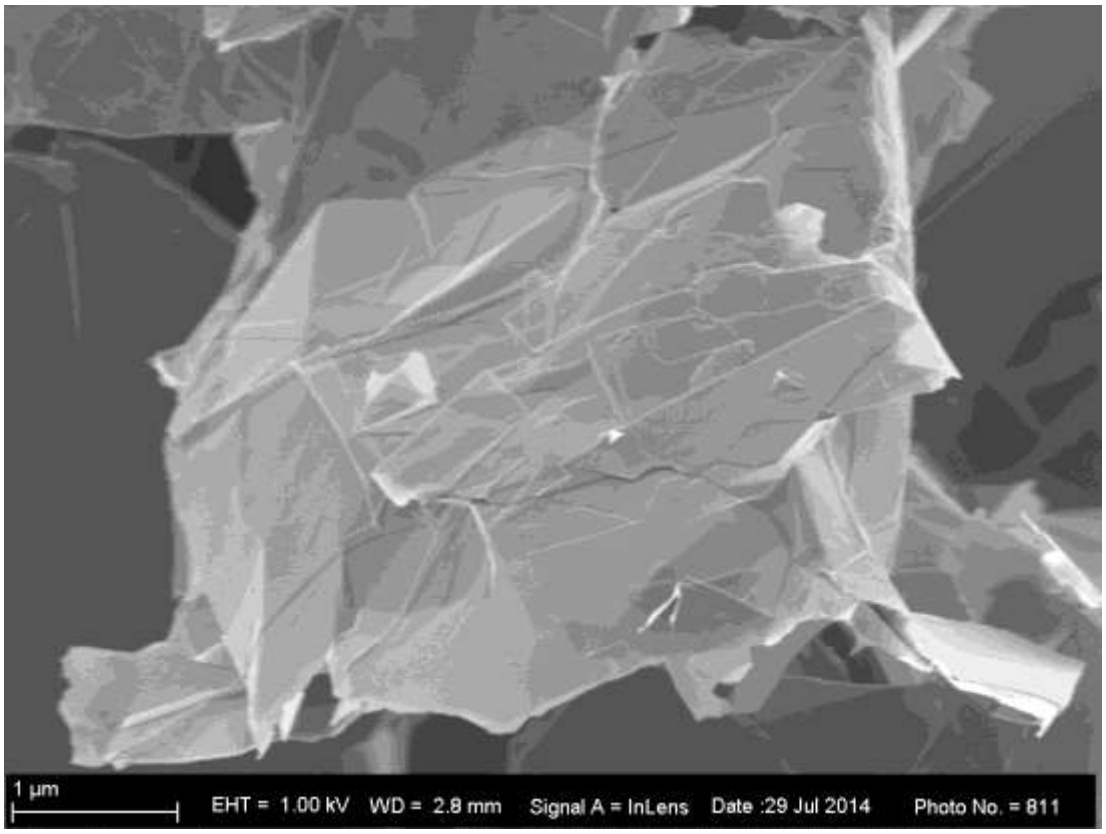

Figure 4-76: SEM of purified electrochemical sample (45000x magnification).

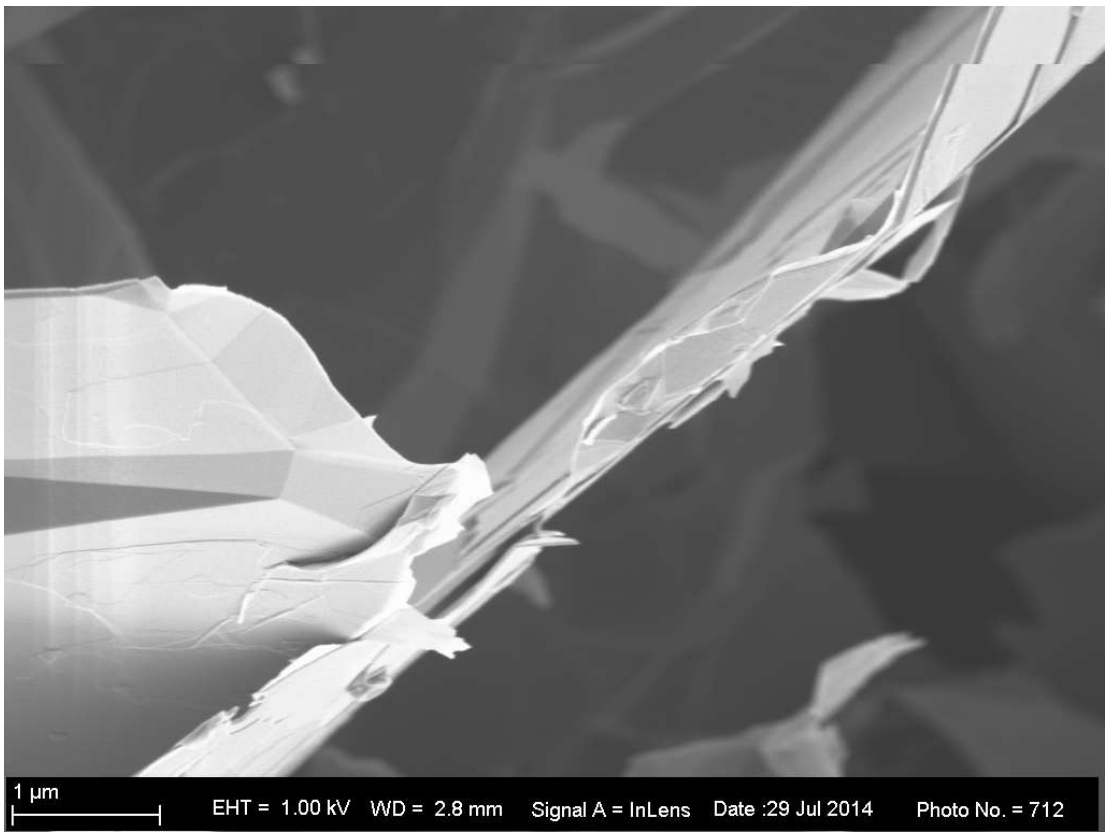

Figure 4-77: SEM of purified electrochemical sample (50000x magnification).

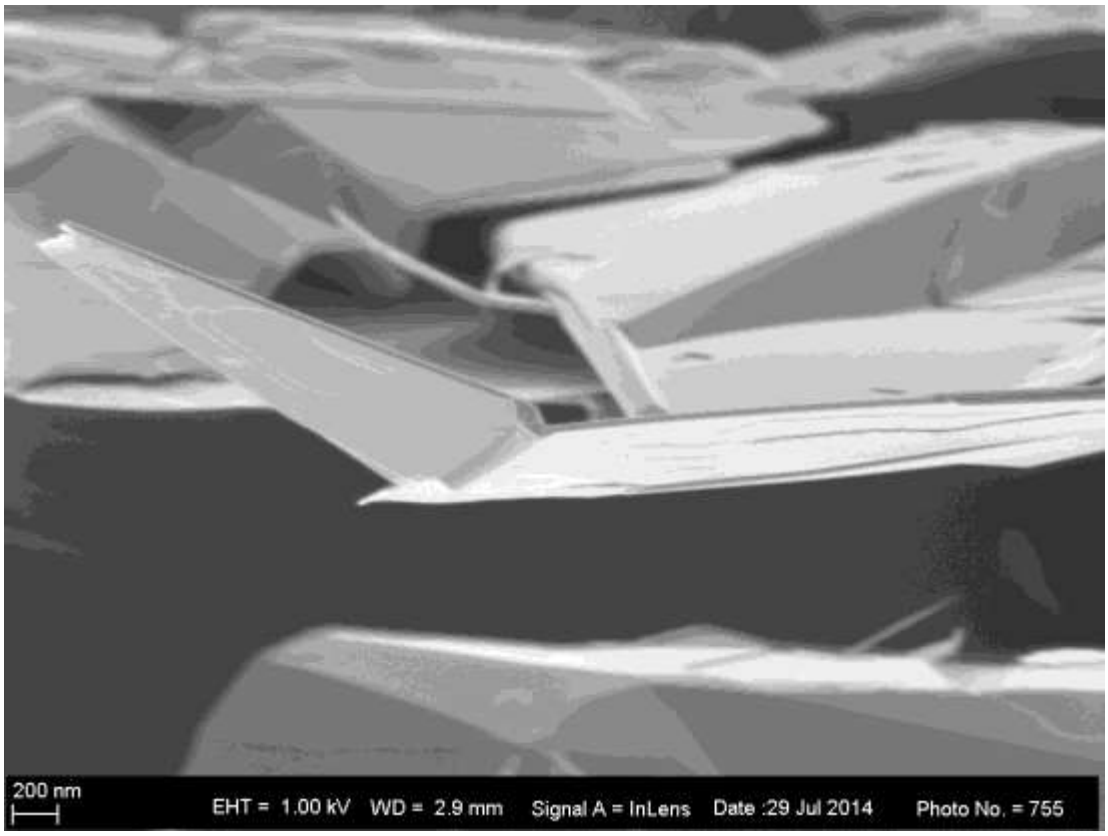

Figure 4-78: SEM of purified best gas phase sample (60000x magnification).

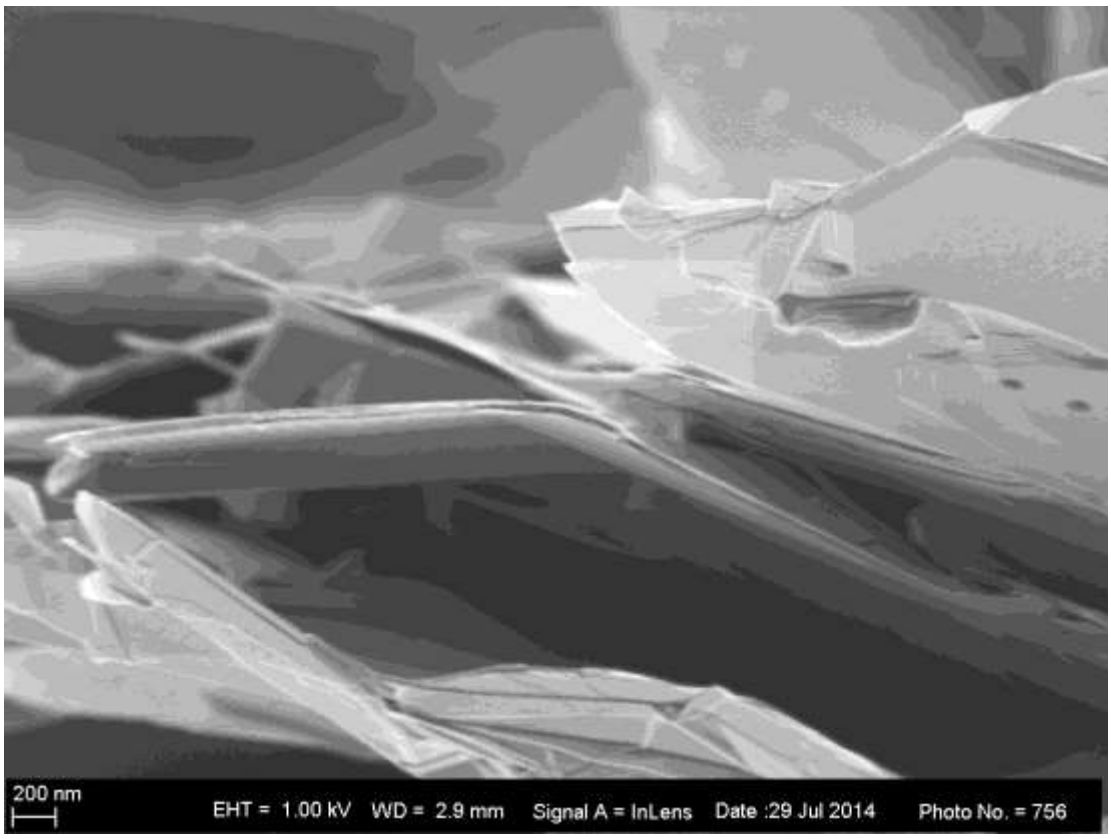

Figure 4-79: SEM of purified best gas phase sample (60000x magnification).

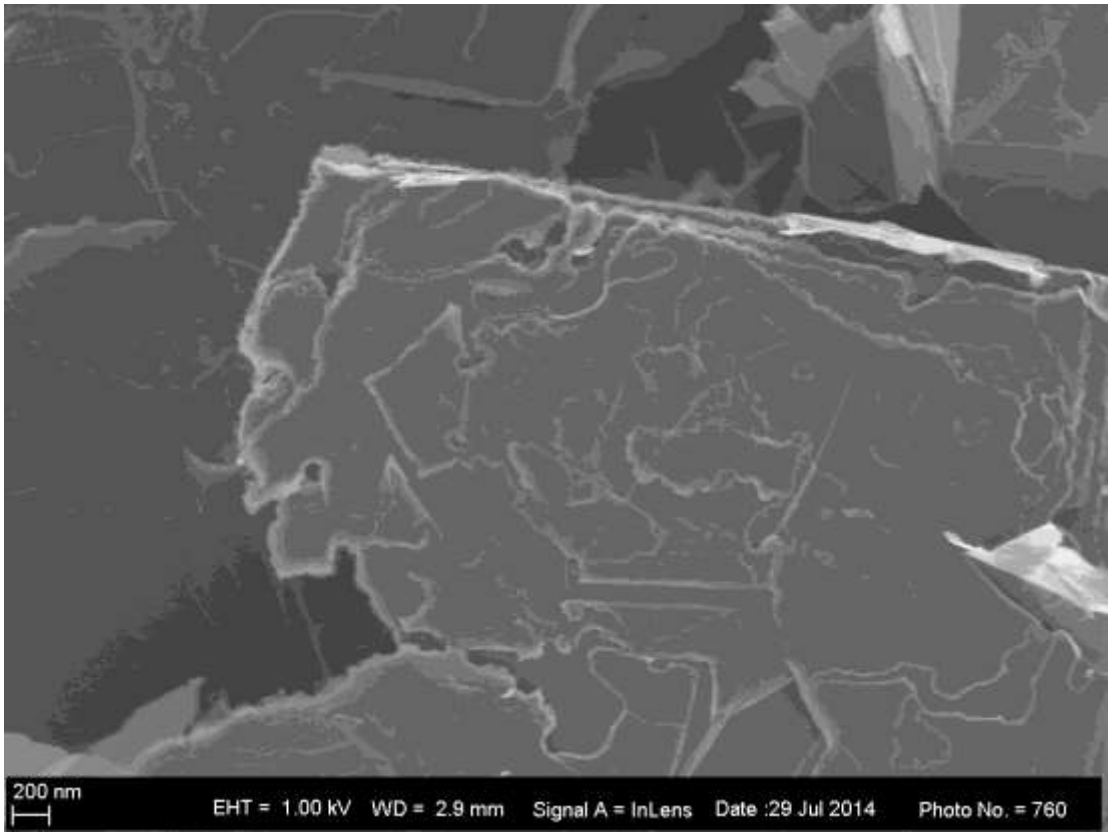

Figure 4-80: SEM of purified best Hummers sample (50000x magnification).

Closer examination of the gas phase sample is illustrated in Figure 4-81, the surface at this magnitude the channels are visible, resulting in cavities. The basal plane seems to be intact, but corrodes inward, making the layered structure visible. Figure 4-82 magnifies the edge, clearly showing the layered structure. The Hummers intercalation sample is magnified in Figure 4-83 and in Figure 4-84, illustrating the edge of the sample. The surface is visible in Figure 4-83, showing the flaky surface, yet smooth edge.

Figure 4-81: SEM of purified best gas phase sample (90000x magnification).

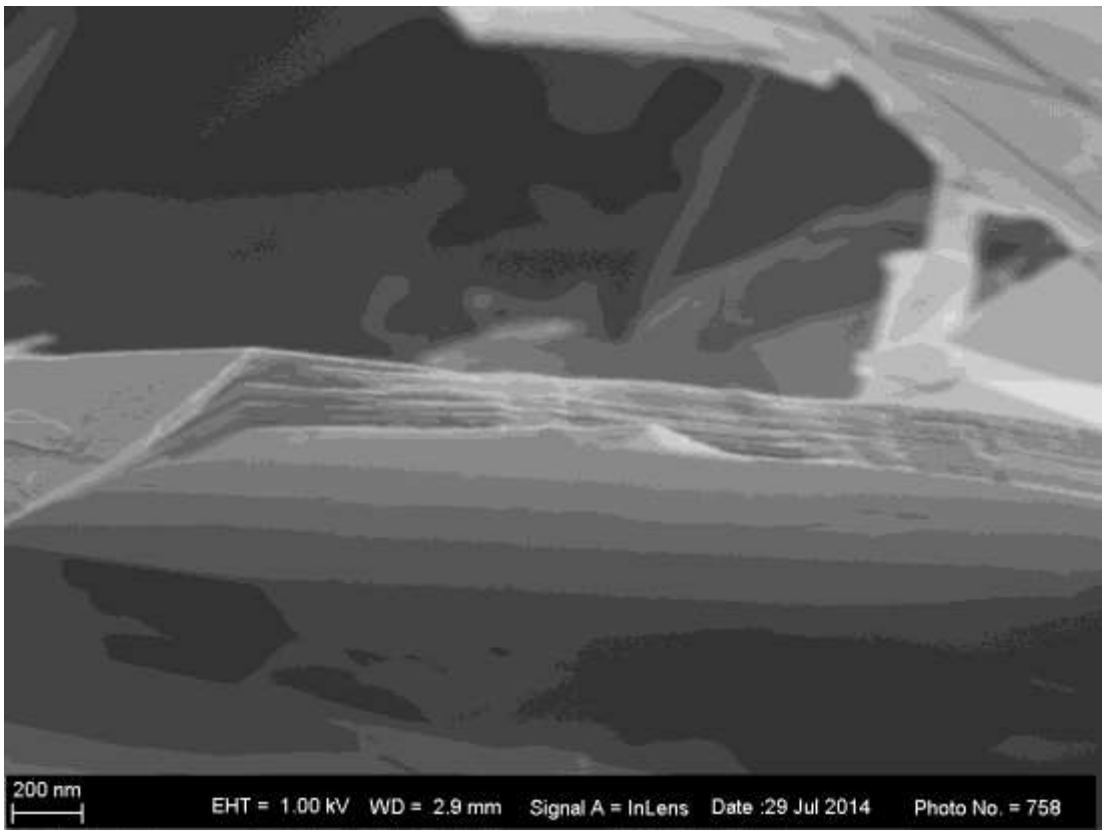

Figure 4-82: SEM of purified best gas phase sample (95000x magnification).

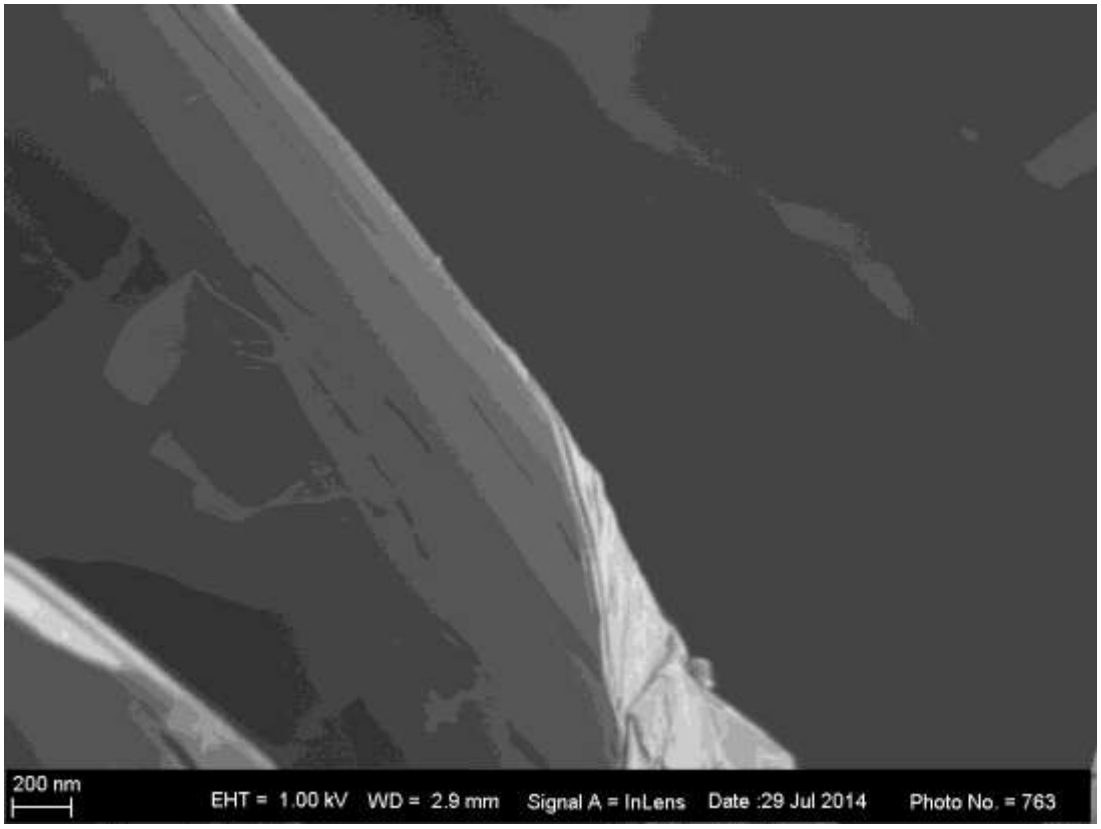

Figure 4-83: SEM of purified best Hummers sample (80000x magnification).

Figure 4-84: SEM of purified best Hummers sample (100000x magnification).

4.7.5 Partially Oxidised Exfoliated Samples

The electrochemical and the best of the gas phase and the Hummers intercalation samples were partially oxidised in order to determine the reactivity of the samples. The amount of impurities or deposits and the extent of damage are directly proportional to the reactivity of the sample. The exfoliated sample of the electrochemical and the best of the gas phase and Hummers methods were partially oxidised to 95 % and 70 % of its original mass in the TGA. These samples were analysed and compared in the SEM

Firstly, the samples that were partially oxidised only 5 % are illustrated. The exfoliated bulk samples magnified 5000 times of the different methods are shown in Figure 4-85 to Figure 4-87. The electrochemical and Hummers sample seems to be similar. The appearance of the gas phase sample is different. The gas phase sample is more reactive than the other two methods. This is also evident in the images of the surface of the different samples at higher magnification (10000 times) in Figure 4-88 to Figure 4-90.

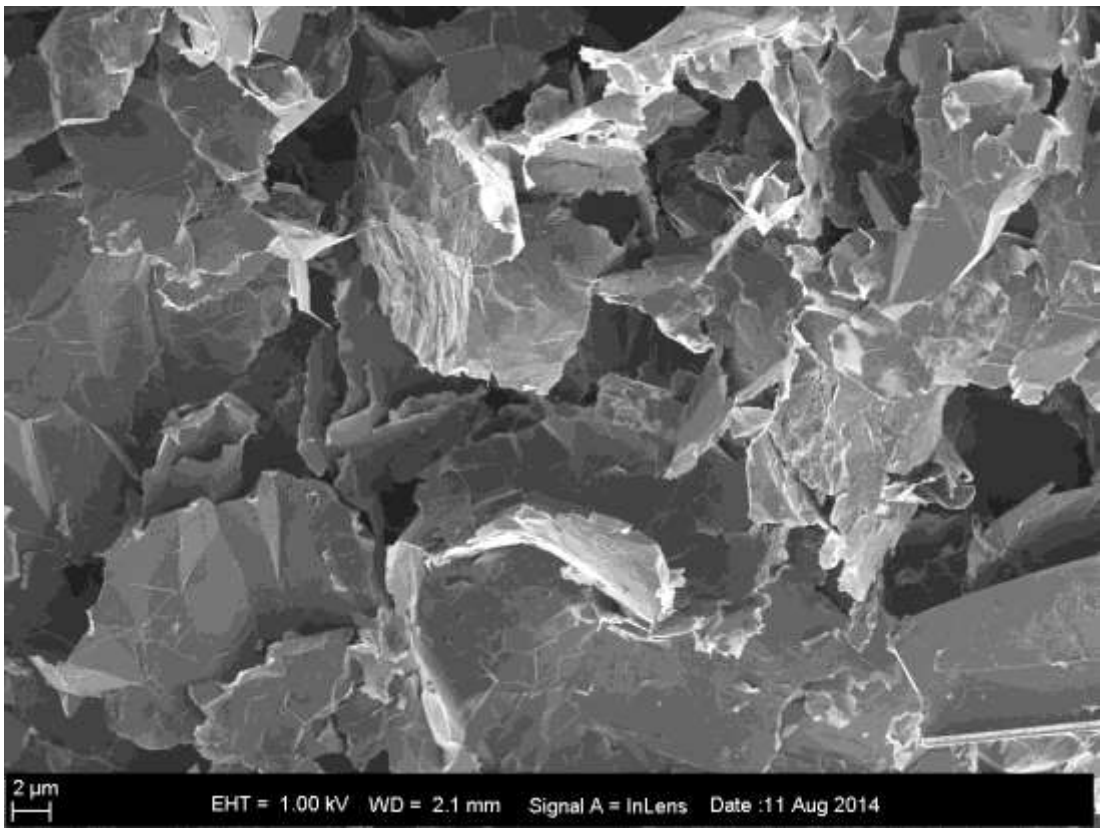

Figure 4-85: SEM of 5% oxidised electrochemical sample (5000x magnification).

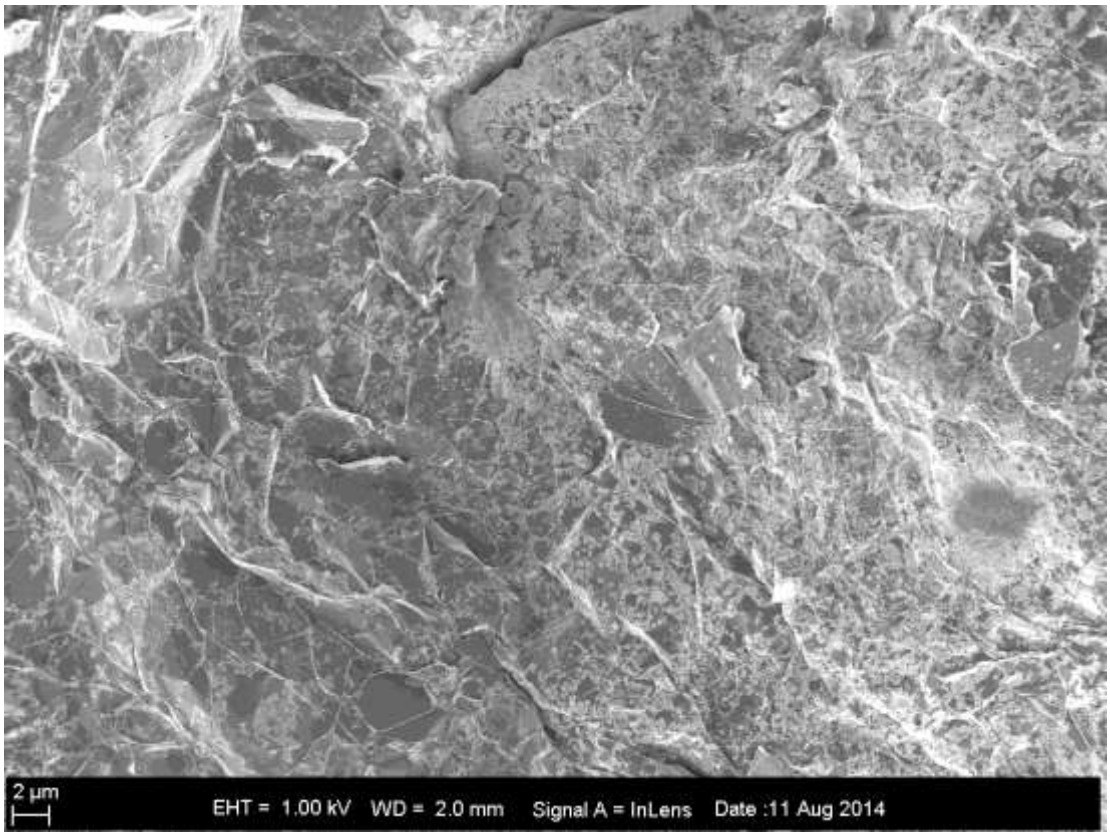

Figure 4-86: SEM of 5% oxidised gas phase sample (5000x magnification).

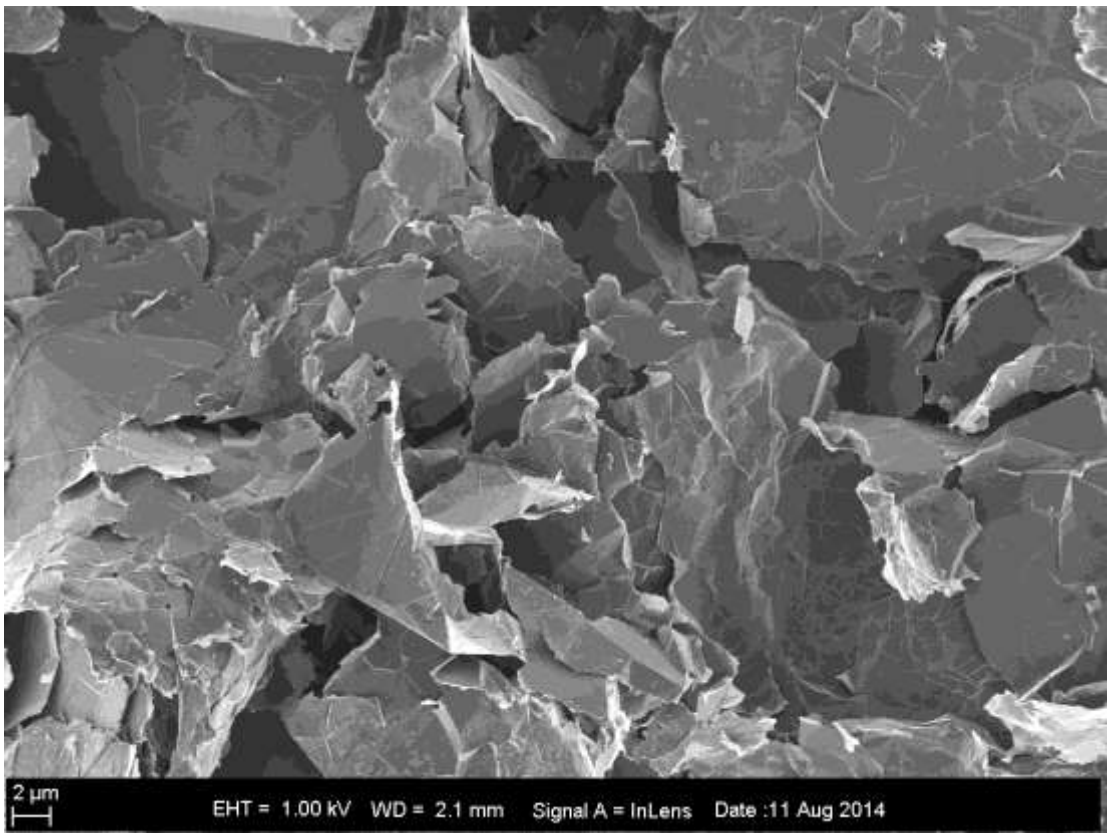

Figure 4-87: SEM of 5% oxidised Hummers sample (5000x magnification).

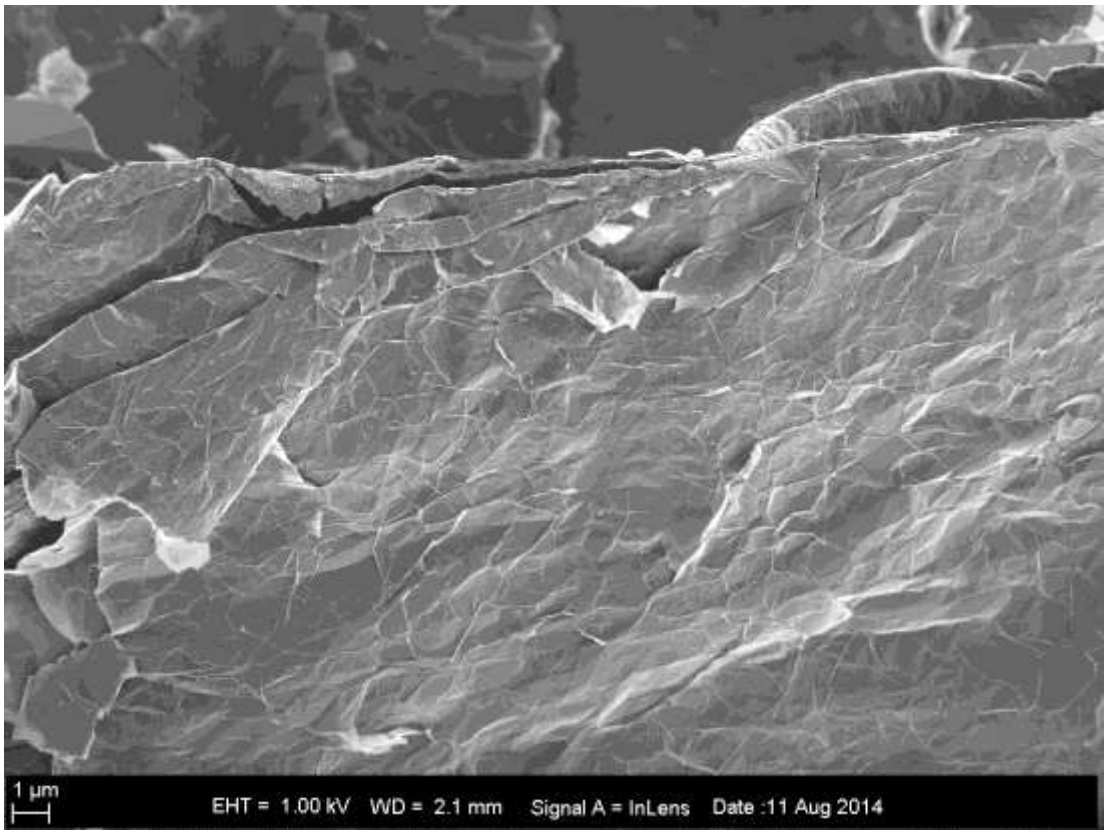

Figure 4-88: SEM of 5% oxidised electrochemical sample (10000x magnification).

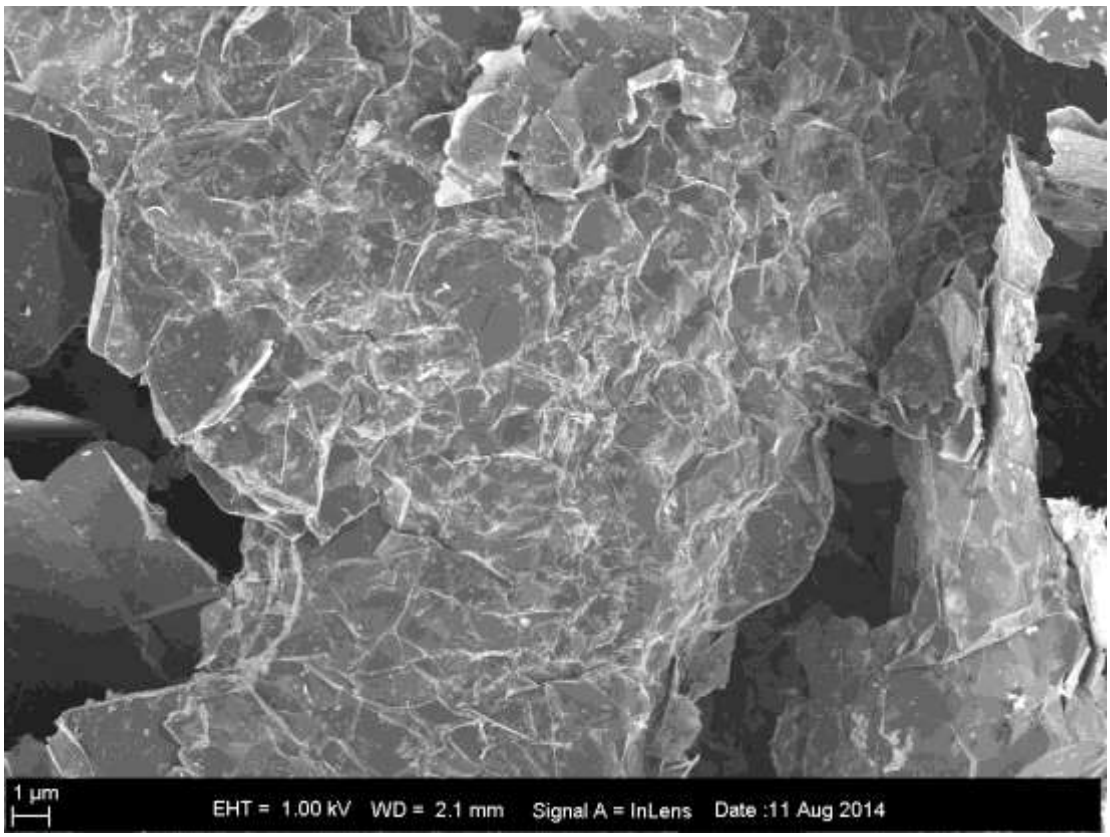

Figure 4-89: SEM of 5% oxidised gas phase sample (10000x magnification).

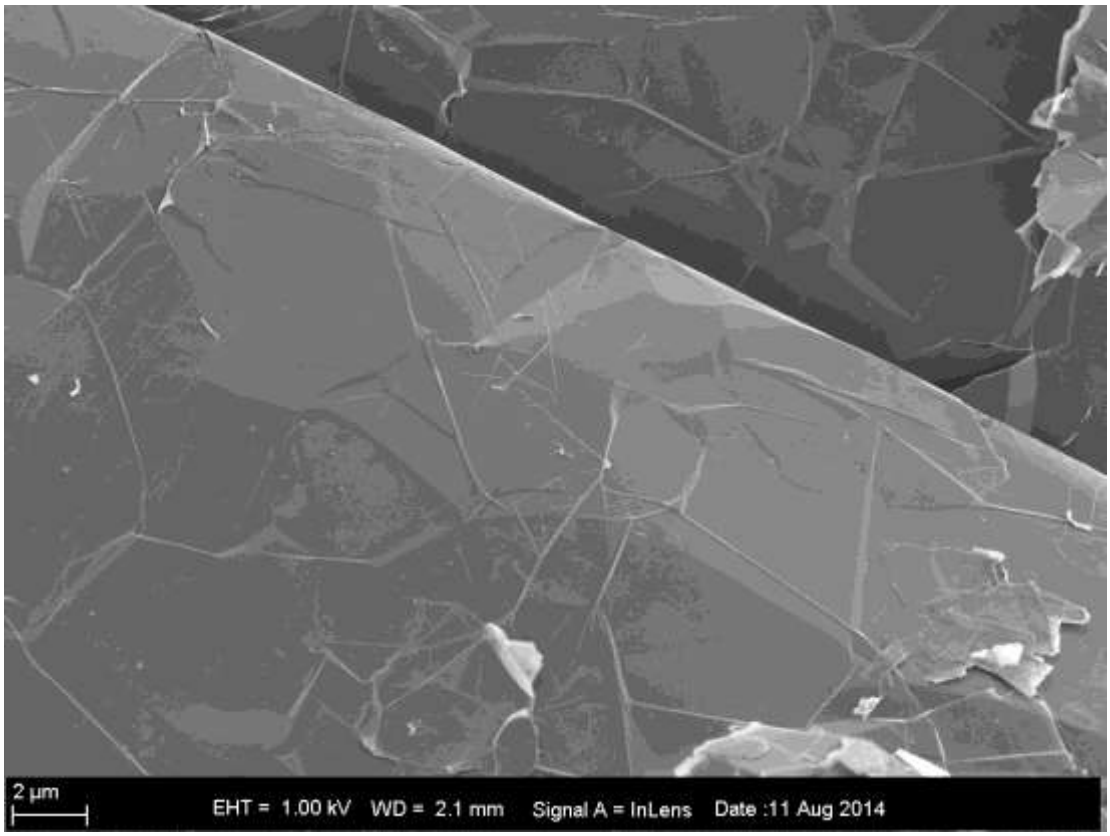

Figure 4-90: SEM of 5% oxidised Hummers sample (10000x magnification).

Figure 4-91 is an image of the exfoliated electrochemical sample at a magnification of 45000 times. Here the edge oxidation is visible. The edges erode inward in circular motion. Figure 4-92 illustrates the gas phase sample magnified 40000 times. Here the deposits are visible. The Hummers method sample is illustrated in Figure 4-93, Figure 4-94 and Figure 4-95. The basal plane in Figure 4-93 is damaged by the oxidation. Oxidation pits are clearly visible over the whole basal plane. Figure 4-94 shows a layer-edge, illustrating the “zig-zag” type damage on the edge. The basal plane is illustrated at higher magnification in Figure 4-95, showing the shrinkage of the flake layers.

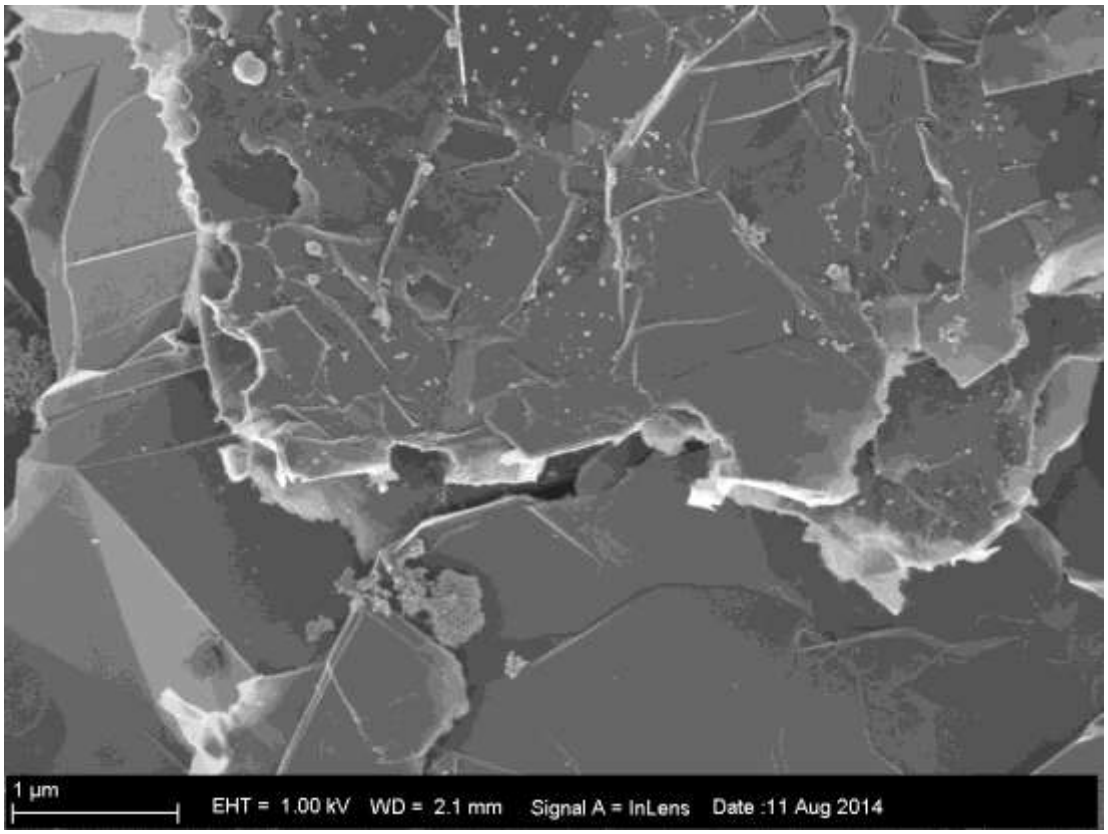

Figure 4-91: SEM of 5% oxidised electrochemical sample (45000x magnification).

Figure 4-92: SEM of 5% oxidised gas phase sample (40000x magnification).

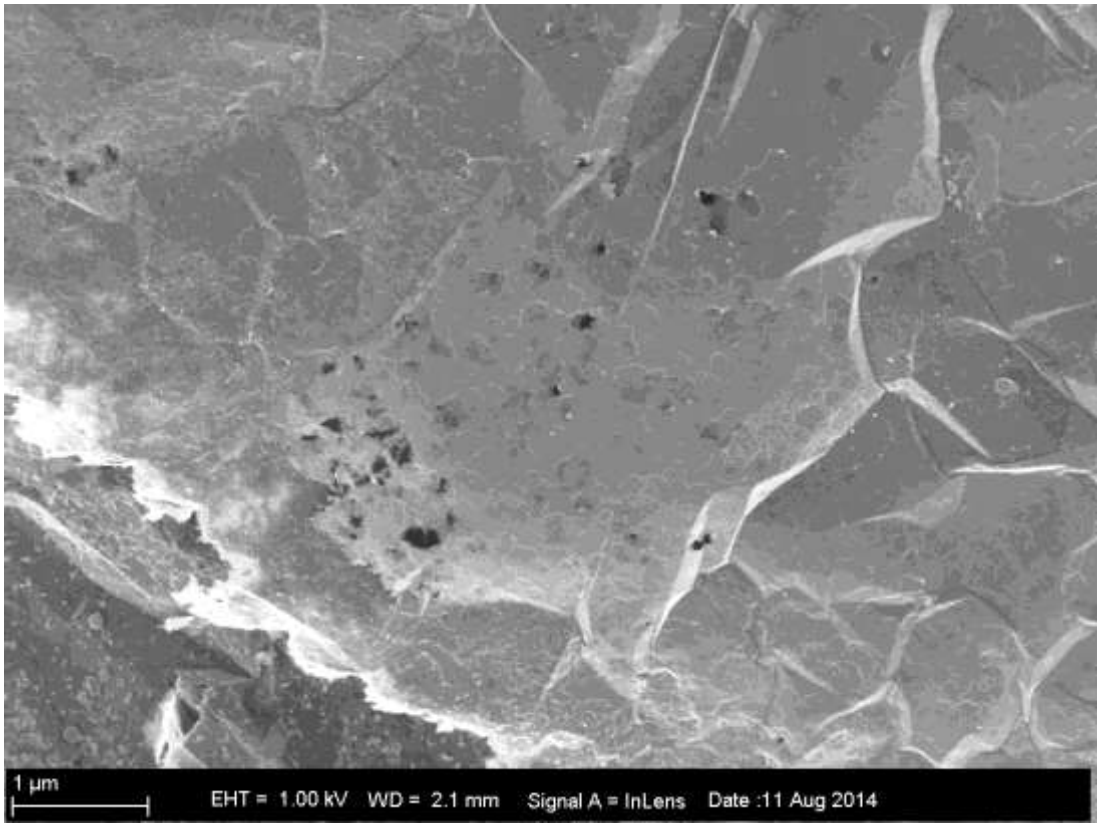

Figure 4-93: SEM of 5% oxidised Hummers sample (37000x magnification).

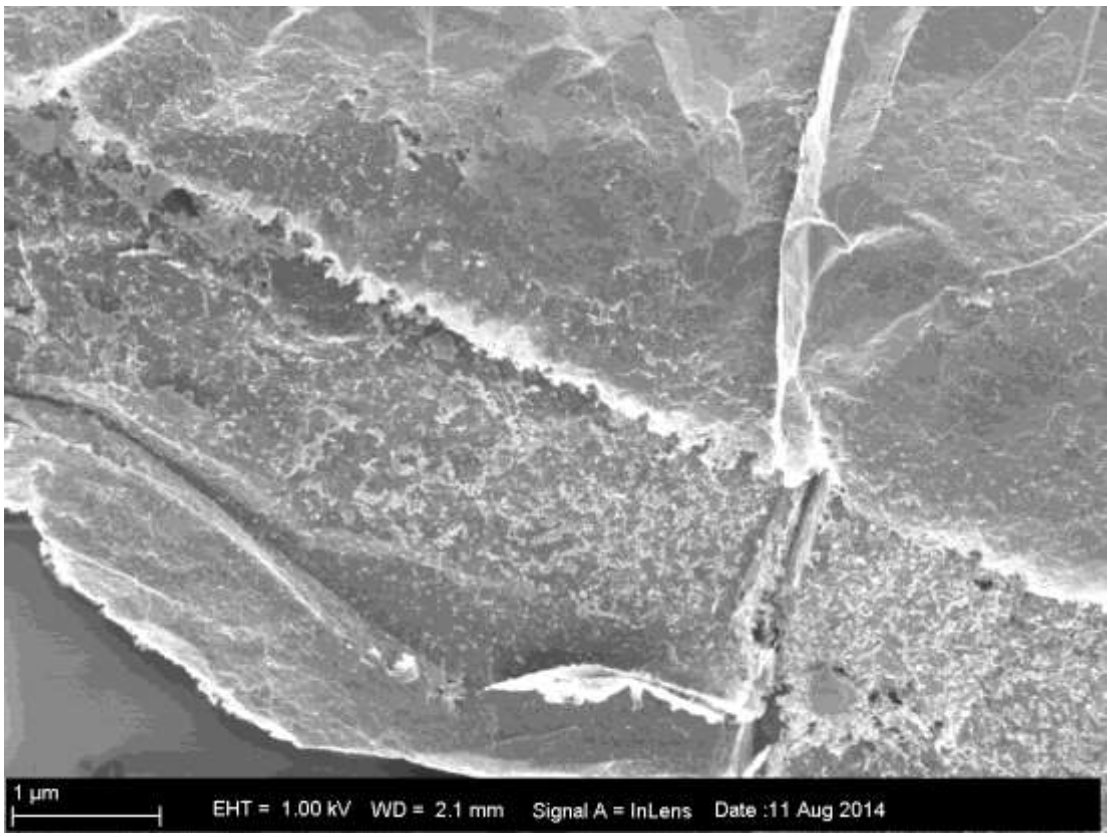

Figure 4-94: SEM of 5% oxidised Hummers sample (40000x magnification).

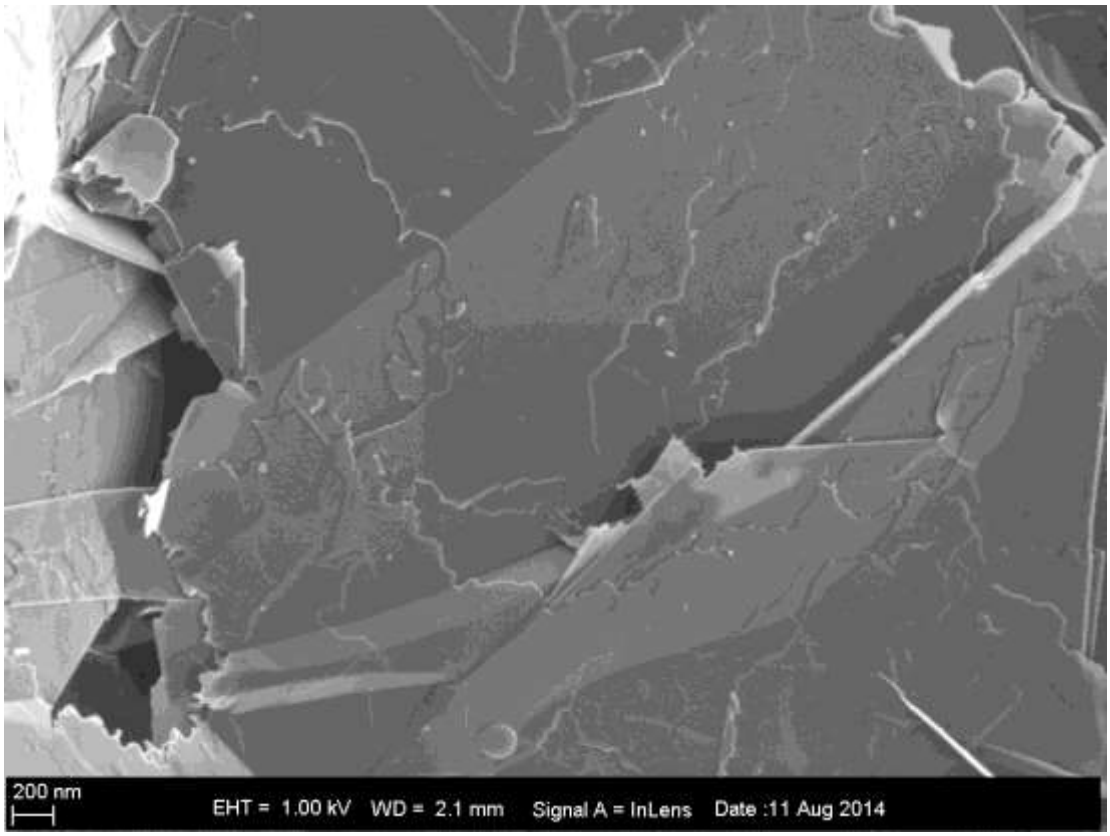

Figure 4-95: SEM of 5% oxidised Hummers sample (55000x magnification).

These exfoliated samples were partially oxidised 30 % as well. On a macro level these samples are visibly very different. The electrochemical sample does not appear to be as damaged in Figure 4-96, whereas the gas phase sample in Figure 4-97 shows a clear residue and in Figure 4-98 the Hummers sample clearly illustrates damage to the edges.

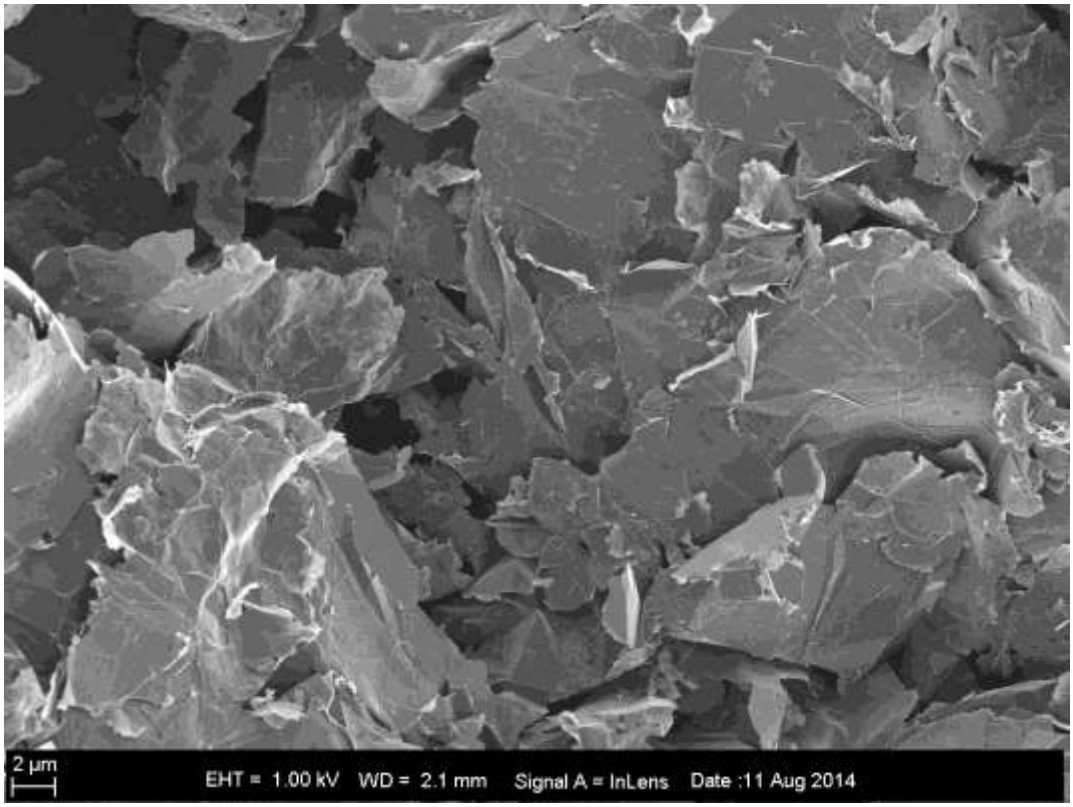

Figure 4-96: SEM of 30% oxidised exfoliated electrochemical sample (6000x magnification).

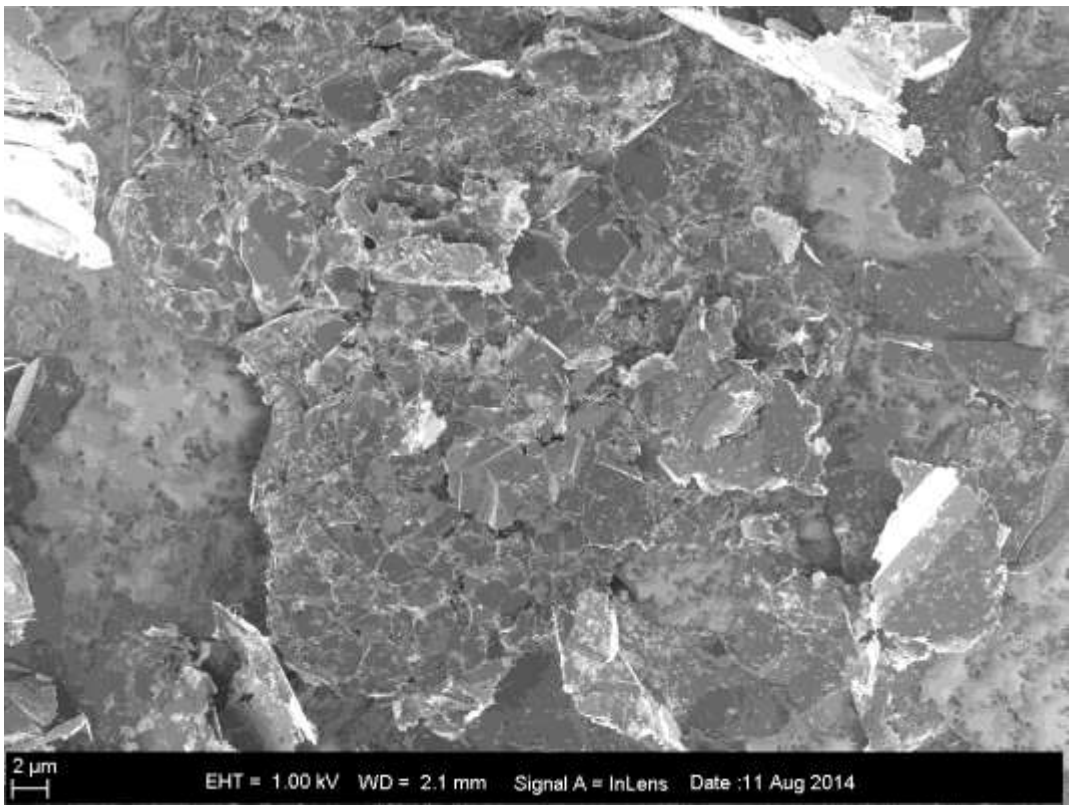

Figure 4-97: SEM of 30% oxidised exfoliated gas phase sample (5000x magnification).

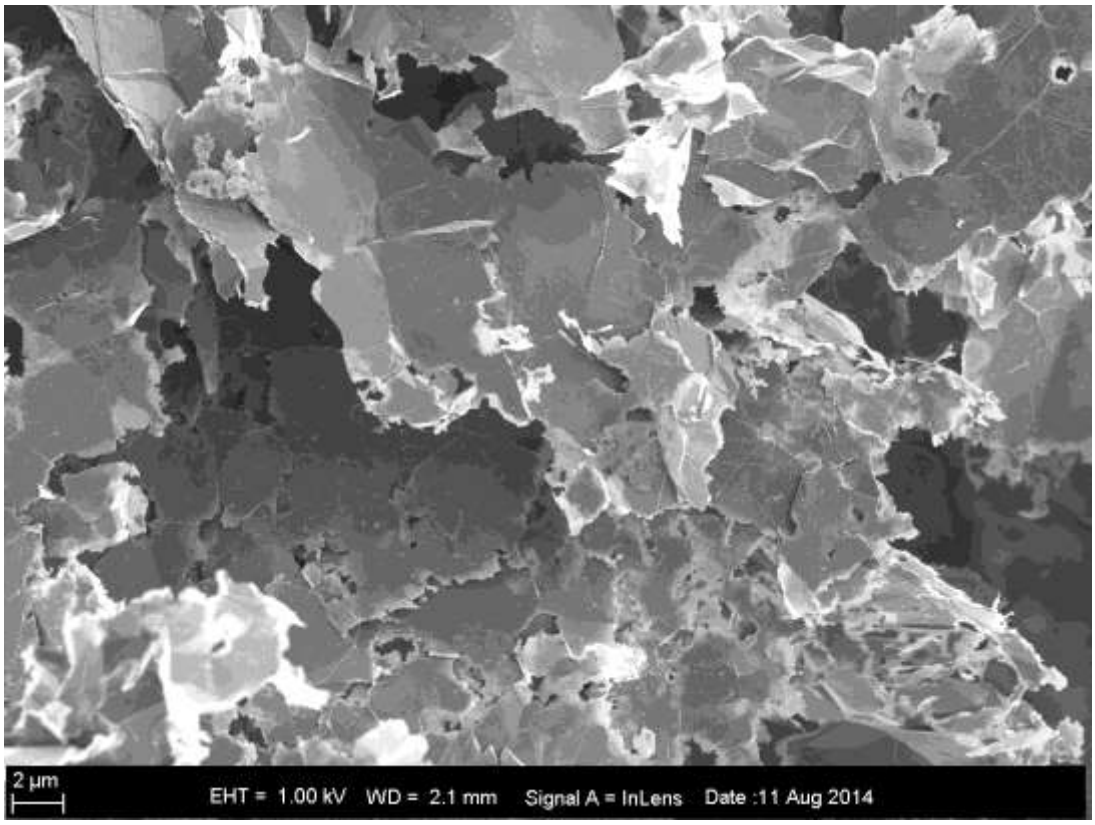

Figure 4-98: SEM of 30% oxidised exfoliated Hummers sample (7000x magnification).

Upon closer inspection, the electrochemical sample is magnified to 20000 times and 55000 times respectively in Figure 4-99 and Figure 4-100. In these samples the damage on the basal plane is clear, with random oxidation pits randomly near the edges and in the centre and an uneven basal plane.

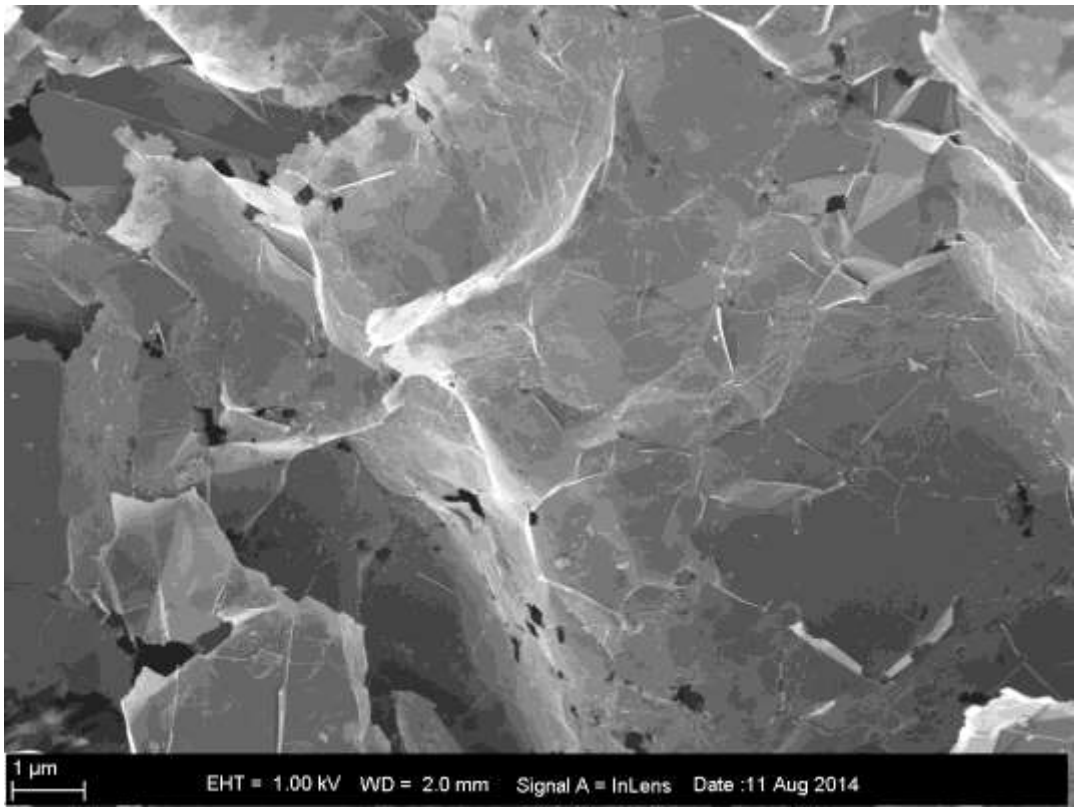

Figure 4-99: SEM of 30% oxidised exfoliated electrochemical sample (20000x magnification).

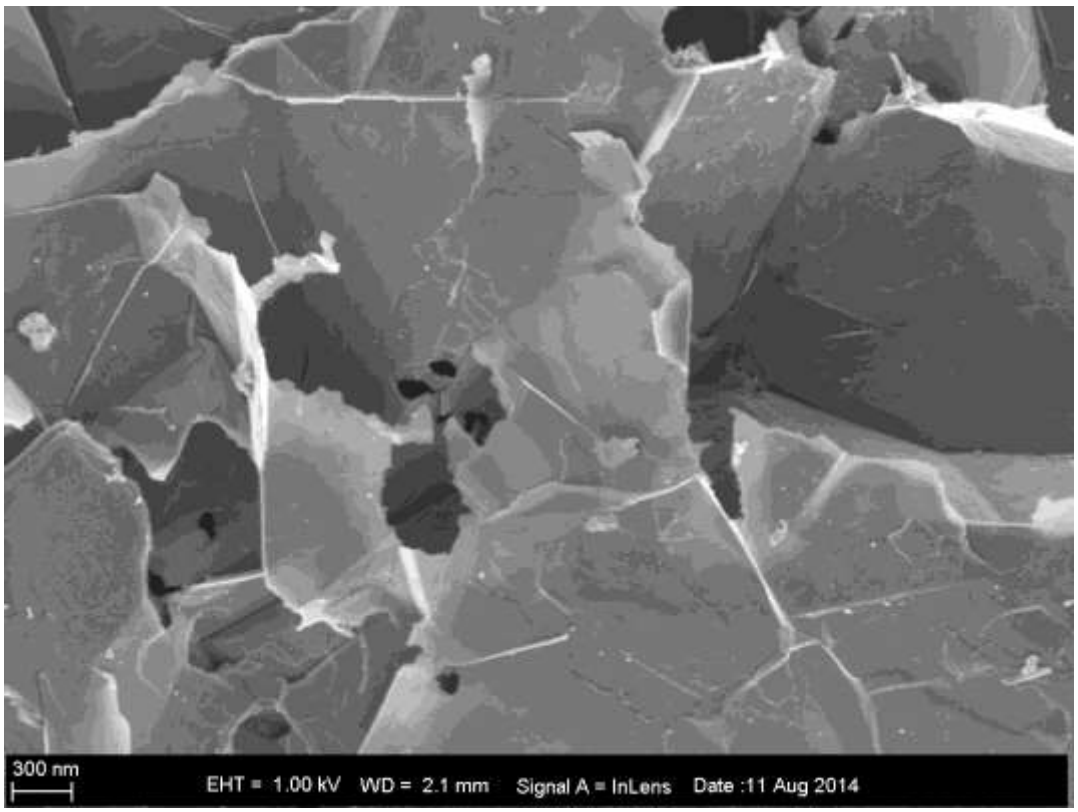

Figure 4-100: SEM of 30% oxidised exfoliated electrochemical sample (55000x magnification).

The gas phase sample is magnified, and the damage and residue becomes more evident. In Figure 4-101 the damage to the edge is very clear, whereas Figure 4-102 clearly enhances residual material, and the basal plane is clearly uneven. At 45000 times magnification in Figure 4-103 the roughened edges are very distinct, and in Figure 4-104 the residue and damaged edges are extensive.

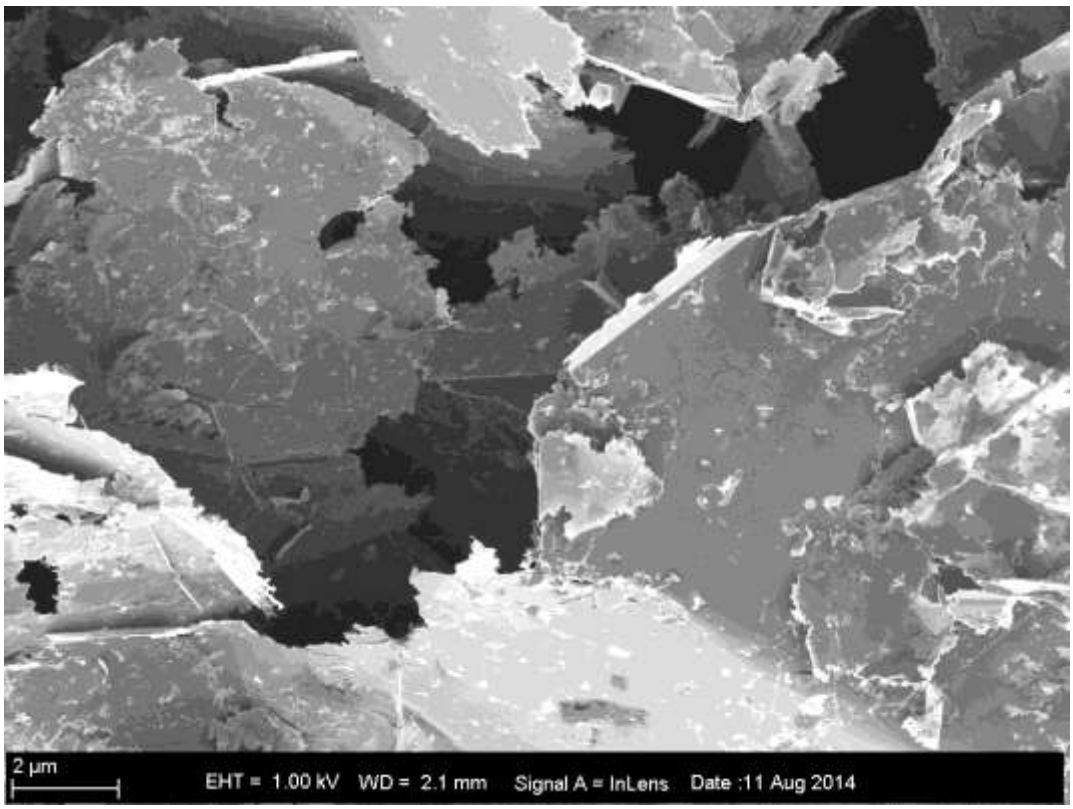

Figure 4-101: SEM of 30% oxidised exfoliated gas phase sample (15000x magnification).

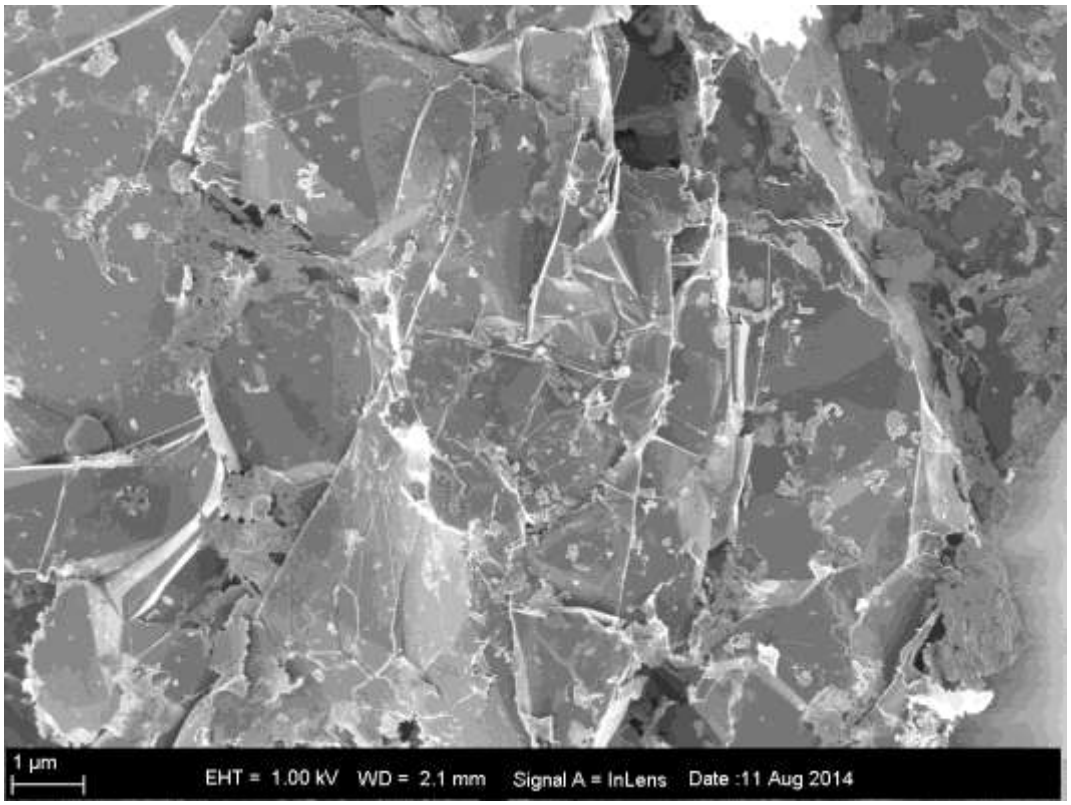

Figure 4-102: SEM of 30% oxidised exfoliated gas phase sample (20000x magnification).

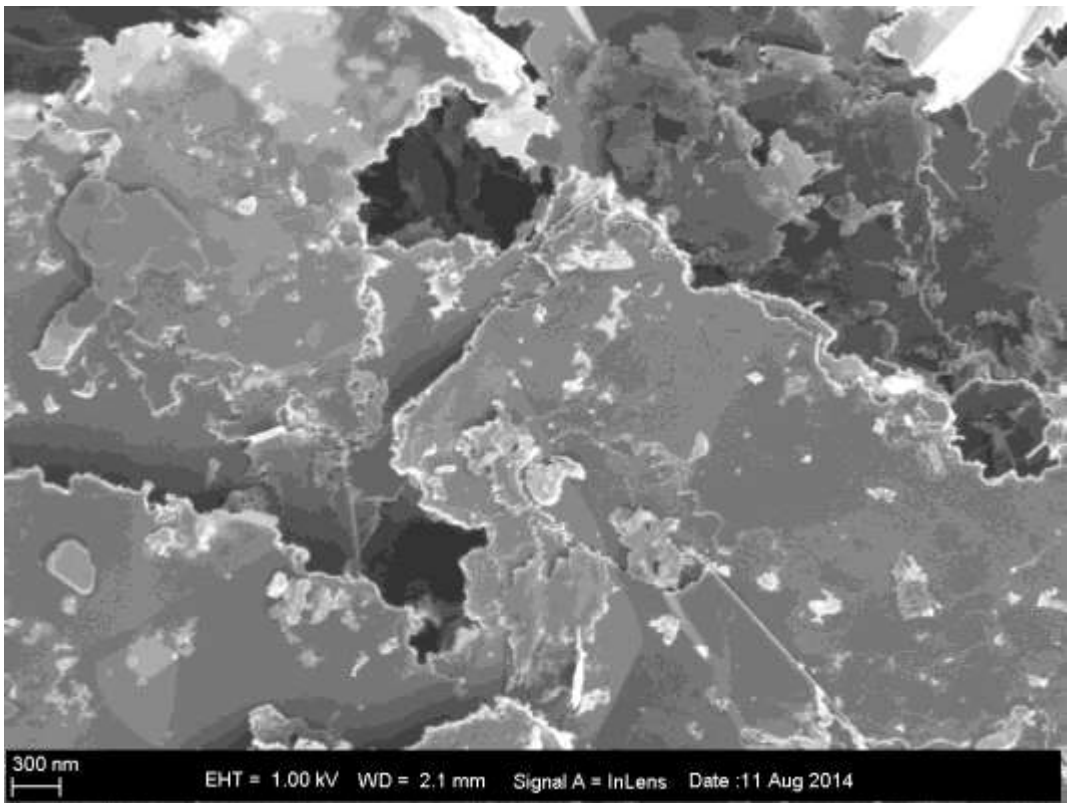

Figure 4-103: SEM of 30% oxidised exfoliated gas phase sample (45000x magnification).

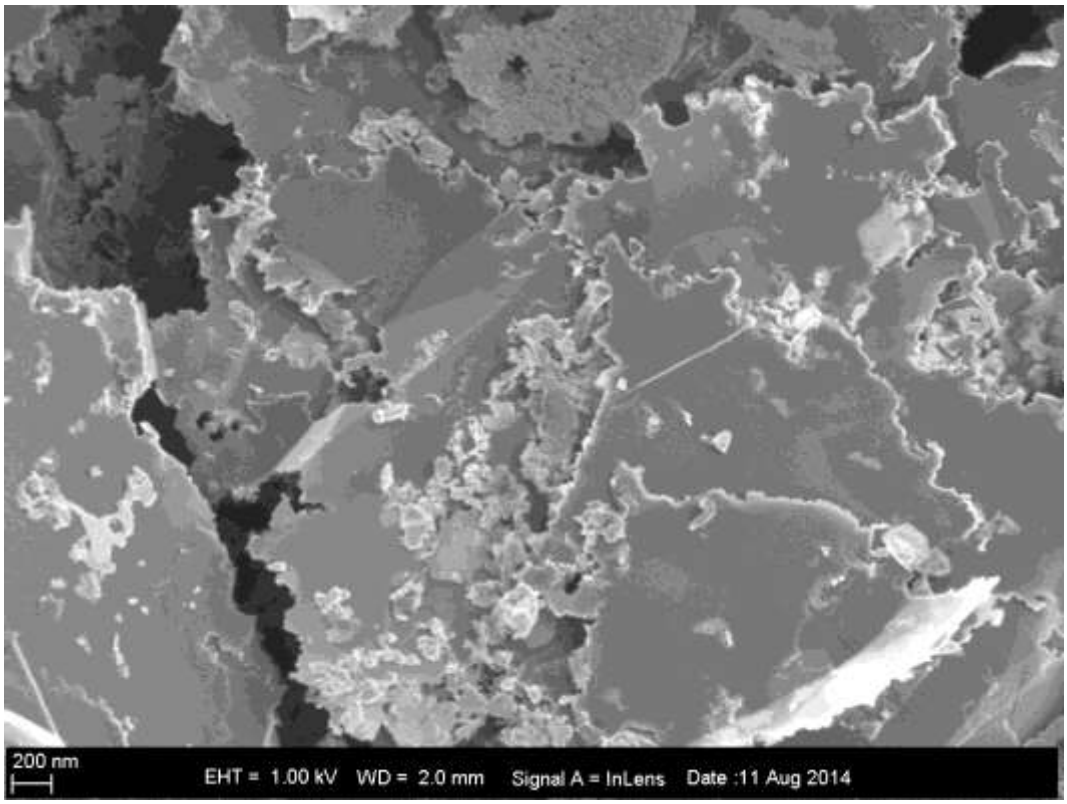

Figure 4-104: SEM of 30% oxidised exfoliated gas phase sample (55000x magnification).

The exfoliated Hummers method sample oxidised 30 % is illustrated below. Figure 4-105 illustrates the extensive damage at a magnification of 15000 times. The edges are completely destroyed. In Figure 4-106 the basal plane has random erosion and shows extreme damage.

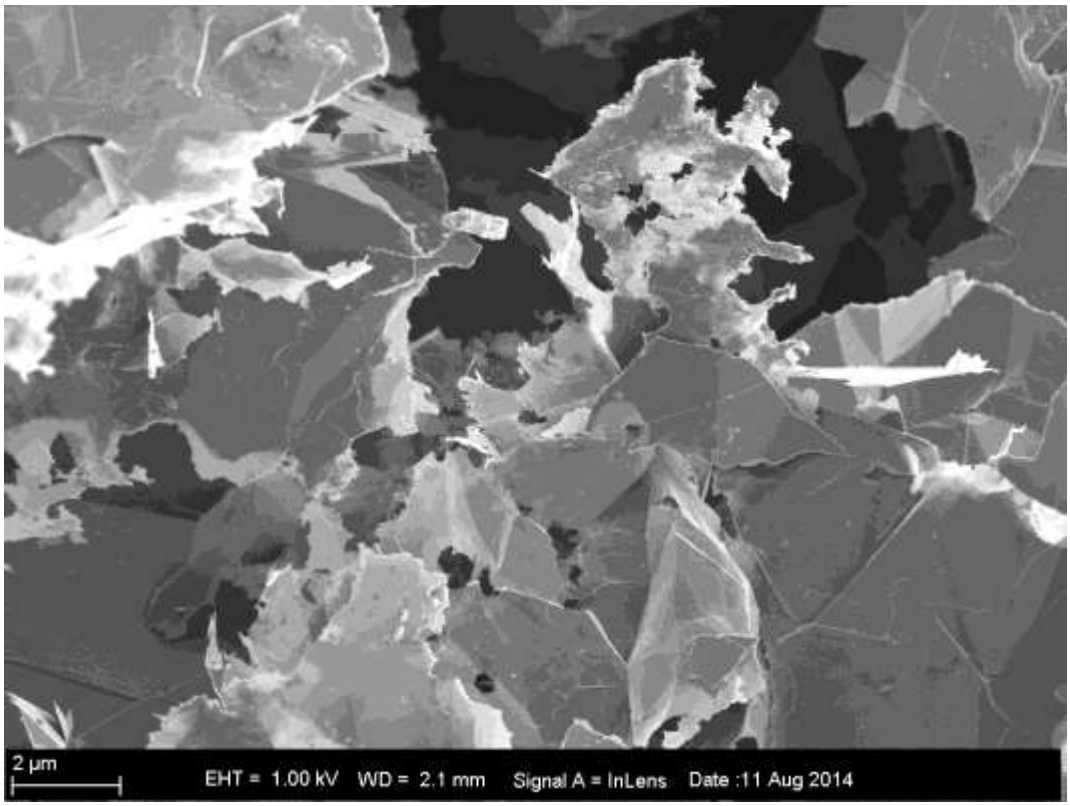

Figure 4-105: SEM of 30% oxidised exfoliated Hummers sample (15000x magnification).

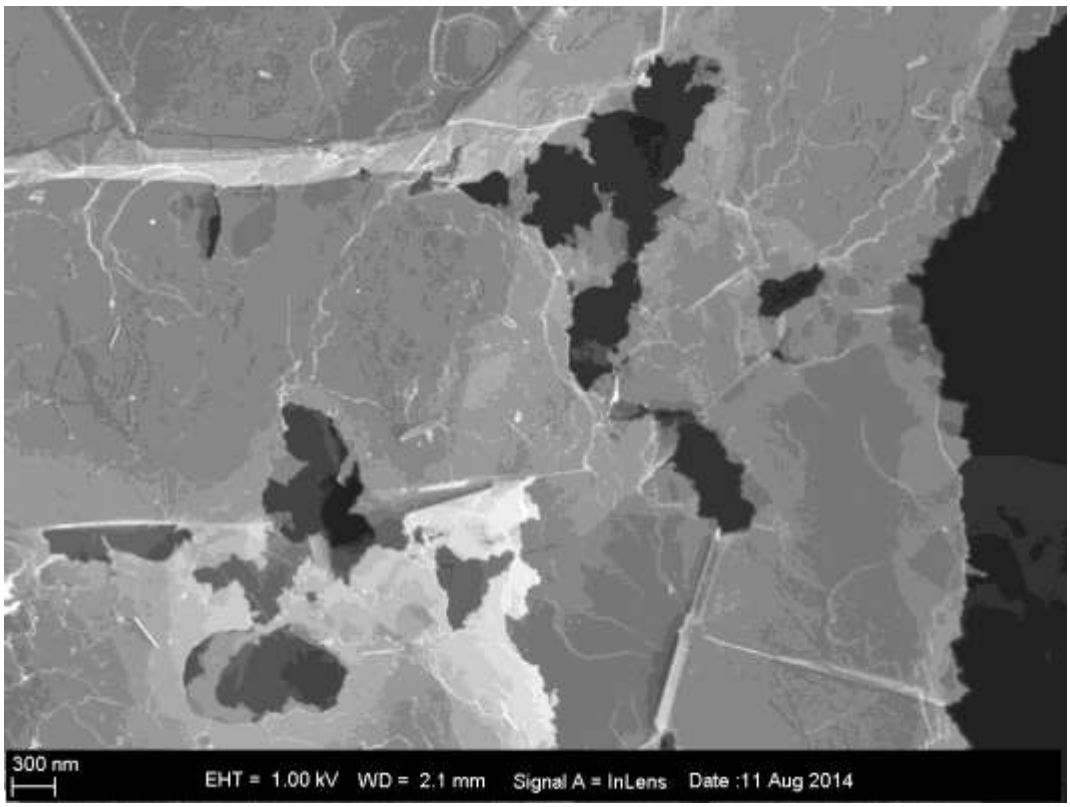

Figure 4-106: SEM of 30% oxidised exfoliated Hummers sample (40000x magnification).

4.7.6 Partially Oxidised Purified Samples

The exfoliated samples were purified, as previously mentioned, which enabled the removal of any impurities, yielding less reactive samples. These samples were partially oxidised 5 %, and clearly are different from the only exfoliated samples. This will be evident from the images shown below. Figure 4-107 to Figure 4-109 are images of the purified electrochemical intercalation sample. These images clearly illustrate the oxidation pits, sometimes eroding through to the centre of the basal plane.

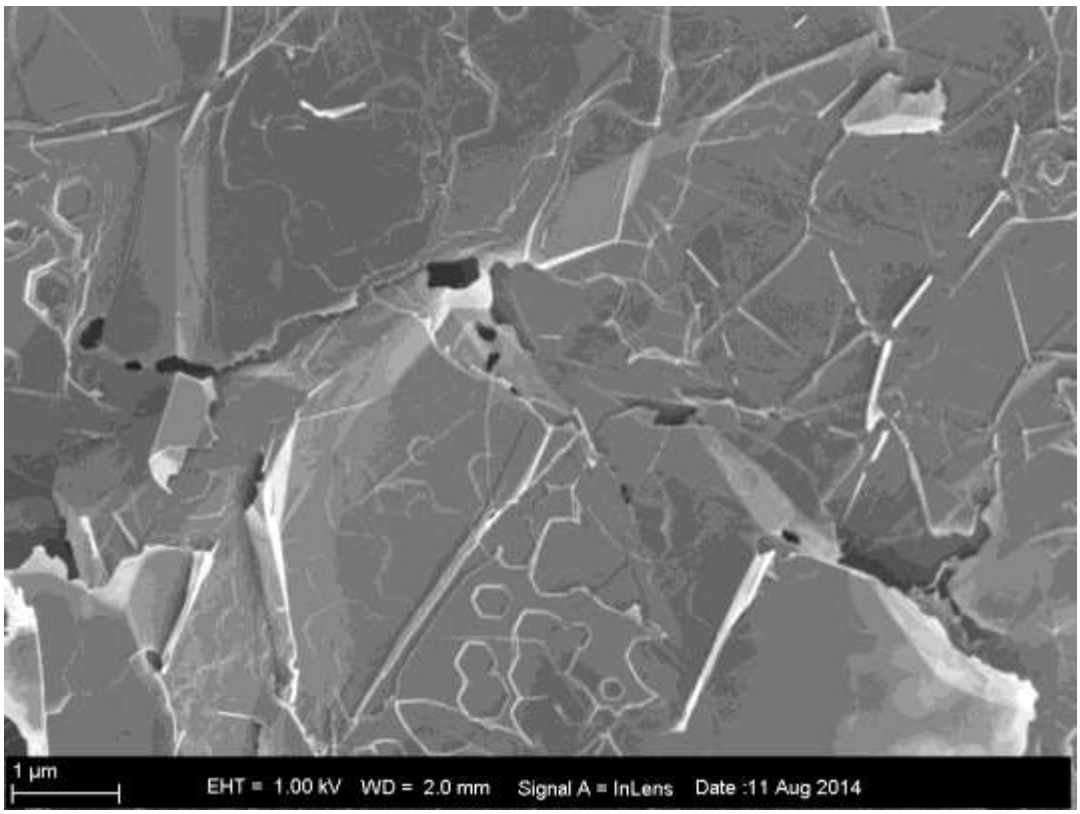

Figure 4-107: SEM of 5% oxidised purified electrochemical sample (30000x magnification).

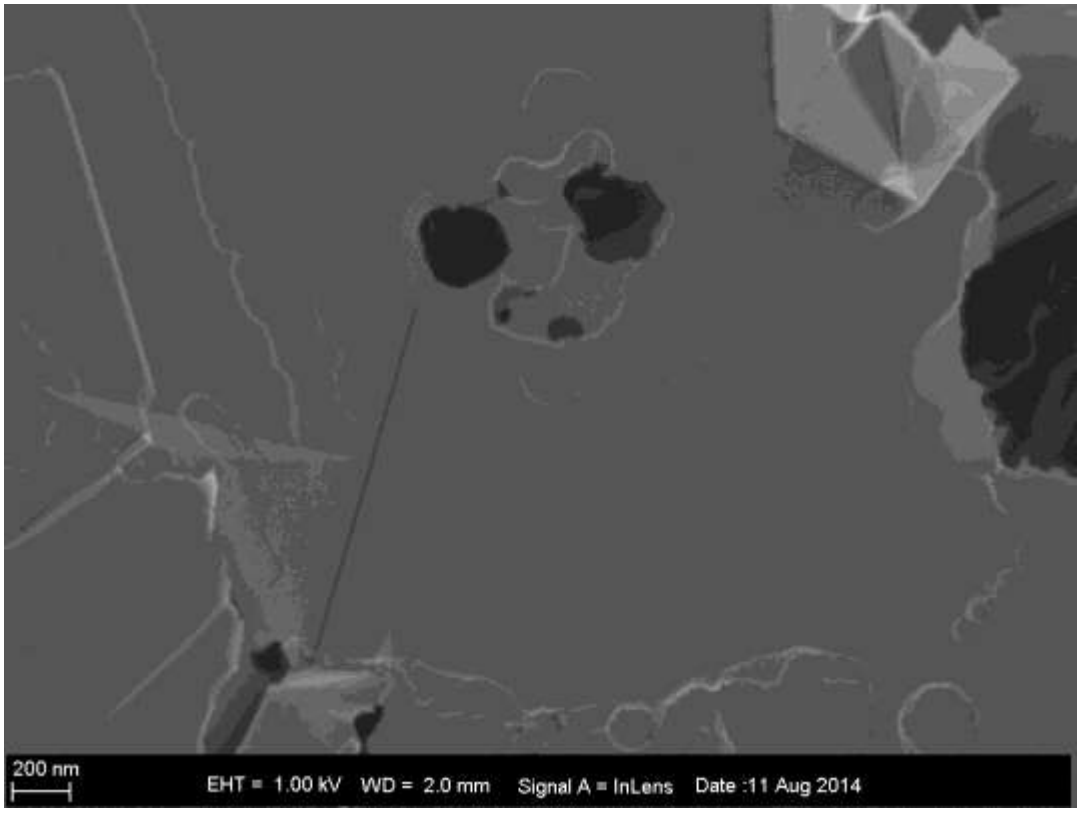

Figure 4-108: SEM of 5% oxidised purified electrochemical sample (80000x magnification).

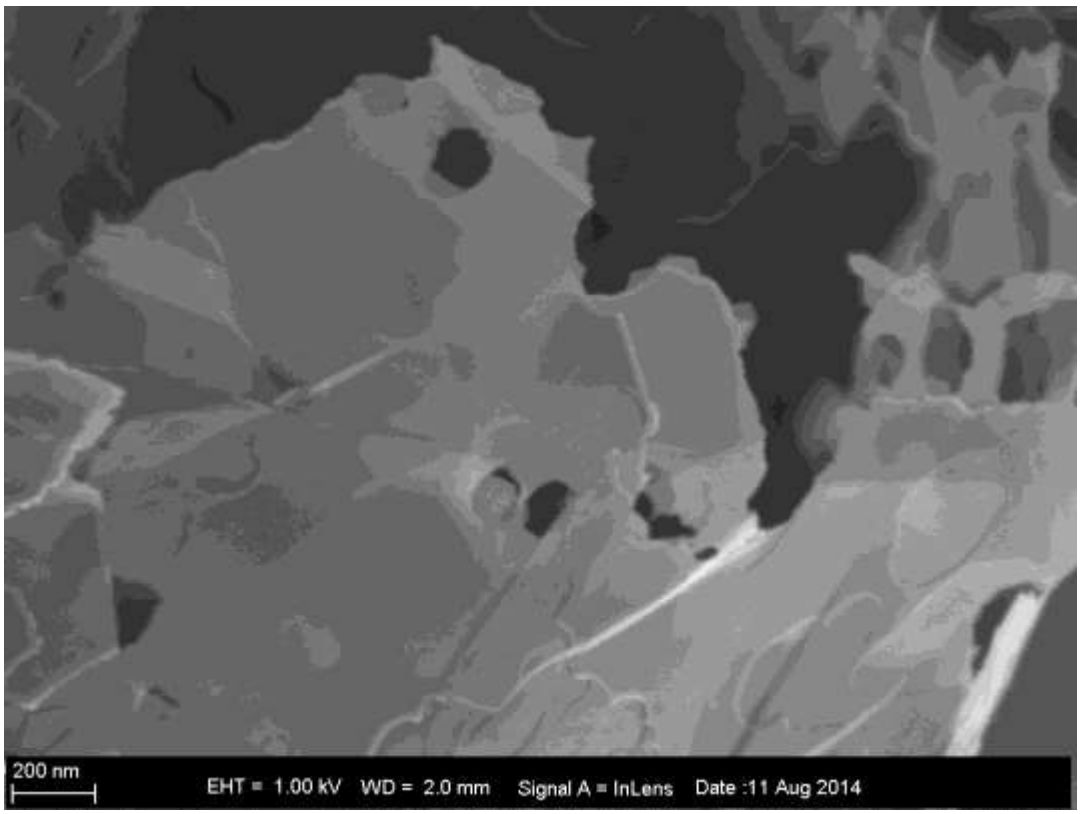

Figure 4-109: SEM of 5% oxidised purified electrochemical sample (115000x magnification).

The purified gas phase intercalation samples oxidised 5% are illustrated in the images below. Figure 4-110 clearly shows many oxidation pits. In Figure 4-111 the pits are magnified and it is clear that these pits are a few layers deep. The basal plane is damaged with random pits and eroded structure. Figure 4-112 illustrates the extreme damage to the structure of the sample, whereas Figure 4-113 shows the edge at a very high magnification. This image shows the extensive damage to the edge, the edge is very roughened and the basal plane also seems to be damaged. In Figure 4-114 and Figure 4-115 the sample is magnified 100 000 times and the damage is extensive. The layers are individually roughened, and oxidation pits are visually evident.

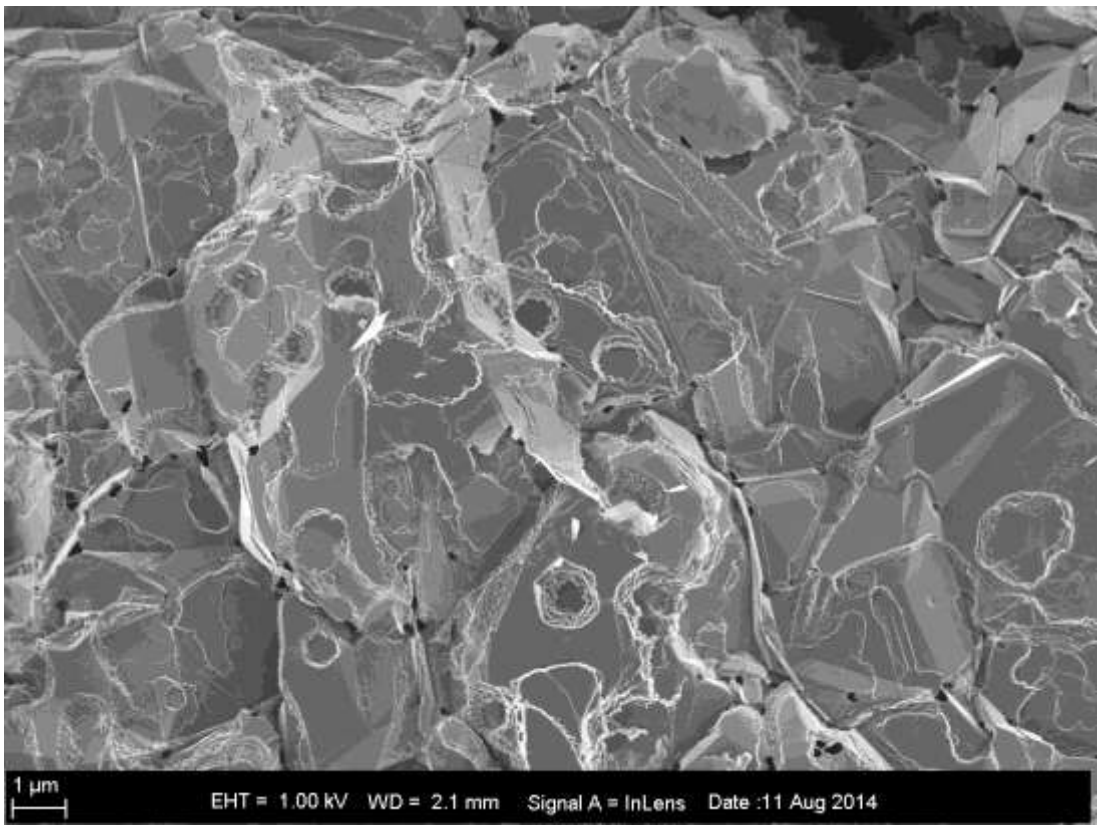

Figure 4-110: SEM of 5% oxidised purified gas sample (15000x magnification).

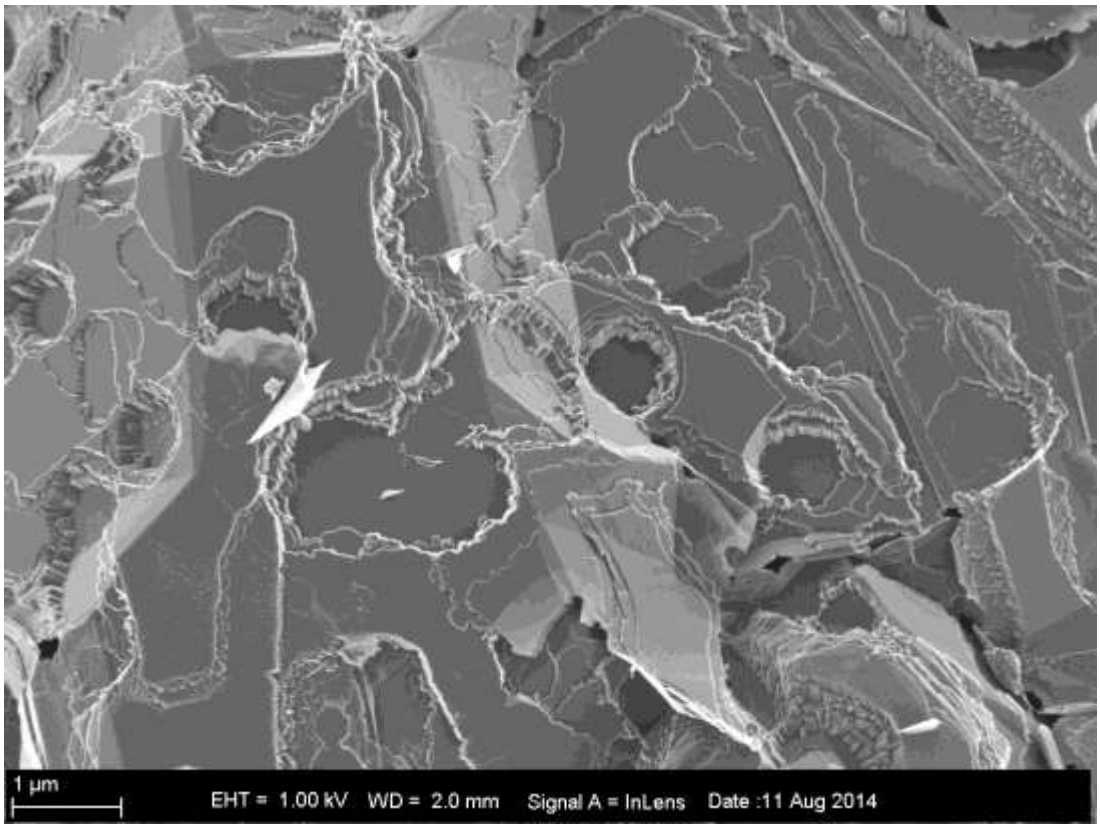

Figure 4-111: SEM of 5% oxidised purified gas sample (30000x magnification).

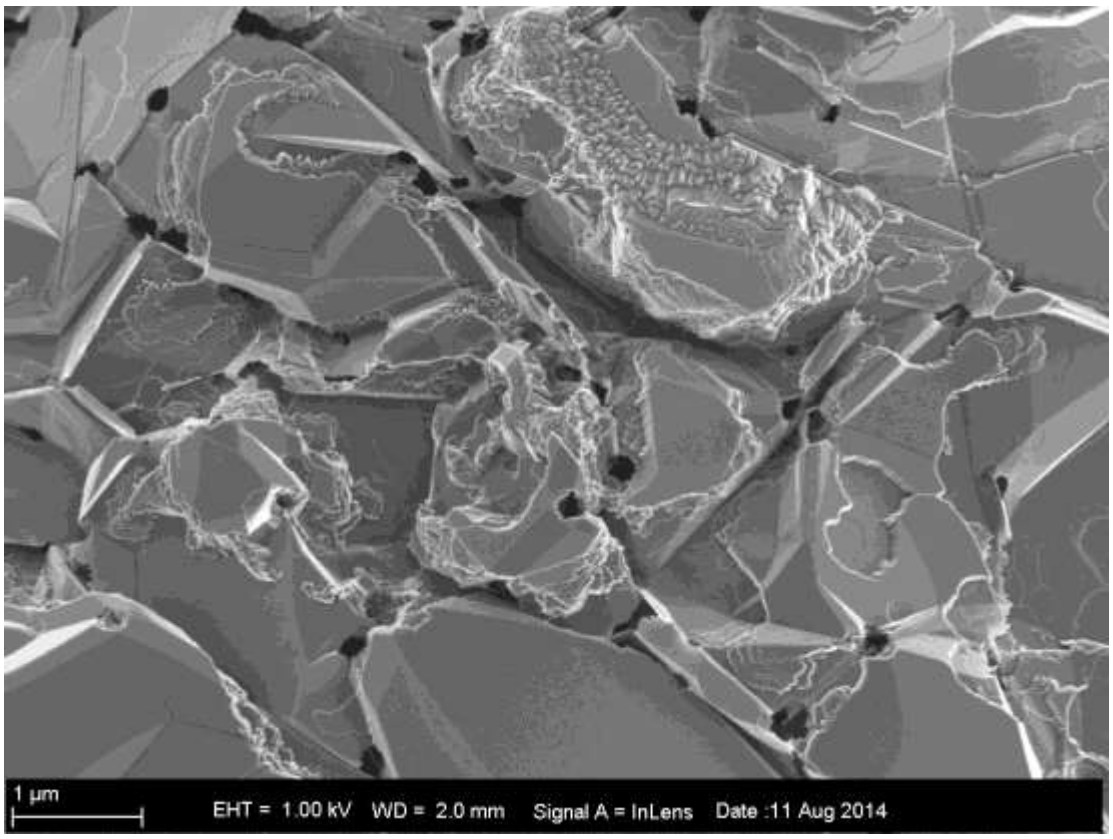

Figure 4-112: SEM of 5% oxidised purified gas sample (35000x magnification).

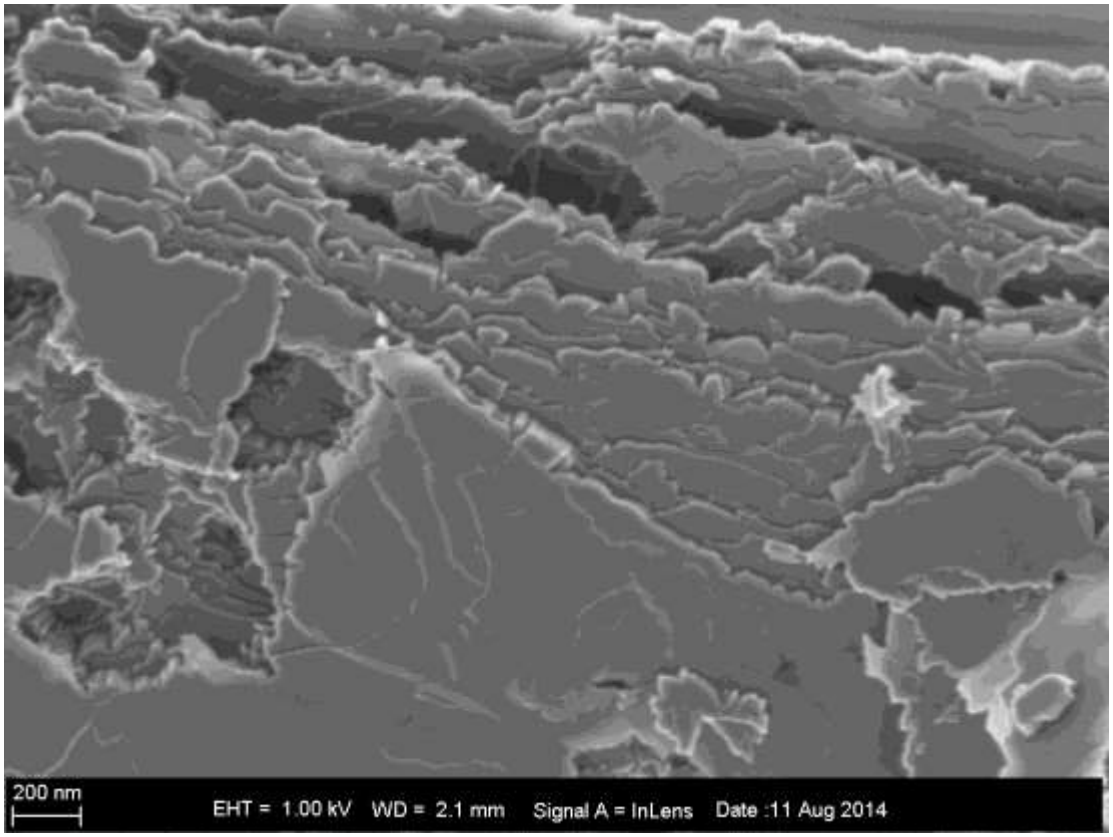

Figure 4-113: SEM of 5% oxidised purified gas sample (90000x magnification).

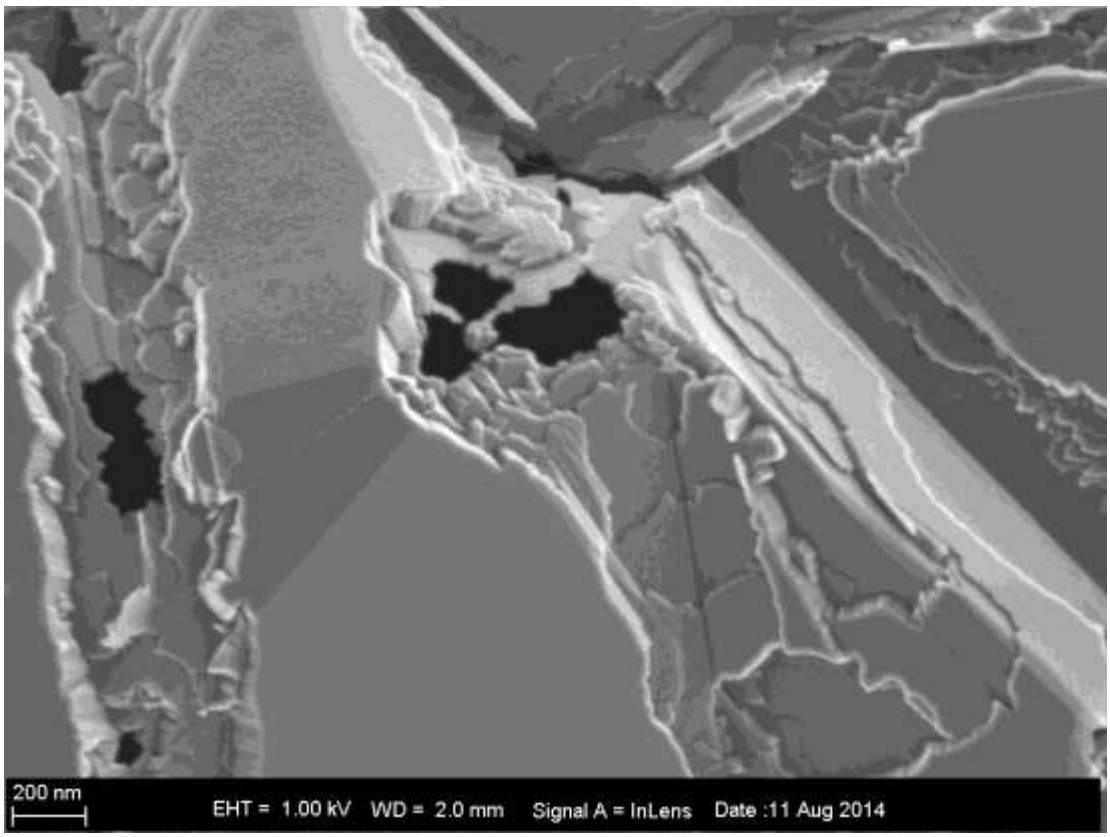

Figure 4-114: SEM of 5% oxidised purified gas sample (100000x magnification).

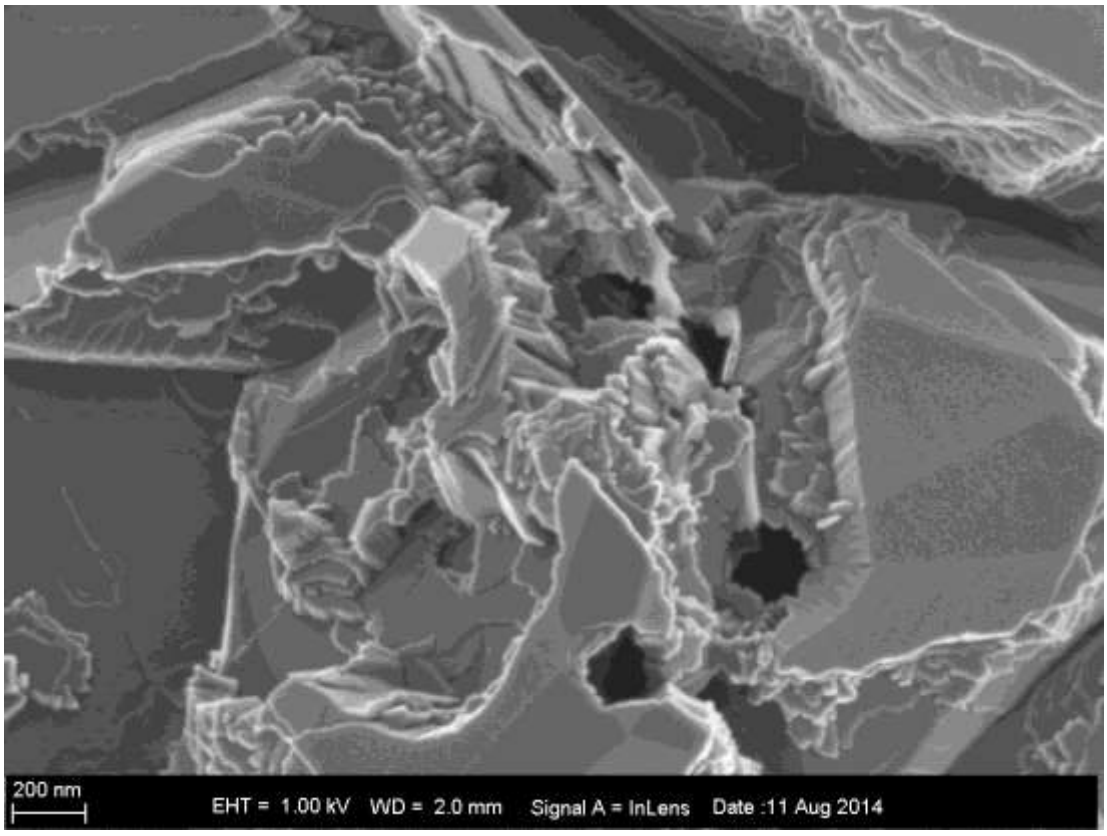

Figure 4-115: SEM of 5% oxidised purified gas sample (100000x magnification).

The 5 % oxidised purified Hummers intercalation method samples are illustrated in the following images. The oxidation pits are immediately visible from a distance, only 6000 times enhanced in Figure 4-116, but magnified 15000 times in Figure 4-117 the pits are more visible. Figure 4-118 shows that the oxidation pits are a few layers deep, also evident in Figure 4-119, illustrating almost exactly hexagonal pits. The randomly distinct pits are visible in both Figure 4-120 and Figure 4-121 illustrating the reactivity of the Hummers sample. This is due to the oxidation agent with which these samples were created. Figure 4-122 shows the layers and the surface erosion which occurred due to the oxidation. At 150 000 times the edge magnified, in this image the zig-zag structure is evident.

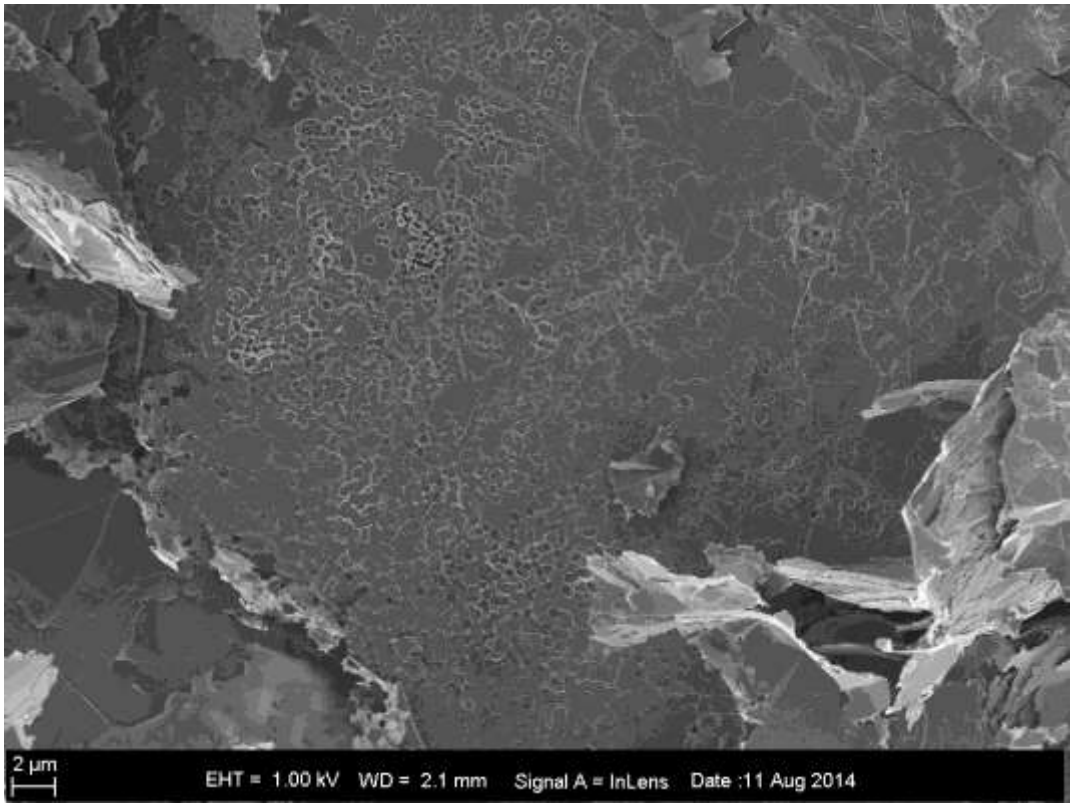

Figure 4-116: SEM of 5% oxidised purified Hummers sample (6000x magnification).

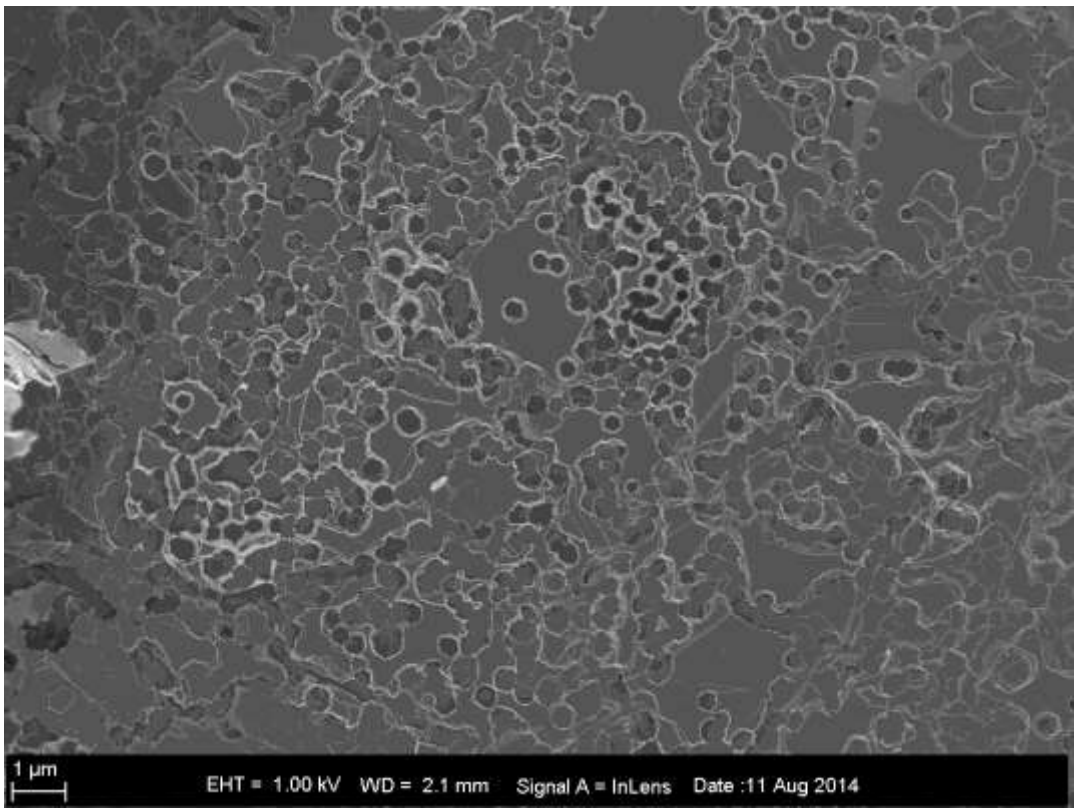

Figure 4-117: SEM of 5% oxidised purified Hummers sample (15000x magnification).

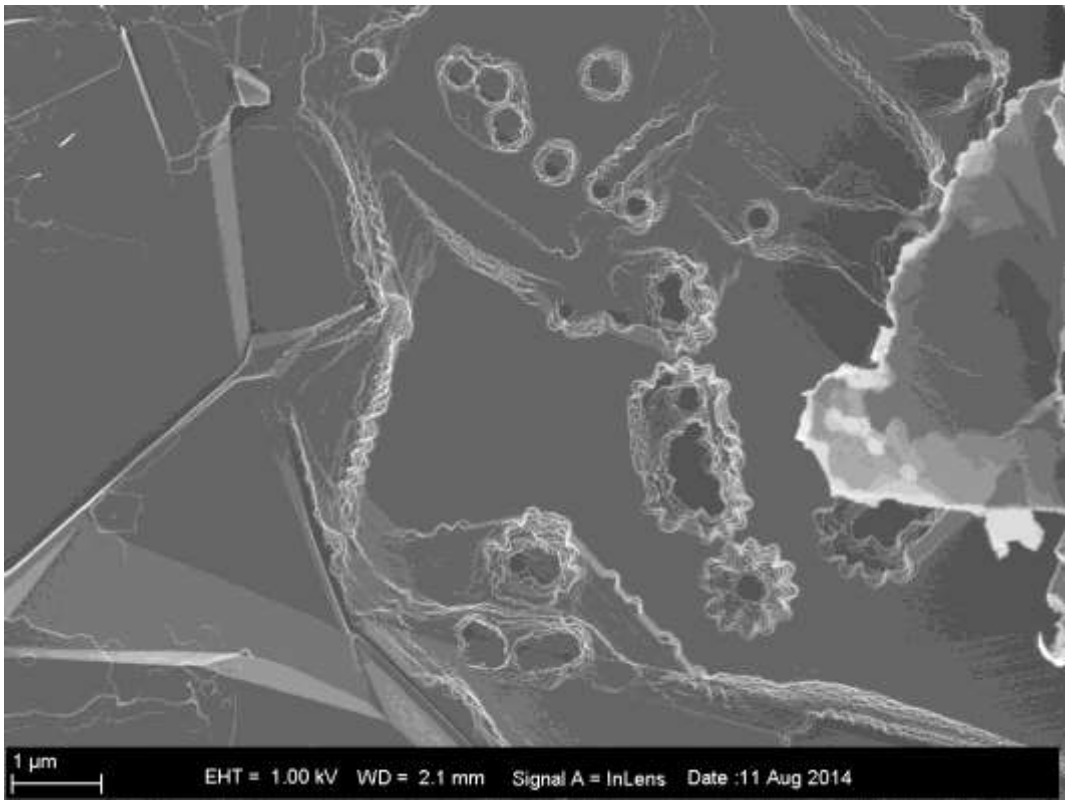

Figure 4-118: SEM of 5% oxidised purified Hummers sample (25000x magnification).

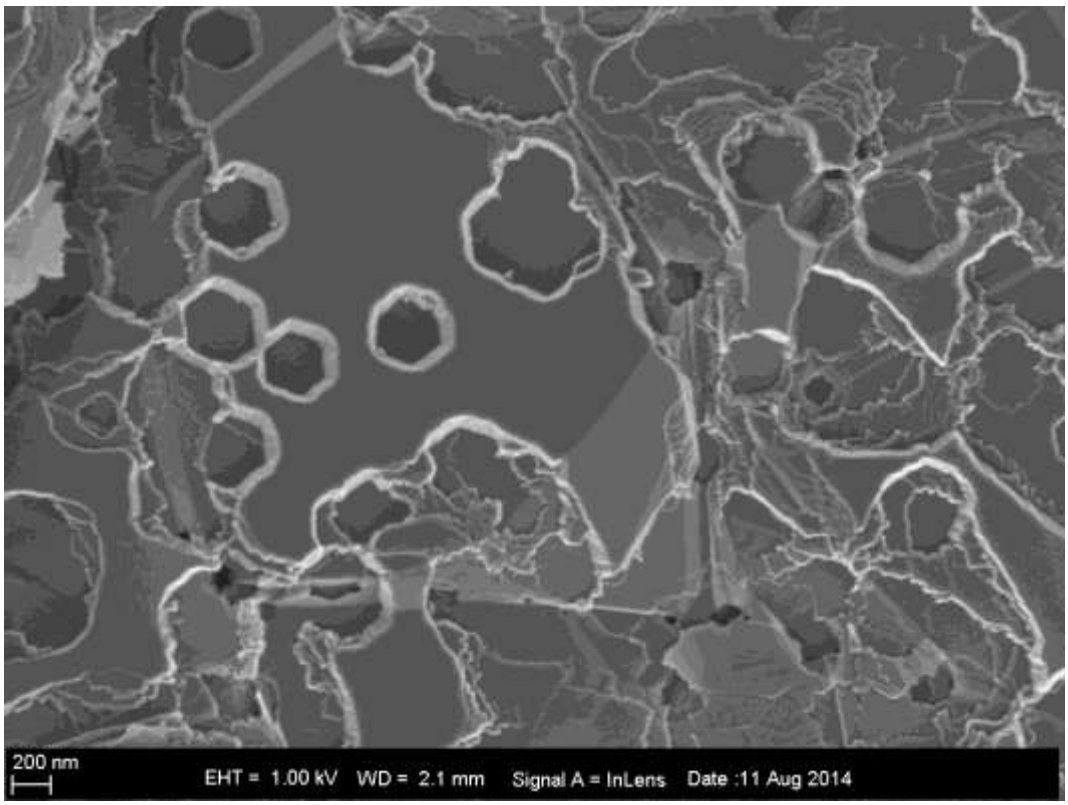

Figure 4-119: SEM of 5% oxidised purified Hummers sample (55000x magnification).

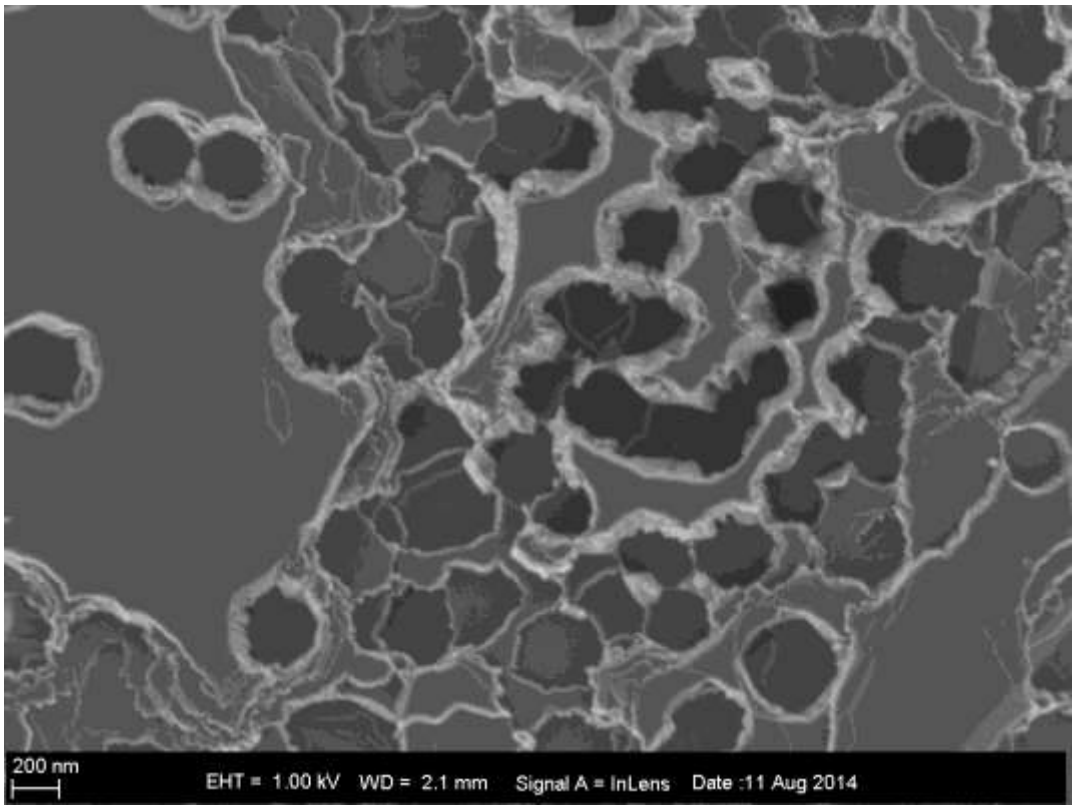

Figure 4-120: SEM of 5% oxidised purified Hummers sample (66000x magnification).

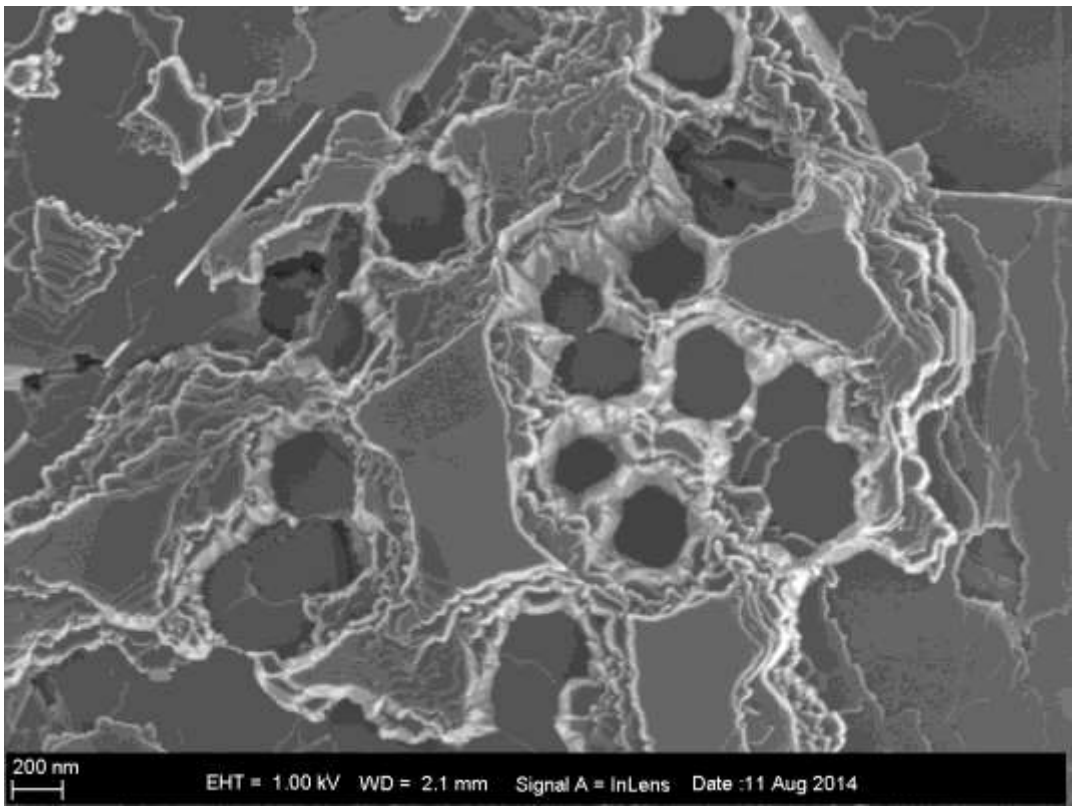

Figure 4-121: SEM of 5% oxidised purified Hummers sample (70000x magnification).

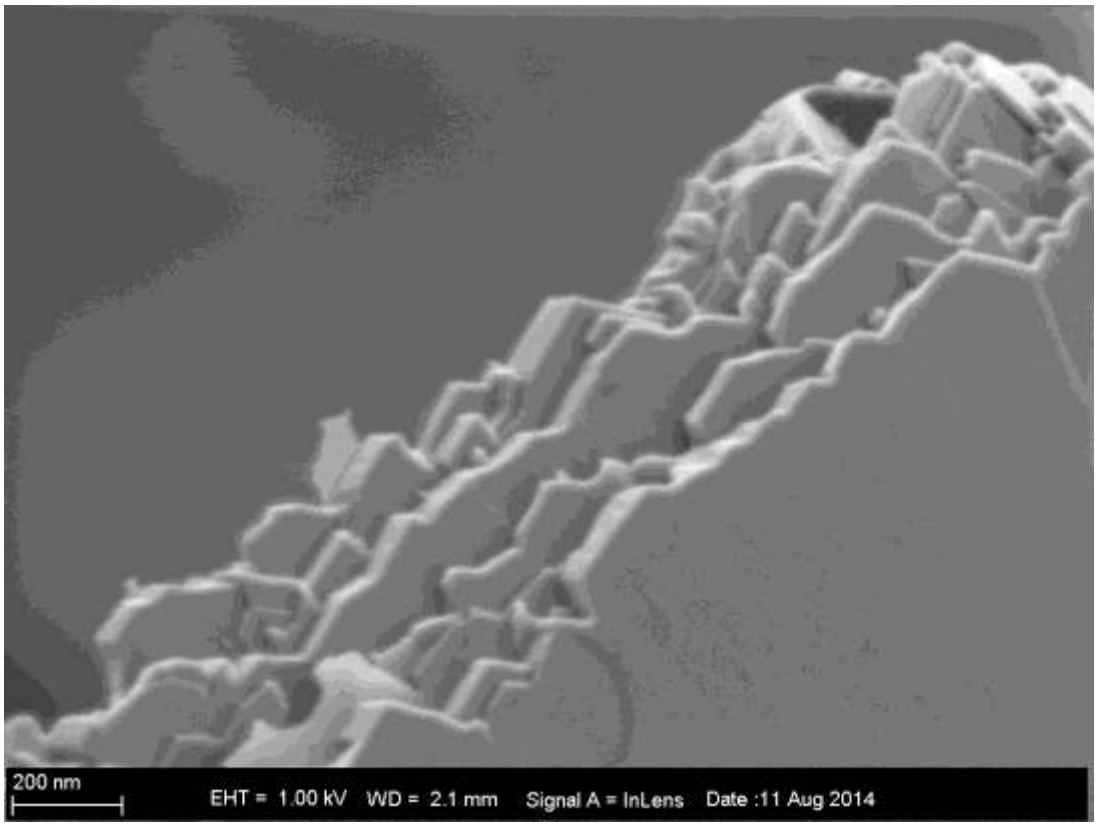

Figure 4-122: SEM of 5% oxidised purified Hummers sample (150000x magnification).

The purified samples were oxidised 30 % and illustrated below. All the images are magnified 5000 times for comparison. It is very clear that the electrochemical sample in Figure 4-123 illustrates damage in the edges, and the visibly shows the pits at a macro level. Figure 4-124 shows the gas phase sample, and the extensive damage is clearly visible. These edges are extremely damaged and random pits are also evident. The Hummers sample is shown in Figure 4-125 with extreme damage to the edge and the basal plane is also damaged with pits visible.

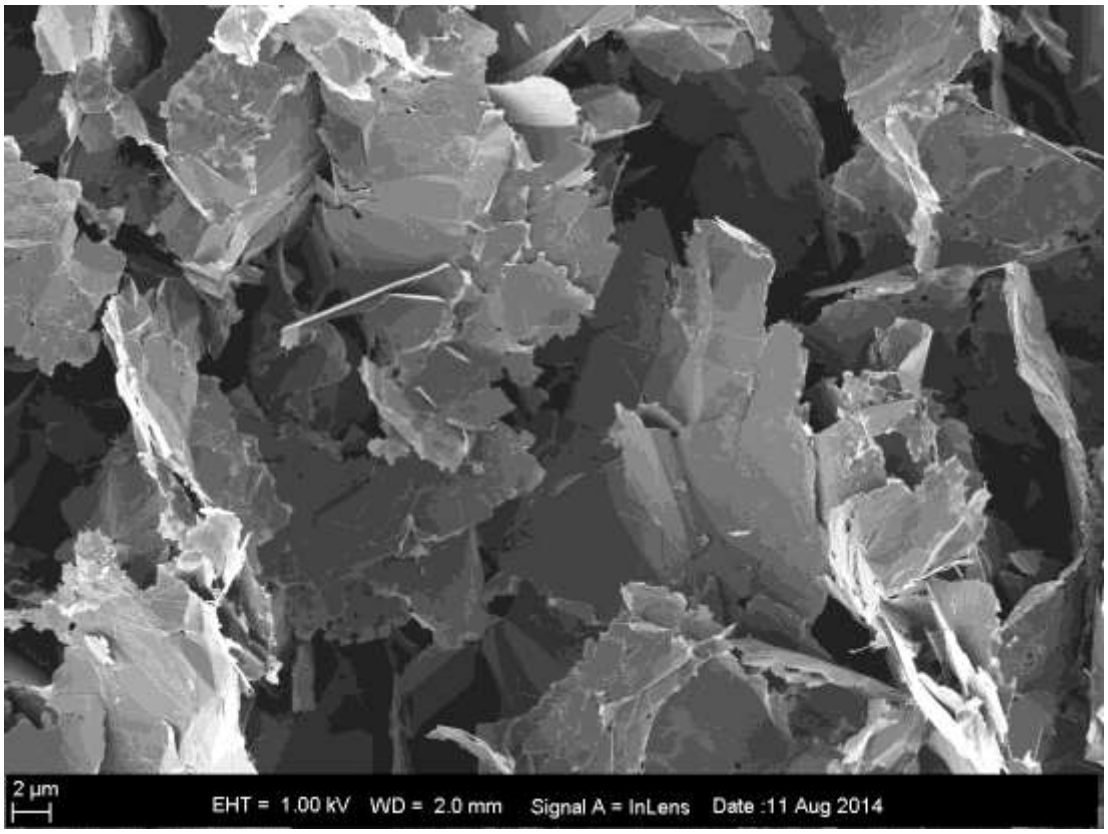

Figure 4-123: SEM of 30% oxidised purified electrochemical sample (5000x magnification).

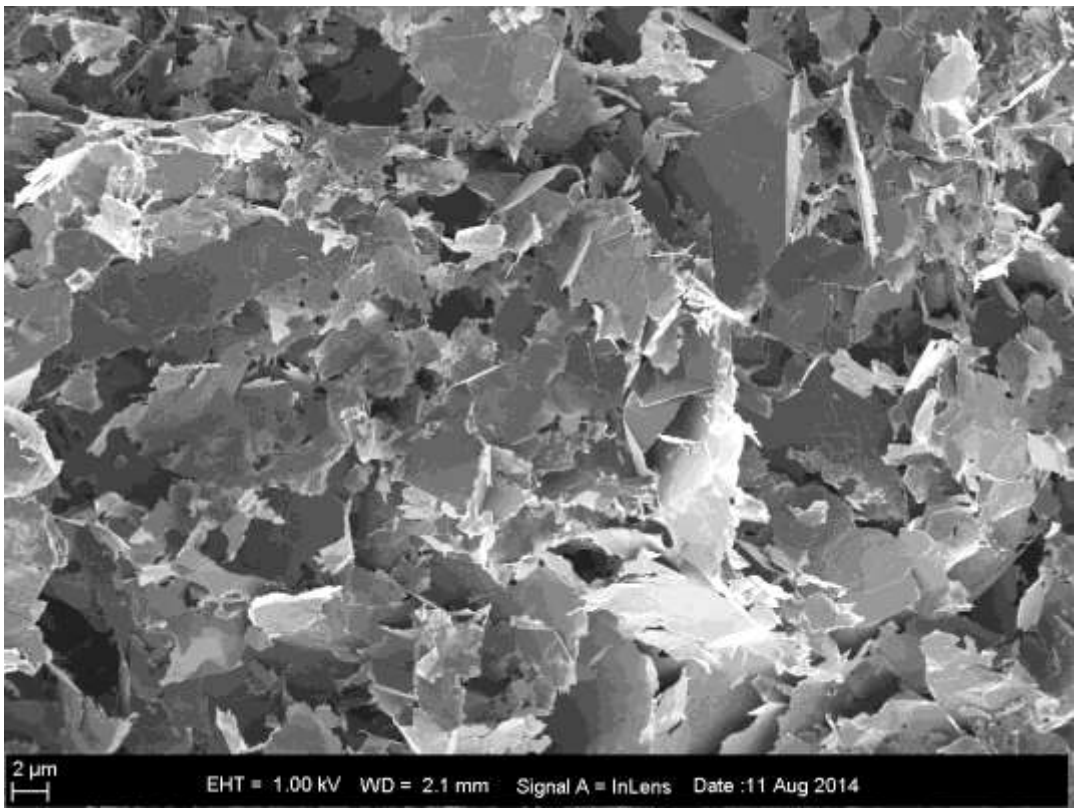

Figure 4-124: SEM of 30% oxidised purified gas phase sample (5000x magnification).

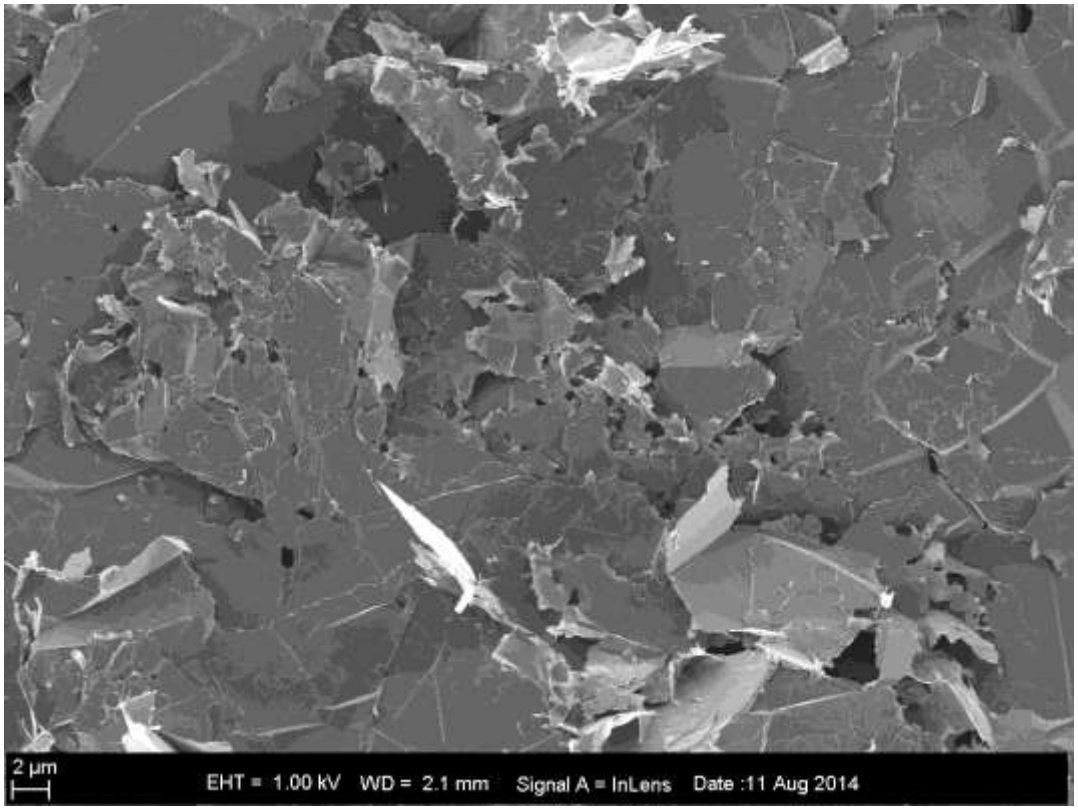

Figure 4-125: SEM of 30% oxidised purified Hummers sample (5000x magnification).

The purified electrochemical sample oxidised 30 % are shown in the following images. Figure 4-126 illustrates oxidation pits, and Figure 4-127 shows the damage incurred onto the edges of the sample, but the basal plane seems to be mostly intact. Figure 4-128 shows an uneven basal plane, with visible pits.

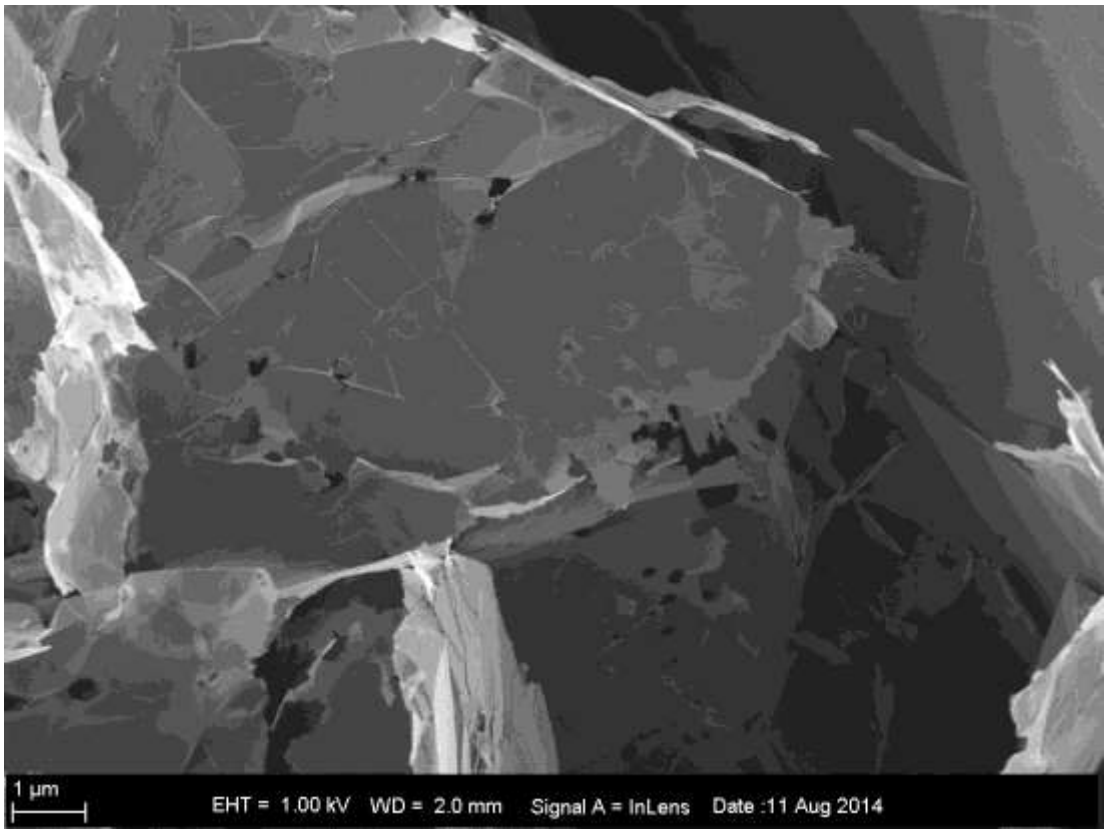

Figure 4-126: SEM of 30% oxidised purified electrochemical sample (20000x magnification).

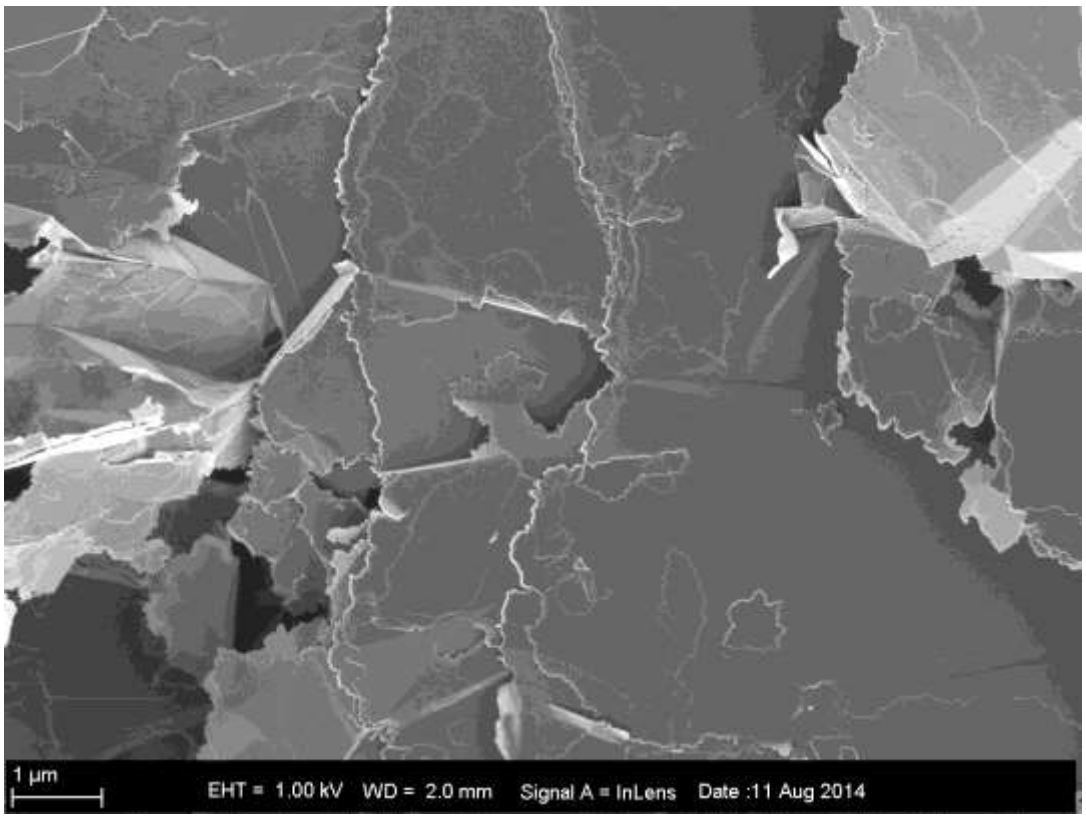

Figure 4-127: SEM of 30% oxidised purified electrochemical sample (25000x magnification).

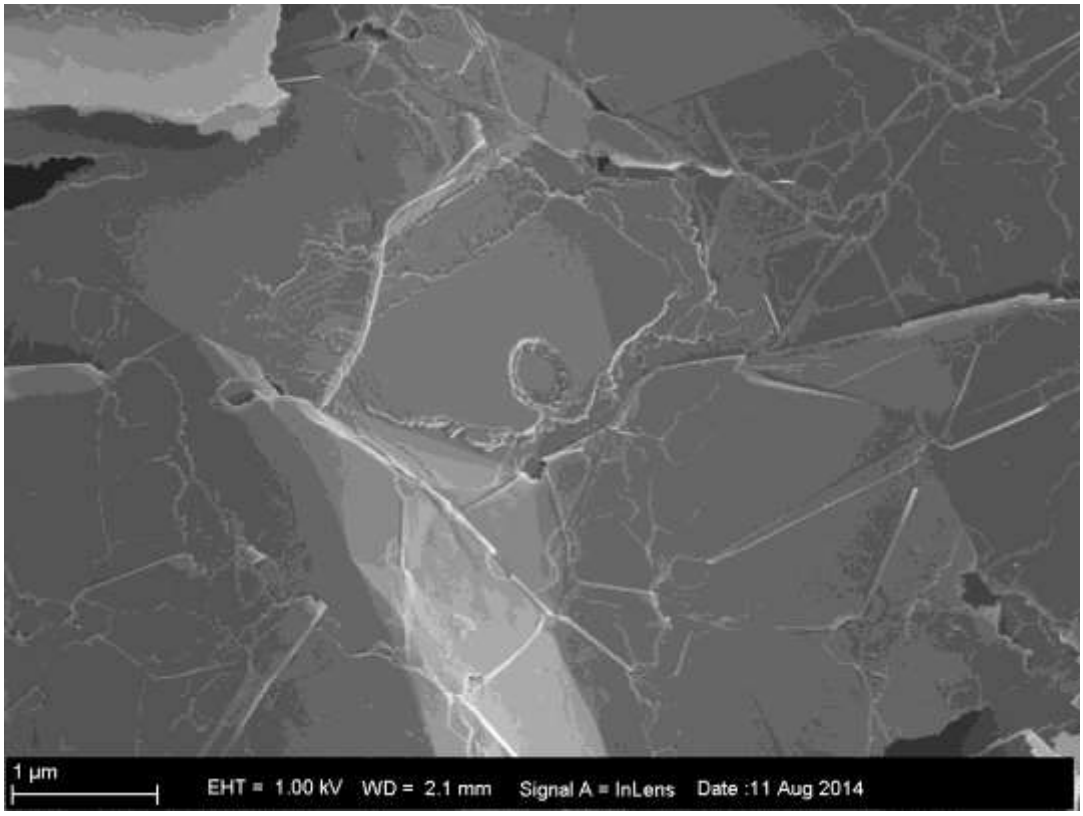

Figure 4-128: SEM of 30% oxidised purified electrochemical sample (40000x magnification).

The gas phase sample is illustrated in the following images. Figure 4-129 shows the edge as well as the basal plane, in this image the basal plane is well intact. The edge is visibly damaged. At higher magnification in Figure 4-130 the basal plane is visibly damaged, with the layers eroded to the centre. Figure 4-131 shows the extent of damage with the edges seems to be zig-zag. This phenomenon is magnified in Figure 4-132. This image shows extensive damage at a magnification of 90000 times.

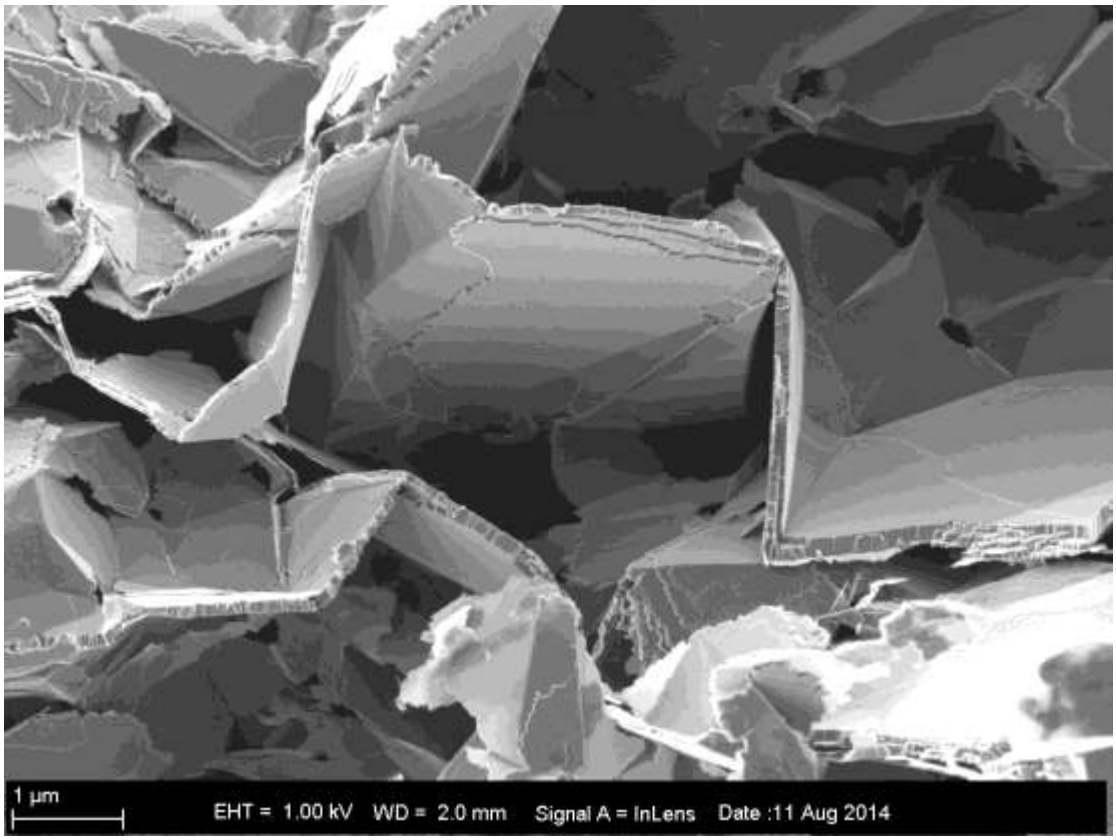

Figure 4-129: SEM of 30% oxidised purified gas phase sample (30000x magnification).

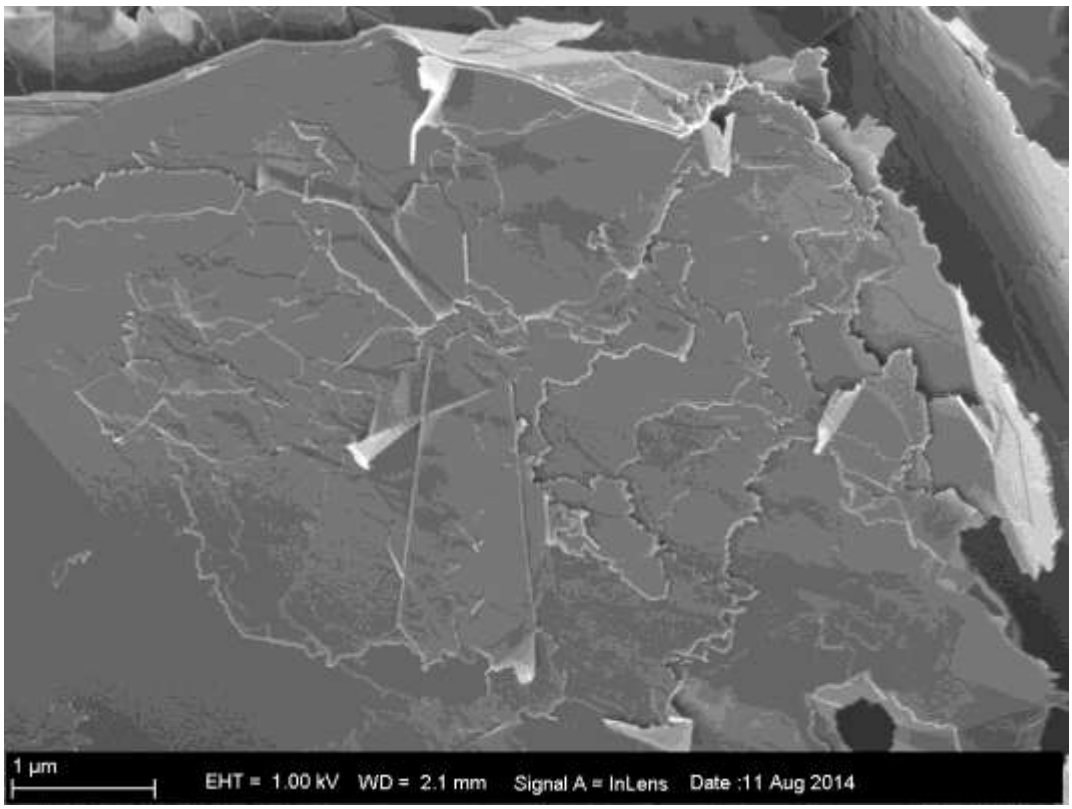

Figure 4-130: SEM of 30% oxidised purified gas phase sample (40000x magnification).

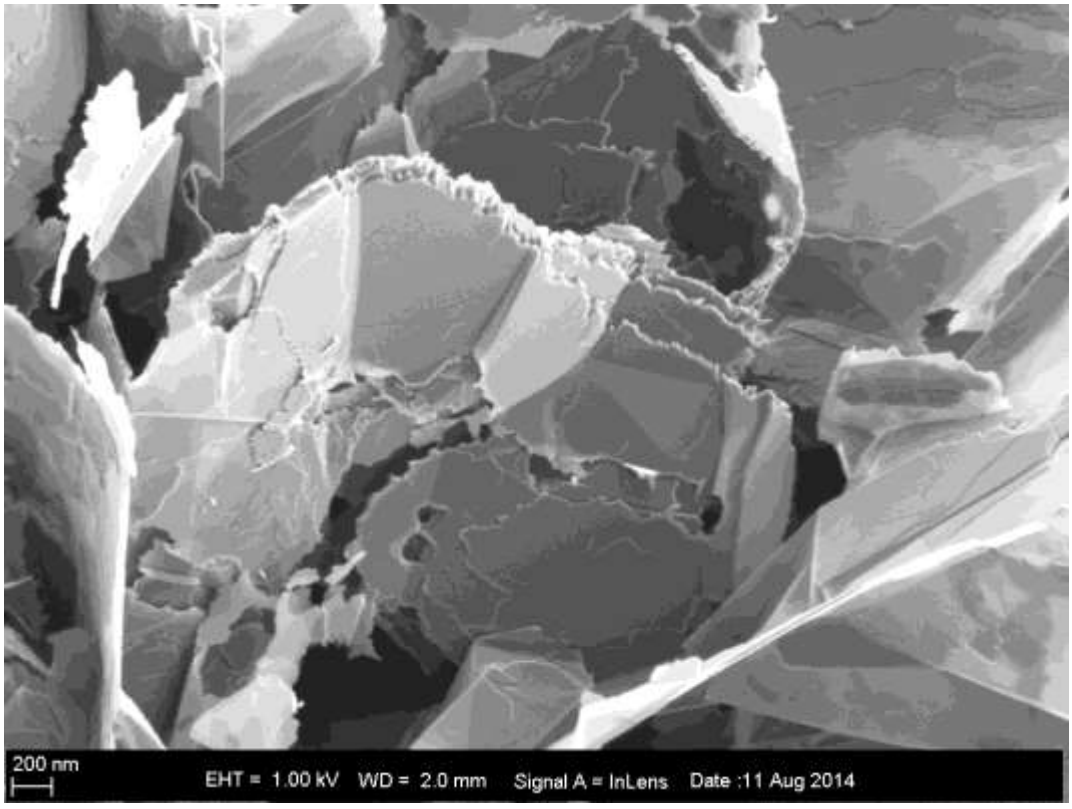

Figure 4-131: SEM of 30% oxidised purified gas phase sample (55000x magnification).

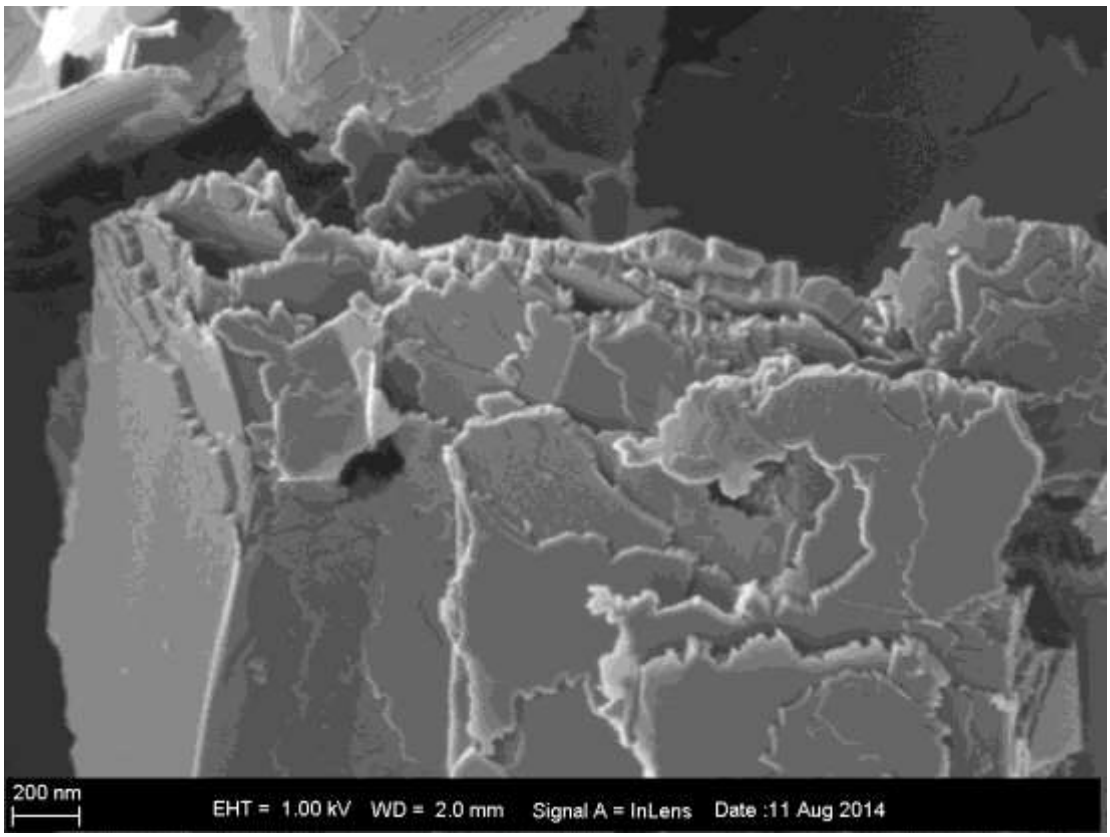

Figure 4-132: SEM of 30% oxidised purified gas phase sample (90000x magnification).

The 30 % oxidised purified Hummers sample is magnified 10000 times in Figure 4-133 and Figure 4-134. The basal plane is clearly damaged, with oxidation pits visible. Figure 4-134 shows the extent of damage. In this image the flake is completely destroyed, with pits and erosion through the entire flake. The Hummers method is undoubtedly from all the various oxidation samples the most damaged. This is due to the preparation method including an oxidation agent, which oxidises the sample further.

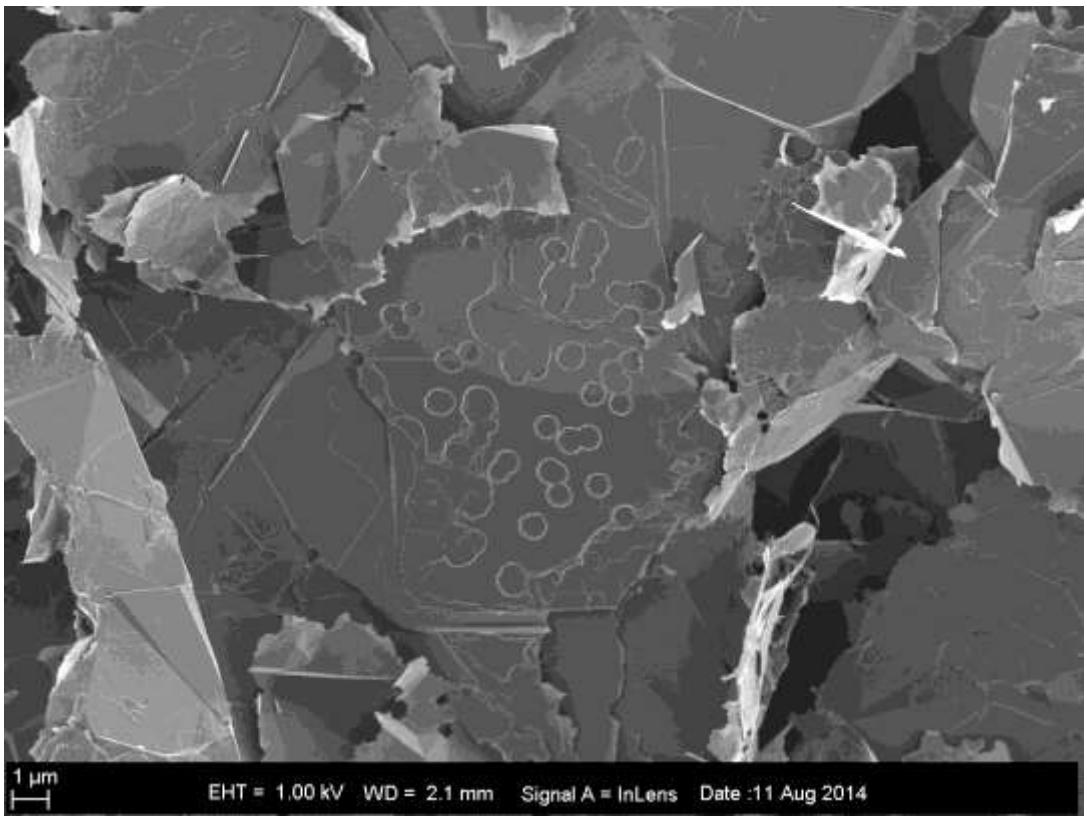

Figure 4-133: SEM of 30% oxidised purified Hummers sample (10000x magnification).

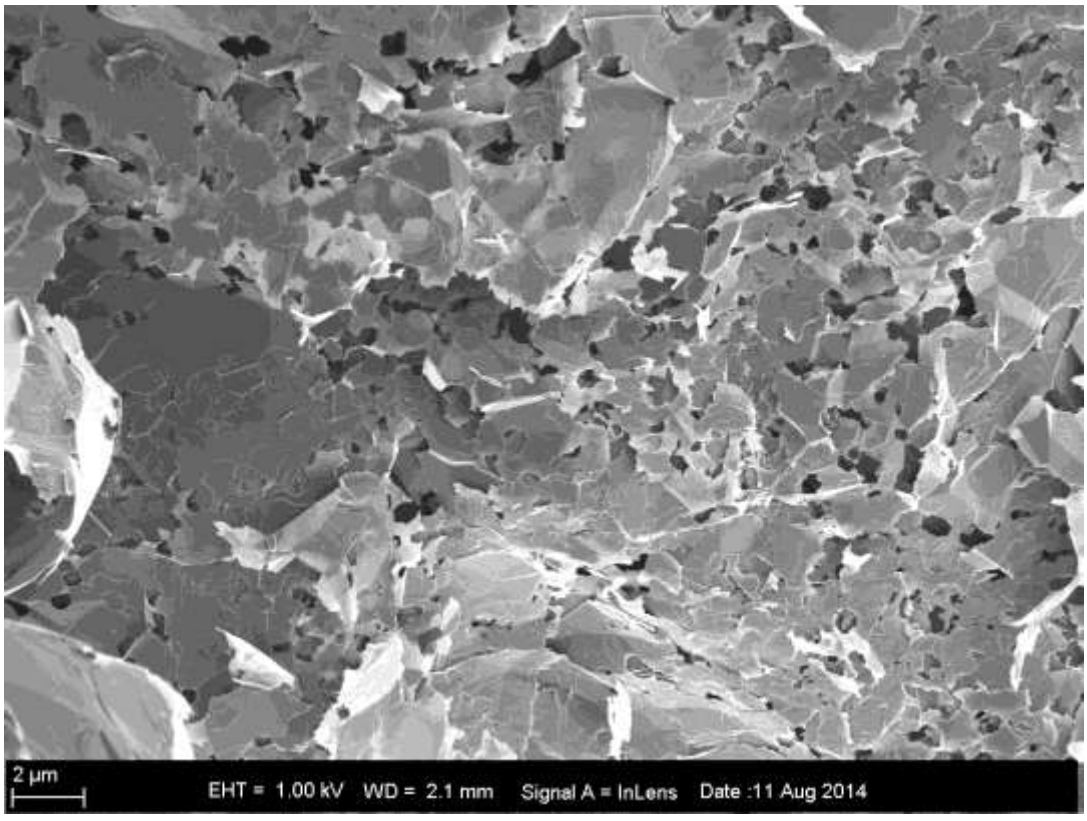

Figure 4-134: SEM of 30% oxidised purified Hummers sample (10000x magnification).

5. Conclusions and Recommendations

The gas phase sample had virtually no mass loss at the point where expansion took place. Therefore it is concluded that this method delivers very efficient intercalation, producing large expansion without significant mass loss. The mass loss which occurs only at the sublimation of iron chloride (320 ºC) indicates the "un-intercalated" or residual iron chloride. After oxidation, the residual mass of the gas phase sample before purification is 25 %; this also proves the presence of impurities in the exfoliated sample. The residual material on the sample acts as catalysts making this sample very reactive.

The Hummers and electrochemical intercalation methods show similar expansion and mass loss curves, therefore it can be concluded that the reaction mechanism for both these methods is alike. For the Hummers and electrochemical samples, expansion and mass loss occurs over a wide temperature range, this indicates that graphite oxide was formed rather than the theoretically expected, "insertion of atoms between the sheets". The mass losses before 200 ˚C of the samples of the Hummers and electrochemical methods are more evidence that graphite oxide and graphite surface complexes with oxygen were produced.

The expansion method using TMA is different from that of microwave expansion, as microwave expansion employs a rapid, intense heating, whereas the TMA uses slow heating. Using manual expansion the electrochemical method shows the best intercalation of a volume expansion of 1500 %, with the gas phase just below with 1450 %. Using the TMA for expansion the gas phase illustrates best intercalation of about 250 % with the electrochemical and Hummers methods approximately 220 %.

The Hummers samples are extremely damaged. This is clear from the several and deep oxidation pits visible throughout the basal plane of these samples. The basal plane and the edges are even eroded before purification and oxidation. This intercalation technique employs oxidisers in the preparation method which additionally oxidises the samples. This explains why the Hummers method renders the most damage.

The residual material on the gas phase sample acts as catalysts making the sample very reactive and consequently damaging the surface during oxidation. The partially oxidised purified gas phase sample visibly shows the pits and roughened edges.

The X-ray diffractograms of the exfoliated samples from both the electrochemical and Hummers methods are similar to that of the original graphite flakes. This indicates that when the intercalated samples have been expanded and sonicated, the original material is nearly restored at the level of the basal plane. The gas phase sample restores the original graphite flake diffractogram to some extent as well.

It is recommended that a more efficient method for removal of residual material in the gas phase samples be explored. It is also recommended that more research be done to determine the reaction mechanisms during the three different intercalation methods. Analyse the graphite surface complexes of the intercalated compounds and determine the evolved gases during expansion.

6. References

Abe, T, Mizutani, Y, Shinoda, N, Ihara, E, Asano, M, Harada, T, Inaba, M and Ogumi, Z (1995) "Debye-Waller factors of $FeCl_3$- and ICl-Graphite Intercalation Compounds" *Carbon*, 33(12), 1789 – 1793.

Afanasov, IM, Shornikova, ON, Kirilenko, DA, Vlasov, II, Zhang, L, Verbeeck, J, Avdeev, VV and Van Tendeloo, G (2010) "Graphite structural transformations during intercalation by HNO_3 and expansion" *Carbon*, 48, 1858 – 1865.

Asano, M, Sasaki, T, Abe, T, Mizutani, Y and Harada, T (1996) "Mass-spectrometric study of vaporization of $FeCl_3$-Graphite intercalation compound" *Journal of Physics and Chemistry of Solids*, 57(8), 787 – 790.

Chung, DDL (1987) "Review Expansion of graphite" *Journal of Materials Science*, 22, 4190 – 4198.

Chung, DDL (2002) "Review Graphite" *Journal of Material Science*, 37, 1475 – 1489.

Dresselhaus, MS and Dresselhaus, G (2002) "Intercalation compounds of graphite" *Advances in Physics*, 51(1), 1 – 186.

Focke, WW, Badenhorst H, Mhike, W, Kruger, HJ and Lombaard, D (2014) "Characterization of commercial expandable graphite fire retardants" *Thermochimica Acta*, 584, 8 – 16.

Graphit Kropfmuhl AG (*sa*) "What is graphite" , http://www.graphite.de/englisch/pdf/blaehgraphitprospekt_e.pdf [2013, July 10].

Hamwi, A, Senhaji, A, Djurado, D and Dupuis, J (1993) "Chloride-fluoride-graphite ternary compounds: Preparation and characterisation" *Carbon*, 31(4), 623 – 628.

Inagaki, M, Tashiro, R, Washino, Y and Toyoda, M (2004) “Expansion process of graphite via intercalation compounds with sulfuric acid” *Journal of Physics and Chemistry of Solids*, 65, 133–137.

Kalucki, K. and Morowski, AW (1987) “Controlled Reactivity of Graphite with Iron (III) Chloride” *Reactivity of Solids*, 4, 269 – 273.

Kalyoncu, RS (1998) “Graphite” *Graphite*, 1 – 2.

Kang, F, Zheng, Y, Wang, H, Nishi, Y and Inagaki, M (2002) “Effect of preparation conditions on the characteristics of expanded graphite” *Carbon*, 40, 1575 – 1581.

Kwon, OY, Choi, SW, Park, KW and Kwon, YB (2003) “The preparation of expanded graphite by using microwave” *J. Ind. Eng. Chem.*, 9(6), 743 – 747.

McCreery, RL (2008) “Advanced Carbon Electrode Materials for Molecular Electrochemistry” *Chem. Rev.*, 108, 2646–2687.

Metz, W and Hohlwein, D (1975) “Charakterisierung von graphit-$FeCl_3$-verbindungen als teilweise geordnete schichtstrukturen” *Carbon*, 13(2), 87-96 (1975).

Nakajima T, and Matsuo Y (1994) “Formation process and structure of graphite oxide, *Carbon,* 32(3), 469 – 475.

Noel, M and Santhanam, R (1998) “Review Electrochemistry of graphite intercalation compounds” *Journal of Power Sources*, 72, 53 – 65.

Savoskin, MV, Yaroshenko, AP, Whyman, GE and Mysyk, RD (2006) “New graphite nitrate derived intercalation compounds of higher thermal stability” *Journal of Physics and Chemistry of Solids*, 67, 1127 – 1131.

Shornikova, ON, Dunaev, AV, Maksimove, NV and Avdeev, VV (2006) “Synthesis and properties of ternary GIC with iron and copper chlorides” *Journal of Physics and Chemistry of Solids*, 67, 1193 – 1197.

Sorokina, NE, Mudretsova, SN, Maiorova, AF, Avdeev, VV and Maksimova NV (2001) “Thermal Properties of Graphite Intercalation Compounds with HNO_3” *Inorganic Materials*, 37(2) 153 – 156.

Toyoda, M and Inagaki, M (2000) “Heavy oil sorption using expanded graphite: new application of expanded graphite to protect heavy oil pollution” *Carbon*, 38, 199 – 210.

Tuinstra, F, Koenig, J (1970) “Raman spectrum of graphite” *Journal of Chemical Physical*, 53, 1280 – 1281.

Wei, T, Fan, Z, Luo, G, Zheng, C and Xie, D (2008) “A rapid and efficient method to prepare expanded graphite by microwave irradiation” *Carbon*, 47, 313 – 347.

Zhao, W, Tan, PH, Liu, J and Ferrari, AC (2011) “Intercalation of Few-Layer Graphite Flakes with $FeCl_3$: Raman Determination of Fermi Level, Layer by Layer Decoupling, and Stability” *Journal of the American Chemical Society*, 133, 5941 – 5946.

Zhu, J, Chen, Z and Wang, C (2003) “Preparation and characterization of $CuCl_2$–$FeCl_3$–H_2SO_4–graphite intercalation compounds by hydrothermal synthesis” *Material letters*, 57, 2145 – 2149.

UNIVERSITEIT VAN PRETORIA
UNIVERSITY OF PRETORIA
YUNIBESITHI YA PRETORIA

DECLARATION OF ORIGINALITY

UNIVERSITY OF PRETORIA

The Department of Chemical Engineering places great emphasis upon integrity and ethical conduct in the preparation of all written work submitted for academic evaluation.

While academic staff teach you about referencing techniques and how to avoid plagiarism, you too have a responsibility in this regard. If you are at any stage uncertain as to what is required, you should speak to your lecturer before any written work is submitted.

You are guilty of plagiarism if you copy something from another author's work (eg a book, an article or a website) without acknowledging the source and pass it off as your own. In effect you are stealing something that belongs to someone else. This is not only the case when you copy work word-for-word (verbatim), but also when you submit someone else's work in a slightly altered form (paraphrase) or use a line of argument without acknowledging it. You are not allowed to use work previously produced by another student. You are also not allowed to let anybody copy your work with the intention of passing if off as his/her work.

Students who commit plagiarism will not be given any credit for plagiarised work. The matter may also be referred to the Disciplinary Committee (Students) for a ruling. Plagiarism is regarded as a serious contravention of the University's rules and can lead to expulsion from the University.

The declaration which follows must accompany all written work submitted while you are a student of the Department of Chemical Engineering. No written work will be accepted unless the declaration has been completed and attached.

Full names of student: Xandra van Heerden

Student number: 29079498

Topic of work: The influence of three different intercalation methods on the properties of expanded graphite

UNIVERSITEIT VAN PRETORIA
UNIVERSITY OF PRETORIA
YUNIBESITHI YA PRETORIA

Declaration

1. I understand what plagiarism is and am aware of the University's policy in this regard.

2. I declare that this thesis is my own original work. Where other people's work has been used (either from a printed source, Internet or any other source), this has been properly acknowledged and referenced in accordance with departmental requirements.

3. I have not used work previously produced by another student or any other person to hand in as my own.

4. I have not allowed, and will not allow, anyone to copy my work with the intention of passing it off as his or her own work.

SIGNATURE .....